MODELLING MATERIAL MASS BALANCES OVER WASTEWATER TREATMENT PLANTS

by

Sven Wilhelm Sötemann

BSc. Eng. (Civil) University of Cape Town
MSc. Eng. (Civil) University of Cape Town
PgDipl. Eng. (Civil) University of Cape Town

Thesis Submitted for the Degree of
Doctor of Philosophy
in Civil Engineering

University of Cape Town
Department of Civil Engineering

August 2005

DECLARATION BY CANDIDATE

I, Sven Wilhelm Sötemann hereby:

(1) Grant the University free licence to reproduce the above thesis in whole or in part, for the purpose of research;

(2) Declare that:

(i) The above thesis is my own unaided work, both in conception and execution, and that apart from the normal guidance of my supervisors, I have received no assistance and

(ii) that neither the substance or any part of the thesis has been submitted for a degree in the University or any other University.

Signed by candidate

ABSTRACT

MODELLING MATERIAL MASS BALANCES OVER WASTEWATER TREATMENT PLANTS

The overall objective of whole wastewater treatment plant (WWTP) modelling is to develop a COD (electron), carbon (C), nitrogen (N), phosphorus (P), alkalinity (proton), calcium (Ca), magnesium (Mg) and inorganic suspended solids (ISS) concentrations mass balances model for unit operations in municipal WWTPs. The development of such a model, for both steady state and dynamic simulation conditions, is an objective greater than this thesis project, however it makes a number of significant steps towards it, viz.:

(1) A simple mass balances (COD, N and P) WWTP steady state and kinetic simulation model (UCTOLD) was set up, including prediction of the inorganic suspended solids concentration for WWTPs comprising: Primary sedimentation, anoxic/aerobic activated sludge and aerobic digestion of primary and waste activated sludge. The kinetic and steady state models gave virtually identical results.

(2) The activated sludge simulation model (ASM1) was extended to incorporate pH as a predictive parameter and validated against literature data. The extension of ASM1 incorporates chemical (weak acid/base aqueous chemistry) and physical (gas exchange) processes and integrates these with the biological processes. This extension is restricted to aerobic and anoxic/aerobic C and N removal activated sludge systems.

(3) The biological processes of anaerobic digestion were integrated into a two phase (aqueous/gas) version of the chemical physical processes model developed by Musvoto *et al.* (1997, 2000) to construct a mass balances (COD, C, N, O, H) based integrated chemical/physical/biological processes model capable of predicting digester pH and it was validated with laboratory and literature data. Although not validated for dynamic loading conditions, the anaerobic digestion model is capable of dealing with such conditions - a brief inhibition of the acetoclastic methanogen group caused irreversible digester failure (pH <6.5).

(4) The dynamic simulation anaerobic digestion model is simplified into a steady state one for initial design of AD systems and integration into the steady state WWTP model (1 above).

(5) The 3 phase (aqueous-gas-solid) mixed weak acid/base chemical physical processes kinetic model including mineral precipitation of calcium and magnesium phosphates and carbonates was applied to aeration treatment of swinery wastewater and sewage sludge anaerobic digester liquor to evaluate the feasibility of producing a three phase mixed weak acid/base chemical, physical and biological processes models for activated sludge and anaerobic digestion. This three phase chemical physical model predicted the time dependent literature data very well, with multiple precipitating minerals competing for the same compounds. This cannot be solved with equilibrium chemistry algebraic equations. The production of three phase activated sludge and anaerobic digestion models therefore appears entirely feasible.

The developed models meet the following requirements: (i) They are combinations of the existing biological models and the mixed weak acid base chemistry, so that the chemical/physical processes within which the biological processes take place are modelled together, (ii) the

integration between the biological and chemical physical processes is seamless with the hydrogen ion (i.e. pH) being modelled as a process compound like all the others and (iii) the models of the different unit operations such as N removal activated sludge, aerobic digestion, anaerobic digestion, primary sedimentation etc. can be readily combined to form a mass balances based kinetic model for a whole wastewater treatment plant because the compounds at the interconnections are common.

Sven Wilhelm Sötemann
Dept. of Civil Engineering
Private Bag
University of Cape Town
Rondebosch 7701
South Africa

August, 2005

SYNOPSIS

MODELLING MATERIAL MASS BALANCES OVER WASTEWATER TREATMENT PLANTS

1. INTRODUCTION

Since the activated sludge system produces the effluent that must comply with legislated effluent criteria, it has been well researched and relatively reliable simple steady state design and complex dynamic simulation models have been developed for it, including biological N and/or P removal. However, little attention has been focussed on modelling the wastewater treatment plant (WWTP) as a whole, where the outflow from one unit operation becomes inflow to downstream or upstream unit operations. The interconnection of individual unit operations of a WWTP means that design and operation optimisation of one unit operation can have unexpected and often unforseen consequences on the performance of both upstream and downstream unit operations, and hence on the WWTP performance as a whole. For example, the recycling of nutrient rich liquors from sludge treatment unit operations to the activated sludge system has a significant impact on the WWTP effluent quality (e.g. Pitman *et al.*, 1991; Wild and Siegrist, 1999), contributing up to 25% of the total N load to the activated sludge system (Janus and van der Roest, 1997).

Accordingly, this thesis project was initiated with the overall objective of working towards developing mass balance models for the entire WWTP. A WWTP mass balances model would have to ensure that materials of importance in any of the individual unit operations are included, so that materials are common at the interconnections between unit operations. The four main links between common unit operations of WWTPs are (i) the primary settling tank - anaerobic digester link, (ii) the activated sludge - aerobic digester link, (iii) the activated sludge system - anaerobic digester link and (iv) the primary settler - aerobic digester link. This may require modelling of parameters in an individual unit operation that may not be of significance to that unit operation, but these parameters may be crucial to a unit operation that receives the output. Unit operations in which transformations of the materials take place and hence to be modelled, are primary sedimentation, biological wastewater treatment in activated sludge systems, including or excluding biological N and P removal, aerobic and anaerobic stabilization of primary and secondary sludges and generic sludge thickening.

Development of materials mass balance models for the entire WWTP require that steady state and dynamic simulation models be developed for those unit operations where these are not available or inadequate. In these developments the main focus is on the unit operations that are not simply physical separations (e.g. settling tanks, dissolved air flotation), but include biologically mediated transformations. In assessing the level of modelling of the various unit operations, one unit operation immediately apparent to require modelling development was that of anaerobic digestion of sewage sludges. Steady state and dynamic simulation modelling of even the biologically mediated reactions in this unit operation has not progressed to the same extent

as for activated sludge. Hence, this was identified as a priority in this thesis project.

2. RESEARCH OBJECTIVES AND AIMS

The overall objective of whole WWTP modelling is to develop a COD (electron), carbon (C), nitrogen (N), phosphorus (P), alkalinity (proton), calcium (Ca) and magnesium (Mg) and inorganic suspended solids (ISS) concentrations mass balances model for unit operations in municipal WWTPs comprising primary sedimentation, secondary treatment with activated sludge and aerobic and anaerobic sludge stabilization of primary (PS) and secondary (waste activated, WAS) sludges. The development of such a model for both steady state and dynamic simulation conditions, is an objective greater than this thesis project. However, this thesis project has a number of significant steps towards this greater objective, viz.

(i) Set up a simple mass balances (COD, N and P) WWTP steady state and kinetic simulation models (UCTOLD) including prediction of the inorganic suspended solids concentration for WWTPs comprising primary sedimentation, anoxic acrobic activated sludge and aerobic digestion of primary and waste activated sludge. Compare and verify kinetic model with the steady state model calculations.

(ii) Extend the activated sludge simulation model (ASM1) to incorporate pH as a predictive parameter and validate against literature data. The extension of ASM1 requires incorporating chemical (weak acid/base aqueous chemistry) and physical (gas exchange) processes and integrating these with the biological processes. These extensions are restricted to acrobic and anoxic/acrobic C and N removal activated sludge systems.

(iii) Integrate the biological processes of anaerobic digestion into a 2 phase (aqueous-gas) version of the chemical physical processes model developed by Musvoto *et al.* (1997, 2000) to construct a mass balances (COD, C, N, O, H) based integrated chemical physical biological processes model capable of predicting digester pH (UCTADM1) and verify it with laboratory and literature data.

(iv) Simplify UCTADM1 into a steady state model for initial design of AD systems and integration into the steady state WWTP model.

(v) Apply the 3 phase (aqueous-gas-solid) mixed weak acid/base chemical physical processes kinetic model for including multiple mineral precipitation of calcium, magnesium phosphate and carbonate based minerals to aeration treatment of swinery wastewater and sewage sludge anaerobic digester liquor to evaluate the feasibility of producing 3 phase mixed weak acid/base chemical, physical and biological processes models for activated sludge and anaerobic digestion.

In the development of these models, requirements were (i) that they should be as far as possible combinations of the existing biological models and the mixed weak acid/base chemistry so that the chemical physical processes within which the biological processes take place are modelled as well as the biological processes themselves, (ii) that the integration between the biological and chemical physical processes is seamless with the hydrogen ion (i.e. pH) being modelled as a process compound like all the others, and (iii) that the models of the different unit operations such as N removal activated sludge, anaerobic digestion, primary sedimentation etc. can be readily combined to form a mass balances based kinetic model for the entire wastewater treatment plant.

3. STEADY STATE MASS BALANCES WWTP MODEL

A steady state WWTP mass balances (COD, N and P) spreadsheet program was developed. This steady state mass balances spreadsheet is capable of:

(i) **Wastewater characterization:**
From the given (measured) concentrations and component fractions, it characterizes the raw and settled wastewaters and primary sludge COD, TKN, FSA, TP and OP, each into their unbiodegradable and biodegradable soluble and particulate components from mass balances around the PST.

(ii) **Activated sludge system design:**
It calculates the design parameters for the fully aerobic, nitrification denitrification (ND) or ND biological excess P removal (BEPR) activated sludge systems treating the raw and settled WW at long and short sludge ages respectively, i.e. volume of reactor, average and peak oxygen demand, effluent COD, TKN, FSA, TP and OP concentrations as well as waste activated sludge (WAS) flow and composition.

(iii) **Aerobic digester design:**
It calculates the design parameters for a single reactor aerobic digester by taking the PS and WAS (excluding BEPR) flows and concentrations (including the liquid stream), blending and concentrating them to the selected thickened concentrations and aerobically digesting the blended and thickened sludge to a selected residual biodegradable organic content, taking due account in N and P released during digestion. It calculates the digester volume, oxygen demand and effluent concentrations, and checks material mass balances (COD, N and P), all for the minimum (T_{min}) and maximum (T_{max}) temperatures.

(iv) **Mass balance checks:**
It checks and compares the COD, N and P mass balances around the WWTP comprising (1) raw WW treatment in a long sludge age AS system, where the sludge age is selected long enough for sludge stabilization in the reactor and direct discharge of WAS to drying beds (i.e. extended aeration), and (2) PST's, short sludge aged activated sludge system, PS and WAS thickening and aerobic digestion of PS and WAS to the same residual biodegradable organics as (1) above (see Fig 1 below). The concentrations of COD (and oxygen demand), N and P in the effluent streams for the AS systems, the thickening units and the aerobic digester are added and balance to within 0.5% of the influent raw wastewater COD, TKN and TP for both T_{min} and T_{max} temperatures. The carbonaceous oxygen utilised in the raw WW system (AS only), and in the settled WW system (AS and aerobic digester) are within 0.5%.

(v) **Comparison with simulation results:**
An Activated Sludge Model No 1 (ASM1, Henze *et al.*, 1985) Aquasim (Reichert, 1998) dynamic simulation model was set up for the raw and settled WW treatment plants above, including thickening and aerobic digestion of PS and WAS (Fig 1). For both systems, the simulation model gives virtually identical results for all the AS and aerobic digestion effluent COD, TKN, FSA, TP, OP, VSS, ISS and TSS concentrations from both systems. There is therefore close correlation between the far more complex dynamic simulation

WWTP model in which ASM1 is used to model the AS and aerobic digester systems and the much simpler steady state model programmed into the spreadsheet described here.

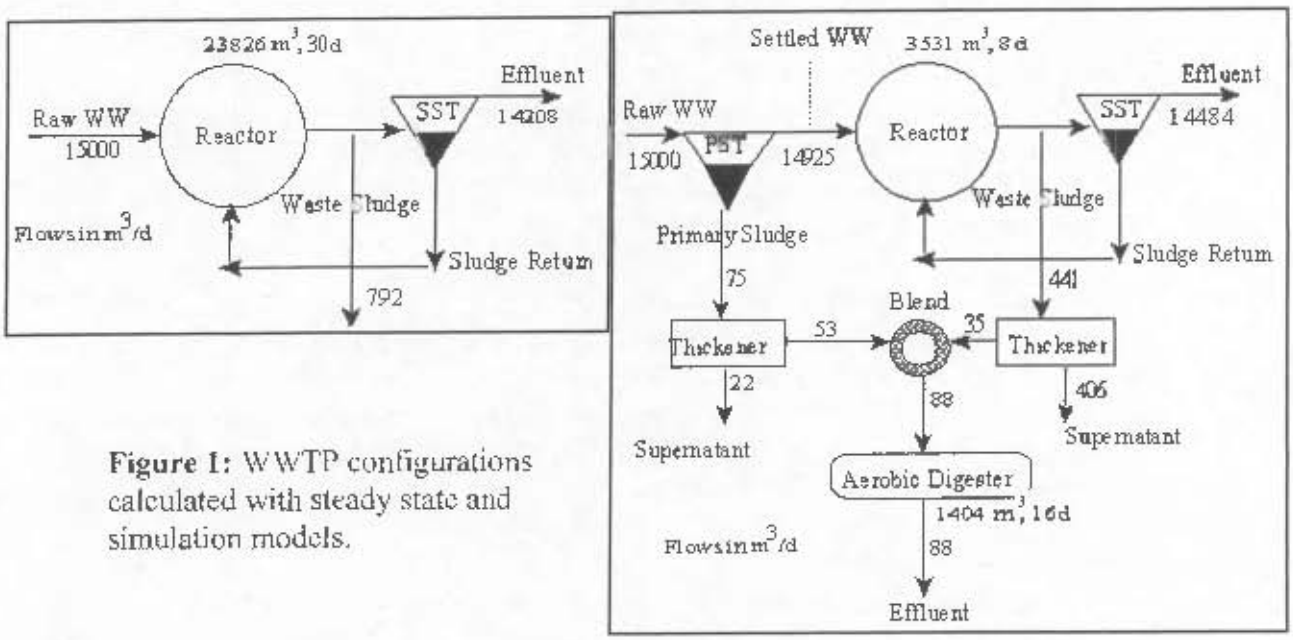

Figure 1: WWTP configurations calculated with steady state and simulation models.

4. INTEGRATED BIOLOGICAL, CHEMICAL AND PHYSICAL PROCESSES KINETIC MODELLING: ANOXIC-AEROBIC C AND N REMOVAL IN THE ACTIVATED SLUDGE SYSTEM

The biological kinetic model ASM1 for carbon (C) and nitrogen (N) removal was integrated with the mixed weak acid/base model of Musvoto *et al.* (1997, 2000) to extend the application of ASM1 to situations where an estimate for pH is important. Because chemical precipitation is generally not significant when treating municipal wastewaters for C and N removal, only gas and liquid phase processes were considered for this integrated model. However, the approach will facilitate ready integration of chemical precipitation processes if required. The biological processes in ASM1 were modified to take into account the effect of the interaction of the weak acid/base species of the ammonia, carbonate and phosphate systems and pH with heterotrophic and autotrophic organism behaviour, which includes generation and utilization CO_2 in metabolism, use of specific weak acid/base species for organism growth and generation and utilization of H^+. With these modifications, simulations with the model were compared with those of ASM1 and experimental data in the literature and a good correlation was obtained. However, these comparisons are only a preliminary validation, because, despite their inclusion, the weak acid/bases and pH do not have a significant effect on the biological processes in the cases considered (i.e. well buffered wastewater). A difficulty in calibrating this model was selection of the oxygen mass transfer coefficient (K_La) value for the aeration system, which affects the pH in the anoxic and aerobic reactors through CO_2 gas exchange. Aerobic reactor outflows from two full-scale wastewater treatment plants with fine bubble aeration systems were found to be around 20% supersaturated with CO_2, whereas simulations indicated higher levels of super-saturation. The performance of a ND activated sludge system with decreasing influent

alkalinity was also evaluated. The developed model extends application of activated sludge simulation models to situations where pH prediction is of importance such as treatment of low alkalinity wastewaters or wastewaters with high N concentrations. This model produces the outputs required for the models of the other unit operations in the WWTP, such as anaerobic digestion of WAS and is therefore an important first step towards modelling the entire wastewater treatment plant because it is central to two important links in a wastewater treatment plant: (i) The activated sludge - anaerobic digester link and (ii) the activated sludge - aerobic digester link.

5. INTEGRATED CHEMICAL/PHYSICAL AND BIOLOGICAL PROCESSES MODELLING: ANAEROBIC DIGESTION OF SEWAGE SLUDGES

A two phase (aqueous-gas) integrated mixed weak acid/base chemistry, physical and biological processes kinetic model for anaerobic digestion (AD) of sewage sludge was developed and validated. The biological kinetic processes for AD are integrated into a two phase subset of the three phase mixed weak acid/base chemistry kinetic model of Musvoto *et al.* (1997, 2000). The approach of characterising sewage sludge into carbohydrates, lipids and proteins, as is done in the International Water Association (IWA) AD model No 1 (ADM1), requires measurements that are not routinely available on sewage sludges. Instead, the sewage sludge is characterized with the COD, carbon, hydrogen, oxygen and nitrogen (CHON) composition. The model is formulated in mole units, based on conservation of C, N, O, H and COD. The model is calibrated and validated with data (Izzett *et al.*, 1992) from laboratory mesophilic anaerobic digesters operating from 7 to 20 days sludge age and fed a sewage primary and humus sludge mixture. These digesters yielded COD mass balances between 107-109% and N mass balances between 91-99%, and hence the experimental data are accepted as reasonable. The sewage sludge is found to be 64 - 68% biodegradable (depending on the kinetic formulation selected for the hydrolysis process) and to have a $C_{3.5}H_7O_2N_{0.196}$ composition. For the selected hydrolysis kinetics of surface mediated reaction (Contois), with a single set of kinetic and stoichiometric constants, for all retention times good correlation is obtained between predicted and measured results for (i) effluent COD concentration, (ii) gas production, (iii) gas composition, (iv) effluent free and saline ammonia (FSA) and (v) alkalinity concentrations and (vi) digester pH (Fig 2). The measured composition of primary sludge from two local wastewater treatment plants ranged between $C_{3.38}H_7O_{1.91}N_{0.21}$ and $C_{3.91}H_7O_{2.04}N_{0.16}$. The predicted composition is therefore within 5% of the average measured composition providing persuasive validation of the model.

The model was also applied to laboratory scale methanogenic anaerobic digesters operating from 5 to 60 days sludge age and fed a 'pure' primary sludge (Ristow *et al.*, 2004a). These digesters yielded COD mass balances between 90-110% and N mass balances between 80-113%, and the primary sludge was found to be 66.5% biodegradable. In total, 4 different batches of primary sludge (feed batches 12, 13, 14 and 15) were fed to the experimental systems over the duration of the investigation, and the compositions were found to be $C_{4.15}H_7O_{2.41}N_{0.22}$, $C_{4.17}H_7O_{2.63}N_{0.22}$, $C_{4.31}H_7O_{3.03}N_{0.24}$ and $C_{4.06}H_7O_{2.43}N_{0.19}$ respectively. The digester feed concentrations ranged between 9 and 42 gCOD/ℓ. For the saturation type hydrolysis kinetics (Contois) with a single set of kinetic and stoichiometric constants calculated by Ristow *et al.* (2004a), good correlation is obtained between predicted and measured results, except for the lower (<8 day, see Fig. 3) retention time digesters. Fig 3 shows the predicted and measured results for the systems that were fed influent COD concentrations between 9 and 13 gCOD/ℓ.

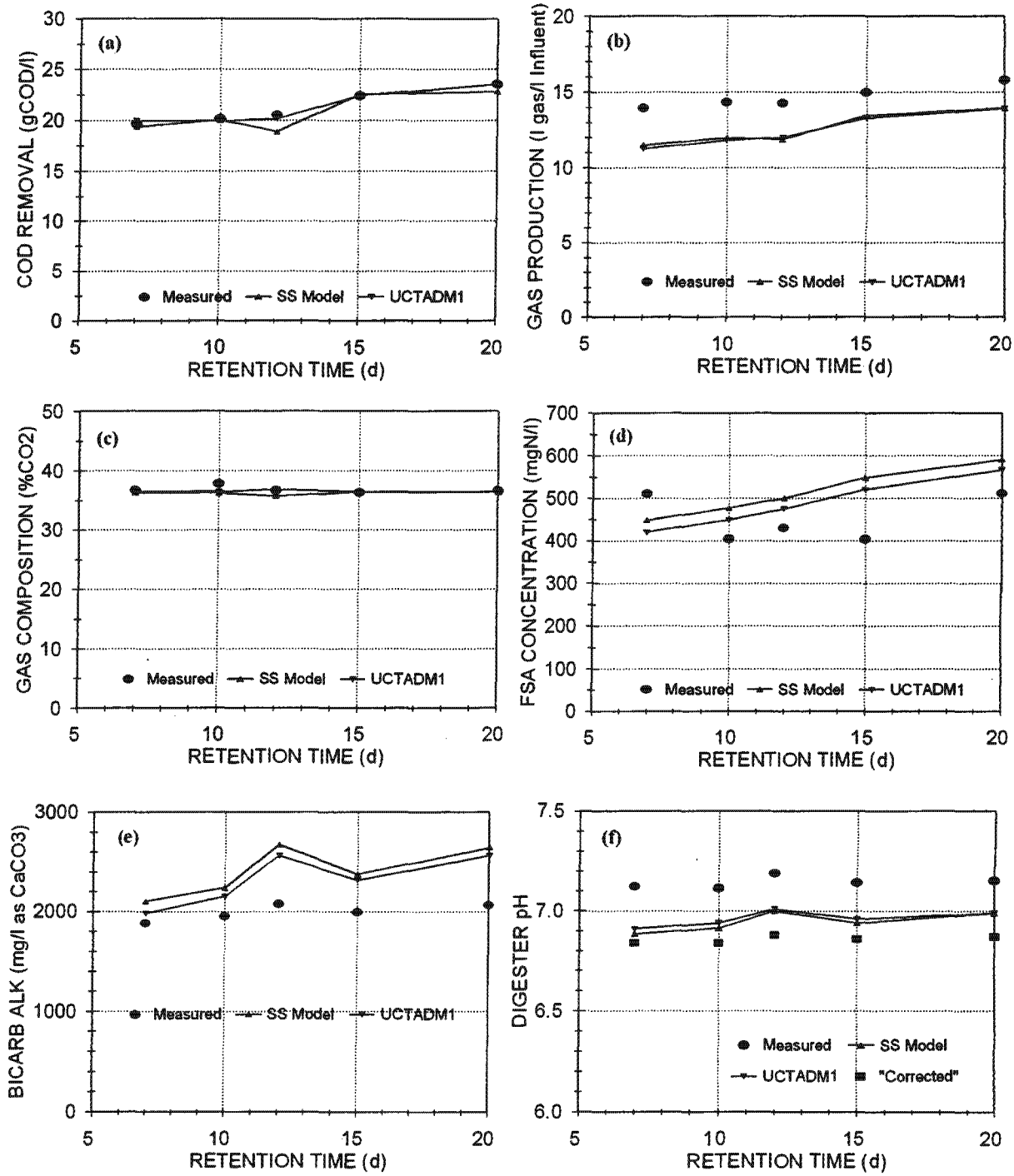

Fig 2: Comparison between kinetic simulation model (UCTADM1) predicted (lines) and measured (points) (a) COD removal, (b) gas production, (c) gas composition, (d) free and saline ammonia, (e) $H_2CO_3^*$ alkalinity and (f) digester pH versus retention time for the Izzett *et al.* (1992) data set; also shown are the predictions of the steady state AD model.

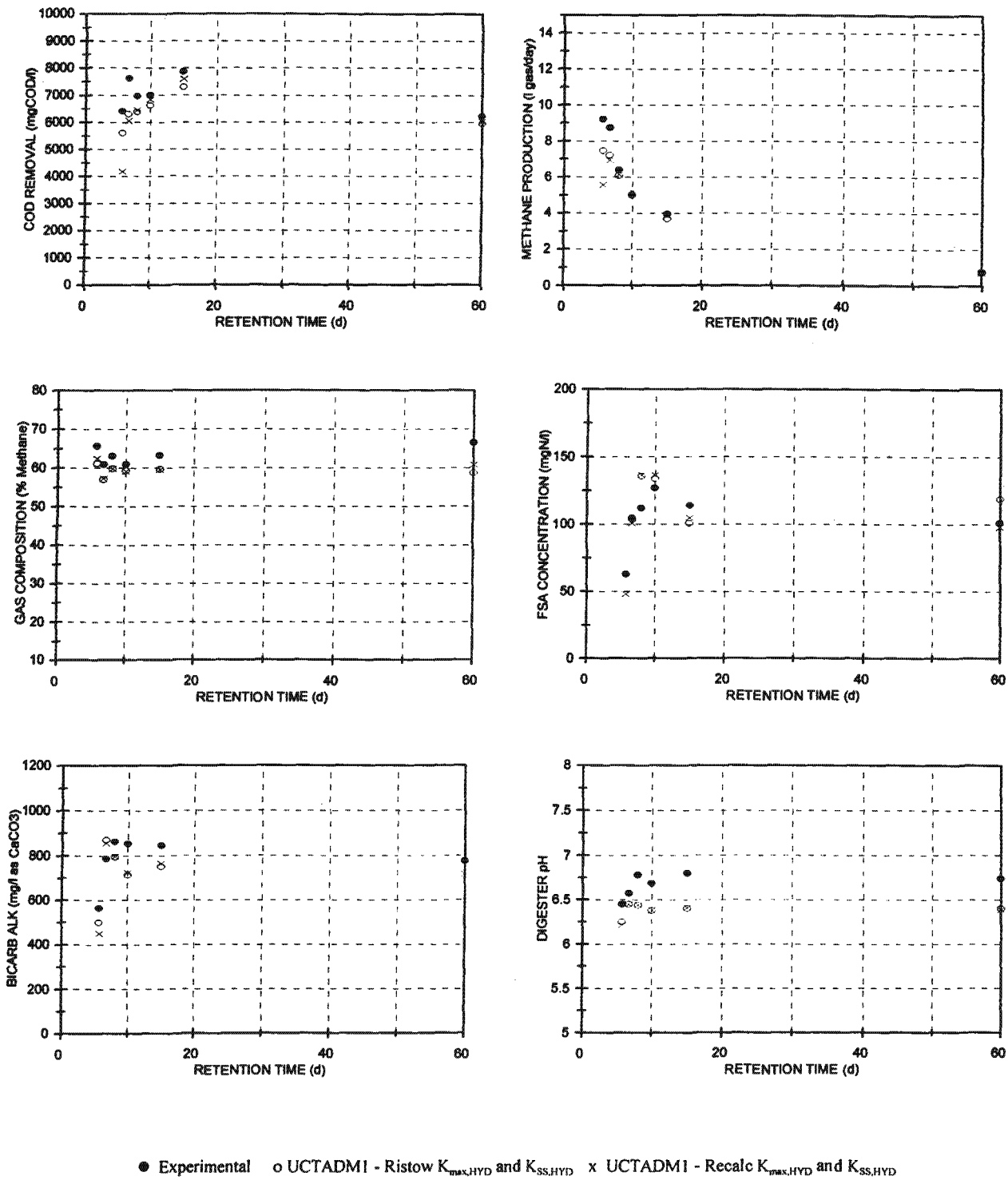

Fig 3: Comparison between kinetic simulation model (UCTADM1) predicted and measured (a) COD removal, (b) gas production, (c) gas composition, (d) free and saline ammonia, (e) $H_2CO_3^*$ alkalinity and (f) digester pH versus retention time for the Ristow *et al.* (2004a) data set for feed COD concentrations between 9 and 13 gCOD/*ℓ*.

Because of the lower correlation between the predicted and measured results at low (<8d) retention times, the hydrolysis rate constants were re-calculated to ascertain whether a different set of hydrolysis rate constants would better predict the low retention time systems. When re-calculating the hydrolysis rate constants, it was not possible to obtain hydrolysis rate constants that resulted in better predictions because of considerable scatter in the data. It was found that many different combinations of hydrolysis rate constants could be chosen without improvement in the model predictions. Therefore, the predicted results show some deviation from the experimental results. This is due to the scatter in the experimental data and not a reflection on the model, indeed, the predicted results on the whole correlate well with the experimental results.

The developed anaerobic digestion model can serve as a stand alone model for simulation of anaerobic digesters treating primary sludges, or can be integrated into a dynamic simulation model for the entire WWTP.

6. A STEADY STATE MODEL FOR ANAEROBIC DIGESTION OF SEWAGE SLUDGES

A steady state model for anaerobic digestion of sewage sludge was developed from the complex simulation one that comprises three sequential parts - (i) a kinetic part from which the % COD removal and methane production are determined for a given retention time, (ii) a stoichiometry part from which the gas composition (or partial pressure of CO_2), ammonia released and alkalinity generated are calculated from the %COD removal and (iii) a carbonate system weak acid/base chemistry part from which the digester pH is calculated from the partial pressure of CO_2 and alkalinity generated. From the stoichiometry and weak acid/base chemistry parts of the model, for a given % COD removal, the digester gas composition, ammonia released, alkalinity generated and digester pH are completely defined by the influent (i) sludge composition, i.e. X, Y, Z and A in $C_XH_YO_ZN_A$ of the hydrolysable organics, (ii) volatile fatty acid (VFA) concentration and (iii) pH. For the kinetic part of the model, four hydrolysis kinetic equations were calibrated against 7 to 60 day retention time anaerobic digesters treating two different sewage sludge types, viz. (i) first order, (ii) first order specific, (iii) Monod and (iv) Contois (saturation). Once calibrated against the two sludge type data sets and taking into account experimental error in effluent COD concentrations and gas productions (i.e. COD mass balance error), each of the four hydrolysis kinetic equations predicted the % COD removal versus retention time equally well, and predicted COD removal and methane production compared well with measured data. For the different sewage sludge types, viz. (i) a primary and humus sludge mixture from a trickling filter plant and (ii) a 'pure' primary sludge, different kinetic rate constants were obtained indicating that the 'pure' primary sludge hydrolysed faster and had a lower unbiodegradable particulate COD fraction ($f_{PS'up}$ = 0.33) than the primary and humus sludge mixture (0.36). With the %COD removal known from the hydrolysis part of the model, and again taking experimental error into account (i.e. C and N mass balances error), the stoichiometry and weak acid/base chemistry parts of the model predicted the gas composition, effluent free and saline ammonia (FSA) concentration, alkalinity generated and digester pH well for a primary and humus sludge composition of $C_{3.5}H_7O_2N_{0.196}$ (Fig 2). From independent measurement of primary sludge CHON composition, this model estimated composition is within 96%, 100%, 95% and 99% of the average measured composition of $C_{3.65}H_7O_{1.97}N_{0.190}$ lending strong support to the developed steady state model. This steady state anaerobic digestion model will be an invaluable aid for the design of anaerobic digesters treating sewage sludges. Further,

the model can be readily integrated into the steady state mass balances model for the entire WWTP, which is still to be completed.

7. MODELLING PHYSICAL CHEMICAL PROCESS IN 3 PHASES - TOWARDS INCORPORATING THE SOLID PHASE IN THE KINETIC MODEL FOR ANAEROBIC DIGESTION (UCTADM1)

In previous research (Musvoto *et al.*, 2002) a three phase (aqueous/gas/solid) mixed weak acid/base chemistry kinetic model was developed. This model formed the framework for the activated sludge and anaerobic digestion kinetic modelling in this project. Accordingly, to further validate this model, it was applied to evaluate the processes operative in the aeration treatment of swine wastewater (SWW) and sewage sludge anaerobic digester liquor (ADL). In both applications, with a single set of constants (except for the aeration rates which are situation specific), close correlation could be obtained between predicted and measured calcium magnesium phosphate, FSA, total inorganic carbon (C_T) concentrations and pH versus time, except for the Ca concentration-time profile in the SWW. For this wastewater, the model application highlighted an inconsistency in the measured Ca data which could not be resolved. This illustrates the value of a mass balance based model in evaluating experimental data. From the model applications, in both wastewaters the dominant minerals precipitating are struvite and amorphous calcium phosphate (ACP), which precipitate simultaneously competing for the same species, P. The absolute and relative masses of the two precipitants are governed by the initial solution state (e.g. C_T, Mg, Ca and P concentrations), their relative precipitation rates (struvite > ACP) and the system conditions imposed (aeration rates and time applied). It is concluded that the 3 phase mixed kinetic model is able to correctly predict the time dependent weak acid/base chemistry reactions and final equilibrium state (in terms of the duration of the experimental batch tests, <48h) for situations where multiple minerals competing for the same species precipitate simultaneously or sequentially, a deficiency in traditional equilibrium chemistry based algebraic models. This indicated that the approach developed for mixed phase and process modelling of mineral precipitation is suitable for integration into any of the kinetic models of unit processes developed here, where mineral precipitation may be of interest, e.g. the anaerobic model.

8. CONCLUSIONS AND FURTHER RESEARCH

This thesis project made some significant advances towards developing mass balances based integrated WWTP models for steady state and diurnal flow and load conditions which links primary sedimentation, activated sludge and aerobic or anaerobic digestion of primary and waste activated sludges. The most significant of these are development of (i) the two phase mixed weak acid/base chemical, physical and biological processes simulation model for anaerobic digestion (AD) of primary sludge (PS) and (ii) the steady state simplification of the two phase AD model.

In further research, the four main links between common unit operations of WWTPs need to be considered further, using the mass balances based steady state models for the activated sludge system and aerobic and anaerobic digestion: (i) the primary settling tank (PST) - anaerobic digester (AD) link, (ii) the activated sludge (AS) system - aerobic digester link, (iii) the AS system - AD link and (iv) the PST - aerobic digester link. Attention should also be given to biological N and P removal AS systems and where required, steady state models developed or extended for unit operations in which the biological processes dominate (e.g. N and P removal

activated sludge, aerobic digestion and anaerobic digestion), to allow integrated design of the different unit operations making up the WWTP. Unit operations in which physical processes dominate, such as primary sedimentation, sludge thickening before and dewatering after sludge digestion should be regarded as solid/liquid separators and solids concentrators only. Several complex issues which require further experimental research remain around aerobic and anaerobic digestion of activated sludge including the polyphosphate accumulating organisms (PAOs), and these biological excess phosphorus removal (BEPR) activated sludge systems also need to be considered.

To develop a steady state and kinetic model for the entire wastewater treatment plant, the following require further work:

Steady state WWTP model:

(i) The steady state anaerobic digestion model needs to be incorporated into the steady state WWTP mass balances tracking model developed so far. This would require that the inputs for the AD model (i.e. the feed sludge characteristics) be included in the upstream unit operations. In addition to the parameters already in the mass balances model, this would include C, alkalinity, and possibly SCFA production in the PST. Also, and very importantly, it needs to be established whether or not the unbiodegradable particulate organic material from the influent wastewater, and that generated in the activated sludge reactor (endogenous residue) as defined by the activated sludge (aerobic) system, are unbiodegradable also under anaerobic digester conditions. Some models have assumed these organics to remain unbiodegradable in anaerobic digesters, but this has not been experimentally proven.

(ii) Recycling of various liquors (e.g. sludge thickening liquors) from downstream unit operations to upstream ones, and the characteristics of these recycle stream would have to be included.

(iii) The steady state mass balances WWTP model needs to be extended to include biological P removal. This is not a simple task. In the activated sludge system, the ordinary heterotrophic (OHO) and polyphosphate accumulating (PAO) organisms have different endogenous respiration/die off rates, the former high (b_{H20} = 0.24 /d at 20 °C) and the latter low (b_{G20} = 0.04 /d at 20°C). These b rates influence the rates at which the nutrients N and P bound in the cell mass are released in aerobic (and anaerobic) digestion. The release rates of N and P from the cell bound phase to the dissolved phase under aerobic and anaerobic digestion conditions also needs to be investigated.

Kinetic WWTP model:

(i) The integrated biological, chemical and physical processes kinetic model for C and N removal in the activated sludge system should be extended to include biological P removal. This would require research into the interaction of the biological aspects of the polyphosphate accumulating organisms with the aquatic chemistry of the bulk liquid - as was done for the heterotrophic and autotrophic organisms in the kinetic C and N removal model.

(ii) The integrated biological, chemical and physical process kinetic model for anaerobic digestion should be extended to include P, for anaerobic digestion of biological N and P

removal waste activated sludge.

(iii) Once P has been included in the kinetic anaerobic model, the solid phase should be integrated to enable the kinetic anaerobic model to predict multiple mineral precipitation, which would be helpful in the design and operation of anaerobic digesters.

(iv) Even though multiple mineral precipitation is not expected to occur in activated sludge systems, the compounds for multiple mineral precipitation should be included in the kinetic activated sludge model, because in a wastewater treatment plant, its output (e.g. WAS) may become input to an anaerobic digester, where mineral precipitation is important.

TABLE OF CONTENT

PUBLICATIONS LIST

Publications to date (August 2005) of the writer of this thesis:

MSc:

Journal Papers Published

Vermande SM, Sötemann SW, Aguilera Soriano G, Wentzel MC, Audic JM and Ekama GA (2002) Comparison of aerobic and anoxic phosphorus uptake in NDBEPR systems (UCT and ENBNRAS). Wat. Sci. Tech., 46(4/5) 201-207.

Hu Z-R, Sötemann SW, Moodley R, Wentzel MC and Ekama GA (2003) Experimental investigation on the external nitrification biological nutrient removal activated sludge (ENBNRAS) system. Biotech & Bioeng, 83(3) 260-273.

Sötemann SW, Vermande SM, Wentzel MC and Ekama GA (2003) Comparison of the performance of an external nitrification biological nutrient removal activated sludge system with a UCT biological nutrient removal activated sludge system. Water SA, WISA 2002 Edn 105-113.

Conference Papers Presented

Söteman SW, Vermande S, Wentzel MC and Ekama GA (2002) Comparison of aerobic and anoxic -aerobic P uptake BEPR in BNR systems. Procs 7th WISA Biennial conference 19-23 May Durban, ISBN 1-86845-844-X, Paper 029.

Reports

Sötemann SW, Wentzel MC and Ekama GA (2000) External nitrification in biological nutrient removal activated sludge systems. Research Report W101, Dept. of Civil Eng., Univ of Cape Town, Rondebosch, 7701, RSA.

Hu Z, Sötemann SW, Vermande SM, Moodley R, Little C, Lakay MT, Wentzel MC and Ekama GA (2002) External nitrification with the aid of fixed media trickling filters (TF) to increase the capacity of biological nutrient removal (BNR) activated sludge (AS) systems - Final report to the Water Research Commission on contract K5/970, UCT Report W109, WRC Report 970/1/02, Water Research Commission, Private Bag X03, Gezina, 0031, RSA.

PhD:

Jornal Papers Accepted

Sötemann SW, Musvoto EV, Wentzel MC and Ekama GA (2005), Integrated biological, chemical and physical processes kinetic modelling Part 1 - Anoxic and aerobic processes of carbon and nitrogen removal in the activated sludge system. Water SA, 31(4) (Accepted).

Sötemann SW, van Rensburg P, Ristow NE, Wentzel MC, Loewenthal RE and Ekama GA (2005) Integrated biological, chemical and physical processes kinetic modelling Part 2 - Anaerobic digestion of sewage sludges. Water SA, 31(4) (Accepted).

Sötemann SW, Ristow NE, Wentzel MC and Ekama GA (2005) A Steady state model for anaerobic digestion of sewage sludge. Water SA, 31(4) (Accepted).

Journal Papaers Submitted

Wentzel MC, Ekama GA and Sötemann SW (2005) Mass balances based whole wastewater treatment plant models - Part 1: Biodegradability of wastewater organics under anaerobic conditions. Water SA (Submitted).

Ekama GA, Wentzel MC and Sötemann SW (2005) Mass balances based whole wastewater treatment plant models - Part 2: Tracking the influent inorganic suspended solids. Water SA (Submitted).

Ekama GA, Sötemann SW and Wentzel MC (2005) Mass balances based whole wastewater treatment plant models - Part 3: Biodegradability of activated sludge organics under anaerobic conditions. Water SA (Submitted).

Sötemann SW, Wentzel MC and Ekama GA (2005) Mass balances based whole wastewater treatment plant models - Part 4: Aerobic digestion of primary and waste activated sludges. Water SA (Submitted).

Conference Papers Presented

Ristow NE, Sötemann SW, Wentzel MC, Ekama GA and Loewenthal RE (2004) Considerations for the use of primary sewage sludge and sulfate-reducing bacteria for the treatment of sulfate-rich wastes. Procs. 8th biennial WISA conference and exhibition, Cape Town, 2-6 May, 1533-1541, CD-ROM ISBN 1-920-01728-3.

Sötemann SW, Musvoto EV, Wentzel MC and Ekama GA (2004) Integrated biological, chemical and physical processes kinetic modelling Part 1 - Anoxic and aerobic processes of carbon and nitrogen removal in the activated sludge system. Procs. 8th biennial WISA conference and exhibition, Cape Town, 2-6 May, 1044-1062, CD-ROM ISBN 1-920-01728-3.

Sötemann SW, van Rensburg P, Ristow NE, Wentzel MC, Loewenthal RE and Ekama GA (2004) Integrated biological, chemical and physical processes kinetic modelling Part 2 - Anaerobic digestion of sewage sludges. Procs. 8th biennial WISA conference and exhibition, Cape Town, 2-6 May, 1327-1344, CD-ROM ISBN 1-920-01728-3.

Ristow NE, Sötemann SW, Wentzel MC, Loewenthal RE and Ekama GA (2004) The effects of hydraulic retention time and feed COD concentration on the hydrolysis rate of primary sewage sludge. Procs Anaerobic digestion 2004 - 10th World Congress - Anaerobic

Bioconversion for Sustainability, Montreal, 29 Aug - 2 Sep., Vol 2, 629-635.

Sötemann SW, Ristow NE, van Rensburg P, Wentzel MC, Loewenthal RE and Ekama GA (2004) Integrated biological, chemical and physical processes kinetic model for anaerobic digestion of sewage sludge. Procs. Anaerobic digestion 2004 - 10th World Congress - Anaerobic Bioconversion for Sustainability, Montreal, 29 Aug - 2 Sep., Vol 3, 1416-1420.

Loewenthal RE, Sötemann SW, Wentzel MC and Ekama GA (2004) Three phase mixed weak acid/base chemistry kinetic modelling of multiple mineral precipitation problems. Procs. CEFIC-CEEP International conference on Struvite: Its role in phosphorus recovery and reuse. Cranfield, UK, 17-18 June.

Sötemann SW, Ristow NE, Wentzel MC and Ekama GA (2005) A steady state mass balances model for anaerobic digestion of organic wastes. IWA/WISA specialized conference on management of residues emanating from water and wastewater treatment, Johannesburg, 9-12 Aug.

Sötemann SW, van Rensburg P, Ristow NE, Wentzel MC, Loewenthal RE and Ekama GA (2005) Integrated chemical, physical and biological processes modelling of anaerobic digestion of sewage sludge. IWA/WISA specialized conference on management of residues emanating from water and wastewater treatment, Johannesburg, 9-12 Aug.

Ristow NE, Sötemann SW, Wentzel MC, Loewenthal RE and Ekama GA (2005) The effects of hydraulic retention time and feed COD concentration on the hydrolysis rate of primary sewage sludge. IWA/WISA specialized conference on management of residues emanating from water and wastewater treatment, Johannesburg, 9-12 Aug.

Conference Papaers Accepted

Sötemann SW, Ristow NE, Wentzel MC and Ekama GA (2005) Characterization of sewage sludge with a mass balance based steady state model for anaerobic digestion. 1st International Workshop on Anaerobic Digestion Model No 1, Copenhagen, 4-6 Sept.

Reports

Ristow NE, Sötemann SW, Loewenthal RE, Wentzel MC and Ekama GA (2004) Hydrolysis of primary sewage sludge under methanogenic, acidogenic and sulfate-reducing conditions. Final WRC Report on K5/1216, Water Research Commssion, PO Box X03, Gezina, 0033, Pretoria.

Sötemann SW, Ristow NE, Loewenthal RE, Wentzel MC and Ekama (2005) Material mass balances and modelling of wastewater treatment plants. WRC Report on K5/1338/1/05, Water Research Commission, PO Box X03, Gezina, 0033, Pretoria.

LIST OF SYMBOLS AND ABBREVIATIONS

Abbreviation	Description
Ac	Acetate
ACP	Amorphous calcium phosphate
AD	Anaerobic digestion
ADL	Anaerobic digester liquor
Alk	Alkalinity
ADM1	Anaerobic digester model No. 1
ADWF	Average dry weather flow
ANO	Autotrophic nitrifier organism
AS	Activated sludge
ASM1	Activated Sludge Model No. 1
ASM2	Activated Sludge Model No. 2
ATP	Adenosine triphosphate
BEPR	Biological excess phosphorus removal
BNR	Biological nutrient removal
C	Carbon
Ca	Calcium
CED	Chemical equilibrium dissociation
CF	Cape Flats
CIP	Chemical ion pairing
COD	Chemical oxygen demand
CP	Chemical / physical
CPB	Chemical / physical / biological
DO	Dissolved oxygen
FA	Fully aerobic
FSA	Free and saline ammonia
Fe	Iron
H	Hydrogen
HAc	Acetic acid
HAP	Hydroxyapatite
HPr	Propionic acid
IDS	Inorganic dissolved solids
ISS	Inert suspended solids
IWA	International Water Association
K	Potassium
Mg	Magnesium
MLE	Modified Ludzack Ettinger
MW	Molecular weight
N	Nitrogen
Na	Sodium
ND	Nitrifying / denitrifying
O	Oxygen
OHO	Ordinary heterotrophic organism

oP	Ortho phosphorus
OrgN	Organic nitrogen
OrgP	Organic phosphorus
OTR	Oxygen transfer rate
OUR	Oxygen utilisation rate
P	Phosphorus
PAO	Polyphosphate accumulating organism
PGE	Physical gas exchange
PMP	Physical mineral precipitation
Pr	Propionate
PS	Primary sludge
PST	Primary settling tank
Q	Flow
R	Hydraulic retention time or sludge age for anaerobic digester
RBCOD	Readily biodegradable COD
SBCOD	Slowly biodegradable COD
SBR	Sequencing batch reactor
SCFA	Short chain fatty acid
SS	Settleable solids
SSADL	Blended PS and WAS digester liquor
SST	Secondary settling tank
SWW	Swine wastewater
T	Temperature
TDS	Total dissolved solids
TKN	Total Kjeldahl nitrogen
TOC	Total organic carbon
TP	Total phosphorus
TSS	Total suspended solids
UASB	Upflow anaerobic sludge bed
UASBDL	Upflow anaerobic sludge bed digester liquor
UCT	University of Cape Town
UCTADM1	University of Cape Town anaerobic digester model1
V	Volume
VFA	Volatile fatty acid
VSS	Volatile suspended solids
WAS	Waste activated sludge
WRC	Water Research Commission
WW	Wastewater
WWTP	Wastewater treatment plant

Symbol	Description
b	Death rate
C_{hsgas}	Head space gas concentration
C_T	Total inorganic carbon
C_{var}	Coefficient of variation
E	Fraction of hydrolysed COD utilised that is converted to biomass
f_{ave}	Effluent active fraction
f_{cv}	COD/VSS ratio
f_{cvPS}	Primary sludge COD/VSS ratio
$f_{e,H}$	Fraction of the active mass that is unbiodegradable in endogenous respiration
f_{iOHO}	Inorganic content of ordinary heterotrophic organisms
f_{iPAO}	Inorganic content of polyphosphate accumulating organisms
f_{iPS}	VSS/TSS ratio of primary sludge
f_m	Monovalent ion activity coefficient
f_n	TKN/VSS ratio of organisms
f_{nPS}	TKN/VSS ratio of primary sludge
f_p	TP/VSS ratio of organisms
f_{pPS}	TP/VSS ratio of primary sludge
f_{psr}	Fraction of COD removed by primary sedimentation
$f_{PS'up}$	Fraction of unbiodegradable COD in the primary sludge
$f_{Sb's}$	Influent RBCOD fraction with respect to the biodegradable COD
$f_{S'up}$	Particulate unbiodegradable COD fraction
$f_{S'us}$	Soluble unbiodegradable COD fraction
f_{tsr}	Fraction solids removal in terms of TSS
f_{vsr}	Fraction solids removal in terms of VSS
f_{XBGP}	Phosphorus content of PAOs
f_{xm}	Unaerated sludge mass fraction
$f_{ZB,N}$	N content of the OHOs
$f_{ZB,P}$	P content of the OHOs
H_c	Dimensionless Henry's law constant
k_G	Gas phase individual mass transfer coefficient
K_h	First order hydrolysis rate constant
K_H	First order specific hydrolysis rate constant
K_I	Inhibition constant (hydrogen ion concentration at which the growth of acetoclastic methanogens is half the normal rate
k_L	Liquid phase individual mass transfer coefficient
K_{La}	Overall liquid phase mass transfer rate coefficient
$k_{max,HYD}$	Maximum specific hydrolysis rate
K_{ppt}	Mineral precipitation rate constant
K_{ra}	Weak acid/base kinetic rate constant
K_{rG}	Gas stripping rate constant
K_{rIP}	Ion pair kinetic rate constant
K_S	Half saturation coefficient
μ_A	ANO maximum specific growth rate
μ_{max}	Maximum specific growth rate

N_{obsi}	Influent organic biodegradable soluble N
P_{atm}	Atmospheric pressure
ρ_{CO2}	Partial pressure of CO_2
ρ_{H2}	Partial pressure of hydrogen
ρ_{N2}	Partial pressure of nitrogen
ρ_{O2}	Partial pressure of oxygen
pK	Weak acid/base equilibrium constant
pK_{ST}	Ion pair kinetic rate constant
P_T	Total phosphorus
P_{tot}	Total gas pressure in head space
q_{gas}	Vent gas flow rate from the head space
Q_{gas}	Total gas production
Q_i	Influent flow
r_h	Volumetric hydrolysis/acidogenesis rate
R_h	Hydraulic retention time
R_{hn}	Nominal hydraulic retention time
R_s	Sludge age
R_{sm}	Minimum sludge age for nitrification
r_{ZAC}	Growth rate of acetogens
r_{ZAD}	Growth rate of acidogens
r_{ZAM}	Growth rate of acetoclastic methanogens
r_{ZHM}	Growth rate of hydrogenotrophic methanogens
R^2	Correlation coefficient
S_{bp}	Biodegradable particulate organics concentration
S_{bpi}	Influent biodegradable particulate organics concentration
S_{bpr}	Biodegradable COD removal
S_{bs}	Biodegradable soluble COD concentration
S_{bsi}	Influent biodegradable soluble COD concentration
S_{bsa}	Soluble COD that is SCFA concentration
S_{bsai}	Influent soluble COD that is SCFA concentration
S_{bsACi}	Influent acetate concentration
S_{bsf}	Soluble COD that is glucose concentration
S_{bsfi}	Influent soluble COD that is glucose concentration
S_{bsHAci}	Influent acetic acid concentration
S_m	Methane concentration
S_{te}	Total effluent COD concentration
S_{ti}	Total influent COD concentration
S_{up}	Unbiodegradable particulate COD concentration
S_{upi}	Influent unbiodegradable particulate COD concentration
Sus	Unbiodegradable soluble COD concentration
S_{usi}	Influent unbiodegradable soluble COD concentration
V_d	Volume of digester
V_r	Volume of reactor
X_{BH}	Heterotrophic active concentration
X_{EH}	Heterotrophic endogenous residue concentration
X_I	Unbiodegradable VSS concentration accumulated in the reactor
X_{Ii}	Influent unbiodegradable VSS concentration

X_{IO}	Accumulated inert suspended solids concentration in the reactor
X_{Ioi}	Influent inert suspended solids concentration
Y_{ZA}	ANO yield coefficient
Y	Yield coefficient
Y_{ZH}	OHO yield coefficient
Y_{ac}	Anabolic yield of acetogens
Y_{ad}	Anabolic yield of acidogens
Y_{am}	Anabolic yield of acetoclastic methanogens
Y_{AC}	True acetogen yield
Y_{AD}	True acidogen yield
Y_{AM}	True acetoclastic methanogen yield
Y_h	Heterotrophic yield
Y_{hm}	Anabolic yield of hydrogenotrophic methanogens
Y_{HM}	True hydrogenotrophic methanogen yield
Z_{AC}	Growth of acetogenic organisms
Z_{AD}	Growth of acidogenic organisms
Z_{AM}	Growth of acetoclastic methanogenic organisms
Z_{HM}	Growth of hydrogenotrophic methanogenic organisms

Note: Only symbols and abbreviations used in the text are included, those in equations are defined below the appropriate equations.

CHAPTER 1

INTRODUCTION

1.1 BACKGROUND

To aid the design and operation of, and research into conventional biological wastewater treatment systems, a variety of mathematical models have been developed. With few exceptions, these models have focused almost exclusively on the biologically mediated processes that lead to the removal of, or change in, the particular compounds of interest. For example, models for the activated sludge system have progressively included the biologically mediated processes of COD removal, nitrification, denitrification and biological excess phosphorus removal (Dold *et al.*, 1980; 1991; Van Haandel *et al.*, 1981; Henze *et al.*, 1987; Wentzel *et al.*, 1992; Henze *et al.*, 1995). In this group of models, by focusing on the biological processes usually it is implicitly assumed that: (i) The biological processes dominate the system response and that (ii) chemical and physical processes (e.g. precipitation and gas stripping respectively) play an insignificant role compared to the biological processes and accordingly can be neglected, (iii) compounds not directly involved in the biological processes or not of interest, even though present, do not significantly influence the behaviour, and (iv) the biological processes take place within a regime of constant pH. This has restricted application of these models to situations where the assumptions remain valid. For the activated sludge system treating municipal or similar types of wastewaters, where the concentrations of compounds that cause changes in reactor pH are low relative to the alkalinity of the waste water, these assumptions usually are valid. For example, in the nitrification of municipal wastewaters it usually is reasonable to assume that the biological processes dominate and that there is sufficient buffer capacity present to absorb the generation of hydrogen ions (H^+) and loss of CO_2 so that the pH does remain approximately constant; some of the models have included the parameter 'Alkalinity' to check that this condition is in fact true (e.g. Dold *et al.*, 1991). However, in the treatment of a number of wastewaters the assumptions are not valid and the biological processes based models cannot be applied. For example, in the nitrification of wastewaters with low buffer capacity and/or high N concentrations, or in the treatment of wastewaters where the generation or utilization of short-chain fatty acids (SCFA), e.g. acetic and propionic acid, is significant, the assumption that the pH remains essentially constant can no longer be accepted.

In particular, the models cannot be applied to situations where chemical and physical processes play a significant role and so cannot be neglected, e.g. in anaerobic digestion and in the treatment of low alkalinity municipal wastewater, trickling filter effluents, anaerobic digester liquors, activated sludge dewatering liquors, landfill leachates, septic tank effluents and waste sludge lagoon effluents. For these systems and wastewaters, chemical and physical processes play a significant role and these processes and their interactions with each other and with the biological processes will have to be included in any model of these treatment systems and wastewaters. In other words, a model integrating the biological, physical and chemical processes of importance will be required. Deterministic models that quantitatively describe the stoichiometry and kinetics

of the biological processes are well advanced for the activated sludge system, e.g. IWA Activated Sludge Model No. 1 (ASM1, Henze *et al.*, 1987; Dold *et al.*, 1991) and ASM2 (Henze *et al.*, 1995) and for anaerobic digestion, e.g. IWA Anaerobic Digestion Model No. 1 (ADM1, Batstone et al., 2002). Similar models need to be developed for the chemical and physical processes important in wastewater treatment and integrated with these biological models. Models including chemical and physical processes will require that the pH parameter/compound is incorporated and accurately determined, as pH is of fundamental importance in the chemical/physical processes, significantly influencing them.

From the discussion above, it is evident that application of the existing biological models for waste-water treatment systems can be enhanced by including pH as a parameter/compound. Further, including the pH will facilitate the integration of chemical and physical processes into the biological models and the development of independent physical/chemical models. Including the pH in turn will require that all the weak acid/bases present that influence the pH (e.g. carbonate, SCFA, free and saline ammonia, FSA and phosphate systems) also will have to be included in some fashion. That is, weak acid/base chemistry 'background' in which the biological processes operate needs to be brought to the 'foreground' and must form an integral part of the models. In the development of these models, requirements were (i) that they should be as far as possible combinations of the existing biological models and the mixed weak acid/base chemistry so that the chemical/physical processes within which the biological processes take place are modeled as well as the biological processes themselves, (ii) that the integration between the biological and chemical physical processes is seamless with the hydrogen ion (i.e. pH) being modeled as a process compound like all the others, and (iii) that the models of the different unit operations such as N removal activated sludge, anaerobic digestion, primary sedimentation etc. can be readily combined to form a mass balances based kinetic model for the entire wastewater treatment plant (WWTP).

1.2 TOWARDS DEVELOPING INTEGRATED CHEMICAL, PHYSICAL AND BIOLOGICAL PROCESSES MASS BALANCES MODELS OVER WASTEWATER TREATMENT PLANTS

To aid the design and operation of, and research into conventional biological wastewater treatment systems, a variety of mathematical models have been developed. For these models the primary focus has been on the individual unit operation of the activated sludge system, since this is the unit operation that produces the effluent that must comply with legislated effluent criteria (Wild and Siegrist, 1999). As a consequence the activated sludge system has been well researched and relatively reliable simple steady state design (e.g. WRC, 1984; Wentzel *et al.*, 1990; Maurer and Gujer, 1994) and complex dynamic simulation models (e.g. Dold *et al.*, 1980, 1991; Wentzel *et al.*, 1992; Henze *et al.*, 1987, 1995) have been developed for the system, including biological N and/or P removal, or not. However, little attention has been focussed on modelling the wastewater treatment plant (WWTP) as a whole, in an integrated fashion.

The WWTP comprises a sequence of individual unit operations (e.g. primary settling, activated sludge, anaerobic digestion). These individual unit operations are interconnected through a web of flows: The outputs from upstream unit operations become inputs to downstream unit operations; further, common practise at WWTPs is to recycle various liquors (e.g. sludge thickening and anaerobic digestion supernatants) from downstream unit operations to upstream

ones. This interconnection of individual unit operations means that design and operation optimisation of one unit operation can have unexpected and often unforseen consequences on the performance of both upstream and downstream unit operations, and hence on the WWTP performance as a whole. For example, the recycling of nutrient rich liquors from sludge treatment unit operations to the activated sludge system has a significant impact on the WWTP effluent quality (e.g. Pitman *et al.*, 1991; Wild and Siegrist, 1999), contributing up to 25% of the total N load to the activated sludge system (Janus and van der Roest, 1997).

To assess and quantify the interdependencies of the various unit operations making up the WWTP, models that track materials of importance through the WWTP on a mass balance basis are required. Such models will be termed: Materials mass balance models. Materials mass balance based models of the entire WWTP would be a valuable tool to aid optimisation of WWTP design and performance. Potential advantages of mass balance based models of the entire WWTP are that they allow for design and operation:

(i) Tracking compounds through the WWTP - currently little more than total settleable solids (TSS) is used mostly manually to assess loads and capacities on different unit operations in a WWTP sequence; TSS is not mass conservative and provides no assessment of mass balances and continuity for the sequence of unit operations at the WWTP.
(ii) Identifying characteristics of streams from one unit operation (e.g. primary settling) to a downstream one (e.g. aerobic/anaerobic digestion); this will assist in design and performance assessment and optimisation of the various unit operations in the WWTP.
(iii) Assessing impact of recycling sludge thickening and dewatering liquors from downstream operations on upstream operations.
(iv) Identifying bottlenecks and overloaded unit operations which limit the capacity of the WWTP.
(v) Optimizing unit operations for maximum unit operation throughput and minimum impact on effluent quality and upstream units.
(vi) Assessing the impact of interventions such as including additional unit operations in the sequence like phosphorus precipitation or nitrification of recycling liquors.
(vii) Identifying WWTP operational and analytical data that do not conform to mass balance and continuity principles - from the writers' experience something as basic as flow measurement can have significant errors up to 50% leading to inefficient and uneconomical operation of the WWTP.

A WWTP mass balances model would have to ensure that materials of importance in any of the individual unit operations are included, so that materials are common at the interconnections between unit operations. The four main links between common unit operations of WWTPs are (i) the primary settling tank - anaerobic digester link, (ii) the activated sludge - aerobic digester link, (iii) the activated sludge system - anaerobic digester link and (iv) the primary settler - aerobic digester link. This may require modelling of parameters in an individual unit operation that may not be of significance to that unit operation, but these parameters may be crucial to a unit operation that receives the output. For example, in activated sludge models carbon (C) is not usually included as a compound, but C is of importance in the anaerobic digestion of sewage sludges, because in this unit operation it determines gas production and composition, and influences the pH established through the weak acid/base chemistry (C also becomes important

in the activated sludge system when pH is included, a necessity for a proton balance). Materials identified as of importance and to be included in such a model are: COD (electron), carbon (C), nitrogen (N), phosphorus (P), alkalinity (proton), calcium (Ca) and magnesium (Mg). Also, because of its importance in accepted design procedures for the various unit operations (e.g. secondary settling tanks), the inorganic concentrations were to be included.

Unit operations in which transformations of the materials take place and hence to be modelled in a WWTP mass balances model are primary sedimentation, biological wastewater treatment in activated sludge systems, including or excluding biological N and P removal, aerobic and anaerobic stabilization of primary and secondary sludges and generic sludge thickening. A WWTP model would have to be developed for both steady state and dynamic simulation conditions.

Steady state models are based on the slowest process kinetic rate that governs the overall behaviour of a WWTP unit operation and relates this process rate to the unit operation's design and operating parameters. Therefore, steady state models allow the individual unit operations design and operating parameters, such as reactor volume and recycle ratios, to be estimated reasonably simply and quickly from system performance criteria specified for the design, such as effluent quality. For example, a steady state aerobic or anaerobic digestion model would be useful to (i) estimate retention time, reactor volume, gas production and composition for a required system performance like COD (or VSS) removal (degree of sludge stabilization), (ii) investigate the sensitivity of the system performance to changes in the design and operation parameters, (iii) provide a basis for cross-checking simulation model results, and (iv) estimate product stream concentrations for design and operation of down- (or up-) stream unit operations of the wastewater treatment plant, e.g. assess the impact of ammonia, nitrate or phosphate return with recycling of digestion liquors. Since the outflow(s) from one unit operation become the inflow(s) to downstream and/or upstream unit operations, is makes sense to link the all the selected unit operations and design each unit operation in its integrated context of the entire WWTP for the particular influent wastewater characteristics. Once approximate design and operating parameters are known, these can serve as input to the more complex simulation models to investigate dynamic behaviour of the unit operation and refine the design and operating parameters.

Development of materials mass balance models for the entire WWTP requires that steady state and dynamic simulation models be developed for those unit operations where these are not available or inadequate. In these developments the main focus is on the unit operations that are not simply physical separations (e.g. settling tanks, dissolved air flotation), but include biologically mediated transformations. In assessing the level of modelling of the various unit operations, one unit operation immediately apparent to require intensive modelling effort was that of anaerobic digestion of sewage sludges. Steady state and dynamic simulation modelling of even the biologically mediated reactions in this unit operation had not progressed to the same extent as for activated sludge. Hence, this was identified as a priority in this thesis project report.

To develop models for anaerobic digestion of sewage sludges, the models need to be considerably more complex than existing models for the activated sludge system. In anaerobic digestion, physical processes are of importance in that considerable gas production of CO_2 and methane (CH_4) takes place, and in the digestion of biological P removal sludges, chemical

processes play an important role in that significant precipitation can occur within the digester or in the liquors leaving the digester. This strongly suggested that the models for anaerobic digestion would have to include in addition to the biological processes, chemical and physical processes, and interactions between all these groups of processes. To include chemical and physical processes requires that the pH parameter/compound is incorporated directly in the models and accurately determined, as pH is of fundamental importance in the chemical and physical processes, significantly influencing them. Furthermore, in anaerobic digestion pH itself is a crucial parameter, as the biological processes are particularly pH sensitive, and produce and consume weak acid/base species (e.g. short-chain fatty acids, SCFA) that can significantly influence the pH, i.e. it is no longer reasonable to accept that the biological processes take place within a regime of constant pH. Hence, inclusion of pH directly within the models for anaerobic digestion is fundamental. Including pH will require that all the weak acid/base systems present that influence the pH (e.g. carbonate, SCFA, free and saline ammonia, FSA and phosphate systems) also be included in some fashion, i.e. aqueous chemical processes require inclusion.

Development of steady state and dynamic simulation models for anaerobic digestion requires that the inputs to the digester (i.e. the sewage sludge) be well defined. Accordingly, primary and secondary sewage sludge characterisation require further investigation. In this regard, of particular importance are COD, weak acid/base chemistry and species (and associated pH), and C and N contents of the input. These parameters would have to be predictable in the outputs from upstream unit operations.

In an anaerobic digestion model, the characteristics of the input (i.e. the sludges) are important for reasonable simulations and calculations, including *inter alia* the pH and associated weak acid/base species (e.g. carbonate, ammonia) and C and N contents. The anaerobic digester input is derived in part from the activated sludge unit operation (the secondary sludge), and hence these inputs would need to be predictable parameters in this unit operation: Current activated sludge models do not include these parameters, and hence would have to be extended to include them (see Chapter 1.1). This requires that the physical processes (for CO_2 loss via gas stripping) and pH be incorporated directly in the activated sludge models in some fashion. Initially, this would be restricted to aerobic COD removal and nitrification, and anoxic/aerobic COD removal, nitrification and denitrification activated sludge systems.

In tracking materials through the WWTP, it became apparent that the inorganics were of significance, in that conventional design procedures for a number of the physical separation unit operations are based on total suspended solids (TSS) concentrations which include the inorganics. Reliable steady state design and dynamic simulation predictive models for the organic (volatile) suspended solids (VSS) concentrations in activated sludge systems are available, and a predictive model for the reactor inorganic suspended solids (ISS), and hence the total suspended solids (TSS = VSS + ISS) concentrations has been developed (Ekama and Wentzel, 2004). Accordingly, the inorganic material (and hence TSS) must be incorporated into the models.

1.3 RESEARCH APPROACH AND THESIS LAYOUT

The development of a mass balances based (COD, C, N and P) steady state and dynamic simulation models for an entire WWTP system, including aerobic and anaerobic digestion of waste sludge, is an objective greater than this thesis project. However, this thesis project takes a number of significant steps towards this higher objective, viz.

(i) Set up a simple mass balances (COD, N and P) WWTP steady state and kinetic simulation models (UCTOLD) with primary sedimentation, anoxic aerobic activated sludge and aerobic digestion of primary and waste activated sludge. Compare and verify kinetic model with the steady state model calculations (Chapter 2).

(ii) Extend the activated sludge simulation model (ASM1) to incorporate pH as a predictive parameter and validate against literature data. The extension of ASM1 requires incorporating chemical (weak acid/base aqueous chemistry) and physical (gas exchange) processes and integrating these with the biological processes. These extensions are restricted to aerobic and anoxic/aerobic activated sludge systems. (Chapter 3).

(iii) Integrate the biological processes of anaerobic digestion into a 2 phase (aqueous-gas) version of the chemical physical processes model developed by Musvoto *et al.* (1997, 2000) to construct a mass balances (COD, C, N, O, H) based integrated chemical physical biological processes model capable of predicting digester pH (UCTADM1) and verify it with laboratory and literature data (Chapter 4).

(iv) Simplify UCTADM1 into a steady state model for initial design of AD systems and integration into the steady state WWTP model (Chapter 5).

(v) Review 3 phase (aqueous-gas-solid) mixed weak acid/base chemical physical processes for inclusion of multiple mineral precipitation of calcium, magnesium phosphate and carbonate based minerals in the kinetic models developed above.

In the development of these models, requirements were (i) that they should be as far as possible combinations of the existing biological models and the mixed weak acid/base chemistry so that the chemical physical processes within which the biological processes take place are modelled as well as the biological processes themselves, (ii) that the integration between the biological and chemical/physical processes is seamless with the hydrogen ion (i.e. pH) being modelled as a process compound like all the others, and (iii) that the models of the different unit operations such as N removal activated sludge, anaerobic digestion, primary sedimentation etc. can be readily combined to form a mass balances based kinetic model for the entire wastewater treatment plant. Details of these developments are presented in the subsequent Chapters as indicated above.

Instead of presenting a combined literature review for the whole thesis project, the literature review is split up and a literature review relating to the content of each Chapter is included with each respective Chapter. This was done because a different model is developed in each Chapter and the literature reviewed does not necessarily relate to any of the other Chapters and therefore would not form a coherent combined literature review.

CHAPTER 2

THE STEADY STATE MASS BALANCES MODEL AND SINGLE (AQUEOUS) PHASE BIOLOGICAL KINETIC MODEL

2.1 INTRODUCTION

Steady state models are relatively simple (stoichiometric) models that utilise constant flows and loads as input to determine the system design parameters. They are based on the slowest process kinetic rate that governs the overall behaviour of the system and relate this process rate to the system design and operating parameters. Therefore a steady state model allows the system design and operating parameters (e.g. reactor volumes, sludge recycle ratios) to be estimated reasonably simply and quickly from the performance criteria for the design, such as effluent quality. For example, for an activated sludge system steady state model the sludge age, wastewater characteristics and average dry weather flow as well as summer/winter temperatures are required as input. From this input the steady state model generates the following information:

(i) Mass of organism, endogenous residue, inorganic and inert material contained in the reactor(s) as a function of COD load and sludge age and hence the
(ii) required reactor volume(s) for a chosen sludge age and reactor TSS concentration.
(iii) Daily sludge production.
(iv) Effluent COD, TKN, FSA, nitrate, total P and ortho-P concentrations.
(v) System carbonaceous and nitrification oxygen requirements.

Individual unit operations in wastewater treatment such as the activated sludge (AS) system have been thoroughly investigated in earlier research and relatively reliable simple steady state models for the system, including biological N and/or P removal, have been developed over the past years. However, little attention has been focussed on the WWTP as a whole in an integrated fashion, where the outputs of the upstream unit processes of the WWTP become inputs to the downstream unit operations based on material mass balances around the sequence of unit operations. Of course in WWTP design, such an integrated approach has been followed by designers but this is done either manually or with very simple mass balance spreadsheets of only a few material components (COD, TSS and perhaps N and P) without due recognition of the interrelationships and changes between the materials.

Therefore an integrated materials mass balance steady state model for the entire wastewater treatment plant comprising:

(i) Primary sedimentation.

(ii) Activated sludge in- or excluding nitrification, denitrification and/or biological excess P removal (BEPR).

(iii) Waste activated sludge (secondary) and/or primary sludge thickening.

(iv) Aerobic and/or anaerobic treatment of primary and/or secondary sludge.

Including COD, TKN, and total P (TP), each in their biodegradable and unbiodegradable and dissolved and particulate forms as well as free and saline ammonia (FSA), dissolved ortho P (OP), nitrate and alkalinity (Alk) will help define for design and operation:

(i) The correct relationship between the raw (unsettled) and settled wastewater characteristics and the composition of the primary sludge (eg % biodegradable materials formed in primary settling tanks). Currently raw and settled wastewater and primary sludge characteristics are selected based on experience which are often inconsistent with mass balances. A correct estimate of the % biodegradable material in the primary sludge is required for design of the primary sludge treatment system whether it be aerobic or anaerobic digestion.

(ii) The concentrations of the input materials COD, VSS, TKN, FSA, OrgN, TP, OP and Alk to the anaerobic digester model (if selected) from the primary and/or secondary sludge characteristics. From the transformations in the anaerobic digester (from a simplified steady state model derived from the complex kinetic one described in Chapter 4, see Chapter 5), the gas volume and composition, heat requirements and generation, %COD and VSS removal and concentrations of mineral precipitation during or after digestion can be predicted.

(iii) The expected loads on the various unit operations of the sequence from estimated loads on the WWTP and the operating conditions in the upstream unit operations. This will help to find bottlenecks, i.e. unit operations which limit the capacity of the WWTP under different organic and hydraulic loading conditions.

2.2 LITERATURE REVIEW

2.2.1 The Activated Sludge Process - Steady State Behaviour

Marais and Ekama (1976) developed a steady state model (carbonaceous material removal and nitrification) which sets out the procedures for the design of the activated sludge process. A review of the steady state model (Marais and Ekama, 1976) is given below.

2.2.1.1 Biological growth kinetics

Marais and Ekama (1976) replaced the BOD_5 as a measure of energy with the COD, because the standardization of the COD test, the short time necessary for the test, the relative ease with which it can be automated and its direct link with the energy in the water provided sufficient incentive for them. They fractionated the influent COD flow into four fractions: The total influent COD (S_o), the biodegradable COD (S_i), the unbiodegradable soluble (S_u) and the unbiodegradable particulate (S_{xii}) COD.

They described the biological growth kinetics on which their steady state model is based as

follows: When a biodegradable substrate (biodegradable COD) is introduced into the bulk liquid, the organism mass removes the biodegradable COD from the bulk liquid and stores it, i.e. the biodegradable substrate is adsorbed onto the cell walls of the organisms. This stored biodegradable COD is utilized by the organisms as energy source for synthesis of new organism mass (anabolism) by (i) incorporating a fraction of the energy into their cell mass and (ii) utilizing the remaining fraction as energy to produce the new cell mass (this energy is lost as heat) with an associated oxygen demand (the associated oxygen demand is directly proportional to the oxygen utilized). A further process that occurs together with, but distinct from the anabolic processes is the process of catabolism. Catabolism is described as the loss of organism mass to provide energy for organism cell maintenance and is termed endogenous respiration. A fraction of the live organism mass remains as an unbiodegradable organic (termed endogenous residue) and the remaining fraction is utilized to provide the energy for cell maintenance. A proportional mass of oxygen (proportional to the biodegradable fraction of the organism utilized for cell maintenance) is required and must be supplied. In order to quantify this model, Marais and Ekama (1976) had to ascertain (i) at what rate the biodegradable substrate is removed from the bulk liquid, (ii) what fraction of, and at what rate is the biodegradable substrate incorporated as cell mass and (iii) what is the rate of endogenous respiration is?

Monod derived an empirical relationship that relates the concentration of nutrient surrounding the organisms with the rate of mass growth of the organism:

$$\frac{dX_{a1}}{dt} = \mu X_a \tag{2.1}$$

$$\text{where } \mu = \frac{\mu_m S_b}{(K_S + S_b)} \tag{2.2}$$

X_a = concentration of organism (1 denoting a specific organism) in mg VSS /ℓ
μ = specific growth rate at concentration S
μ_m = maximum specific growth rate for the specific organism, substrate and condition
K_S = substrate concentration at which $\mu = 0.5\mu_m$ (mgCOD/ℓ)
S_b = concentration of biodegradable substrate (energy) in mgCOD /ℓ.

It was experimentally proven that Monod's relationship is not valid for the period after a step change in nutrient concentration occurred, because it was observed that for a period after the step change in the nutrient concentration, the organisms continued to remove the nutrient at the same rate as before the step change was introduced. The rate then increased gradually to a new steady state level, as the organisms developed additional adsorption sites. It was concluded that under steady state conditions, Monod's rate function is valid, because the rate of COD utilization is generally lower than the adsorption rate constant, i.e. with a constant COD concentration in the bulk liquid, the adsorption rate increases until it equals the rate of utilization of the stored COD. Accepting that Monod's relationship was valid under steady state conditions, Marais and Ekama (1976) derived the following equations to give a quantitative description of organism growth:

The organism mass synthesized with respect to the mass of energy utilized (dS_b) is given by:

$$dX_{a1} = Y_h dS_b \tag{2.3}$$

where Y_h = growth yield coefficient (mass of organisms synthesized per unit mass substrate utilized) in mgVSS/mgCOD utilized.

Substituting for dX_{a1} from Equation 2.3, then Equation 2.1 can be rewritten relating dS/dt to the growth rate to derive a form widely used in activated sludge treatment kinetics:

$$\frac{dS_b}{dt} = \frac{K_m S_b}{K_S + S_b} X_a \tag{2.4}$$

where $K_m = \mu_m / Y_h$.

For the endogenous respiration process, Marais and Ekama (1976) derived the following:

Per unit of time, the nett loss due to endogenous respiration is proportional to the active mass in the bulk liquid, and therefore the rate of change of the active mass due to endogenous respiration can be written as:

$$\frac{dX_{a2}}{dt} = - b_h X_a \tag{2.5}$$

where b_h = specific endogenous respiration rate (mgVSS/mgVSS.d)
2 = denotes the live mass lost in endogenous respiration.

Only 80% of the active organism mass that is used for endogenous respiration is biodegradable, 20% remains as unbiodegradable endogenous residue. Hence the fraction remaining as endogenous residue:

$$\frac{dX_e}{dt} = -\frac{dX_{a2}}{dt} f = f b_h X_a \tag{2.6}$$

where f = fraction of active mass remaining as endogenous residue.

Therefore the mass of the active organisms that is biodegradable under endogenous respiration can be written as $(1-f)b_h X_a$.

2.2.1.2 Process kinetics

In the activated sludge system, the system design and operating parameters (e.g. the mixing regime, the sludge recycle ratios) influence the behaviour and the response of the system, hence consideration must be given to the reactor kinetics. Marais and Ekama (1976) believed that an understanding of the kinetic behaviour of the completely mixed system is basic to modelling the process over a range of mixing regimes from plug flow to completely mixed.

They derived equations for steady state solutions for the completely mixed activated sludge process after establishing what parameters needed to be determined:

(i) Active mass: The nett live mass resulting from the growth (increase in mass) of organisms and the loss of organism mass due to endogenous respiration.
(ii) Endogenous residue mass: The 20% of the active organism mass that is unbiodegradable under endogenous respiration.
(iii) Inert mass: Accumulation of unbiodegradable volatile solids from the influent when the sludge age is longer than the hydraulic retention time.
(iv) Oxygen consumption: The organisms require oxygen for synthesis, endogenous respiration and nitrification. This oxygen requirement has to be met for optimum nutrient removal.

Marais and Ekama (1976) defined the reactor sludge age (R_s) as:

$$Rs = \frac{\text{mass of sludge in reactor}}{\text{mass of sludge wasted per day}} \tag{2.7}$$

To obtain the required sludge age, sludge is drawn directly from the reactor, so that the reactor and waste concentrations are the same. The constant draw off for any desired sludge age can be calculated from:

$$Rs = \frac{V}{q} \tag{2.8}$$

where V = volume of the reactor
q = waste sludge flow rate.

To derive equations for each of the parameters that need to be determined (see above), Marais and Ekama (1976) performed mass balances (i.e. $dX_a/dt = 0$) on the (i) active organism mass, (ii) endogenous residue (iii) substrate (S_b) and (iv) inert volatile solids to derive the five equations that form the basis for the design of an activated sludge plant:

$$S = \frac{1 + b_h Rs}{Y_h K Rs} \tag{2.9}$$

which defines the effluent quality,

$$X_e = 0.2 b_h X_a Rs \tag{2.10}$$

$$X_a = \frac{Y_h(S_{bi} - S_b)}{1 + b_h Rs} \frac{Rs}{R_h} \tag{2.11}$$

$$X_i = X_{ii} \cdot \frac{R_h S_b}{R_h} \qquad (2.12)$$

which define the endogenous residue, active organism and inert concentrations respectively, and

$$dO/day = (1-1.42Y_h)\frac{(S_{bi}-S_b)}{R_h} + 1.42 \cdot 0.8 \cdot b_h \cdot X_a \quad (\text{per } \ell \text{ reactor volume}) \qquad (2.13)$$

where S_{bi} = initial substrate concentration
R_h = hydraulic retention time
X_{ii} = influent inert concentration

which defines the oxygen demand. Marais and Ekama (1976) stated that greater insight into the process behaviour is obtained by considering the masses of X_a, X_e, S_{bi}, S_b and O, rather than their concentrations. The mass parameters are obtained by multiplying the concentrations by the reactor volume (for X_a, X_e X_i and X_o) or the influent flow (for S_{bi}). By multiplying each side of Equations 2.10, 2.11 and 2.12 by the reactor volume V, and noting that that $R_h = V/Q$, these equations can be expressed in mass parameters. With the mass of active organisms (MX_a), endogenous residue (MX_e), inert material (MX_i) and oxygen required (MO) known, the total volatile solids mass (MX_v) is the sum of the active organism mass, the endogenous residue and the inert volatile solids. The volume of reactor required can then be calculated from the value specified for the VSS concentration (X_v) by:

$$V = \frac{MX_v}{X_v} \qquad (2.14)$$

and the hydraulic retention time (R) is determined from the flow per day, by dividing the reactor volume by the influent flow. From the above equations , Marais and Ekama (1976) derived a number of equivalent forms and functional inter-relationships that are relevant for the design of an activated sludge system.

2.2.1.3 Nitrification

Marais and Ekama (1976) included nitrification in their steady state model. Nitrification is the biological process whereby free and saline ammonia is converted to nitrites and nitrates in a two step process: Two autotrophic bacteria groups mediate the process of nitrification, the *Nitrosomonas* convert the free and saline ammonia to nitrite, and the *Nitrobacter* convert the nitrite to nitrate. The *Nitrosomonas* represent the rate limiting bacteria group, because they are slower than the *Nitrobacter*. Consequently it is not necessary to model nitrification as a two step process, it is sufficient to model the rate limiting organism group (the *Nitrosomonas*) because it can be assumed that all the nitrite produced by the *Nitrosomonas* will rapidly be converted by the faster *Nitrobacters*.

Marais and Ekama (1976) modelled the growth of the autotrophs in conformity with the growth of ordinary heterotrophic organisms (see above):

$$\frac{dX_n}{dt} = \mu_n X_n = \left(\frac{\mu_{nm} N_a}{K_n + N_a}\right) X_n \qquad (2.15)$$

where X_n = concentration of Nitrosomonas (mg/ℓ)
μ_n = growth rate of Nitrosomonas (mg/mg.d)
μ_{nm} = maximum specific growth rate (mg/mg.d)
K_n = concentration of free and saline ammonia where $\mu = 0.5\mu_{nm}$
N_a = concentration of free and saline ammonia (mg/ℓ)

They assumed that the endogenous respiration rate for the autotrophic organisms is so low, that it can be neglected. Therefore, they included no endogenous respiration process for the autotrophic organisms. They performed a mass balance on X_n, neglecting endogenous respiration and derived the following equation:

$$\frac{1}{Rs} = \frac{\mu_{nm} N_a}{K_n + N_a} \qquad (2.16)$$

They plotted a graph of Equation 2.16 and showed that as the sludge age is reduced, the free and saline ammonia concentration in the reactor increases until it is equal to that in the influent flow. Any further reduction of the sludge age would cause the autotrophic organisms to be washed out of the system and nitrification would cease. Substituting $N_a = N_{ai}$(influent) in Equation 2.16 gives the minimum sludge age necessary for nitrification to occur in the system:

$$\frac{1}{R_{sm}} = \frac{\mu_{nm} N_{ai}}{N_{ai}} = \mu_{nm}, \text{ or } R_{sm} = \frac{1}{\mu_{nm}} \qquad (2.17)$$

Dissolved oxygen is a prerequisite for nitrification. Nitrification requires greater surety of oxygen supply than that for COD removal, because the ordinary heterotrophs adsorb their substrate and can therefore store it until an oxygen supply is available again. In contrast, nitrification ceases as soon as the oxygen drops below a critical level. The oxygen demand for nitrification is simply 4.57 mgO/mgN times the concentration (or mass) of nitrate produced per day.

2.2.1.4 Steady state aerobic digestion

Aerobic digestion was also included in the steady state model of Marais and Ekama (1976). They stated that two problems are faced when designing an aerobic digester: (i) What are the active and inert masses in the digester influent, (ii) at what rate does the active mass reduce and (3) what is the oxygen demand?

Waste activated sludge entering an aerobic digester contains inert material and active organism mass. During aerobic digestion, the inert fraction of the influent remains unchanged, however the active fraction reduces due to endogenous respiration, generating an oxygen demand and unbiodegradable settleable solids (see above). Marais and Ekama (1976) assumed that the active mass degrades according to Eq. 2.5 and a fraction, f (see above) remains as unbiodegradable particulate material in accordance with Eq. 2.6. They defined the sludge mass by its volatile settleable solids (VSS) instead of by its total settleable solids (TSS) because they argued that the VSS/TSS ratio changes, particularly if nitrification occurs. They defined:

X_a = active solids concentration (mgVSS/ℓ)
X_I = inert solids concentration (mgVSS/ℓ)
X_e = endogenous residue (unbiodegradable particulate) concentration (mgVSS/ℓ)
X_v = total solids concentration = Xa+Xe+XI (mgVSS/ℓ)
i,t = subscripts referring to influent and time respectively
f = fraction of active mass that is unbiodegradable particulate
b_h = endogenous respiration rate (mgVASS/mgVASS.d)

Usually aerobic digesters are of the flow through completely mixed type, i.e. $R_h = R_s$. For aerobic digestion in a completely mixed single reactor Marais and Ekama (1976) developed the following model by doing mass balances over the reactor for active endogenous and inert masses:

$$\frac{dX_a}{dt} = \frac{dX_{ai}}{R_h} - \frac{X_a}{R_h} - b_h X_a \qquad (2.18)$$

At steady state, $dX_a/dt = 0$ and

$$X_a = \frac{X_{ai}}{1 + b_h R_h} \qquad (2.19)$$

Similarly, for the endogenous residue and the inert mass, at steady state:

$$X_e = f b_h X_a R_h = f(X_{ai} - X_a) \qquad (2.20)$$

$$X_I = X_{ii} \qquad (2.21)$$

The total inert mass in the effluent from the digester, X_{if} is then:

$$X_{if} = X_{ii} + X_e = X_{ii} + f(X_{ai} - X_a) \qquad (2.22)$$

The total volatile mass in the effluent, X_{vf} is:

$$X_{vf} = X_{if} + X_a \qquad (2.23)$$

Oxygen is required for the oxidation of the carbonaceous material plus nitrification, and Marais and Ekama (1976) give the total oxygen demand as:

$$\frac{MO_T}{d} = 1.42(1 - f) b_h M X_a + 4.6 \cdot f_n (1 - f) b_h M X_a \qquad (2.24)$$

where f_n = N content of the active organism mass (mgNH_3-N/mgVSS)
4.6 = oxygen requirement for nitrification of 1 mg NH_3-N (mg)

Eq. 2.24 represents the carbonaceous oxygen demand plus the nitification oxygen demand to give the total oxygen required for the aerobic digestion process.

2.2.1.5 Closure

Since Marais and Ekama (1976) developed the steady state model described above, the process of denitrification (van Haandel *et al.*, 1981) and the processes of biological phosphorus removal (Wentzel *et al.*, 1990) have been added to the steady state model, to form a complete carbonaceous material removal, nitrification, denitrification and biological excess phosphorus removal steady state model. This steady state model formed the basis of the steady state mass balances spreadsheet discussed in this Chapter.

2.2.2 A Model for Calculating the Reactor Inorganic Suspended Solids Concentration in Activated Sludge Systems

Ekama and Wentzel (2004) developed a model for inorganic material in activated sludge systems. They reasoned that many steady state and dynamic simulation models for the volatile suspended solids (VSS) in activated sludge systems had been developed, however models for the reactor inorganic solids (ISS) and total suspended solids (TSS = VSS + ISS) had not been developed. They noted that estimates of the TSS concentrations are of importance because the TSS concentration influences the design and operation of down stream unit operations, e.g. secondary settling tanks and sludge treatment systems such as aerobic and anaerobic digestion. Further, the VSS is not mass conservative through a wastewater treatment system, and hence mass balances on VSS cannot be performed. The influent ISS, however, should be mass conservative because they are inorganic and do not take part in any biological or chemical reactions and therefore a mass balance on the ISS can be performed. Therefore Ekama and Wentzel (2004) developed a predictive model for the ISS concentration in the activated sludge reactor, excluding the ISS from chemical precipitant dosing. In this model, the ISS is conceptualized as the sum of inorganics from the influent and that form in the TSS test procedure, i.e. it is based on the influent ISS that accumulates in the activated sludge reactor and on an uptake of inorganic dissolved solids (IDS) by heterotrophic organisms. The uptake of IDS by the heterotrophic organisms has been included because the active organisms retain water inside their cell walls (intracellular or bound water) which contains IDS that precipitates as ISS in the test drying step and so will reflect in the TSS concentration obtained from a TSS test.

The Ekama and Wentzel (2004) conceptual ISS model is therefore based on the following: The influent ISS (X_{Ioi}) accumulates in the reactor proportionally to the sludge age and inversely proportional to the nominal hydraulic retention time (from mass balance principles). Precipitation of minerals as well as the dissolution of influent ISS are considered negligible and it is assumed that slowly biodegradable particulate organic material does not contain ISS. Further, Ekama and Wentzel (2004) include IDS taken up by ordinary heterotrophic (OHOs) and phosphate accumulating organisms (PAOs) as part of their intra-cellular cell mass, which precipitates as inorganic solids when dried and incinerated in the TSS test procedure. Autotrophic organisms are assumed to contribute negligibly to the intra-cellular IDS, because they make up less than 2% of the total active mass in a reactor. In addition to the intra-cellular IDS described above, PAOs take up additional IDS which is stored as polyphosphate with the associated counter ions. Lastly, unbiodegradable particulate organic material, including endogenous residue, is assumed to contain no inorganic material. After integrating the above concepts into the Wentzel *et al.* (1990) steady state nitrification/denitrification biological excess phosphorus removal model, Ekama and Wentzel (2004) give the masses of VSS, ISS and TSS in an activated sludge reactor as:

$$\frac{MX_v}{MS_{ti}} = (1 - f_{S'us} - f_{S'up})\left[\left(1 - \frac{\%}{100} f_{Sb's}\right)\frac{Y_H R_s}{(1 + b_{HT} R_s)}(1 + f_{EH} b_{HT} R_s)\right.$$

$$+\frac{\%}{100}f_{Sb's}\frac{Y_G R_s}{(1+b_{GT}R_s)}(1+f_{EG}b_{GT}R_s)]+\frac{f_{S'up}}{f_{cv}}R_s \quad \text{kgVSS/(kgCOD load/d)} \qquad (2.25)$$

$$\frac{MX_{Io}}{MS_{ti}}=(1-f_{S'us}-f_{S'up})\left[(1-\frac{\%}{100}f_{Sb's})\frac{Y_H R_s}{(1+b_{HT}R_s)}f_{iOHO}+\frac{\%}{100}f_{Sb's}\frac{Y_G R_s}{(1+b_{GT}R_s)}f_{iPAO}\right]+\frac{X_{Ioi}}{S_{ti}}R_s$$

kgISS/(kgCOD load/d) (2.26)

$$\frac{MX_t}{MS_{ti}}=(1-f_{S'us}-f_{S'up})[(1-\frac{\%}{100}f_{Sb's})\frac{Y_H R_s}{(1+b_{HT}R_s)}(1+f_{EH}b_{HT}R_s+f_{iOHO})$$

$$+\frac{\%}{100}f_{Sb's}\frac{Y_G R_s}{(1+b_{GT}R_s)}(1+f_{EG}b_{GT}R_s+f_{iPAO})]+[\frac{f_{S'up}}{f_{cv}}+\frac{X_{Ioi}}{S_{ti}}]R_s \quad \text{kgTSS/(kgCOD load/d)} \qquad (2.27)$$

$$f_i = \frac{MX_v}{MX_t} \quad \text{kgVSS/kgTSS} \qquad (2.28)$$

where

b_{HT}, b_{GT}	=	endogenous respiration rate for OHOs and PAOs at T °C
	=	0.24/d and 0.04/d respectively at 20°C (θ_b = 1.029 for both)
f_{cv}	=	COD/VSS ratio of organics = 1.48 mgCOD/mgVSS
f_{EH}, f_{EG}	=	endogenous residue fraction of the OHOs and PAOs
	=	0.20 and 0.25 respectively
f_i	=	VSS/TSS ratio of reactor sludge mass
f_{iOHO}	=	inorganic content of OHO cell mass = 0.15 mgISS/mgOHOVSS
f_{iPAO}	=	total inorganic solids content of PAOs (mgISS/mgPAOVSS)
$f_{S'up}$	=	influent unbiodegradable particulate COD fraction
$f_{S'us}$	=	influent unbiodegradable soluble COD fraction
$f_{Sb's}$	=	influent readily biodegradable (RB)COD fraction with respect to biodegradable COD.
MS_{ti}	=	COD mass load on reactor (kgCOD/d) = Q_i S_{ti}
MX_{Io}	=	mass of ISS in reactor (kgTSS)
MX_t	=	mass of TSS in reactor (kgTSS)
MX_v	=	VSS mass in reactor (kgVSS)
Q_i	=	average dry weather flow (ADWF, Mℓ/d)
R_s	=	system sludge age (days)
S_{ti}	=	flow weighted average influent COD concentration entering biological reactor (mgCOD/ℓ)
X_{Io}	=	ISS concentration in biological reactor (mgISS/ℓ)
X_{Ioi}	=	influent ISS concentration entering biological reactor (mgISS/ℓ)
X_v	=	VSS concentration in the reactor (mgVSS/ℓ)
Y_H, Y_G	=	yield coefficient for OHOs and PAOs = 0.45 mgVSS/mgCOD
%	=	Percentage of influent readily biodegradable COD taken up by PAOs

In Equation 2.26 three unknown parameters need to be determined (X_{Ioi}, f_{iOHO} and f_{iPAO}). The influent ISS concentration (X_{Ioi}) is measured directly, and the inorganic contents of the OHOs and PAOs, which cannot be measure directly, were calculated indirectly by matching measured and model predicted reactor ISS concentrations from the data of 22 experimental investigations measured in the University of Cape Town's Water Research Laboratory over the past 15 years. From enhanced PAO culture investigations fed artificial wastewater, the PAO ISS content (f_{iPAO}) for 100% aerobic P uptake was calculated to be 1.30 mgISS/mgPAOVSS and from nitrification/denitrification systems fed artificial wastewater, the OHO ISS content (f_{iOHO}) was calculated to be 0.15 mgISS/mgOHOVSS. These calibrated values were then applied to nitrification/denitrification BEPR systems. For the systems with >90% aerobic P uptake BEPR Ekama and Wentzel (2004) found that the predicted ISS correlated very well with the measured ISS. However, for systems with significant anoxic P uptake BEPR, they found the correlation to be very poor. They explained this poor correlation for the systems with significant anoxic P uptake BEPR by virtue of the lower P content in PAOs present in systems with significant anoxic P uptake. As the P content was lower for those PAOs, it seemed reasonable to accept that the ISS content also would be lower. Hence they established a linear relationship between P and ISS contents of the PAOs with the enhanced PAO culture P content at the one extreme and zero P content (equivalent to that of OHOs) at the other extreme:

$$f_{iPAO} = f_{iPAOBM} + 3.286\,(f_{XBGP} - f_{XBGPBM}) \qquad \text{mgISS/mgPAOVSS} \qquad (2.29)$$

f_{iPAOBM}	=	inorganic solids content of the PAO active biomass (mgISS/mgVSS)
	=	0.15 mgISS/mgPAOVSS (without polyphosphate)
f_{XBGP}	=	total P content of PAOs (= $f_{XBGPBM} + f_{XBGPP}$)
f_{XBGPBM}	=	P content of the PAO cell mass = 0.03 mgP/mgPAOVSS

Equation 2.29 implied that the PAO P and ISS contents without polyphosphate are the same as the ISS content of OHOs and that the 3.286 factor describes the ISS content of the polyphosphate in the PAOs.

Ekama and Wentzel (2004) validated the model with data measured on 48 aerobic, anoxic-aerobic nitrification/denitrification and anaerobic-anoxic-aerobic nitrification/denitrification BEPR systems operated in the Water Research Laboratory at the University of Cape Town over the past 15 years. The validation was based on the consistency of the predicted and measured ISS concentrations and the reasonable correspondence between predicted influent ISS/COD ratios.

The Ekama and Wentzel (2004) ISS model can readily be integrated into the existing steady state or dynamic simulation models, and it was integrated in both the steady state mass balances spreadsheet and the UCTOLD dynamic activated sludge models discussed in this Chapter.

2.2.3 The University of Cape Town Dynamic Activated Sludge Model (UCTOLD)

The UCT dynamic activated sludge model incorporated in the UCTOLD program (Dold *et al.*, 1980 and 1991) was built on the steady state aerobic model of Marais *et al.*, (1976). This steady state model was developed from a number of previous models for COD and nitrogen (N) conversion and removal. The most important features of this steady state model are:

(i) The influent COD is divided into three fractions (biodegradable, unbiodegradable particulate and unbiodegradable soluble COD) and the influent TKN into four fractions

(unbiodegradable soluble, unbiodegradable particulate, biodegradable organic and free and saline ammonia).

(ii) A distinction is made between active (organism), endogenous (unbiodegradable residue left after organism death) and inert sludge fractions.

(iii) The biological reactions are formulated in terms of the active organism mass.

(iv) The oxygen utilization rate is linked to the organism synthesis and endogenous processes and an oxygen requirement for nitrification is formulated.

(v) Nitrogen is incorporated into all of the sludge fractions, including active and endogenous sludge mass.

The UCT dynamic model for the activated sludge system was based on mechanistic conceptualization of the aerobic and denitrification kinetic behaviour of the organisms prevalent in such a system. The following concepts were incorporated in this dynamic model:

(i) The bisubstrate hypothesis (Stern and Marais, 1974):
This hypothesis proposed that the influent biodegradable COD consists of two fractions, a readily biodegradable (RBCOD) and slowly biodegradable (SBCOD) fraction. The RBCOD consists of molecules (in the liquid phase) that can easily and directly pass through the organism cell wall by active or passive uptake by the organism. The specific growth rate of the active mass on the RBCOD is therefore fast.
The SBCOD consists of larger, more complex molecules which cannot pass through the organism cell wall. For the organisms to be able to utilize the SBCOD, the SBCOD has to be enmeshed by the sludge mass and adsorbed onto the organism surface. Once adsorbed, the SBCOD is broken down outside the cell wall, by means of enzymatic breakdown. The products of the enzymatic breakdown can then pass directly through the cell wall for the organism metabolism. The enmeshment of the SBCOD is assumed to be instantaneous, and therefore it was not explicitly modelled. Some of the enmeshed SBCOD is adsorbed onto the surface of the active biomass at a defined kinetic rate. The enzymatic breakdown (or hydrolysis) of the adsorbed SBCOD is considered slow and therefore it represents the rate limiting process. This resulted in the utilization of SBCOD being modelled as a two stage process, the adsorption of the material by the organism mass and subsequent hydrolysis of the adsorbed SBCOD. The hydrolysis and utilization of adsorbed SBCOD was modelled with an active site surface kinetic reaction in which the rate is expressed as a Monod type function, but the substrate concentration is expressed as a proportion of active sites occupied by adsorbed SBCOD, i.e. X_{bs}/X_{bh} rather than with respect to the bulk liquid.

(ii) Nitrification / Denitrification (van Haandel *et al.*, 1981):
Van Haandel *et al.*, (1981) incorporated denitrification in the Dold *et al.*, (1991) model to produce a general nitrification/denitrification activated sludge kinetic model. They found that the bisubstrate theory could also be applied to the denitrification kinetic behaviour. The same formulations for the utilization of RBCOD and SBCOD under aerobic conditions could be applied to model their utilization under anoxic conditions, albeit with a SBCOD utilization rate which is a third less than that under aerobic conditions.

(iii) The death-regeneration hypothesis:
In earlier models organism 'death', natural or predation, was modelled by the endogenous respiration concept. This concept was used to explain a reduction in active organism mass with time after all organic material was depleted. This phenomenon was explained by the concept of organism maintenance: A fraction of the organism mass is utilized by the organisms to provide energy for cell maintenance.
The death-regeneration model separates the reactions that take place when an organism 'dies'. The reduction in active organism mass with time after all organic material is depleted is hypothesized to be a combined effect of (i) 'death' of the organisms and (ii) the regeneration of organisms that utilize the 'dead' organisms as food source. When the organisms 'die', their cell content is released into the bulk liquid (lysis), a fraction of which is unbiodegradable and remains in the bulk liquid as endogenous residue. The remainder, which is considered biodegradable, becomes SBCOD in the bulk liquid, and it is utilized by the living organisms as if it were SBCOD from the wastewater. This results in an associated oxygen demand termed endogenous oxygen demand.

(iv) Nitrogen transformations:
It was found that (i) and (ii) above could be integrated with the transformation of nitrogen in synthesis, death-regeneration and nitrification/denitrification..

From Dold *et al.* (1980) and van Haandel *et al.* (1981), the processes and their interactions with the compounds that are incorporated in the UCTOLD (Dold *et al.*, 1991) model are described below:

Aerobic growth of heterotrophs on RBCOD:
A fraction of the RBCOD is utilized by the organisms for growth (active organism production or synthesis) and the balance of the RBCOD is utilized for energy to fuel the growth process, resulting in an associated oxygen demand for synthesis. Growth of the organisms is modelled by Monod kinetics. The N source for synthesis is either ammonia or nitrate. Ammonia is utilized first, and once the ammonia concentration in the bulk liquid reduces to near zero, nitrate is utilized as an alternative N source. This results in two processes describing aerobic growth of heterotrophs on RBCOD: One utilising ammonia as the N source (Process 1), the other utilizing nitrate (Process 2). In the model, this is facilitated by a switching function that is dependent on the ammonia concentration in the bulk liquid. As the ammonia concentration in the bulk liquid approaches zero, Process 1 is switched off (i.e. the increase in organism mass by Process 1 equals zero) and simultaneously Process 2 is switched on. Should both the ammonia and the nitrate be depleted, both processes are switched off. To ensure that Processes 1 and 2 are active only in the presence of oxygen, a further switching function is incorporated that switches both processes off if the dissolved oxygen concentration reduces to zero and a switch is made to anoxic growth of heterotrophs on RBCOD.

Anoxic growth of heterotrophs on RBCOD:
In the absence of oxygen, the heterotrophic organisms use nitrate as terminal electron acceptor and RBCOD as substrate. As for the aerobic growth of heterotrophs on RBCOD described above, anoxic growth is modelled by Monod kinetics, and two processes describe anoxic growth of heterotrophs on RBCOD: One utilising ammonia as the N source (Process 3), the other utilizing nitrate (Process 4), and both are controlled by a switching function dependent on the ammonia concentration, which switches the processes on or off depending on the ammonia concentrations in the bulk liquid. To ensure that Processes 3 and 4 are active only in the presence of nitrate in

the bulk liquid, a further switching function is incorporated that switches both processes off if the nitrate concentration reduces to zero.

Aerobic growth of heterotrophs on adsorbed SBCOD:
The organisms utilize the adsorbed SBCOD under aerobic conditions in two steps. First the adsorbed SBCOD is hydrolysed by enzymes outside the cell wall, and then the products formed by the hydrolysis are directly utilized for cell synthesis, resulting in an associated oxygen demand. Since the hydrolysis is the rate limiting step, only the hydrolysis step is modelled. In the model described here, Levenspiel's surface reaction kinetics (Dold *et al.*, 1980) are used to model the hydrolysis step. As for the growth of heterotrophs on RBCOD described above, the aerobic growth of heterotrophs on RBCOD is modelled in two processes: One utilising ammonia as the N source (Process 5), the other utilizing nitrate (Process 6), and both are controlled by a switching function dependent on the ammonia concentration. Switching functions also ensure that Processes 5 and 6 only operate in the presence of oxygen. At very low oxygen concentrations, there is a switch to anoxic growth of heterotrophs on SBCOD.

Anoxic growth of heterotrophs on adsorbed SBCOD:
Anoxic growth of heterotrophs on adsorbed SBCOD is modelled the same as the two processes of Aerobic growth of heterotrophs on adsorbed SBCOD, except that the hydrolysis kinetic rate is multiplied by a factor (η_G) to take cognisance of the slower hydrolysis rate under anoxic conditions. As before, either ammonia (Process 7) or nitrate (Process 8) is utilized as N source, controlled by a switching function dependent on the ammonia concentration. A further switching function ensures that both Processes 7 and 8 are switched off when the bulk liquid nitrate concentration reaches zero.

Death of heterotrophs:
This process (Process 9) is modeled by the death-regeneration hypothesis. The heterotrophic organisms die at a certain rate, and a portion of the cell mass adds to the unbiodegradable endogenous residue, while the remainder adds to the SBCOD. The N content of the biodegradable portion (SBCOD) adds to the particulate organic N. The process of death is active under aerobic, anoxic and anaerobic conditions.

Adsorption of SBCOD:
It is assumed that as soon as the SBCOD enters the reactor in the influent flow, it enmeshes in the sludge mass in that reactor. Therefore the adsorption process (Process 10) simply transfers the enmeshed SBCOD to adsorbed COD.

Hydrolysis of particulate organic N:
The N content of the biodegradable particulate (SBCOD) organic material is released as soluble organic nitrogen (Process 11) during the hydrolysis process, for both aerobic and anoxic SBCOD utilization.

Ammonification of soluble organic N:
The heterotrophic organism mass mediates the conversion of soluble organic N to ammonia (Process 12). The hydrogen ions taken up in this process result in a change in the alkalinity.

Aerobic growth of autotrophs:
Ammonia is converted to nitrate in one step by the autotrophs, resulting in the growth of the autotrophic organism mass (Process 13) and an associated nitrification oxygen demand. Because

nitrification requires the presence of oxygen, a switching function switches the process off when the dissolved oxygen concentration reaches zero.

Death of autotrophs:
This process (Process 14) is identical to the heterotrophic death process.

Most of these processes were taken up into the IWA Activated Sludge Model No1 (ASM1, Henze *et al.*, 1987) with some modifications: (i) The adsorption rate of SBCOD was omitted, (ii) the hydrolysis/utilization rate of SBCOD was split into two with the hydrolysis process generating RBCOD which was released to the bulk liquid, adding to the influent RBCOD pool, and (iii) anoxic and aerobic growth on RBCOD with nitrate as N source was omitted. Essentially, for sludge ages longer than 5 days, for which enmeshment/adsorption can be accepted as instantaneous and complete, there is little to choose between the two models - both give virtually the same results for the same systems. Because of the history of experience with the UCTOLD model at UCT, the UCTOLD model will form the basis of the dynamic model that is compared with the steady state mass balances spreadsheet in this Chapter.

2.3 THE STEADY STATE MASS BALANCES (COD, ISS, VSS, TSS, N AND P) WASTEWATER TREATMENT PLANT MODEL

2.3.1 The Steady State Aerobic Digestion Model

In the steady state aerobic digestion model of Marais and Ekama (1976, see also van Haandel et al., 1998a) reviewed above, extended here to include the ISS model of Ekama and Wentzel (2004), it is assumed that (i) the unbiodegradable organics in the influent to the digester, which comprises both (a) the wastewater unbiodegradable particulate organics (S_{upi}) that accumulate in the activated sludge reactor as VSS (X_I) and (b) the OHO unbiodegradable particulate organics (endogenous residue, X_{EH}) generated in the activated sludge reactor, remain unaffected with the result that their concentrations do not change in the digester. These two concentrations are lumped together and denoted X_{Ii}, viz. the influent unbiodegradable VSS to the digester, (ii) the inorganic suspended solids (ISS) concentration from the (original) influent wastewater also does not change during digestion, i.e. no precipitation or dissolution of inorganics takes place in the digester and (iii) the OHOs (X_{BH}) decrease in the digester via endogenous respiration. This decrease in OHO concentration gives rise to five ancillary effects, i.e. (iv) a generation of unbiodegradable VSS in the form of 'new' endogenous residue (X_{EH}) which is 20% (f_{EH}) of the OHOs that are 'lost' in endogenous respiration, (v) a decrease in the ISS concentration proportional with the OHO decrease, (vi) the utilization of oxygen for endogenous respiration, (vii) the release of ammonia and ortho-phosphate (OP) to the bulk liquid, the former of which may be nitrified and (viii) the utilization of oxygen for nitrification.

The equations for the steady state single reactor completely mixed aerobic digester model were derived from the above assumptions. In the interests of brevity, their derivation is not given, but the equations of the model in terms of the VSS and TSS concentration measures are listed in Table 2.1 (Equations 2.30 to 2.49).

2.3.1.1 Aerobic digestion of primary sludge - steady state modelling

The steady state aerobic digestion model for WAS (Table 2.1) can also be applied to stabilization of primary sludge (PS). This hinges around calculating the equivalent influent active fraction of the PS, which is possible provided the $f_{PS'up}$ fraction of the PS is known. The $f_{PS'up}$ can be calculated from a mass balance around the PST. For example, in a PST in which 40% and 15% COD and TKN removal are obtained for typical raw and settled wastewater characteristics listed in Table 2.2 (the same influent that was used in the comparison of the steady state mass balances spreadsheet and the dynamic UCTOLD model in Chapter 2.3.3), the PS generated has the following characteristics: COD/VSS ratio (f_{cvPS}) = 1.64 mgCOD/mgVSS, TKN (orgN)/VSS ratio (f_{nPS}) = 0.049 mgN/mgVSS, $f_{PS'up}$ = 0.314, unbiodegradable particulate TKN fraction = 0.59 and VSS/TSS ratio (f_{iPS}) = 0.83. Unless the COD/VSS ratio of the biodegradable or unbiodegradable organics is known, the unbiodegradable VSS fraction in PS cannot be calculated from the raw and settled wastewater and PS characteristics.

From anaerobic digestion of PS, it was established that the COD/VSS (f_{cv}) and TKN/COD ($f_{ZB,N}$) ratios of the particulate unbiodegradable organics are higher than those for the particulate biodegradable organics, and that these ratios of the unbiodegradable organics are lower than the ratios that have been assumed previously for these organics in activated sludge. Because the implications of these differences for the activated sludge system have not been fully explored yet,

Table 2.1: Equations of the steady state aerobic digestion model based on the steady state activated sludge model of Marais and Ekama (1976) and the ISS model of Ekama and Wentzel (2004).

Parameter	Model in terms of VSS	Model in terms of TSS
Influent active fraction (f_{avi}, f_{ati})	$\beta = 1/f_{avi} - (1 - f_{EH})$ ...(2.30)	$\delta = 1/f_{ati} - (1 + f_{iOHO})$...(2.40)
Effluent active fraction (f_{ave}, f_{ate})	$\alpha = 1/f_{ave} - (1 - f_{EH})$ ...(2.31)	$\gamma = 1/f_{ate} - (1 + f_{iOHO})$...(2.41)
Retention time (R_h, d)	$R_h = \frac{1}{b_{HT}}\left[\frac{\alpha}{\beta} - 1\right]$...(2.32)	$R_h = \frac{\gamma - \delta}{b_{HT}(\delta + f_{EH})}$....(2.42)
Effluent active fraction (f_{ave}, f_{ate})	$\alpha = \beta(1 + b_{HT} R_h)$....(2.33)	$\gamma = \delta + b_{HT} R_h (\delta + f_{EH})$...(2.43)
Fraction solids removal (f_{vsr}, f_{tsr})	$f_{vsr} = f_{avi}(1 - f_{EH})\ (1 - \beta/\alpha)$...(2.34)	$f_{tsr} = 1 - \frac{f_{ati}}{f_{ate}(1 + b_{HT} R_h)}$...(2.44)
Organic Oxygen Demand (kgO/d)	$V_d O_c = f_{cv} f_{vsr} Q_i X_{vi}$...(2.35)	$V_d O_c = f_{cv} Q_i X_{ti} f_{tsr} (1 - f_{EH})/(1 + f_{iOHO} - f_{EH})$.....(2.45)
Nitrif. Oxygen Demand (kgO/d	$V_d O_n = 4.57 f_n f_{vsr} Q_i X_{vi}$....(2.36)	$V_d O_n = 4.57 f_n Q_i X_{ti} f_{tsr} (1 - f_{EH})/(1 + f_{iOHO} - f_{EH})$.....(2.46)
Total Oxygen Demand (kgO/d)	$V_d O_t = (f_{cv} + 4.57 f_n) f_{vsr} Q_i X_{vi}$...(2.37)	$V_d O_t = (f_{cv} + 4.57 f_n) Q_i X_{ti} f_{tsr} (1 - f_{EH})/(1 + f_{iOHO} - f_{EH})$.....(2.47)
Effluent Ammonia Conc (mgN/ℓ)	$N_{ae} = N_{ne} = f_n X_{vi} f_{vsr}$.....(2.38a & 2.38b)	$N_{ae} = N_{ne} = f_n X_{ti} f_{tsr} (1 - f_{EH})/(1 + f_{iOHO} - f_{EH})$.....(2.48a & 2.48b)
Effluent Ortho-P Conc (mgP/ℓ)	$P_{se} = f_p X_{vi} f_{vsr}$.....(2.39)	$P_{se} = f_p X_{ti} f_{tsr} (1 - f_{EH})/(1 + f_{iOHO} - f_{EH})$.....(2.49)
VSS/TSS ratio	$f_{ii} = \frac{f_{ati}}{f_{avi}}$..(2.50); $f_{ie} = \frac{f_{ate}}{f_{ave}}$..(2.51); $f_{ie} = \frac{(1 - f_{vsr})}{(1 - f_{tsr})} f_{ii}$..(2.52a); $f_{ie} = \frac{f_{ii}[1/(b_H R_h) + 1] - f_{ati}(1 - f_{EH})}{[(1/(b_H R_h) + 1] - f_{ati}(1 + f_{iOHO} - f_{EH})}$..(2.52b)	

Notes: (1) For known influent active fraction (f_{avi}, f_{ati}) if (i) effluent active fraction is specified (i.e. a level of sludge stability), then use Eqs 2.31 or 2.41 to calculate α or γ and Eqs 2.32 or 2.42 to calculate the required retention time (R_h) or (ii) if R_h is known, then use Eqs2.33 or 2.43 to calculate α or γ and Eqs 2.31 or 2.41 to calculate the resulting effluent active fraction. (2) **Symbols:** f_{avi}, f_{ati}, f_{ave} f_{ate} = active fraction with respect to VSS (subscript v) and TSS (subscript t) for the influent (subscript i) and effluent (subscript e) sludges, f_{vsr}, f_{tsr} = fraction of VSS (subscript v) and TSS (subscript t) solids removed; f_{ii}, f_{ie} = VSS/TSS ratio of the influent (subscript i) and effluent (subscript e) solids; V_d= digester volume; Q_i = influent flow; O_c, O_n, O_t = organic, nitrification and total oxygen utilization rates - mgO/(ℓ.d); f_{EH} and b_{HT} = unbiodegradable fraction and endogenous respiration rate of the OHOs in the endogenous respiration model (i.e. 0.20 and 0.24/d at 20°C); f_{iOHO} = ISS content of OHOs = 0.15 mgISS/mgOHOVSS. N_{se}, N_{ne} and P_{se} are the effluent ammonia (no nitrification, N_{ne}=0), nitrate(complete nitrification, N_{ae}=0) and phosphorus concentrations.

Table 2.2: Raw and settled wastewater and primary sludge characteristics calculated from a mass balance around the primary settling tank (PST) for raw and settled wastewater unbiodegradable particulate COD fractions ($f_{S'up}$) of 0.15 and 0.04 and raw wastewater soluble unbiodegradable and biodegradable COD fractions ($f_{S'us}$ and $f_{S'bs}$) of 0.07 and 0.25 respectively.

Parameter	RawWW	Settled WW	Primary Sludge	Units
Flow	15000	14925	75	m^3/d
Total COD (S_{ti})	750	450	60450	mgCOD/ℓ
Unbiodegradable particulate COD (S_{upi})	112	18	18818	mgCOD/ℓ
Unbiodegradable soluble COD (S_{usi})[4]	53	53	53	mgCOD/ℓ
Biodegradable particulate COD (S_{bpi})	439	233	41433	mgCOD/ℓ
Biodegradable soluble COD (S_{bsi})[4]	146	146	146	mgCOD/ℓ
Unbiodegradable COD fraction of PS	-	-	0.312[1]	
Total TKN (N_{ti})	60.0	51.1	1831	mgN/ℓ
Free and saline Ammonia (N_{ai})	45.0	45.0	45.0	mgN/ℓ
Unbiodegradable particulate OrgN (N_{oupi})[2]	7.6	1.2	1281	mgN/ℓ
Unbiodegradable soluble OrgN (N_{ousi})[3]	1.8	1.8	1.8	mgN/ℓ
Biodegradable particulate OrgN (N_{obpi})[4]	3.9	1.4	501	mgN/ℓ
Biodegradable soluble OrgN (N_{obsi})[4]	1.7	1.7	1.7	mgN/ℓ
Unbiodegradable TKN fraction of PS			0.719	
Total suspended solids (TSS)	301	78.7	44459	mgTSS/ℓ
Volatile suspended solids (VSS)	253	69.2	36829	mgVSS/ℓ
Inorganic suspended solids (ISS)	48	9.5	7650	mgISS/ℓ

[1] Obtained from a strict mass balance.

[2] Calculated from a TKN/COD ratio ($f_{ZB,N}$) = 68.6 mgN/gCOD or equivalently f_n = 0.10 mgN/mgVSS and COD/VSS = 1.48 mgCOD/mgVSS for the influent unbiodegradable particulate organics.

[3] Based on a raw wastewater FSA/TKN ratio and unbiodegradable soluble TKN fraction of (f_{na} and f_{nu}) of 0.75 and 0.03 respectively.

[4] Based on 0.45μm membrane filtered COD and TKN concentrations of 199 mgCOD/ℓ and 3.5 mgN/ℓ, and accepting that 0.45μm membrane filtrate concentrations are soluble.

the commonly accepted COD/VSS and TKN/COD ratios of activated sludge have been assumed for the unbiodegradable particulate organics in this analysis, i.e. f_{cv} = 1.48 mgCOD/mgVSS and $f_{ZB,N}$ = 67.6 mgN/gCOD (f_n = 0.10 mgN/mgVSS).

The biodegradable COD in PS is utilized in the aerobic digester and transformed to OHO biomass in the same way as it would be in the activated sludge system if raw wastewater were treated. The COD/VSS ratio (f_{cv}) of the OHO biomass formed is 1.48 mgCOD/mgVSS, the same as that formed in the activated sludge system. Once the OHO biomass has formed, it is degraded via endogenous respiration (or death regeneration) in the aerobic digester in the identical way as WAS described by Marais and Ekama (1976). However, one important difference is that the

oxygen utilized in the digester is the sum of that used for synthesis of OHO biomass and endogenous respiration of the formed OHO biomass (including nitrification, if this takes place). If a fraction $f_{PS'up}$ of the PS particulate COD is unbiodegradable, the biodegradable fraction is (1-$f_{PS'up}$). The OHO biomass that grows from this is Y_H (1- $f_{PS'up}$) kgOHOVSS/kg PS COD. The unbiodegradable COD has the same COD/VSS ratio as this material in the activated sludge reactor treating raw wastewater, which for the purposes of this analysis is f_{cv} = 1.48 mgCOD/mgVSS. Hence, the VSS mass of the unbiodegradable organics is $f_{PS'up}/f_{cv}$ kgVSS/kg PS COD. The total VSS mass is the sum of the OHO VSS and unbiodegradable VSS, i.e. Y_H (1-$f_{PS'up}$) + $f_{PS'up}/f_{cv}$ kgVSS/kg PS COD. The ratio of the OHO and total VSS masses gives the equivalent active fraction of the PS (f_{avPS}), which is given by:

$$\frac{1}{f_{avPS}} = 1+\frac{f_{PS'up}}{f_{cv}Y_H(1-f_{PS'up})} \qquad (2.53)$$

The oxygen demand for synthesis of the OHO VSS mass, O_s is:

$$V_d O_s = Q_i S_{tPS} (1-f_{cv}Y_H)(1-f_{PS,up}) \text{ kgO/d} \qquad (2.54)$$

where V_d is the volume of the digester, and Q_i and S_{tPS} the PS influent flow and total COD concentration respectively.

For example, for the WWTP in Fig 2.2, Chapter 2.3.3and the wastewater characteristics in Table 2.2, the primary sludge COD concentration is 60450 mgCOD/ℓ in a flow of 75 m³/d, i.e. 4534 kgCOD/d. From Eq 2.53, the unbiodegradable fraction of this PS COD ($f_{PS'up}$) = 0.315. Hence the OHO VSS concentration synthesized is 0.45(1-0.315)60450 = 18634 mgVSS/ℓ, the unbiodegradable VSS concentration = 0.315x60450/1.48=12866 mgVSS/ℓ and the total VSS concentration = 18634 + 12866= 31500 mgVSS/ℓ. The PS ISS concentration is 7560 mgISS/ℓ and the OHO ISS contribution to this (after OHO formation) = 0.15(18634) = 2795 mgISS/ℓ, making the total ISS = 10445 mgISS/ℓ. Hence the TSS equals 31500 + 10445 equals 41945 mgTSS/ℓ. From these concentrations the active fractions of the VSS and TSS and VSS/TSS ratio are 0.592, 0.444 and 0.751 respectively.

By specifying an effluent active fraction (f_{ave} or f_{ate}), the retention time and oxygen demand for the OHO biomass breakdown are given by Eqs 2.30 to 2.35 or 2.40 to 2.45 in Table 2.1. To this oxygen demand, the oxygen demand for synthesis must be added to give the total oxygen demand (kgO/d). From this total oxygen demand and an acceptable oxygen transfer rate [OTR, kgO/(m³.h)] of the aeration system, the volume of the digester (V_d) is calculated. With the retention time (R_h) known, the influent sludge flow rate is determined ($Q_i = V_d/R_h$). The ratio of the actual PS flow rate and the digester feed flow rate (Q_i) is the degree of PS thickening required by gravity sedimentation. For example, if the primary sludge is to be stabilized to an active fraction with respect to VSS (f_{ave}) of 0.235, then from Eq 2.31 α = 3.455, Eq 2.30 β = 0.889, Eq 2.32 R_h = 14.3d, Eq 2.34 f_{vsr} = 0.351 and Eq 2.35 $V_d O_e$ = 1.48x0.352x0.075x31500 = 1230 kgO/d. Adding the 1037 kgO/d synthesis oxygen demand gives the total oxygen demand = 2268kgO/d. If a maximum OTR of 125 mgO/(ℓ.h) is accepted for the aeration system, then a digester volume of 2268x1000/(24x125) = 756 m³ is required. To obtain 14.3 days retention time, the influent flow rate (Q_i) is 756/14.3 = 52.8 m³/d. The PS thus can be thickened by 75/52.8=1.42 times by gravity thickening, or to a TSS concentration of 44459x1.42 = 63072 mgTSS/ℓ or 6.3% solids.

Higher (or lower) maximum OTRs for the aeration system will result in smaller (or greater) digester volumes and higher (or lower) thickened digester feed concentrations.

Because the unbiodegradable TKN (and TP) fractions of PS are so much higher than the unbiodegradable COD fraction (most of the PS TKN and TP are locked up in the unbiodegradable organics, Table 2.2), the PS does not contain sufficient available N (and P) for OHO growth. Therefore, ammonia and phosphate need to be dosed to the aerobic digester to facilitate non nutrient deficient OHO growth. Because the yield of biomass under anaerobic conditions is only 1/10th of that under aerobic conditions, nutrient dosing usually is not necessary for anaerobic digestion of PS and is one of several good reasons why PS is usually anaerobically digested. In the aerobic digester, even though the synthesis process is much faster than the endogenous process, N and P are released during endogenous respiration and become available for synthesis of biomass, which reduces the N and P dose and reduces nitrification (provided N is not overdosed). For example, from Table 2.2, the ammonia and biodegradable organic nitrogen available in the PS for OHO synthesis, taking due account of PS thickening, is 45+501x1.42+1.7 = 758 mgN/ℓ. The concentration of N required for OHO synthesis at 0.10 mgN/mgVSS is 0.10x18634x1.42= 2646 mgN/ℓ. However, N is released to the bulk liquid during endogenous respiration and becomes available as an N source for synthesis, i.e. 0.10x0.352x31500x1.42=1575 mgN/ℓ. Therefore the net N deficit is 2646-758-1575=313 mgN/ℓ or 313x0.054=16.9 kgN/d. The P supplement, as kgP/d, is calculated the same way and is approximately between 20 - 30% of the N addition.

With regard to the ISS, this concentration initially increases in the aerobic digester treating PS due to OHO growth, but then decreases due to OHO biomass loss with endogenous respiration. The VSS/TSS ratio therefore changes from that of the influent PS value as aerobic digestion progresses. The aerobic digestion model in terms of TSS also can be used, but then the equivalent influent active fraction of the PS needs to be expressed with respect to TSS, i.e. f_{atPS}. The ISS concentration on which f_{atPS} is based is the sum of the ISS concentration from the influent wastewater that settles out in the PST plus the ISS contribution of the OHO that forms. The latter is given by $f_{iOHO}\ Y_H\ (1- f_{iPS'up})\ S_{tPS}$. For example, from Table 2.2, the influent fixed ISS concentration to the PS digester is 7650x1.42 = 10863 mgISS/ℓ in a flow of 52.8 m^3/d. The effluent fixed ISS concentration therefore also is 10863 mgISS/ℓ. However, the effluent active OHO concentration adds to the fixed ISS. The effluent active fraction of the VSS is 0.235 and the fraction of VSS removed is 0.352. Hence, the effluent OHO concentration is 0.235(1-0.315)1.42x31500 = 6807 mgOHOVSS/ℓ, making its ISS contribution = 0.15x6807=1021 mgISS/ℓ. The effluent ISS concentration thus is 10863+1021=11884 mgISS/ℓ. This is higher than the influent. The effluent VSS concentration is (1-0.315)31500x1.42=27911 mgVSS/ℓ, making the effluent VSS/TSS ratio 27911/(27911+11884)=0.701.

In the calculations for aerobic digestion of PS above, the following is noted :

(i) COD is conserved, but not VSS. This is because the COD/VSS ratio is different before and after OHO formation. For the example wastewater, the COD/VSS ratio for the PS before OHO formation (f_{cvPS}) is 1.64. This is an average value of a $(1- f_{iPS'up})$ to $f_{PS'up}$ mixture of biodegradable organics with a high COD/VSS ratio (1.71) and unbiodegradable organics with a COD/VSS ratio f_{cv} = 1.48 mgCOD/mgVSS. After OHO VSS formation, the PS is similar to WAS with the same COD/VSS ratio (f_{cv}) = 1.48

mgCOD/mgVSS for both the OHO VSS and the unbiodegradable VSS, and with a defined active fraction with respect to VSS (f_{avPS}). It may be argued that it is not necessary to use VSS in the steady state aerobic digester model and use COD throughout, as simulation models like ASM1 do. However, at some point the COD/VSS ratio of the sludge mass (and its components) is required in order to express the activated sludge concentrations as VSS or TSS to relate the model outputs to parameters commonly measured in practice at WWTPs. Whether this is at the beginning or end of the model calculations is irrelevant.

(ii) The influent wastewater ISS that settles out in the PST is conserved through the aerobic digester. This ISS concentration can be determined by measurement on the primary sludge. However, the VSS/TSS ratio (f_{iPS}) measured on the PS (before OHO formation i.e. f_{iPS} = 0.83, Table 2.2) changes to different values after OHO formation and during aerobic digestion of the PS. These changes arise from changes in both VSS and ISS concentrations during digestion due to the decreasing OHO concentration.

(iii) Like for the COD/VSS ratio (f_{cv}) (see i above), it has been assumed in this analysis that the N (and P) contents of the VSS (f_n) of the unbiodegradable organics (as VSS) in the PS are the same as activated sludge at 0.10 mgN/mgVSS. Primary sludge characterization with anaerobic digestion indicates that for modelling the whole WWTP, it will be necessary to assign different ratio values to the influent particulate unbiodegradable organics (and perhaps the endogenous residue) as the active (OHO) biomass to more accurately track the COD, VSS and N through the different unit operations of WWTPs. Activated sludge Model No 2 (Henze et al., 1995) does this - it assigns 70, 40 and 30 mgN/gCOD to the OHO (and PAO) biomass, biodegradable particulate COD and unbiodegradable particulate organics respectively, but the experimental source for these ratios are not given. This aspect requires further investigation.

(iv) The difference in COD/VSS ratio of the PS biodegradable and unbiodegradable organics does not affect the COD balance and aerobic digester model because all the biodegradable COD is transformed to OHO active VSS with a COD/VSS ratio of 1.48 mgCOD/mgVSS, the same as activated sludge. Similarly, the TKN/VSS (and TP/VSS) ratios of biodegradable (particulate) organics in PS are much lower than the measured average PS TKN/VSS (f_{nPS}) (and TP/VSS, f_{pPS}) ratios, but those of the OHO active VSS formed are the same as those of activated sludge, i.e. f_n = 0.100 mgN/mgVSS (and f_p = 0.030 mgP/mgVSS).

2.3.1.2 Aerobic digestion of primary sludge and waste activated sludge blends - steady state modelling

Aerobic digestion of blends of waste activated (WAS) and primary (PS) sludges can be modelled with the equations and procedure developed above for the two different sludges, but the blended sludge characteristics need to be defined. These are obtained from the individual WAS and PS characteristics. Like with PS only, the biodegradable COD in the PS is utilized in the aerobic digester and transformed to OHO active mass. The active fraction of the VSS mass formed and the synthesis oxygen demand in this process are given by Eqs 2.30 and 2.31. The COD/VSS ratio (f_{cv}) of the OHO VSS mass formed is 1.48 mgCOD/mgVSS, the same as that of the WAS. This OHO VSS mass, as well as that in the WAS, is degraded via endogenous respiration (or death regeneration) in the aerobic digester in the identical way as WAS alone, as demonstrated for PS above. Like with PS only, the oxygen demand in the digester is the sum of the synthesis and endogenous oxygen demands, where now the latter is that by the OHOs from the PS and WAS.

The characteristics of the WAS and PS blend are obtained by adding the mass flows of like components in the WAS and PS and making ratios of selected blended mass flow rates to calculate the blended sludge characteristics. The process design of the digester is based on the blend characteristics *after* OHO VSS formation, such as active fraction with respect to VSS, the VSS/TSS ratio, and the fraction of PS VSS mass (after OHO formation) in the blend.

Once the WAS equivalent blended sludge characteristics after OHO VSS formation are known, the WAS aerobic digestion model equations apply (Table 2.1), i.e. (i) for a specified effluent active fraction (f_{ave}), the retention time (R_h) for a single reactor digester is given by Eq 2.32, and (ii) the fraction of VSS solids removed and organic oxygen demand are given by Eqs 2.34 and 2.35. The oxygen demand for synthesis of OHO mass from the PS biodegradable organics (Eq 2.31) is added to the endogenous oxygen demand. For example, with $f_{avi} = 0.619$, $\beta = 0.816$ (Eq 2.30) and digesting the sludge to the same effluent active fraction as the WAS from the extended aeration (30d sludge age) activated sludge system treating raw wastewater, i.e. $f_{ave} = 0.235$, yields $\alpha = 1/0.235\text{-}0.8 = 3.455$ (Eq 2.31). Hence $R_h = 16.0$d (Eq 2.32), $f_{vsr} = 0.378$ (Eq 2.34) and $V_dO_c = 1.48 \times 0.378 \times 0.089 \times 43065 = 2146$ kgO/d (Eq 2.35). Adding the 1037 kgO/d synthesis oxygen demand gives the total oxygen demand $= 2146+1037 = 3183$ kgO/d. If a maximum OTR of 93 mgO/(ℓ.h) is accepted for the aeration system, then a digester volume of $3183 \times 1000/(24 \times 93) = 1430$ m^3 is required. With the fraction of VSS removed (f_{vsr}) = 0.378, the effluent VSS concentration = (1-0.378) 43065 = 26786 mgVSS/ℓ. From the calculated f_{ave}, f_{atc} and f_{ic} (Eqs 2.50 and 2.51), the different components of the digester effluent sludge can be calculated.

With WAS and PS blends, ammonia and phosphate dosages for non nutrient deficient OHO growth are much lower or not required than for PS alone. This is because the OHO active mass in the WAS releases N and P to the bulk liquid during aerobic digestion. The released N can be readily nitrified in aerobic digesters stabilizing blended PS and WAS sludges because the WAS is likely to contain nitrifiers. However, the contribution of the nitrification oxygen to the total generally will be low, so it can be ignored when calculating the WAS and PS sludge thickening from the maximum OUR in the digester. For example, the ammonia and biodegradable organic nitrogen available in the PS for OHO synthesis, taking due account of PS thickening to 54m^3/d, i.e. 1.38 times, is $(45+501 \times 1.38+1.7)0.054 = 40.1$ kgN/d. The concentration of N required for OHO synthesis at 0.10 mgN/mgVSS is $0.10 \times 18634 \times 0.075 = 139.9$ kgN/d. The N released to the bulk liquid during endogenous respiration = $f_n f_{vsr} X_{vi} Q_i = 0.10 \times 0.378 \times 43065 \times 0.089 = 144.9$ kgN/d. Hence, the net ammonia N released is 40.1-139.9+144.9 = 45.2 kgN/d, which in a flow of 89 m^3/d is 508 mgFSA-N/ℓ. This FSA will be nitrified to nitrate. Adding the digester influent nitrate concentration from the WAS (39.4 mgN/ℓ), appropriately diluted by the primary sludge flow to $39.4 \times 35/89 = 15.5$ mgNO_3-N/ℓ, yields an effluent nitrate concentration of 508+15= 523 mgNO_3-N/ℓ. This gives a nitrification oxygen demand of 213 kgO/d, which is less than 10% of the carbonaceous oxygen demand. Because more N is released than required for growth, no N needs to be dosed in this case. The same would apply to P. The relatively high N (and P) content of the WAS supplies (overall) the N (and P) requirement for a OHO synthesis on the PS biodegradable organics.

2.3.2 The Steady State Mass Balances Spreadsheet

The steady state design and operation WWTP mass balances spreadsheet (in Corel Quattro Pro 8), comprises 15 sheets:

1. *'Input'*: Primary sludge (PS) and wastewater (WW) fractions are entered directly or they can be calculated from the results of PS/WW characterization tests such as the Imhoff cone settling and membrane filtration for the PS and a laboratory scale (AS) system and membrane filtration for the WW characterisations. Kinetic and stoichiometric metric constants for the AS models for BNR are also entered in this sheet.

2. *'Loads'*: This sheet provides for the input of diurnal variations in flow as well as in COD, TKN, FSA, TP, OP and settleable solids (SS) concentrations. From this diurnal data estimates of the COD, OrgN, OrgP, VSS, ISS and TSS removal in primary settling are calculated, after which the diurnal variation in settled WW COD, TKN, FSA, TP, OP concentrations are also calculated. Further, estimates of COD, TKN, FSA, TP and OP loads on the biological reactor for raw and settled WWs are also presented. The PS composition (COD, VSS, ISS, TSS, OrgN and OrgP, each into their unbiodegradable and biodegradable soluble and particulate components) from mass balances around the PST is also characterized.

3. *'Char'*: In this sheet the raw and settled WWs COD, TKN, FSA, TP and OP are characterized, each into their unbiodegradable and biodegradable soluble and particulate components, utilizing the concentrations and fractions that are entered and/or calculated in sheets 1. and 2. above. The characterization of the raw and settled WW is presented graphically in corresponding block diagrams.

4. *'ASTmin'*, 5. *'ASTmax'*: Here the design parameters (i.e. volume of reactor, average and peak oxygen demand, effluent COD, TKN, FSA, nitrate, TP and OP concentrations and waste activated sludge (WAS) flow and composition) for fully aerobic raw and settled WW AS systems are calculated for both long and short sludge ages which can be chosen independently by the user. The parameters are calculated for both maximum ('ASTmax') and minimum ('ASTmin') expected temperatures.

6. *'AerDigSgl'*: The design of a single reactor aerobic digester. From the PS and WAS flows and concentrations (including the liquid stream): PS and WAS are blended and concentrated to the selected thickened concentration. The blend is aerobically digested to a selected residual biodegradable organic content, taking due account of the N and P release during digestion. The digester volume is calculated together with the oxygen demand and all effluent concentrations. Material mass balances (COD, N and P) are performed over the aerobic digester. The calculations are performed for the WAS from the fully aerobic system (sheets 4. and 5. above), N removal (MLE system, sheet 11. below) and N&P removal (UCT system, sheet 12. below) at both maximum and minimum design temperatures.

7. *'AerDTmin'*, 8. *'AerDTmax'*: These two sheets explore aerobic digestion of fully aerobic and nitrification/denitrification (ND) WAS sludges in single, double and triple

compartment digesters with and without PS and with separate PS and WAS thickening before blending, where the degree of thickening is governed by (i) selected upper limits of PS and WAS thickening by gravity sedimentation and flotation respectively or (ii) selected maximum OUR in the digester. This study showed that:

(i) Compartmentalizing the aerobic digester is only beneficial (smaller volume) for WAS digestion. Only for WAS can the digester volume be reduced by compartmentalization (as a result of the first ordered digestion rate) due to reduction in retention time, compared with a single completely mixed digester. For WAS only, the digester volume is governed by flotation thickening limitations, not by oxygen transfer limitations in the digester. Compartmentalizing the digester for PS and PS/WAS blends is not beneficial. The high OUR stimulated by the PS biodegradable organics limits the thickened feed sludge concentration to the first compartment to well below PS thickening capacity of gravity thickening.
(ii) Step feeding PS and PS/WAS blends in proportion to the digester compartment volumes equalizes the OUR in the compartments, but the retention time is then not long enough to achieve the required residual biodegradable organics in the effluent (i.e. reduced sludge stabilization). Only if the digester retention time is increased to that for the single reactor digester, is the required degree of stabilization achieved with step feeling. Therefore for PS and PS/WAS blends, it is the OUR in the digester that governs the digester volume and the degree of sludge thickening required.

Denitrification kinetics in WAS anoxic aerobic digesters have been measured experimentally and the simulation model UCTOLD (similar to ASM#1 (Henze *et al.*, 1987)) simulated the dynamic behaviour very well (Warner *et al.*, 1986). A much simpler steady state model has also been developed for anoxic aerobic digesters, but this has not been integrated into the spreadsheet, which so far is for fully aerobic digesters only.

9. *'MBalAE'*: This sheet checks the COD, N and P mass balances around the WWTP comprising (i) raw WW treatment in a long sludge age AS system, where the sludge age is selected long enough for sludge stabilization in the reactor and direct discharge of WAS to drying beds, and (ii) Primary settling tanks (PSTs), short sludge aged activated sludge system, PS and WAS thickening and aerobic digestion of PS and WAS to the same residual biodegradable organics as (i) above. The concentrations of COD (and oxygen demand), N and P in the effluent streams for the AS system, the thickening units and the aerobic digester are added and balance to within 0.5% of the influent raw wastewater COD, TKN and TP for both maximum and minimum temperatures. Also the carbonaceous oxygen utilised in the raw WW system (AS only), and in the settled WW system (AS and aerobic digester) are within 0.5%. The total oxygen demand also is close, but cannot be used as a mass balance check because the effluent FSA concentration from the short sludge aged system is higher than that from the long sludge age, resulting in somewhat lower nitrification oxygen demand in the settled WW system.

10. *'MLEUCTConst'*: Collects the required input data for a MLE N removal and a UCT N&P removal AS system design and makes the necessary temperature adjustments to the kinetic constants.

11. *'MLESys'*, 12. *'UCTSys'*: Does the complete design for the MLE and UCT systems at maximum and minimum design temperatures for both the raw and settled WW. Anaerobic, anoxic and aerobic reactor volumes, recycles ratios, oxygen demand, effluent concentrations and WAS flow and composition are calculated.

13. *'MLEBal'*, 14. *'UCTBal'*: These two sheets calculate the COD, N and P mass balances over the WWTP treating the raw and settled WW for the MLE and UCT systems respectively, as 9. above does for the fully aerobic system. COD, N and P mass balances over both raw and settled WWTPs are within 0.2%.

15. *'Tables'*, 16. *'Summary'*: Tabulates and summarises the results calculated in the various spreadsheet pages above.

The steady state spreadsheet described in this Chapter is capable of the following:

It characterizes the raw and settled WWs COD, TKN, FSA, TP and OP, each into their unbiodegradable and biodegradable soluble and particulate components, from the given (measured) concentrations and fractions and the PS COD, VSS, ISS, TSS, OrgN, OrgP, also each into their unbiodegradable and biodegradable soluble and particulate components from mass balances around the PST. The design parameters for the fully aerobic, ND or NDP biological excess P removal (BEPR) systems treating the raw and settled WW at long and short sludge ages respectively are calculated, i.e. volume of reactor, average and peak oxygen demand, effluent COD, TKN, FSA, TP and OP concentrations as well as WAS flow and composition. It also calculates the design parameters for a single reactor aerobic digester by taking the PS and WAS flows and concentrations (including the liquid stream), blending and concentrating them to the selected thickened concentrations, aerobically digesting the blended and thickened sludge to a selected residual biodegradable organic content, taking due account in N and P released during digestion. Digester volume, oxygen demand and effluent concentrations are calculated, and the material mass balances (COD, N and P) checked over the aerobic digester. WAS can be from fully aerobic, N removal (MLE) and N&P removal (UCT) systems at maximum and minimum temperatures. Further, the spreadsheet explores aerobic digestion of fully aerobic and ND WAS sludge in single, double and triple compartment digesters with and without PS and with separate PS and WAS thickening before blending, where the degree of thickening is governed by (i) selected upper limits of PS and WAS thickening by gravity sedimentation and flotation respectively or (ii) selected maximum OUR in the digester. Checks are performed on the COD, N and P mass balances around the WWTP ensuring consistency throughout the spreadsheet.

This steady state mass balances spreadsheet provides a useful tool to (i) determine the system design and operating parameters for fully aerobic, ND or NDP biological excess P removal (BEPR) AS systems treating raw and/or settled WW and furthermore for aerobic digestion of PS, WAS, or a blend of the PS and WAS, (ii) investigate the sensitivity of the system performance to the design and operating parameters, (iii) estimate product stream concentrations for design of down- (or up-) stream unit operations of the WWTP and (iv) provide a basis for cross checking kinetic simulation model results.

This steady state mass balances spreadsheet brings a step closer the modelling of a WWTP as a whole, in an integrated fashion, rather than focussing only on each unit operation by itself. A

WWTP comprises a sequence of individual unit operations (e.g. primary settling, AS and anaerobic or aerobic digestion). These individual unit operations are interconnected through a network of flows: The outputs from upstream units become inputs to downstream units and further, common practice at a WWTP is to recycle various liquors (e.g. sludge thickening and anaerobic digestion supernatant) from downstream unit operations to upstream ones. This interconnection of individual unit operations means that design and operation optimisation of one unit may have unexpected and often unforseen consequences on the performance (and economics) of both upstream and downstream unit operations, and hence on the WWTP as a whole. To assess and quantify the interdependencies of the various unit operations making up a WWTP, models that track materials of importance through a WWTP on a mass balance basis are required, and this spreadsheet is such a steady state model and it includes a link (i) between the primary settler and the aerobic digester and (ii) between the AS system and the aerobic digester.

Integrating the steady state model for anaerobic digestion developed in Chapter 5 into the spreadsheet described here would add two further links (i) between the primary settler and the anaerobic digester and (ii) between the AS system and the anaerobic digester. This integration would provide a material mass balances steady state model for an entire WWTP, comprising any combination of primary sedimentation, AS and anaerobic or aerobic digestion.

Once the overall WWTP scheme is established and the main system defining parameters of the individual unit operations estimated, more complex kinetic simulation models can be applied to the individual unit operations to refine their design and evaluate their performance under cyclic flow and load conditions.

2.4 SINGLE PHASE BIOLOGICAL PROCESS KINETIC MODEL

2.4.1 Introduction

Two kinds of mathematical models are generally developed for the mathematical modelling of WW treatment systems. These two models are (i) the steady state model and (ii) the dynamic model. The steady state models have constant flows and loads and they tend to be relatively simple mathematical models, which makes them useful for design purposes. In steady state models complete descriptions of system parameters are not required, because the models are orientated more towards determining the important system design parameters. Dynamic models on the other hand have varying flows and loads and accordingly include time as a parameter, which makes dynamic models generally more complex than the steady state ones. The dynamic models are useful in predicting time dependent system responses of existing or proposed WWTPs, however the complexity of the dynamic models means that for application, the system parameters have to be completely defined.

While a simpler steady state model is useful to determine the required design parameters for a particular WW treatment system, a more complex dynamic model which requires the design parameters obtained from the corresponding steady state model as input, is useful because it may:

(i) Provide information that is not apparent from laboratory or pilot scale investigations.

(ii) Provide additional information / solutions that were not covered by laboratory, pilot scale

or other studies.

(iii) Help identify areas that require further research, thereby guiding the selection of laboratory or pilot scale work; This can be particularly useful if the system under investigation is a complex one.

(iv) Assist in identifying parameters that significantly influence a systems response.

(v) Help in evaluating a system design under dynamic flow and load conditions that will be encountered at full scale.

(vi) Assist in identifying possible causes for an existing full scale system malfunction, failure and/or poor performance, i.e. it may be very useful as a diagnostic and trouble shooting tool.

Numerous dynamic single phase biological processes kinetic models for the N removal AS system have been developed in the past (e.g. Dold *et al.*, 1980, 1991; Henze *et al.*, 1987). The dynamic activated sludge system model incorporated into the UCTOLD program (Dold *et al.*, 1991) reviewed above, was selected and coded into the simulation program AQUASIM (Reichert, 1998). This model was chosen because it was comprehensively validated against experimental data in earlier research at UCT (Dold *et al.*, 1980; van Haandel *et al.*, 1981 and Warner *et al.*, 1986) and was built on the Marais and Ekama (1976) steady state model which formed the basis of the steady state mass balances spreadsheet described earlier in this Chapter.

The matrix representation of the dynamic activated sludge system model incorporated into the UCTOLD program (Dold *et al.*, 1991) is shown in Figure 2.1 below. This dynamic model includes COD and N removal only and not BEPR. The matrix was coded into AQUASIM (Reichert, 1998) as it is shown in Figure 2.1 with no amendments, other than the omission of the compound Alk (Compound 12 in Figure 2.1). The compound 'alkalinity' was omitted since it is not required for a comparison with the results for the steady state mass balances spreadsheet, because in its current form the spreadsheet does not include the alkalinity. The remaining 13 state variables and the 14 processes together with the associated stoichiometry and kinetic process rates were entered into AQUASIM (Reichert, 1998).

2.4.2 The Dynamic Activated Sludge System Model (UCTOLD, Dold *et al.*, 1991) Coded In AQUASIM (Reichert, 1998)

The model was programmed into AQUASIM (Reichert, 1998) in such a way, that the input required to fully characterize the WW is limited to the total influent COD concentration (S_{ti}), total influent TKN concentration (N_{ti}) and FSA concentration (N_{ai}). The characterization is then performed by the program, using the applicable fractions (e.g. the fraction of the influent that is unbiodegradable particulate, f_{up}) in the same way that the characterization is done in the steady state mass balances spreadsheet.

AQUASIM (Reichert, 1998) provides only completely mixed reactors and makes no provision for settling tanks or sludge thickeners. The settling tanks and thickeners are simulated as follows:

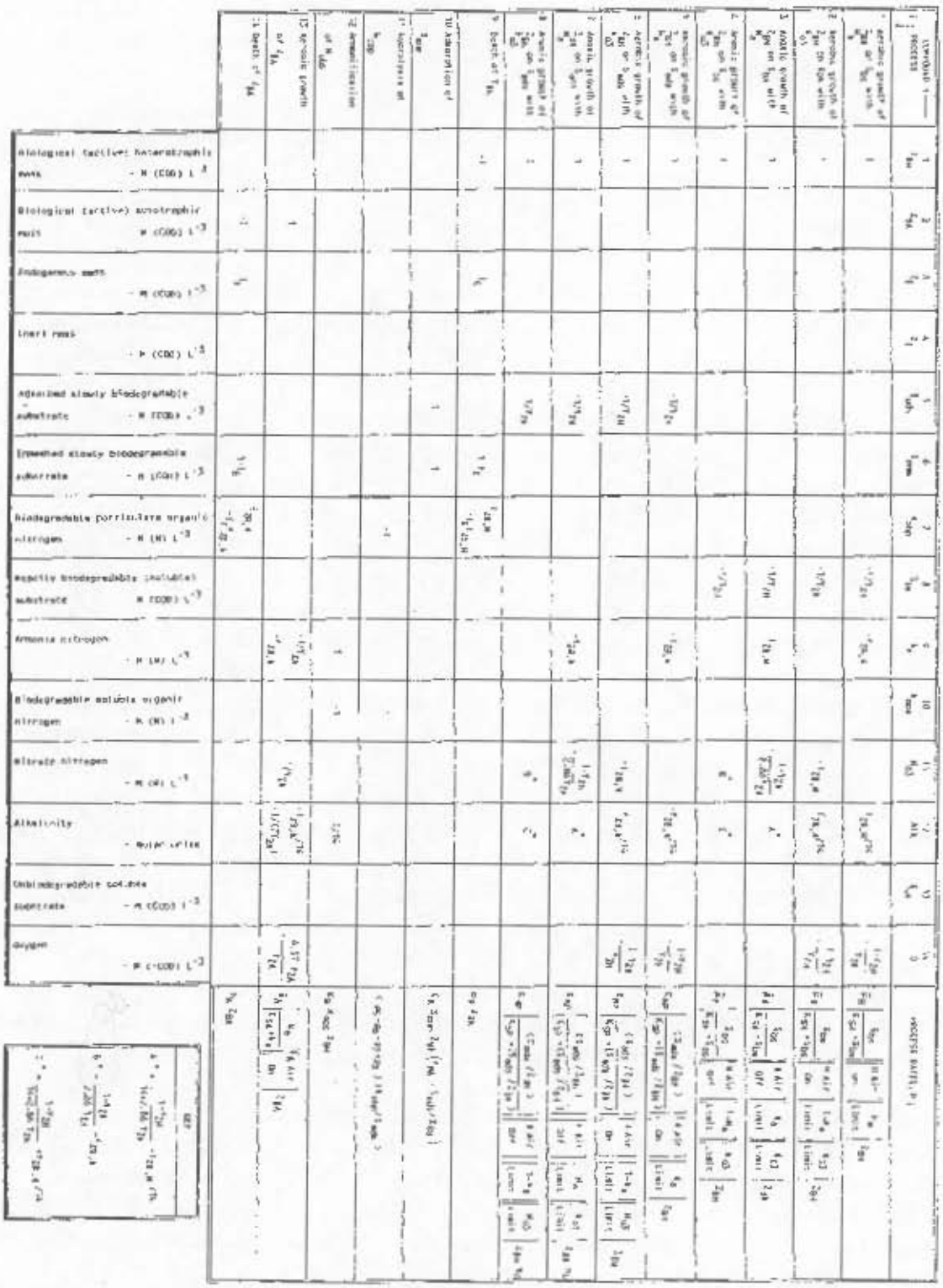

Figure 2.1: Matrix representation of the UCTOLD dynamic model (Dold *et al.*, 1991)

(i) Secondary settling tank: The secondary settling tank is simulated as a completely mixed reactor, which has a very small volume (1 unit of volume). A bifurcation from the link that connects the secondary settling tank to the effluent, routes all the particulate material back to the beginning of the system (i.e. the bifurcation simulates the sludge return), while the dissolved material remains as effluent. In effect this setup acts as a secondary settler that is 100% efficient, i.e. no solid material leaves the system with the effluent.

(ii) Primary settling tank: The primary settling tank is simulated in the same way as the secondary settling tank in (i) above, however for the primary settling tank a bifurcation is taken from the link between the primary settling tank and the AS reactor. Effectively the raw WW flows through the primary settling tank and is separated into settled WW and PS at the bifurcation, which routes the PS (raw WW concentrations less the settled WW concentrations) away from the primary settling tank/AS reactor link, leaving only the settled WW (concentrations) to continue into the AS reactor.

(iii) Sludge thickener: The sludge thickener is again simulated in the same way as the settling tanks in (i) and (ii) above. A bifurcation is taken from the link between the thickener and the unit process that is fed by the thickener. This bifurcation routes the supernatant flow containing only dissolved material away from the link, which results in thickened flow only in the link. The supernatant abstraction rate has to be calculated manually, from the degree of thickening required.

No modifications needed to be made for the simulation of the aerobic digester. Since the aerobic digester is simply an aerated reactor with the same processes active that are active in the AS reactor, the simulation of an aerobic digester in AQUASIM (Reichert, 1998) is straight forward.

In order to simulate aerobic reactors, an aeration process had to be added, which can be activated for aerobic reactors and deactivated for all other reactors. The aeration process was described by the following process rate:

$$dO/dt = K_{LA}(O_{sat} - O) \qquad (2.55)$$

where K_{LA} = Oxygen mass transfer coefficient
O_{sat} = Oxygen saturation concentration
O = Dissolved oxygen concentration

The K_{LA} was calibrated to a value so that the residual dissolved oxygen concentration in the aerobic reactor bulk liquid was approximately equal to 2 mgO/ℓ.

Once the model was completely coded into AQUASIM (Reichert, 1998), flow balances as well as COD and N mass balances were performed to check for possible errors in programming. The flow balance and the COD and N mass balances must be 100%, if they are not 100%, it is indicative of an error in the programming of the model. With the dynamic activated sludge UCTOLD model and the system design parameters programmed into AQUASIM, a number of simulations were performed and the results compared to the results calculated from the steady state spreadsheet.

2.4.3 Comparison of the Results Calculated by the Steady State Mass Balances Spreadsheet and the Dynamic Activated Sludge Model (UCTOLD, Dold *et al.*, 1991)

The UCTOLD (Dold *et al.*, 1991) Aquasim (Reichert, 1998) dynamic simulation model was set up for the raw and settled WW treatment plants shown in Figure 2.2 below. This plant includes thickening and aerobic digestion of PS and WAS to compare the results with the output from the steady state mass balances spreadsheet. The raw wastewater entering the primary settling tank (PST) exits the PST as settled wastewater, which flows into the AS reactor. The primary sludge is thickened and blended with the thickened waste activated sludge. The blended sludge flows into the aerobic digester for sludge stabilisation. The influent (raw) and settled wastewater characteristics and the design and operating parameters are listed in Tables 2.3 and 2.4 respectively.

From the wastewater characteristics and the design and operating parameters, the steady state spreadsheet calculates the following parameters for the treatment plant (see also Figure 2.2):

Primary Sludge:

(i) Flow from PS thickener 53 m^3/d at 6% TSS concentration.

Activated sludge:

(i) Reactor volume 3531 m^3 at 8d sludge age, 14°C and 4 gTSS/ℓ concentration
(ii) Waste flow 441 m^3/d
(iii) Flow from WAS thickener 35 m^3/d at 5% TSS concentration.

Aerobic digester:

(i) Influent flow 88 m^3/d at 5.6% TSS concentration
(ii) 16 day retention time for required effluent active fraction with respect to VSS ($f_{a,v}$) = 0.235
(iii) Reactor volume (88 m^3/d x 16 d) 1404 m^3.

The above parameters are required as input to the model, hence the values of steady state models.

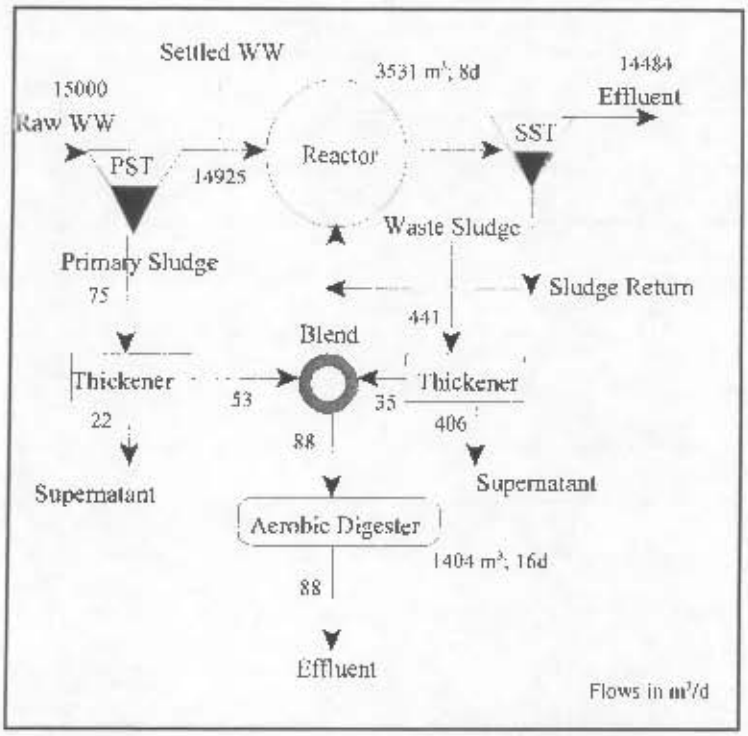

Figure 2.2: Schematic of the WWTP modelled using the steady state mass balances spreadsheet and ASM#1.

This model was used to simulate the performance of the wastewater treatment plant (Figure 2.2) for constant flow and load conditions, to enable the results to be compared directly with the results obtained from the steady state mass balances spreadsheet. Table 2.5 shows the results from the steady state mass balances spreadsheet and the results obtained from the dynamic UCTOLD (Dold *et al.*, 1991) model.

From Table 2.5 it can be seen that the dynamic model gives virtually identical results for all the effluent AS and aerobic digester COD, TKN, FSA, TP, OP, VSS, ISS and TSS concentrations. Small differences are evident, for example the slightly lower carbonaceous OUR of the dynamic model (43.5 vs. 44.4 mgO/lreactor/hr). The lower OUR result from the dynamic model can be attributed to the fact that in the dynamic model, not all biodegradable COD is utilised: A fraction remains as adsorbed COD on the organisms, while another small fraction remains enmeshed in the sludge. This is in contrast with the steady state model, where it is assumed that all biodegradable COD is utilised, resulting in a higher carbonaceous OUR. This difference can be expected to increase with decreasing sludge age, because the lower the sludge age, the less time is available to the organisms in the dynamic model to utilize the available COD, hence more of the biodegradable COD will remain enmeshed in the sludge.

Table 2.3: Raw and settled wastewater characteristics.

	RAW WASTEWATER	SETTLED WASTEWATER
Influent flow (Mℓ/d)	15.000	14.925
COD (mgCOD/ℓ):		
Sti	750.0	450.0
Sbsi	146.0	146.0
Sbpi	439.0	233.5
Susi	52.5	52.5
Supi	112.5	18.0
TKN (mgN/ℓ):		
Nti	60.0	51.0
FSA	45.0	45.0
Nobsi	1.7	1.7
Nobpi	3.9	1.3
Nousi	1.8	1.8
Noupi	7.6	1.2

Table 2.4: System design and operating parameters.

	WASTEWATER
Min.; Max. Temperature (°C)	14°; 22°
Characteristics	See Table 2.3
	ACTIVATED SLUDGE SYSTEM
Influent flow (Mℓ/d)	14.925
Sludge age (d)	8
Design reactor concentration (kgTSS/ℓ)	4.0
Aeration power (kWh/kgO)	1.20
	AEROBIC DIGESTER
Effluent active fraction	0.235
Aeration power (kWh/kgO)	1.20
	PS THICKENER
Effluent sludge concentration (kgTSS/ℓ)	60.0
	WAS THICKENER
Effluent sludge concentration (kgTSS/ℓ)	50.0

A further difference in the results of the steady state model and the UCTOLD (Dold *et al.*, 1991) model can be seen in the effluent nitrogen compounds. The effluent TKN from the dynamic model is higher than that from the steady state mass balances model, while the converse is true for the nitrate, which is expected. The higher effluent TKN from the dynamic model is a result of a higher effluent FSA and a higher effluent soluble biodegradable organic N, compared to the effluent from the steady state model. In the steady state model it is assumed that all the biodegradable organic N is converted to FSA, as for the biodegradable COD. This is not the case for the dynamic model. Therefore in the dynamic model, there is an effluent soluble biodegradable organic N, which in the steady state model is zero. This, combined with the fact that for the dynamic model there is residual biodegradable particulate COD, which contains N, enmeshed in the sludge and adsorbed on the organisms, results less N being nitrified in the dynamic model, which leads to a lower effluent nitrate concentration.

In the UCTOLD dynamic model simulations of nitrifying aerobic digestion of waste activated sludge, nitrate utilization for ordinary heterotrophic organism (OHO) growth can occur even when there is sufficient ammonia available (this will not happen in ASM1 because ASM1 does not include heterotrophic growth on nitrate as N source, only ammonia). In UCTOLD this happens because the rate of nitrification is faster than the rate of OHO growth, which is limited by the supply rate of SBCOD from the OHO death process. This leads to the uptake of nitrate for OHO growth but the release of ammonia in OHO death. This released ammonia is then nitrified with an associated OUR for nitrification. The consequence is an artificially high nitrification OUR from the continual supply of ammonia nitrogen from the death process, N that was taken up by the OHOs as nitrate. This problem can be eliminated in the dynamic model by reducing the switching function K value which controls the switch from ammonia to nitrate uptake for OHO growth to a very low value (0.0001). This stops the OHO growth process from slowing down when the ammonia concentration gets low, allowing it to successfully 'compete' for ammonia against the nitrification process. In aerobic digestion of waste activated sludge, there is always sufficient ammonia for growth because the ammonia released in OHO death is always greater than that taken up for OHO growth on the SBCOD released in OHO death. The same problem can happen with aerobic digestion of primary sludge, even when sufficient ammonia is dosed for sludge production from the primary sludge particulate biodegradable organics. This problem therefore has nothing to do with ammonia deficiency but everything to do with the relative rates of processes competing for the same compounds, in this case ammonium (NH_4^+). *K values of switching functions on processes competing for the same compounds are therefore very import to watch in dynamic modelling of aerobic digestion.*

Overall there is very close correlation between the formal complex dynamic simulation WWTP model in which the UCTOLD (Dold *et al.*, 1991) model is used to model the AS and aerobic digestion systems and the much simpler steady state model programmed into the spreadsheet described here in this Chapter.

Table 2.5: Simulated results of the WWTP shown in Figure 2.2 from the steady state mass balances spreadsheet and the UCTOLD (Dold *et al.*, 1991) model.

COMPOUND	UNITS	STEADY SATE MODEL	ASM#1
Activated Sludge (14°C)			
Reactor active organism conc.	mgVSS/ℓ	2207	2273
Reactor endogenous residue conc.	mgVSS/ℓ	714	729
Reactor inert organic conc.	mgVSS/ℓ	411	411
Reactor volatile solids conc.	mgVSS/ℓ	3333	3413
Reactor inorganic solids conc.	mgVSS/ℓ	667	667
Reactor total solids conc.	mgTSS/ℓ	4000	4080
Active fraction (w.r.t. VSS)	-	0.662	0.666
Effluent soluble COD	mgCOD/ℓ	52.50	52.50
Effluent soluble biodegradable organic N	mgN/ℓ	0.00	1.20
Effluent soluble unbiodegradable organic N	mgN/ℓ	1.80	1.80
Effluent FSA	mgN/ℓ	0.01	1.21
Effluent TKN	mgN/ℓ	1.81	4.21
Effluent NO_3	mgN/ℓ	42.30	36.30
Carbonaceous OUR	mgO/ℓreactor/h	44.4	43.5
Nitrification OUR	mgO/ℓreactor/h	31.7	28.4
Total OUR	mgO/ℓreactor/h	76.1	71.9
Aerobic Digester (14°C)			
Effluent active organism conc.	mgVSS/ℓ	6382	6652
Effluent endogenous residue conc.	mgVSS/ℓ	4132	4435
Effluent inert organic conc.	mgVSS/ℓ	16630	16630
Effluent volatile solids conc.	mgVSS/ℓ	27144	27717
Effluent inorganic solids conc.	mgVSS/ℓ	10316	10316
Effluent total solids conc.	mgTSS/ℓ	37460	38033
Active fraction (w.r.t. VSS)	-	0.235	0.239
Effluent soluble COD	mgCOD/ℓ	52.50	52.50
Effluent soluble biodegradable organic N	mgN/ℓ	0.00	1.20
Effluent soluble unbiodegradable organic N	mgN/ℓ	1.80	1.80
Effluent FSA	mgN/ℓ	0.00	0.05
Effluent soluble TKN	mgN/ℓ	1.80	3.05
Effluent NO_3	mgN/ℓ	536.00	528.20
Carbonaceous OUR	mgO/ℓreactor/h	94.4	94.8
Nitrification OUR	mgO/ℓreactor/h	6.2	6.0
Total OUR	mgO/ℓreactor/h	100.6	100.8

2.5 CLOSURE

The steady state mass balances spreadsheet described in this Chapter is capable of the following:

(i) Characterizes the raw and settled WWs COD, TKN, FSA, TP and OP, each into their unbiodegradable and biodegradable soluble and particulate components, from the given (measured) concentrations and fractions and PS COD, VSS, ISS, TSS, OrgN, OrgP, also each into their unbiodegradable and biodegradable soluble and particulate components from mass balances around the PST.

(ii) Calculates the design parameters for the fully aerobic, ND or ND BEPR systems treating the raw and settled WW at long and short sludge ages respectively.

(iii) Calculates the design parameters for a single reactor aerobic digester by taking the PS and WAS flows and concentrations (including the liquid stream), blending and concentrating them to the selected thickened concentrations, aerobically digesting the blended and thickened sludge to a selected residual biodegradable organic content. Checks material mass balances (COD, N and P) over the aerobic digester.

(iv) Explores aerobic digestion of fully aerobic and ND WAS sludge in single, double and triple compartment digesters with and without PS and with separate PS and WAS thickening before blending.

(v) Checks the COD, N and P mass balances around the WWTP comprising (i) raw WW treatment in a long sludge age AS system, where the sludge age is selected long enough for sludge stabilization in the reactor and direct discharge of WAS to drying beds (i.e. extended aeration), and (ii) PSTs, short sludge aged activated sludge system, PS and WAS thickening and aerobic digestion of PS and WAS to the same residual biodegradable organics as (i) above.

This steady state mass balances spreadsheet brings a step closer the modelling of a WWTP as a whole, in an integrated fashion. The steady state mass balances spreadsheet includes a link (i) between the primary settler and the aerobic digester and (ii) between the AS system and the aerobic digester which assess and quantify the interdependencies of the PS, AS and anaerobic digester unit operations.

For the steady state mass balances spreadsheet to model an entire WWTP, the following still need to be integrated:

(i) The anaerobic digestion of the sewage sludges: A steady state model for anaerobic digestion of sewage sludges has been developed (see Chapter 5), and this needs to be included in the mass balances tracking model. This will require that the inputs required for the anaerobic digestion model (i.e. the sludge characteristics) be included in the upstream unit operations. In addition to the parameters already in the mass balances model, this will include C, alkalinity and possible short chain fatty acid production in the PST.

(ii) Recycling of various liquors (e.g. sludge thickening liquors) from downstream unit operations to upstream ones, and the characteristics of these recycle stream would have to be included.

This Chapter shows further, that there is a close correlation between the formal complex dynamic simulation WWTP model in which UCTOLD (Dold *et al.*, 1991) is used to model the AS and aerobic digester systems and the much simpler steady state model programmed into the spreadsheet described here.Only one parameter had to be changed in the UCTOLD (Dold *et al.*, 1991) model, i.e. the K value of the switching function for the nitrogen requirement for aerobic growth from 0.10 to 0.0001 mgN/ℓ. This switching function controls the uptake of FSA for growth, and if insufficient, allows nitrate to be taken up instead.

In moving towards developing an integrated *steady state* mass balances model for an entire WWTP system, implicitly there is a need to develop a similar integrated *dynamic* model for an entire WWTP system that is built up around the same mass balances principle of the steady state mass balances model and that is able to track the same compounds that are tracked in the steady state model across the same unit processes links, i.e. the links between the most common unit operations of a WWTP:

(i) The PST - anaerobic digester link
(ii) The AS system - aerobic digester link
(iii) The AS system - anaerobic digester link
(iv) The PST - aerobic digester link

The following Chapter (Chapter 3) outlines the modifications to an existing AS dynamic model, so that it can be integrated into a dynamic model for an entire WWTP, i.e. an existing activated sludge model is modified to include the specific compounds in the phases that they occur so that the resulting modified dynamic AS model can link up with the dynamic models of other unit processes (e.g. link (ii) and (iii) above) to make up a dynamic model of an entire WWTP.

CHAPTER 3

INTEGRATED BIOLOGICAL, CHEMICAL AND PHYSICAL PROCESSES KINETIC MODELLING: ANOXIC-AEROBIC C AND N REMOVAL IN THE ACTIVATED SLUDGE SYSTEM

3.1 INTRODUCTION

A number of mathematical models describing the kinetics of the biological processes for carbon (C), nitrogen (N) and phosphorus (P) removal by the activated sludge system have been developed, e.g. the C and N removal models of van Haandel *et al.* (1981) and Activated Sludge Model No.1 (ASM1, Henze *et al.*, 1987), and the C, N and P removal models UCTPHO (Wentzel *et al.*, 1992) and ASM2 and 2d (Henze *et al.*, 1995, 1999). These models are commonly used in research, design, operation and system development and can be coded into computer shell packages such as ASim (Gujer, 1998) and Aquasim (Reichert, 1998) and various versions of them are commercially available.

In all these models, it is assumed that the biological processes operate in an aqueous phase of constant pH, i.e. that there is sufficient buffer capacity in the aqueous phase to absorb or supply the protons (H^+) required or generated directly or indirectly (via e.g. the weak acid/base species) by the biological processes without a change in pH. For most applications with municipal wastewater, where the concentrations of C, N and P are low, this is a reasonable assumption. In fact, in some models, the parameter Alkalinity is included to check that this condition remains true (e.g. ASM1, Henze *et al.*, 1987; UCTOLD and IAWPRC, Dold *et al.*, 1991). However, in the treatment of a number of wastewaters this assumption is not valid, e.g. in the nitrification of wastewaters with low buffer capacity and/or high nitrogen (N) concentrations, or in the treatment of wastewaters where the generation or utilisation of short-chain fatty acids (SCFA) is significant.

In this Chapter, the biological processes of C and N removal in activated sludge systems are integrated into the three phase mixed weak acid/base chemical-physical kinetic model developed by Musvoto *et al.* (1997, 2000a,b,c). This chemical-physical model includes kinetic descriptions for (i) the ionic equilibrium reactions of the important weak acid/base systems that govern pH in wastewater treatment systems, i.e. the ammonia, carbonate (inorganic carbon), short chain fatty acid (SCFA), phosphate and water systems, (ii) CO_2 and NH_3 gas exchange between aqueous and gas phases, (iii) ion pairing and (iv) precipitation of common minerals associated with Calcium (Ca), Magnesium (Mg), carbonate and phosphate system species. Because in the activated sludge system, mineral precipitation usually is not significant, only parts (i) and (ii) of the model, i.e. the aqueous and gas phase processes, are considered. Furthermore, because of the complex interaction between pH and biological excess P removal (BEPR), only the biological processes of C and N removal are included into the integrated model at this stage. By incorporating the two phase mixed weak acid/base kinetic model into the ASM1 dynamic model (Dold *et al.*, 1991), an interface is provided for the addition of a anaerobic digestion kinetic model to be added, which represents a significant step forward towards an integrated kinetic model for an entire

wastewater treatment system by providing the anaerobic digester - activated sludge system link. In Chapter 4, the biological processes of anaerobic digestion are incorporated into the model, but initially also only in two (aqueous-gas) phases.

3.2 LITERATURE REVIEW

3.2.1 The IAWPRC Dynamic Activated Sludge Model

The ASM1 dynamic model (formerly IAWPRC model in Dold *et al.*, 1991) is based largely on the UCTOLD model (Dold *et al.*, 1991) which is reviewed in Chapter 2 of this thesis. While the ASM1 model (Henze *et al.*, 1987) is similar to the UCTOLD model, two conceptual changes were implemented in (i) the enmeshment / storage and (ii) in the hydrolysis hypotheses, by a Task Group appointed to review activated sludge system modelling.

The ASM1 model also includes the concept of instantaneous enmeshment of the influent particulate material by the sludge mass as included in the UCTOLD model. However, it does not incorporate the concept of slowly biodegradable COD (SBCOD) adsorption onto the organism itself. Instead it proposed that the ordinary heterotrophic organisms (OHOs) release enzymes into the bulk liquid, and these enzymes hydrolyse the enmeshed SBCOD to readily biodegradable COD (RBCOD), adding to the RBCOD from the influent flow (i.e. adding to the RBCOD pool available in the bulk liquid). The OHOs then utilise the RBCOD in the bulk liquid for organism synthesis. The second concept not incorporated in ASM1 is that of nitrate utilisation as N source for OHO growth. In the UCTOLD model, when the ammonia concentration in the bulk liquid approaches zero, nitrate is used as the N source for OHO synthesis. This concept was included in a later version of ASM1 (Dold *et al.*, 1991) which is the version that is reviewed here.

The biological processes and their interactions with the compounds that are incorporated in the Dold *et al.* (1991) ASM1 version used in this integrated chemical, physical and biological model task are described below (see Fig. 3.1):

In the IAWPRC model, the OHOs grow on RBCOD only:

Aerobic growth of heterotrophs:
RBCOD from the influent and RBCOD generated from the hydrolysis of SBCOD are removed under aerobic conditions. A fraction of the RBCOD is utilized for cell mass (growth) and the remainder is oxidized for energy, giving rise to an associated oxygen demand. Growth of the organisms is modelled by Monod kinetics. The N source for synthesis is either ammonia or nitrate. Ammonia is utilized first, and once the ammonia concentration in the bulk liquid reduces to near zero, nitrate is utilized as an alternative N source. This results in two processes describing aerobic growth of heterotrophs: One utilising ammonia as the N source (Process 1), the other utilizing nitrate (Process 2). In the model, this is facilitated by a switching function that is dependent on the ammonia concentration in the bulk liquid. As the ammonia concentration in the bulk liquid approaches zero, Process 1 is switched off (i.e. the increase in organism mass by Process 1 equals zero) and simultaneously Process 2 is switched on. Should both the ammonia and the nitrate be depleted, both processes are switched off. To ensure that Processes 1 and 2 are active only in the presence of oxygen, a further switching function is incorporated that switches both processes off if the dissolved oxygen concentration reduces to zero and a switch is made to

anoxic growth of heterotrophs.

Anoxic growth of heterotrophs:
In the absence of oxygen, the heterotrophic organisms use nitrate as terminal electron acceptor and RBCOD as substrate. As for the aerobic growth of heterotrophs described above, anoxic growth is modelled by Monod kinetics, and two processes describe anoxic growth of heterotrophs: One utilising ammonia as the N source (Process 3), the other utilizing nitrate (Process 4), and both are controlled by a switching function dependent on the ammonia concentration, which switches the processes on or off depending on the ammonia concentrations in the bulk liquid. To ensure that Processes 3 and 4 are active only in the presence of nitrate in the bulk liquid, a further switching function dependent on the nitrate concentration is incorporated, that switches both processes off if the nitrate concentration reduces to zero.

Death of heterotrophs:
The death process of heterotrophs (Process 5) is modelled according to the death-regeneration hypothesis. When the organisms die, a portion of the cell material is unbiodegradable and adds to the unbiodegradable endogenous residue concentration in the bulk liquid. The remaining fraction of the dead cell mass adds to the SBCOD pool in the bulk liquid, from where it will be hydrolysed to RBCOD and utilised by other organisms as substrate for growth and energy. The death process is active under anaerobic, anoxic and aerobic conditions.

Hydrolysis of SBCOD to RBCOD:
SBCOD from the influent and from the death of the heterotrophs in the system is enmeshed in the sludge and broken down by enzymes that are released into the bulk liquid by the heterotrophs. This hydrolysis (Process 6) is modelled on the basis of Levenspiel's surface reaction kinetics, and it occurs only under aerobic or anoxic conditions. Under anoxic conditions the hydrolysis rate is reduced compared to the hydrolysis rate in the presence of oxygen, and to account for the reduced anoxic hydrolysis, the aerobic hydrolysis rate is multiplied by a factor (η_s). A switching function dependent on the oxygen and nitrate concentrations ensures that the hydrolysis process occurs only under aerobic and anoxic conditions.

Hydrolysis of particulate organic nitrogen:
The N content of the SBCOD is broken down (Process 7) to soluble organic N at the rate defined by the hydrolysis of SBCOD to RBCOD above. The soluble organic N that is release adds to the pool of soluble organic N in the bulk liquid.

Ammonification of soluble organic N:
The biodegradable soluble N is converted to free and saline ammonia (Process 8) by the heterotrophs. Because this process takes up hydrogen ions, it results in a change of the bulk liquid alkalinity.

j	PROCESS	1 Z_{BH}	2 Z_{BA}	3 Z_E	4 Z_I	5 S_{ams}	6 N_{obp}	7 S_{bs}	8 N_a	9 N_{obs}	10 N_{o3}	11 Alk	12 S_{us}	13 O	PROCESS RATES, ρ_j
1	Aerobic growth of Z_{BH} with N_a	1						$-1/Y_{ZH}$	$-i_{XB,N}$			$-i_{XB,M}/14$		$-\frac{1-Y_{ZH}}{Y_{ZH}}$	$\hat{\mu}_H \left[\frac{S_{bs}}{K_{SH}+S_{bs}}\right]_{On} \left[\frac{N_a}{Limit}\right] Z_{BH}$
2	Aerobic growth of Z_{BH} with N_{o3}	1						$-1/Y_{ZH}$			$-\frac{1-Y_{ZH}}{2.86Y_{ZH}}$	$i_{XB,M}/14$		$-\frac{1-Y_{ZH}}{Y_{ZH}}$	$\hat{\mu}_H \left[\frac{S_{bs}}{K_{SH}+S_{bs}}\right]_{On} \left[\frac{N_a}{Limit}\right] \left[\frac{N_{o3}}{Limit}\right] Z_{BH}$
3	Anoxic growth of Z_{BH} with N_a	1						$-1/Y_{ZH}$	$-i_{XB,M}$		$-\frac{1-Y_{ZH}}{2.86Y_{ZH}}$	$i_{XB,M}/14$			$\hat{\mu}_H \left[\frac{S_{bs}}{K_{SH}+S_{bs}}\right]_{Off} \left[\frac{N_a}{Limit}\right] \left[\frac{N_{o3}}{Limit}\right] Z_{BH} \eta_g$
4	Anoxic growth of Z_{BH} with N_{o3}	1						$-1/Y_{ZH}$			8*	C*			$\hat{\mu}_H \left[\frac{S_{bs}}{K_{SH}+S_{bs}}\right]_{Off} \left[\frac{N_a}{Limit}\right] \left[\frac{N_{o3}}{Limit}\right] Z_{BH} \eta_g$
5	Death of Z_{BH}	-1		f_E											$b_H Z_{BH}$
6	Hydrolysis of S_{ams}					-1		1							$K_H \left[\frac{(S_{ams}/Z_{BH})}{K_X+(S_{ams}/Z_{BH})}\right] \left[\left[\frac{N_a}{On}\right]_{Air} + \eta_g \left[\frac{N_a}{Off}\right]_{Air} \left[\frac{N_{o3}}{Limit}\right]\right] Z_{BH}$
7	Hydrolysis of N_{obp}						-1			1					$\rho_6 (N_{obp}/S_{ams})$
8	Ammonification of N_{obs}								1	-1		1/14			$K_a N_{obs} Z_{BH}$
9	Aerobic growth of Z_{BA}	1	1						$-1/Y_{ZA}$ $-i_{XB,M}$		$1/Y_{ZA}$	$-i_{XB,M}/14$ $-1/(7Y_{ZA})$		$-\frac{4.57-Y_{ZA}}{Y_{ZA}}$	$\hat{\mu}_A \left[\frac{N_a}{K_{SA}+N_a}\right] \left[\frac{A}{On}\right]_{Air} Z_{BA}$
10	Death of Z_{BA}	-1		f_E		$1-f_E$	$f_{XB,M}$ $-f_E i_{XE,M}$								$b_A Z_{BA}$

KEY	
$A^* = \frac{1-Y_{ZH}}{14\times2.86\,Y_{ZH}} - i_{XB,M}/14$	
$B^* = \frac{1-Y_{ZH}}{2.86\,Y_{ZH}} - i_{XB,M}$	
$C^* = \frac{1-Y_{ZH}}{14\times2.86\,Y_{ZH}} + i_{XB,M}/14$	

Figure 3.1: IAWPRC process model (Dold *et al.*, 1991) in matrix form.

Aerobic growth of autotrophs:
Ammonia is oxidized to nitrate in a single step, resulting in the growth of autotrophic organisms (Process 9). The growth of autotrophic organisms results in an associated oxygen demand. As the process requires the presence of oxygen as terminal electron acceptor, a switching function that depends on the dissolved oxygen concentration of the bulk liquid switches the process off when the dissolved oxygen concentration reaches near zero. As with heterotrophic organism growth, ammonia is utilised as the N source for organism growth.

Death of autotrophs:
Autotroph death (Process 10) is modelled in the same way as heterotrophic organism death.

The IAWPRC process model is presented in matrix format in Figure 3.1 above. This dynamic model is the basis of the 2 phase integrated biological, chemical and physical dynamic model developed in this Chapter.

3.2.2 Mathematical Modelling of Mixed Weak Acid/Base Systems

Traditionally, an equilibrium chemistry based approach that includes the mass parameter of alkalinity for the weak acid/bases species, has formed the basis on which most chemical conditioning (determining the chemical type and dosing to achieve a final state or conversely to determine the final state of a water after addition/removal of a known amount of a specified chemical) algorithms have been developed (e.g. Loewenthal *et al.*, 1991). However, in reviewing this approach to develop an integrated chemical/physical/biological kinetic model for the treatment of high nutrient (N and P) low organic (COD) wastes, Musvoto *et al.*, (1997) noted that the equilibrium chemistry approach, although possibly feasible, presented a number of practical difficulties in implementation, because of the presence of a number of weak acid/bases and a number of processes acting simultaneously on the species concentrations of these weak acid/bases. They therefore concluded that this makes selection of reference species required for the solution procedure to solve the repeated calculations necessary to reach steady state very difficult and cumbersome.

To overcome these difficulties, Musvoto *et al.*, (1997) developed a kinetic approach to modelling mixed weak acid/base systems. In this approach, the weak acid/base equilibria are formulated in terms of the kinetics of the forward and reverse reactions for dissociation. This enabled the parameter H^+ and all the individual weak acid/base systems to be explicitly included in the model so that pH could be calculated directly from $pH = -\log(H^+)$. Musvoto *et al.*, (1997) noted that the advantages of the kinetic approach over the more traditional equilibrium based approach are that kinetics are used throughout and this expedites integration of weak acid/base processes with existing biological kinetic models, and that the approach is general and can be applied to include any weak acid/base of interest. Musvoto *et al.*, (1997) evaluated the kinetic approach to modelling mixed weak acid/base systems by comparing the predicted results with such a model to predictions with equilibrium chemistry based models; very close correspondence was achieved.

The Musvoto *et al.*, (1997) kinetic model for mixed weak acid/base systems is reviewed in more detail below, because this same approach was followed to develop the integrated chemical, physical and biological processes activated sludge model.

From the discussion above, it is evident that the principal requirement for a mixed weak acid/base chemistry model is that the pH is explicitly incorporated and accurately determined. In the kinetics based model, H^+ is included explicitly in the model as a compound (in mole units); pH can be calculated directly from H^+ via $pH = -\log(H^+) = -\log f_m.[H^+]$. Further, all weak acid/base species that significantly influence the pH are included as compounds (in mole units). The weak acid/base equilibria are described in terms of the kinetics of the forward and the reverse dissociation reactions. For example, consider the $H_2CO_3^*/HCO_3^-/CO_3^{2-}$ weak acid/base system:

The dissociation equation for $H_2CO_3^*/HCO_3^-$ subsystem is given by:

$$H_2CO_3^* \leftrightarrow HCO_3^- + H^+ \tag{3.1}$$

The rate of the forward reaction is:

$$r_f = K_{fcl}(H_2CO_3^*) = K_{fcl} \cdot f_m \cdot [H_2CO_3^*] = K'_{fcl}[H_2CO_3^*] \tag{3.2}$$

where:

r_f = rate of forward reaction
K_{fcl} = specific rate constant for the forward reaction
() = activity
f_m = monovalent activity coefficient
[] = molar concentration
K'_{fcl} = apparent specific rate constant for forward reaction

And the rate of the reverse reaction is:

$$r_r = K_{rcl}(HCO_3^-)(H^+) = K_{rcl} \cdot f_m \cdot [HCO_3^-] \cdot f_m \cdot [H^+] = K'_{rcl}[HCO_3^-][H^+] \tag{3.3}$$

where

r_r = rate of reverse reaction
K_{rcl} = specific rate constant for the reverse reaction
f_m = monovalent activity coefficient
K'_{rcl} = apparent specific rate constant for the reverse reaction.

The dissociation equation for the $H_2CO_3^*/HCO_3^-$ weak acid/base subsystem can be represented by these two half-reactions and both kinetic equations are modelled as separate processes. Similarly, the kinetics of the forward and reverse dissociation equations for any other weak acid/base species of importance can be included in a model.

The apparent specific rate constants of the forward and reverse dissociation reactions are selected such that the rates are so rapid that the equilibrium can be considered to be reached effectively

instantaneously. Since H^+ (and correspondingly pH) is included as a compound in the model, and also in the kinetic equations for the forward and reverse dissociation reactions, its value can be calculated at any given time. If any of the weak acid/base species are added or removed from the solution (e.g. by biological processes occurring in the bulk liquid), the kinetic equations for the forward and the reverse dissociation reactions will cause the relative species concentrations (including H^+) to readjust very rapidly (effectively instantaneous) to the new condition. Since all the weak acid/bases have the H^+ species in common, all would be influenced and would thus readjust. The apparent specific rate constants that operate under true equilibrium conditions may be calculated from the corresponding equilibrium constants. Continuing with the same $H_2CO_3^*/HCO_3^-$ subsystem above:

$$r_f = r_r \tag{3.4}$$

at equilibrium (from the law of mass action) and so

$$K'_{fc1}[H_2CO_3^*] = K'_{rc1}[HCO_3^-][H^+] \text{ and therefore} \tag{3.5}$$

$$\frac{K'_{fc1}}{K'_{rc1}} = \frac{[HCO_3^-][H^+]}{[H_2CO_3^*]} = K_{c1} \tag{3.6}$$

where K_{c1} is the equilibrium constant for the $H_2CO_3^*/HCO_3^-$ subsystem. To obtain the apparent equilibrium constant (K'_{c1}) for the $H_2CO_3^*/HCO_3^-$ subsystem:

$$\frac{f_m[HCO_3^-]f_m[H^+]}{[H_2CO_3^*]} = K_{c1} \text{ and therefore} \tag{3.7}$$

$$\frac{[HCO_3^-][H^+]}{[H_2CO_3^*]} = \frac{K_{c1}}{f_m^2} = K'_{c1} \tag{3.8}$$

where f_m = monovalent activity coefficient.

Because the forward and reverse reactions occur almost instantaneously, they cannot be measured in practice; Their exact values however have little bearing from a practical point of view. In order to ensure that the reactions are effectively instantaneous, the reverse rate constant (K'_r) is given a very high theoretical value to ensure that the new equilibrium is reached in a very short period of time - as short as three seconds. The value of the forward rate constant (K'_f) is then calculated through the relationship with the apparent equilibrium constant (K'_{c1}, Equations 3.6, 3.7 and 3.8) so that the modelled kinetic equilibrium will correspond to the equilibrium chemistry:

$$K'_{fc1} = K'_{rc1}K'_{c1} = K'_{rc1} \cdot \frac{10^{-pKc1}}{f_m^2} \tag{3.9}$$

where pK_{c1}=3404.7/T - 14.8435 + 0.03279T (Loewenthal *et al.*, 1989) where T is the temperature in Kelvin.

The advantage of this approach over the alkalinity/equilibrium chemistry approach is that kinetics are used throughout, which means that this approach can easily be incorporated into computer simulation packages such as AQUASIM (Reichert *et al.*, 1998). Moreover, the approach is general, which means it can be applied to include any weak acid/base system in the model.

Musvoto *et al.*, (1997) also developed rate equations for NH_3 and CO_2 stripping and integrated them with their aqueous phase weak acid/base kinetic model to produce a combined aqueous/gas phase kinetic model. Musvoto *et al.*, (1997) stated that CO_2 exchange occurs when (i) aeration is the driving force, stripping the dissolved CO_2 from the bulk liquid and (ii) whenever there is a difference in the partial pressure of the CO_2 dissolved in the liquid and the partial pressure of CO_2 gas in the atmosphere or headspace: This pressure difference drives CO_2 exchange across the liquid/gas interface (expulsion/diffusion) until an equilibrium is reached. Musvoto *et al.*, (1997) represented the latter CO_2 exchange by considering the equilibrium between the dissolved and gaseous CO_2 as outlined below:

The dissolved CO_2 (which is equivalent to the $H_2CO_3^*$ in solution) and hence $H_2CO_3^*$ tends to equilibrium with the partial pressure of the CO_2 gas outside the liquid, i.e.:

$$CO_2\ gas \leftrightarrow H_2CO_3^* \tag{3.10}$$

The resulting CO_2 exchange at the liquid/gas interface causes loss (expulsion) or gain (dissolution) of the $H_2CO_3^*$ in solution, and therefore also in the total carbonate species ($H_2CO_3^*/HCO_3^-/CO_3^{2-}$) concentration. Thus Musvoto *et al.*, (1997) included CO_2 loss or gain into their model, following the same approach as for the weak acid/base dissociation described above, i.e. by modelling the rate of the forward and reverse reactions in Equation 3.10 separately. For the forward reaction:

$$r_f = K'_{fCO2}[CO_2(g)] \tag{3.11}$$

where r_f = the rate of the forward reaction
K'_{fCO2} = the apparent specific rate constant for the forward reaction.

Similarly, for the reverse reaction:

$$r_r = K'_{rCO2}[H_2CO_3^*] \tag{3.12}$$

where r_r = the rate of the reverse reaction
K'_{rCO2} = the apparent specific rate constant for the reverse reaction.

The concentration of CO_2 (g), i.e. the CO_2 gas, is assumed to be constant and it is calculated from the partial pressure of CO_2 with Dalton's law of partial pressure:

$$[CO_2\,(g)] = \frac{\rho CO_2}{RT} \tag{3.13}$$

where pCO_2 = partial pressure of CO_2
R = universal gas constant
T = temperature in Kelvin.

For Equations 3.11 and 3.12 the apparent specific rate constants need to be calculated. The relative values of K'_{fCO2} and K'_{rCO2} are important because they establish the equilibrium concentration of $H_2CO_3^*$. At equilibrium the rate of the forward reaction is equal to the rate of the reverse reaction and therefore:

$$\frac{K'_{fCO2}}{K'_{rCO2}} = \frac{[H_2CO_3^*]}{[CO_2\,(g)]} = K'_{eqCO2} \tag{3.14}$$

where K'_{eqCO2} = apparent equilibrium constant for CO_2 exchange. From Equation 3.14:

$$K'_{fCO2} = K'_{eqCO2} \cdot K'_{rCO2} \tag{3.15}$$

The relative value of K'_{fCO2} can be calculated if K'_{eqCO2} is known and a value for K'_{rCO2} is selected; Then the correct equilibrium condition will be established and the correct concentration of $H_2CO_3^*$ will be given. K'_{eqCO2} at equilibrium is calculated from Henry's Law:

$$K'_{H,CO2} = \frac{K'_{eqCO2}}{RT} \tag{3.16}$$

where $K'_{H,CO2}$ = Henry's law constant for CO_2
$K'_{eqCO2} = K'_{D,CO2}$
$K'_{D,CO2}$ = mass law distribution constant.

To model the CO_2 and NH_3 stripping, Musvoto *et al.*, (1997) integrated the following equation with the weak acid/base part of their model:

$$-\frac{dC_L}{dt} = K_La(C_L - C_e) \tag{3.17}$$

where K_La = overall liquid phase mass transfer rate coefficient = K_L^*a
K_L = overall liquid phase mass transfer rate coefficient
a = specific interfacial area
C_L = concentration in the bulk liquid
C_e = equilibrium concentration in the gas phase.

For NH_3 stripping they assumed that the atmosphere acts as an infinite sink for NH_3, hence the

equilibrium concentration in the gas phase was neglected for NH_3 stripping. For CO_2 exchange, however, the atmosphere cannot be considered to be an infinite sink, and an equilibrium is established between the CO_2 dissolved in solution and the atmospheric (or headspace) CO_2 concentration. Musvoto *et al.*, (1997) calculated the dissolved CO_2 equilibrium concentration from Dalton's and Henry's laws:

$$C_{eCO2} = K'_{H,CO2} \cdot \rho CO_2 \tag{3.18}$$

where $K'_{H,CO2}$ = Henry's law constant for CO_2
pCO_2 = partial pressure of CO_2

The values of the overall liquid phase mass transfer rate coefficients can be determined from individual measurements for each component, however this is time consuming especially when several compounds are being stripped with the same method of aeration. Hence Musvoto *et al.*, (1997) introduced the concept of measuring a single K_{La} value for a reference compound, which was then applied to calculate the K_{La} values for the other compounds (Munz and Roberts, 1989).This approach is briefly outlined below:

Models that simulate mass transfer are based an the assumption that the liquid phase resistance controls the rate of interphase mass transfer if the solutes are sufficiently volatile. This assumption is valid for values of the dimensionless Henry's coefficient H_C>0.19, where H_C is defined as the ratio of the interfacial concentration in the gas phase to that in the liquid phase, i.e. $H_C = C_G / C_L$ and is related to the other equilibrium parameters as follows:

$$H_C = \frac{1}{K_H RT} = \frac{K}{RTM_W} \tag{3.19}$$

where K_H = Henry's law constant
K = conventional equilibrium constant
M_W = molar volume of water
R = universal gas constant
T = temperature in Kelvin.

These mass transfer models are also based on the principle that in general the rate constants for volatile solutes are proportional to one another. The use of a reference compound to predict the extent of mass transfer of organic compounds at gas/liquid interfaces is convenient, because only the mass transfer coefficient for the reference compound needs to be measured, and since the geometric and hydrodynamic conditions in a given reactor do not change, the mass transfer coefficient for the other compounds can be calculated from the reference compound. The rate of mass transfer of compound 'i' is thus related to the rate of mass transfer of the reference compound 'r' by the proportionality factor Ψ, and this proportionality factor depends on the liquid phase diffusivity ratio $D_{L,i} / D_{L,r}$ of the particular compound 'i' and the reference compound 'r'. This can be represented as follows:

$$\Psi_i = \frac{K_{L,i}}{K_{L,r}} = \left(\frac{D_{L,i}}{D_{L,r}}\right)^n \tag{3.20}$$

where Ψ_i = transfer rate constant proportionality factor
$K_{L,i}$ = overall liquid phase mass transfer rate coefficient of compound i
$K_{L,r}$ = overall liquid phase mass transfer rate coefficient of compound r
$D_{L,i}$ = liquid phase molecular diffusion coefficient for compound i
$D_{L,r}$ = liquid phase molecular diffusion coefficient for compound r
n = diffusivity coefficient.

Oxygen was found to be most suitable as a reference compound because is satisfies the volatility criterion, and oxygen transfer is usually the main objective during aeration in wastewater treatment. Munz and Roberts (1989) defined the proportionality factor Ψ such that it became applicable for all compounds irrespective of their volatility (but not their dimensionless Henry's law constant). With oxygen as the reference compound, Ψ was given by:

$$\Psi = \left[\frac{D_{L,i}}{D_{L,O2}}\right]^n \left[1 + \frac{1}{\frac{k_G}{k_L} \cdot H_{c,i}}\right]^{-1} \tag{3.21}$$

where k_G = gas phase individual mass transfer coefficient
k_L = liquid phase individual mass transfer coefficient
$H_{c,i}$ = dimensionless Henry's constant for compound i.

The rate of stripping of compound 'i' in a given situation is then calculated by multiplying the proportionality factor with the corresponding measured or otherwise estimated rate of stripping or absorption of oxygen for the particular situation.

The Musvoto *et al.*, (1997) mixed weak acid/base model incorporating CO_2 diffusion/expulsion and gas stripping was chosen as the basis of integrating the weak acid/base chemistry and the gaseous phase into ASM1 to form an integrated biological, chemical and physical processes kinetic model for anoxic/aerobic C and N removal in activated sludge systems. The Musvoto *et al.*, (1997) model was chosen specifically, because their approach is general, and it can be applied to include (or exclude) any weak acid/base system as well as the stripping of virtually any gas. Since their model uses kinetics throughout, derivatives of their model can easily be incorporated with other kinetic models and coded into computer simulation packages such as AQUASIM (Reichert *et al.*, 1998). Musvoto *et al.* (1997) also included the kinetics of mineral precipitation of $CaCO_3$. However this aspect is not reviewed here as it is not relevant to the development of a two phase (aqueous/gas) chemical, physical and biological processes activated sludge model. This aspect is reviewed in Chapter 6 for the development of a 3 phase chemical physical model.

3.3 MODEL DEVELOPMENT

Central to the mixed weak acid/base chemical-physical model of Musvoto *et al.* (1997, 2000a,b,c) is that the hydrogen ion (H^+) is included explicitly as a compound. Integrating the biological processes of C and N removal of ASM1 into this chemical-physical model requires a number of interactions between the chemical and biological processes to be defined, such as (i) the influence of the biological processes on the weak acid/base systems species and H^+ concentrations, i.e. production and/or utilization of H^+, CO_2, ammonia and phosphate in the growth and death (endogenous respiration) processes, and (ii) the effect of pH on the biological process rates where these are expected to be significant, e.g. on the autotrophic nitrifier organism (ANO) maximum specific growth rate. Additionally, interactions with the physical processes require consideration, such as (i) production of N_2 and loss of this species via gas exchange and (ii) input of O_2 via aeration and utilization of dissolved oxygen in biological processes.

The mixed weak acid/base kinetic model of Musvoto *et al.* (1997) comprises (see their Table 1):

(1) The aqueous phase forward and reverse dissociation chemical processes of the ammonia, carbonate, phosphate, SCFA and water weak acid/base system species, i.e. processes 1-6 and 9-18 involving compounds 1-5 and 7-14.
(2) The gas and solid phase physical processes of the carbonate system, i.e. CO_2 gas exchange (dissolution and expulsion) and $CaCO_3$ precipitation, i.e. processes 7, 8 and 19 respectively involving compounds 3, 6 and 15.

Keeping the same numbering of processes and compounds, Musvoto *et al.* (2000a) extended this model to include (see their Tables 1b and 3):

(3) Ion pairing of Ca and Mg with hydroxide and the various species of the carbonate and phosphate systems; this added 22 processes, i.e. the aqueous phase forward and reverse dissociation chemical processes of the 11 ion pairs (processes 20-41) and 12 compounds, i.e. Mg and 11 ion pair species (compounds 16-27) respectively (see their Table 1b.)
(4) The gas and solid phase physical processes of the ammonia, carbonate and phosphate systems, i.e. ammonia gas stripping and mineral precipitation of four additional minerals associated with Ca and Mg and species of the ammonia, carbonate and phosphate systems, i.e. struvite ($MgNH_4PO_4$), newberyite ($MgHPO_4$), amorphous calcium phosphate [ACP, $Ca_3(PO_4)_2$] and $MgCO_3$; this added 5 additional processes i.e. 42 to 46 but no new compounds as the precipitated minerals were not included explicitly (see their Table 3).

Before incorporating the biological processes of ASM1 into the mixed weak acid/base chemical physical (CP) model of Musvoto *et al.* (1997, 2000a), all the processes and compounds were categorized into chemical (C), physical (P) and biological (B) groups and subgroups (Table 3.1). This was done for ease of discussion of the assembly of a particular integrated chemical - physical - biological (CPB) processes model, be it aerobic or anaerobic. For easy cross reference to the source chemical physical (CP) and biological (B) models, the numbers of the processes and compounds were not changed from those in the source models. The following general groups and subgroups of processes and compounds were adopted, which are summarized in Table 3.1:

(1) The chemical (C) processes, which comprise those of equilibrium dissociation (CED -

forward and reverse weak acid/base dissociation) and ion pairing (CIP). These are processes 1-41 in the Musvoto *et al.* (2000a) CP source model, but the physical (P) processes 7, 8 and 19 are excluded. These processes have the same numbers as in the source model, but the prefix C is added, i.e. C1-C41. The 27 compounds associated with these chemical processes are also numbered identically to the source model, but have the prefix C added, i.e. compounds C1-C5 and C7-C14 involved in the equilibrium dissociation (CED) processes and compounds C4, C5, C8, C10-C12 and C15-C27 involved in the ion pairing (CIP) processes. The only compound that does not belong to this group is the CO_2 gas (C6). CO_2 is included with the compounds associated with the physical (P) processes and so is labelled P1.

(2) The physical (P) processes, which comprise those of mineral precipitation (PMP) and gas exchange (PGE). The five mineral precipitation processes 19 and 42 to 45 in the Musvoto *et al.* (2000a) CP source model are renumbered P1 to P5. Since the precipitants are not explicitly included, these processes involve only existing compounds in the model (viz. C1, C5, C11, C12, C15 and C16) and so add no new compounds. Physical gas exchange (PGE) combines gas dissolution (forward) and expulsion (reverse) processes. The two physical gas exchange processes for CO_2 (dissolution, 7 and expulsion, 8) of Musvoto *et al.* (1997), are numbered P6 and P7, but from the link with the inter-phase mass transfer developed by Musvoto *et al.* (1997), the rate formulations are expressed directly in terms of the more conventional mass transfer rate coefficient and the CO_2 partial pressure (p_{CO2}) (Table 3.3). Summing these two processes (P6 and P7) is directly equivalent to the conventional inter-phase mass transfer gas exchange. For ammonia, the expulsion ('stripping') process (46) of Musvoto *et al.* (2000a) is numbered P8 (Table 3.3). For this gas, the gas phase is accepted to contain zero ammonia (infinite sink) and hence a gaseous ammonia compound is omitted and so also a dissolution process. Added to the PGE processes of the source model to form the integrated CPB activated sludge model are the gas exchange processes for N_2 (dissolution P9 and expulsion P10) formulated in the same manner as for CO_2. Also added is the process for O_2 dissolution by aeration, P11 (Table 3.3). The new compounds associated with these additional PGE processes are the dissolved and gaseous compounds of oxygen and nitrogen. Dissolved oxygen (A8) and nitrogen (A14) are compounds of the biological processes part of the model (see below) so only 2 physical compounds need to be added for the CPB activated sludge model, i.e. gaseous oxygen (P2) and gaseous nitrogen (P3).
No additional physical gas exchange processes would need to be added to incorporate the biological processes of anaerobic digestion, only one gaseous compound methane (CH_4) - it can be assumed that because CH_4 is very insoluble, CH_4 gas is formed directly by the biological processes. Also in anaerobic digestion, dissolved hydrogen is produced and utilized but hydrogen gas production is negligible compared with CO_2 and CH_4 and hence hydrogen need be included only as a dissolved species (Table 3.1).

In model application, the gas exchange processes can be passive (no gas bubbling) or active (with gas bubbling, e.g. aeration). For both cases, the gas exchange formulations apply, except that of O_2 dissolution (P11), which specifically requires aeration. However, the values of the gas exchange constants (K_{La}) differ significantly for the two situations.

(3) The biological (B) processes comprise the biological C and N removal process of activated sludge (ASM1) with prefix A and in Chapter 4 of anaerobic digestion with prefix D (Table 3.1). Also for the biological processes and compounds of the activated sludge model, the same numbers of ASM1 were retained, except the prefix A was added to each, i.e. processes A1 to A8 and compounds A1 to A13. However, two biological processes are added, viz. aerobic and anoxic growth of heterotrophs (OHOs) with nitrate as N source (Dold and Marais, 1985), because these two processes affect reactor pH and these were numbered A1b and A2b. Of the 13 compounds in ASM1, two become redundant in the integrated CPB model - (i) the free and saline ammonia (FSA, A10) because NH_3 and NH_4^+ are in the chemical compounds group and (ii) the Alkalinity (A13), which is now obsolete. Apart from the ammonium (NH_4^+, C1), three other compounds in the source CP model are also involved with the biological processes, i.e. $H_2CO_3^*$ (C3) through CO_2 generation or uptake, H^+ (i.e. pH, C7) through ammonification, nitrification, denitrification and OHO growth/death and HPO_4^{2-} through uptake for OHO growth and release from OHO death.

Following the grouping and numbering system above (Table 3.1), the integrated two phase (aqueous-gas) chemical physical biological (CPB) activated sludge model for C and N removal was assembled by including:

(1) The chemical equilibrium dissociation (CED) processes for the weak acid/bases (C1-C6 and C9-C18) with associated compounds C1-C5 and C7-C14 (Table 1 of Musvoto *et al.*, 1997, not repeated here). Although the SCFA weak acid/base system is included, in the application here the SCFA are set to zero (see below).

(2) The biological activated sludge processes (BA) of C and N removal from ASM1 (A1 to A8), including aerobic and anoxic OHO growth on ammonium (processes A1a and A2a) and nitrate (processes A1b and A2b), with their associated new compounds NH_4^+ (C1), $H_2CO_3^*$ (C3), H^+ (C7), HPO_4^{2-} (C11) and the remaining original 11 activated sludge system compounds (A1-A9, A11-A12) (see Table 3.2).

(3) The physical gas exchange stripping (PGE) processes of ammonia (C46/P8), carbon dioxide (P6 and P7) and nitrogen (P9 and P10) gases and aeration dissolution of oxygen (P11) with their associated compounds dissolved ammonia (C2) and dissolved and gaseous carbon dioxide (C3 and C6), oxygen (A8 and P2) and nitrogen (A14 and P3). A gaseous ammonia compound is not included, because the gas stream is accepted to contain zero ammonia (Table 3.3).

Not included in the integrated CPB activated sludge model are (i) the chemical ion pairing (CIP) processes (C20-C41), because this was not considered important for activated sludge systems treating municipal wastewater (TDS < 1000 mg/ℓ) and (ii) the physical mineral precipitation (PMP) processes (C19, C42-C45 or P1-P5), because only the gas and aqueous phases are considered in this first integrated AS model.

For brevity, only the biological (B) and physical gas exchange (PGE) processes parts of the integrated CPB activated sludge model with their associated compounds are shown in the Petersen matrix of the model (Tables 3.2 and 3.3). Because the chemical and physical parts of the model have units mol/ℓ, these were changed to reflect the usual units in biological models, viz.

Table 3.1: Petersen matrix overview of the integrated chemical-physical-biological processes model for simulating wastewater treatment plant unit operations.

Integrated CPB model matrix structure			COMPOUNDS				
			CHEMICAL (C)		PHYSICAL (P)	BIOLOGICAL (B)	
			Equilibrium Dissociation (CED)	Ion Pairing (CIP)	Gas Exchange	Activated Sludge (BA)	Anaerobic Digest (BD)
PROCESSES	CHEMICAL	Equilibrium Dissociation	15 compounds of the 6 weak acid base systems: C1-C5[a], C7-C14[a], C28-C29[d] 18 chemical equilibrium dissociation processes of the 6 weak acid base systems: C1-C6[a], C9-C18[a], C47-C48[d]	13 compounds associated with 22 ion pairing processes including Ca and Mg: C15-C27[b]	3 compounds CO_2 gas P1 (C6)[a] O_2 and N_2 gases P2-P3[c]	13 compounds for activated sludge (A) : A1 - A14; 13 from ASM1 minus A10 (FSA = C1+C2) plus A14 (dissolved N_2 gas) and replacing in A13 S_{lost} for Alk now obsolete	8 compounds for anaerobic digestion (D): D1-D7 and P4. CH_4 (P4) is produced directly as a gas due to its insolubility and H_2 (D3) is completely utilized as a dissolved gas
		Ion Pairing	22 chemical ion pairing processes (CIP) of 11 ion pairs: C20-C41[b]				
	PHYSICAL	Mineral Pptn	5 physical mineral precipitation processes (PMP): P1 (C19)[a], P2-P5 (C42-C45)[b] No additional compounds - all included with CIP				
		Gas Exchange			4 physical gas exchange (PGE) dissolution and expulsion processes; 2 for CO_2 and 2 for N_2, P6-P7c (C7-C8)[a] and P9-P10[c]. 1 physical gas exchange (PGE) expulsion process for NH_3; P8[c] (C46)[a] 1 physical gas exchange (PGE) dissolution process for O_2; P11[c] CH_4 in BD produced directly as a gas (insoluble). H_2 in BD considered soluble and negligible with respect to CO_2 and CH_4 K_{La} rates different with aeration (active) or not (passive).		
	BIOLOGICAL	Activ Sludg				12 biological (B) activated sludge (BA) processes, i.e. all 8 of ASM1 plus aerobic and anoxic heterotrophic growth with nitrate (A1b and A2b)[c] and anoxic hydrolysis of slowly biodegradable organics (COD, S_{bp}) (A9)[c] and organic N (N_{obp}, A10)[c].	
		Anaer Digst					10 biological (B) anaerobic digestion (BD) processes. [d]

Notes: 1 [a] see Table 1 of Musvoto *et al.* (1997); b see Tables 1b, 1c and 3 of Musvoto *et al.* (2000a); [c] see Tables 3.2 and 3.3 in this chapter; [d] see Table 4.2 in Chapter 4;.

[2] Only reactant compounds are specified. Product and inert (unbiodegradable) are omitted but implicit, e.g. mineral precipitates, water, non-reactive sink gases and unbiodegradable COD and OrgN.

Table 3.2: Matrix representation of the biological processes of ASM1, including anoxic and aerobic growth of OHOs on nitrate (processes A1b and A2b), combined with parts of the mixed weak acid/base chemical-physical model of Musvoto *et al.* (2000a) to yield the two phase (aqueous-gas) integrated chemical-physical-biological (CPB) processes activated sludge system model for C and N removal (see Table 3.3 for physical processes).

	No, i	C3	C7	C11	A1	A2	A3	A4	A5	A6	A7	A8	A9	C1/A10	A11	A12	A13	A14	
No j	Compounds / Processes	$H_2CO_3^*$	H^+	HPO_4^{2-}	S_I	S_{bs}	X_I	S_{enm}	Z_{BH}	Z_{BA}	Z_E	O dissolved	NO_3^-	NH_4^+	N_{obs}	N_{obp}	S_{Lost}	N_2 dslvd	Process rate , ρ_j
A1a	Aerobic growth of Z_{BH} with NH_4^+	$(1-Y_{ZH})/(3Y_{ZH})$	$f_{ZB,N}/14-2f_{ZB,P}/31$	$-f_{ZB,P}$		$-1/Y_{ZH}$			1			$-(1-Y_{ZH})/Y_{ZH}$		$-f_{ZB,N}$					$\mu_H \left[\frac{S_{bs}}{K_{SH}+S_{bs}}\right]\left[\begin{matrix}HAir\\On\end{matrix}\right]\left[\frac{NH_4^+}{limit}\right] Z_{BH}$
A1b	Aerobic growth of Z_{BH} with NO_3^-	F*	$-f_{ZB,N}/14-2f_{ZB,P}/31$	$-f_{ZB,P}$		$-1/Y_{ZH}$			1			$-(1-Y_{ZH})/Y_{ZH}$	$-f_{ZB,N}$				-64/14 $f_{ZB,N}$		$\mu_H \left[\frac{S_{bs}}{K_{SH}+S_{bs}}\right]\left[\begin{matrix}HAir\\On\end{matrix}\right]\left[\frac{1-NH_4^+}{limit}\right]\left[\frac{NO_3}{limit}\right] Z_{BH}$
A2a	Anoxic growth of Z_{BH} with NH_4^+	$(1-Y_{ZH})/(3Y_{ZH})$	A*	$-f_{ZB,P}$		$-1/Y_{ZH}$			1				$-(1-Y_{ZH})/(2.86Y_{ZH})$	$-f_{ZB,N}$				D*	$\mu_H \left[\frac{S_{bs}}{K_{SH}+S_{bs}}\right]\left[\begin{matrix}HAir\\Off\end{matrix}\right]\left[\frac{NH_4^+}{limit}\right]\left[\frac{NO_3}{limit}\right] Z_{BH}\,\eta_G$
A2b	Anoxic growth of Z_{BH} with NO_3^-	F*	C*	$-f_{ZB,P}$		$-1/Y_{ZH}$			1				B*				-64/14 $f_{ZB,N}$	D*	$\mu_H \left[\frac{S_{bs}}{K_{SH}+S_{bs}}\right]\left[\begin{matrix}HAir\\Off\end{matrix}\right]\left[\frac{1-NH_4^+}{limit}\right]\left[\frac{NO_3}{limit}\right] Z_{BH}\,\eta_G$
A3	Aerobic growth of Z_{BA}	-3/8	$f_{ZB,N}/14+1/(7Y_{ZA})$							1		$-(4.57-Y_{ZA})/Y_{ZA}$	$1/Y_{ZA}$	$-(1/Y_{ZA})-f_{ZB,N}$					$\mu_A \left[\frac{NH_4^+}{K_{SA}+NH_4^+}\right]\left[\begin{matrix}A\ Air\\On\end{matrix}\right] Z_{BA}$
A4	Death of Z_{BH}		$2(f_{ZB,P}-f_E f_{ZE,P})/31$	$f_{ZB,P}-f_E f_{ZE,P}$				$1-f_E$	-1		f_E					$f_{ZB,N}-f_E f_{ZE,N}$			$b_H Z_{BH}$
A5	Death of Z_{BA}							$1-f_E$		-1	f_E					$f_{ZB,N}-f_E f_{ZE,N}$			$b_A Z_{BA}$
A6	Ammonification of N_{obs}		-1/14											1	-1				$K_R N_{obs} Z_{BH}$
A7	Hydrolysis of S_{enm}					1		-1											E^* ;
A8	Hydrolysis of N_{obp}														1	-1			$E^*.(N_{obp}/S_{enm})$
	Units	gC/m^3	gH/m^3	gP/m^3	$gCOD/m^3$	$gCOD/m^3$	$gCOD/m^3$	$gCOD/m^3$	$gCOD/m^3$	$gCOD/m^3$	$gCOD/m^3$	$-gCOD/m^3$	gN/m^3	gN/m^3	gN/m^3	gN/m^3	$+gCOD/m^3$	gN/m^3	

$$A^* = -\frac{1-Y_{ZH}}{14*2.86Y_{ZH}} + \frac{f_{ZB,N}}{14} - 2*\frac{f_{ZB,P}}{31} \qquad B^* = -\frac{1-Y_{ZH}}{2.86Y_{ZH}} + f_{ZB,N} \qquad C^* = -\frac{1-Y_{ZH}}{14*2.86Y_{ZH}} - \frac{f_{ZB,N}}{14} - 2*\frac{f_{ZB,P}}{31} \qquad D^* = \frac{1-Y_{ZH}}{2.86Y_{ZH}}$$

$$E^* = K_H \left[\frac{(S_{enm}/Z_{BH})}{K_X+(S_{enm}/Z_{BH})}\right]\left(\left[\begin{matrix}HAir\\On\end{matrix}\right]+\eta_S\left[\begin{matrix}H\ Air\\Off\end{matrix}\right]\left[\frac{NO_3}{limit}\right]\right) Z_{BH} \qquad F^* = \frac{1-Y_{ZH}}{3Y_{ZH}} + \frac{64}{14x3} f_{ZB,N}$$

Notes: (1) Compound A1-A13 numbered identically to ASM1, except NH_4^+, which is C1 in Musvoto *et al.* (1997) and 10 in ASM1. NH_4^+ in ASM1 is actually the free (NH_3) and saline (NH_4^+) ammonia (FSA), where here it is only the saline. H_2CO_3* alkalinity (compound 13) is no longer required. Ammonium (C1), dissolved CO_2 (C3) and dinitrogen (A14), H^+ (C7) and mono-hydrogen phosphate (C11) are included here because they are involved with the biological activated sludge processes.

Table 3.3: Matrix representation of the physical gas exchange (PGE) processes incorporated in the integrated two-phase chemical-physical-biological (CPB) model for C and N removal in the activated sludge system (see Table 3.1 for biological processes).

	No	C2	C3	A8	A14	P1(C6)	P2	P3	
No	Compound→ Process↓	NH_3 dissolved	$H_2CO_3^*$ CO_2 diss	O_2 dissolved	N_2 dissolved	CO_2 gas	O_2 gas	N_2 gas	Rate
P6	Gas exchange of CO_2 - dissolution		1			-1			$K_{La\text{-}CO2}\, p_{CO2}\, K_{H\text{-}CO2}$
P7	Gas exchange of CO_2 - expulsion		-1			1			$K_{La\text{-}CO2}\, [H_2CO_3^*]$
P8	Gas exchange of NH_3 - expulsion	-1							$K_{La\text{-}NH3}\, [NH_{3diss}]$
P9	Gas exchange of N_2 - dissolution				1			-1	$K_{La\text{-}N2}\, p_{N2}\, K_{H\text{-}N2}$
P10	Gas exchange of N_2 - expulsion				-1			1	$K_{La\text{-}N2}\, [N_{2diss}]$
P11	Aeration - dissolution of O_2			1			-1		$K_{La\text{-}O2}\, ([O_{2sat}] - [O_{2diss}])$
	Units	mol/ℓ	mol/ℓ	mgO/ℓ	mol/ℓ	mol/ℓ	mol/ℓ	mol/ℓ	

gC/m^3, gN/m^3 and gP/m^3. Hence, when the H^+ interacts with C, N or P species, it was divided by the molar mass of C, N and P respectively. Also, the kinetic rate equations for the biological processes were modified to take into account the effect of H^+ where this effect is significant. This was done in two ways: (i) Where there is a direct influence of pH on the biological process rate, pH was included in the kinetic rate formulation, and (ii) the kinetic rates of the biological processes were reformulated to utilize specific species of the weak acid/base systems - stoichiometric coefficients were added and existing ones modified to take this into account.

The modifications outlined above were developed for the two organism groups included in ASM1, i.e. ordinary heterotrophic (OHOs) and autotrophic nitrifier (ANOs) organisms. For both groups, information in the literature on their behaviour was used for the modifications and the derivation of the stoichiometric coefficients of the integrated model are discussed briefly below. A review of bioenergetics and activated sludge model development is not given since these topics are already covered in detail in the literature (e.g. McCarty, 1964, 1972; Dold *et al.*, 1980; van Haandel *et al.*, 1981; Henze *et al.*, 1987; Ohron *et al.*, 1996, Casey *et al.*, 1999, Sperandio *et al.*, 1999). Only aspects relevant to the integration are discussed to clarify the additions and changes to the stoichiometric coefficients and kinetic rates in Tables 3.2 and 3.3.

3.4 MODIFICATIONS TO THE ASM1 TO ACCOMPLISH INTEGRATION

3.4.1 Ordinary Heterotrophic Organisms (OHOs)

The processes that involve the OHOs in ASM1 are growth (A1 and A2), death (A4), hydrolysis of enmeshed particulate biodegradable organics (A7) and associated particulate biodegradable organic nitrogen (A8) and ammonification of soluble biodegradable organic nitrogen (A6). The growth of OHOs is described by four processes, two under aerobic conditions using either ammonia (A1a) or nitrate (A1b) as N source, and two under anoxic conditions also using either ammonia (A2a) or nitrate (A2b) as N source. These processes were modified to include (i) production of CO_2 in metabolism, (ii) uptake or release of specific weak acid/base N and P species for growth and death, and (iii) utilization or production of H^+.

3.4.1.1 OHO metabolism

The bioenergetics of OHO growth are quantified in terms of the lumped electron donating capacity parameter COD, because in wastewater treatment the different organics involved in the growth processes are not known. This is possible because the free energy released per electron (e^-) transferred in the breakdown of different types of organics varies in the narrow range 105 to 121 kJ/e^-eq. The integrated model requires a carbon balance to be made over the activated sludge system. Thus the mass CO_2 generated in the growth process needs to be known, which requires the COD/TOC ratio of the wastewater organics to be known. For the range of different organics listed in Table 3.4, the COD/TOC ratio was calculated and varies between 2.67 and 4.0. Because most of the organics in wastewater are of carbohydrate/sugar type with a relatively small proportion of organics with high COD/TOC ratios, an average COD/TOC ratio would seem to be around 3.0. Because CO_2 is generated only in catabolism, the CO_2 generation is proportional to the oxygen utilized, i.e.

$$O_2 \text{ utilised in producing 1 g OHOs as COD} = (1-Y_{ZH})/Y_{ZH} \qquad (3.22a)$$

where

Y_{ZH} = OHO yield coefficient (mg COD OHOs formed/mg COD organics utilized)

Hence the CO_2 generated in producing 1 gOHOCOD

$$= O_2 \text{ utilised}/(\text{COD/TOC ratio}) = (1-Y_{ZH})/(3.0\ Y_{ZH}) \qquad (3.22b)$$

The CO_2 released during metabolism is in the dissolved form and accepted to add to the $H_2CO_3^*$ concentration in the bulk liquid. Hence, the stoichiometric coefficient $(1-Y_{ZH})/(3Y_{ZH})$ is added to the compound $H_2CO_3^*$ in the integrated model matrix (Table 3.2).

The COD/TOC ratio accepted will not significantly influence the activated sludge system mixed liquor pH. This is because in the breakdown of the organics listed in Table 3.4, no direct release of H^+ is envisaged to take place. The CO_2 is generated as $H_2CO_3^*$, but with aeration this is mostly stripped from the bulk liquid which is controlled by gas exchange (higher partial pressure than the atmosphere). Hence, the CO_2 generated is mostly lost to the gaseous phase. Further, if some final dissolved CO_2 state is achieved (e.g. equilibrium with the atmosphere or super-saturation), then any COD/TOC ratio variation is essentially absorbed by the gas phase, not to the bulk liquid and hence does not cause a significant pH change. In contrast, on oxidation the proteins release their N content as NH_3, which at pH between 6.5 and 8.0, takes up a H^+ to form NH_4^+, a process called ammonification. This increases the alkalinity of the bulk liquid and at constant CO_2 partial pressure (pCO_2) will produce a pH increase. In contrast to the CO_2, significant NH_3 loss to the gas phase does not occur (see later). Therefore, in the breakdown of organics, it is not the generation of CO_2 that affects the pH so much as the uptake of a H^+ by the NH_3 released from the breakdown of organic N (proteins). Hence, to predict the pH correctly, the COD/TOC ratio does not need to be known accurately, but the organic N content of the wastewater and its ammonification do need to be known accurately.

Table 3.4: COD/TOC ratio of some organic compounds.

Organic compound	Formula	COD/TOC Ratio
Carbohydrates	$C_n(H_2O)_n$	2.67 for all n
Sugars	$C_n(H_2O)_{n-2}$	2.67 for all n
[1]Carboxylic acids (SCFA and LCFA)	$CH_3(CH_2)_nCOOH$	$4(3n+2)/[3(n+1)]$ = 3.33 for n=1;= 3.94 for n=20
Primary amines	$CH_3\ (CH_2)_n\ NH_2$	4 for all n
Amino acids	$H(CH_2)_nC_2H_4O_2N$	$4(n+1)/(n+2) < 4$
Alkanes	$H(CH_2)_nH$	$4(3n+1)/3n \approx 4$
Alcohols	$H(CH_2)_nOH$	4 for all n

[1]Unsaturated fats have slightly lower COD/TOC ratio because for every double C bond (C=C), there are 2 Hs fewer.

Table 3.5: Stoichiometric and matrix representation of the aerobic and anoxic growth processes with ammonia and nitrate as N source taking account of the substrate required for the reduction of nitrate to ammonia in the chemical-physical-biological (CPB) processes model for C and N removal in the activated sludge system (see Table 3.2 for biological processes).

	No	A2 S_{bs}	A13 S_{bLost}	C1 A10	C7	A9	C7	A9	A8	A5	C3	C3	A14	-	-	-
No	Compound→ Process↓	$C_6H_{12}O_6$ Growth	$C_6H_{12}O_6$ Reductn	NH_4^+ Growth	H^+ Denit	NO_3 Denit	H^+ Growth	NO_3 Growth	O_2 Growth	$C_5H_7O_2N$ Biomass	CO_2 Growth	CO_2 Reductn	N_2 Denit	H_2O Growth	H_2O Reductn	H_2O Denit
A1a	Aerobic growth with ammonia	-1	0	-y	0	0	+y	0	-(6-5y)	+y	+(6-5y)	0	0	+(6-2y)	0	0
A1b	Aerobic growth with nitrate	-1	-y/3	0	0	0	-y	-y	-(6-5y)	+y	+(6-5y)	+2y	0	+(6-2y)	+y	0
A2a	Anoxic growth with ammonia	-1	0	-y'	$-\frac{8}{10}(6-5y')$	$-\frac{8}{10}(6-5y')$	+y'	0	0	+y'	+(6-5y')	0	$+\frac{4}{10}(6-5y')$	+(6-2y')	0	$+\frac{4}{10}(6-5y')$
A2b	Anoxic growth with nitrate	-1	-y'/3	0	$-\frac{8}{10}(6-5y')$	$-\frac{8}{10}(6-5y')$	-y'	-y'	0	+y'	+(6-5y')	+2y'	$+\frac{4}{10}(6-5y')$	+(6-2y')	+y'	$+\frac{4}{10}(6-5y')$
	Units	mol	mol	mol	mol	mol	mol	mol	mol	mol	mol	mol	mol	mol	mol	mol
A1a	Aerobic growth with ammonia	$-\frac{1}{Y_{ZH}}$	0	$-f_{ZB,N}$	0	0	$\frac{f_{ZB,N}}{14}$	0	$-\frac{(1-Y_{ZH})}{Y_{ZH}}$	1	$\frac{(1-Y_{ZH})}{3Y_{ZH}}$	0	0	-		-
A1b	Aerobic growth with nitrate	$-\frac{1}{Y_{ZH}}$	$-\frac{64}{14}f_{ZB,N}$	0	0	0	$\frac{-f_{ZB,N}}{14}$	$-f_{ZB,N}$	$-\frac{(1-Y_{ZH})}{Y_{ZH}}$	1	$\frac{(1-Y_{ZH})}{3Y_{ZH}}$	$\frac{64}{14x3}f_{ZB,N}$	0	-	-	-
A2a	Anoxic growth with ammonia	$-\frac{1}{Y'_{ZH}}$	0	$-f_{ZB,N}$	$-\frac{(1-Y'_{ZH})}{14x2.86Y'_{ZH}}$	$-\frac{(1-Y'_{ZH})}{2.86Y'_{ZH}}$	$\frac{f_{ZB,N}}{14}$	0	0	1	$-\frac{(1-Y'_{ZH})}{3Y'_{ZH}}$	0	$\frac{(1-Y'_{ZH})}{2.86Y'_{ZH}}$	-	-	-
A2b	Anoxic growth with nitrate	$-\frac{1}{Y'_{ZH}}$	$-\frac{64}{14}f_{ZB,N}$	0	$-\frac{(1-Y'_{ZH})}{14x2.86Y'_{ZH}}$	$-\frac{(1-Y'_{ZH})}{2.86Y'_{ZH}}$	$\frac{-f_{ZB,N}}{14}$	$-f_{ZB,N}$	0	1	$-\frac{(1-Y'_{ZH})}{3Y'_{ZH}}$	$\frac{64}{14x3}f_{ZB,N}$	$\frac{(1-Y'_{ZH})}{2.86Y'_{ZH}}$	-	-	-
	Units	gCOD	gCOD	gN	gH	gN	gH	gN	gO	gCOD	gC	gC	gN			

Notes:

(1) For an aerobic yield coefficient (Y_{ZH}) of 0.67 mgOHOCOD/mgCOD organics y= Y_{ZH}x192/160=0.67x192/160=0.804 mol OHO/mol organics.

(2) For an anoxic yield coefficient of (Y'_{ZH}) 0.54 mgOHOCOD/mgCOD organics y'= 0.54x192/160=0.648 mol OHO/mol organics.

(3) The water production is included in the molar stoichiometric part of the table (upper) to allow element (C, H, O ,N) mass balance checks. The COD based stoichiometry in the lower half is calculated from the molar stoichiometry, e.g. y mol biomass (160 gCOD/mol) is synthesized from 1 mole glucose (192 gCOD/mol), so 1 gCOD biomass requires 192/(160y) g glucose; substituting y= Y_{ZH}x192/160 from (1) above yields 1 gCOD biomass requires 1/Y_{ZH} gCOD glucose (-ve for consumption) and y mol biomass (160 gCOD/mol) production yields (6-5y) mol CO_2 in growth process, so 1 gCOD biomass produces 12 (6-5Y_{ZH}192/160)/(192Y_{ZH}) gCO_2-C = +72(1-Y_{ZH})/(192Y_{ZH}) where 72/192 = TOC/COD ratio of glucose; for a TOC/COD ratio of 1/3 this = (1-Y_{ZH})/(3Y_{ZH}).

Under anoxic conditions, nitrate (NO_3^-) serves as terminal electron acceptor and the specific yield coefficient is decreased to ~80% of the aerobic value. With nitrate as electron acceptor approximately the same quantity of free energy from the organics is available to the organism as when oxygen is the electron acceptor, but *ideally* only 2 ATP moles are formed per pair of electrons transferred to the nitrate (Payne, 1981) compared with 3 ATP moles per pair of electrons with oxygen. Measurements by Orhon *et al.* (1996), Sperandio *et al.* (1999) and Muller *et al.* (2003) confirm this reduction in yield experimentally with artificial and real domestic wastewaters. This reduction in yield under anoxic conditions is not recognised in early activated sludge models like UCTOLD (Dold *et al.*, 1991), ASM1 (Henze *et al.*, 1987), UCTPHO (Wentzel *et al.*, 1992) and ASM2 (Henze *et al.*, 1995), but is accepted in later models like ASM2d (Henze *et al.*, 1999) and Biowin (Barker and Dold, 1997). This reduction also has been accepted in the model developed here, so that under anoxic conditions, about 20% less OHO biomass and 40% more CO_2 are generated than under aerobic conditions (Table 3.5). As mentioned earlier, this lower CO_2 generation does not affect the reactor pH but the lower loss of CO_2 to the gas phase (no aeration) does increase the pH above that of the aerobic reactor.

3.4.1.2 Use of specific weak acid/base species for OHO growth

The nitrogen required for OHO synthesis is obtained from either ammonia (processes A1a and A2a) or, in the absence of ammonia, nitrate (processes A1b and A2b). Phosphorus is also incorporated in OHO mass. The concentrations of N and P required for synthesis are quantified in ASM1 and similar biological models as and N and P content of the active biomass i.e. $f_{ZB,N}$ = 0.068 mgN/mgOHOCOD and $f_{ZB,P}$ = 0.020 mgP/mgOHOCOD respectively, but it is not specified which of the ammonia and phosphate weak acid/base system species are taken up for synthesis.

From the literature on bioenergetics, it is accepted that the non-ionic ammonia and phosphate system species are taken up for synthesis, i.e. NH_3 and H_3PO_4. However, it has been accepted in this model that the most abundant species of the systems in the pH range typical for activated sludge systems of 6.5 to 8.5, NH_4^+ and HPO_4^{2-}, are taken up, releasing one and taking up two protons respectively during cell synthesis. In this operating pH range, the concentrations of NH_3 and H_3PO_4 are extremely low and their use in kinetic models for synthesis can lead to numerical instability.

When ammonia is depleted , NO_3^- is taken up by the OHOs as the N source for growth. However, the NO_3^- must be first reduced to NH_4^+ by accepting $8H^+$ and $8e^-$, which are supplied by the biodegradable organics and two additional H^+ are taken up from the bulk liquid, viz.

$$NO_3^- + 2H^+ + (8H^+ + 8e^-) \rightarrow NH_4^+ + 3H_2O \qquad (3.23a)$$

One of the two H^+ is returned to the bulk liquid when NH_4^+ is taken up for growth, but the other is required in the reduction reaction and therefore increases the bulk liquid pH. Hence, the net change in H^+ concentration with NO_3^- as N source and P uptake as HPO_4^{2-} for OHO growth is

$$= -f_{ZB,N}/14 - 2f_{ZB,P}/31 \qquad mgH^+/\ell \qquad (3.23b)$$

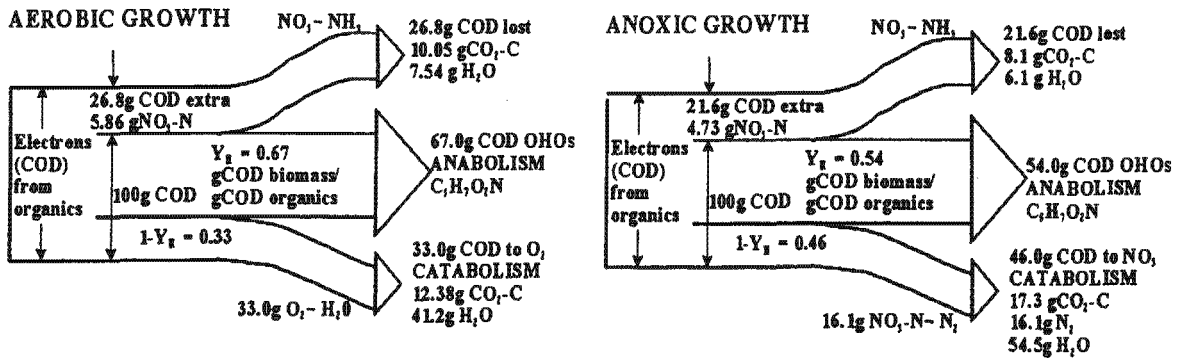

Fig 3.2: Schematic and quantitative representation of aerobic (left) and anoxic (right) OHO growth using nitrate as nitrogen source (assimilative denitrification) taking account of the organics (electrons) required to reduce nitrate to ammonia.

The biodegradable organics that supply the $8H^+$ and $8e^-$ for the nitrate reduction (Eq 23a) are 'lost' from the system, i.e. are no longer available for growth, which is shown quantitatively in Fig 3.2. Even though nitrate reduction (Eq 23a) thermodynamically is an energy generating reaction, bioenergetically the OHOs get no energy from it. It is, therefore, not correct to change the yield coefficient to account for this additional H^+ and e^- consumption. Accordingly, the yield coefficients under aerobic and anoxic conditions remain $Y_{ZH} = 0.67$ and $Y'_{ZH} = 0.54$ mgOHOCOD formed/mgCOD organics utilized. To take account of the COD 'lost' by nitrate reduction for growth, the compound S_{bLost} (A13) is added to the model as a compound so that (i) the magnitude of this 'lost' COD is tracked and (ii) COD balances can still be used to verify the model. Integrating the stoichiometry of the reduction of nitrate to ammonia into the growth processes using glucose as an example substrate is shown in Table 3.5. The Petersen matrix coefficients of the aerobic and anoxic growth processes (1 and 2) in Table 3.2 were calculated from Table 3.5. It can be seen that (i) additional CO_2 is generated when nitrate is utilized as N source for growth, but this additional CO_2 generation does not affect the reactor pH, and (ii) H^+ are taken up from the bulk liquid in the reduction of NO_3^- to NH_3 which will cause a pH increase.

In completely mixed single aerobic reactor systems, the ammonia is unlikely to be depleted sufficiently for NO_3^- to be utilized as the N source - this situation is more likely to occur in plug flow type and sequencing batch reactor (SBR) systems. In anoxic reactors, whether completely mixed or plugflow, invariably ammonia is present in excess of synthesis requirements. In completely mixed nitrifying aerobic digestion of waste activated sludge there always should be sufficient ammonia for growth because the ammonia released in OHO death is always greater than that taken up for OHO growth on the slowly biodegradable (SB) COD released in OHO death. However, in application of the model to aerobic digestion (Chapter 2) nitrate utilization for OHO growth nevertheless can occur. This can also occur with model application to aerobic digestion of primary sludge even when sufficient ammonia is dosed for net OHO biomass production from the primary sludge particulate biodegradable organics. As explained in Chapter 2, this apparent ammonia deficiency in the model arises because the rate of nitrification is faster than the rate of OHO growth, which is limited by the supply rate of SBCOD from the OHO death process. This leads to uptake of nitrate for OHO growth, but to the release of ammonia in OHO death. This released ammonia is then nitrified with an associated OUR for nitrification. The consequence is an incorrectly predicted high nitrification OUR from the continual supply of

ammonia nitrogen from the death process, nitrogen that is taken up as nitrate by the OHOs. This problem was eliminated in the model by reducing the switching function K value which controls the switch from ammonia to nitrate uptake for OHO growth to a very low value (0.0001 mgN/ℓ)). This prevents the OHO growth process from slowing down when the ammonia concentration gets low, allowing it to successfully 'compete' for ammonia against the nitrification process. This problem therefore has nothing to do with ammonia deficiency but everything to do with the relative rates of processes competing for the same compounds, in this case ammonium (NH_4^+). *K values of switching functions on processes competing for the same compounds therefore require very careful scrutiny in simulation models.*

3.4.1.3 Utilization and generation of H^+ in OHO growth and death (endogenous respiration)
When NH_4^+ (or NO_3^-) and HPO_4^{2-} are taken up for synthesis, a proton is released (or taken up) and two protons taken up respectively to convert these species to their unionised forms NH_3 and H_3PO_4. This changes the H^+ concentration which has to be taken into account, viz.

Concentration NH_4^+ (or NO_3^-) taken up for synthesis = $f_{ZB,N}$ (gN/gOHOCOD) (3.24a)
Concentration HPO_4^{2-} taken up for synthesis = $f_{ZB,P}$ (gP/gOHOCOD) (3.24b)

Hence the change H^+ concentration in synthesis with NH_4^+ = $f_{ZB,N}$ /14 -2 $f_{ZB,P}$ /31 mgH^+/ℓ (3.24c)
and the change H^+ concentration in synthesis with NO_3^- = -$f_{ZB,N}$ /14 -2 $f_{ZB,P}$ /31 mgH^+/ℓ (3.24d)

If the unionized N and P species (NH_3 and H_3PO_4) are used instead for synthesis, virtually the same net effect on H^+ will occur, due to the redistribution of the weak acid/base species via the CED kinetic processes.

In organism death, since the death-regeneration approach is followed, (Dold *et al.*, 1980), the difference in N contents of the active biomass lost and the endogenous residue formed is released as biodegradable particulate N. Hence, this process has no direct influence on the H^+ concentration. In contrast, to reduce complexity in phosphorus compounds, the corresponding P is released as HPO_4^{2-}, with associated H^+ to maintain neutrality. This changes the H^+ concentration which has to be taken into account, viz.

Concentration HPO_4^{2-} released in OHO death = $f_{ZB,P}$ - f_E $f_{ZE,P}$ (gP/gOHOCOD) (3.25a)
Associated change H^+ concentration = +2($f_{ZB,P}$ - f_E $f_{ZE,P}$)/31 (3.25b)

3.4.1.4 Ammonification of soluble organic nitrogen
Ammonification is the process mediated by OHOs (A6) whereby biodegradable soluble organic nitrogen (N_{obs}), which is in the unionized 'NH_3' form, is converted to saline ammonia (NH_4^+). Associated with ammonification therefore is a decrease in the H^+ concentration of the bulk liquid due to uptake of a H^+ by the NH_3 to form NH_4^+. The H^+ taken up in ammonification is 1/14 gH^+/gN Organic N ammonified.

In ASM2, the ammonification process is omitted. Instead, the conversion of soluble biodegradable organic N (N_{obs}) to ammonia is linked to the utilization of readily biodegradable

organics (RB COD) of which it is part. So if a wastewater has an influent biodegradable soluble organic N to RBCOD ratio (N_{obsi}/S_{bsi}) of say 0.03 (i_{NSF} in ASM2), the ammonia (NH_3) released is 0.03 times the rate of RBCOD utilization. The release of ammonia from the particulate biodegradable organic N is modelled in the identical way in ASM1 and ASM2. Two models were developed and compared, one conforming strictly to ASM1 including the ammonification process, and the other linking the release of ammonia from the soluble organic N to the utilization of RBCOD. No significant differences were noted between the predictions of the two model versions, provided the ammonification kinetic rate constants were correctly selected.

3.4.1.5 A note on the utilization of SCFA in OHO growth

Inclusion of the SCFA weak acid/base system in the model arises from the earlier application of the chemical - physical part of the model to aeration treatment of anaerobic digester liquor (ADL) (Musvoto, 2000a,c), where it was required to establish the correct pH. Practically, the SCFA are not explicitly required in this integrated CPB model because the influent SCFA concentration usually is very low and hence is included in the RBCOD. However, if the SCFA concentration is significant, such as with activated sludge treatment of anaerobic digester liquor, then SCFA utilization will influence the pH significantly and will need to be explicitly included in the model. This will require that the SCFA are modelled separately as a subfraction of the RBCOD and that four processes be added to the model, viz. processes A1c and A1d - aerobic growth of OHOs on acetate with ammonia (A1c) and nitrate (A1d) as N source, and processes A2c and A2d which are the anoxic equivalents. These processes will have identical stoichiometry as growth on RBCOD, but the substrate utilization is deducted from the HAc species of the SCFA system. Also, the SCFA concentration would need to be deducted from the RBCOD to correctly reflect the RBCOD as the remaining fermentable RBCOD, as is done in UCTPHO (Wentzel *et al.*, 1992) or ASM2 (Henze *et al.*, 1995), where SCFA is modelled separately from the fermentable RBCOD for biological P removal.

3.4.2 Autotrophic Nitrifier Organisms (ANOs)

3.4.2.1 Autotrophic metabolism

Although mediated by a number of different ammonia oxidizing and nitrite oxidizing organisms in two sequential steps from ammonia to nitrite and nitrite to nitrate, in ASM1 nitrification is modelled as a single step from ammonia to nitrate by a generic group of autotrophic nitrifier organisms (ANOs). The nitrification rate is defined by the slower process rate of the sequence, which under most circumstances is the ammonia oxidition. Stoichiometrically, nitrification of saline ammonia requires 2 mol (64gO) oxygen and produces 1mol nitrate and 2 mol protons, i.e.

$$NH_4^+ + 2O_2 \rightarrow NO_3^- + H_2O + 2H^+ \qquad (3.26)$$

The ANOs obtain their anabolic carbon requirements from dissolved CO_2 ($H_2CO_3^*$) and their catabolic energy (e^-) requirements from oxidizing ammonia to nitrate. Accepting that $C_5H_7O_2N$ represents the C, H, O and N content of the ANOs and has a COD content of 160g/mol, then five mol CO_2 are required to synthesize one mol ANOs viz.

$$5\,CO_2 + NH_4^+ + (20H^+ + 20e^-) \rightarrow C_5H_7O_2N + 8\,H_2O + H^+ \qquad (3.27)$$

which includes also the ammonia requirement for cell synthesis.

The catabolic ammonia (e^- and H^+) requirement is determined from the ANO yield coefficient, i.e.

Y_{ZA} = 0.15 (gANOCOD synthesized/gNH_4^+-N nitrified)
= 0.15*14/160 (mol ANOs/mol NH_4^+-N nitrified)

From Eq 3.27, the mol CO_2 required is 5 times the mol of ANOs formed. Hence

$$CO_2 \text{ required} = (5*12/160) = 3/8 \ (gCO_2\text{-}C/gANOCOD \text{ synthesized}) \qquad (3.28)$$

This stoichiometric ratio for CO_2 utilised by the ANOs is added to the model, accepting that the CO_2 taken up is in the dissolved form and represented as $H_2CO_3^*$ (Table 3.2).

The ANOs are conventionally considered to use the NH_4^+ species because this is the most abundant species in the optimum pH range for nitrification, i.e. 7.2-8.5. However, Suzuki (1974), in studies on *Nitrosomonas europae* concluded that the NH_3 species is used in the oxidation process. Also, Drozd (1976) argued that *Nitrosomonas* uses the NH_3 form because a rapid decrease in pH was noticed in the medium in growing cultures suggesting that a proton remains on the exterior of the cell wall in the medium. In this integrated model, it has been accepted that the unionized NH_3 species is used in oxidation, but that NH_4^+ species is taken up from solution with the release of H^+. In the operating pH range for nitrification, the NH_3 concentration is extremely low and its use in mathematical models can lead to numerical instability.

3.4.2.2 Production/utilisation of H^+ in ANO growth and death

The change in H^+ during nitrification (NH_4^+ oxidation and uptake for ANO growth) is derived from Eqs 3.26 and 3.27 and the stoichiometric coefficient for NH_4^+ in the ASM1 model is;

Concentration of NH_4^+-N nitrified to produce 1 gANOCOD/m^3 = $1/Y_{ZA}$ = 1/0.15
From Eq 3.26, 14 g of NH_4^+-N nitrified produce 2g H^+
So $1/Y_{ZA}$ g NH_4^+-N nitrified produces $1/(7Y_{ZA})$ gH^+

Also, from Eq 3.26, the NH_4^+ incorporated into ANO biomass during synthesis releases a H^+. The concentration of N incorporated into ANO mass is defined by the N content of the ANOs , which is accepted to be equal to that of the OHO, i.e. $f_{ZB,N}$ = 0.068 mgN/mgANOCOD. So from Eq 3.27,

14 g NH_4^+-N is incorporated into ANOs releases 1 g H^+
$\therefore$ $f_{ZB,N}$ g NH_4^+-N incorporated into ANOs releases $f_{ZB,N}$ /14 g H^+

Thus in total, during nitrification $1/(7Y_{ZA}) + f_{ZB,P}/14$ gH^+ are released per gANOCOD generated. For ANO death, N transformations are as for OHOs above.

Because the ANO mass constitutes such a small part of the measured reactor COD (or VSS) concentration and the endogenous respiration rate is so low, P uptake and release in ANO growth and death respectively are ignored as negligibly small. However, these can be readily incorporated if required, by following the concepts of the OHOs developed above.

3.4.2.3 Effect of pH on maximum specific growth rate of ANOs

The maximum specific growth rate of nitrifiers μ_A is very sensitive to pH, with nitrification rates declining sharply outside the optimum pH range of 7.0-8.5. In the activated sludge system treating reasonably well buffered wastewaters, quantitative modelling of the effect of pH on nitrification is not critical because pH reduction can be limited or completely obviated by including anoxic zones thereby ensuring alkalinity recovery via denitrification. However, in poorly buffered wastewaters, or wastewaters with high influent N (such as anaerobic digester liquors), the interaction between the biological processes, pH and nitrification is the single most important one for the N removal activated sludge system. Hence, it is essential to include the effect of pH on the nitrification rate in the integrated model to simulate this important interaction.

Quantitative modelling of the effect of pH on μ_A has been hampered by a lack of information and the general expected trends have been formulated based on empirical assumptions. Many studies have shown that μ_A can be expressed as a percentage of the highest value at optimum pH. Accepting this approach and that μ_A is highest and remains approximately constant in the pH range for 7.2<pH<8.5 and decreases as the pH decreases below 7.2 (Downing *et al.*, 1964; Loveless and Painter, 1968), WRC (1984) modelled the μ_A - pH dependency as:

For $7.2<pH<8.5$, $\mu_{ApH} = \mu_{A7.2}$ (3.29a)

For $5<pH<7.2$, $\mu_{ApH} = \mu_{A7.2}\theta_{ns}^{(pH-7.2)}$ (3.29b)

where

θ_{ns} = sensitivity coefficient ≈ 2.35

WRC (1984) considered additionally an increase in half saturation concentration (K_n, mgN/ℓ) with decrease in pH, i.e. $K_{npH} = K_{n7.2}\,\theta_{ns}^{(7.2-pH)}$ with θ_{ns} also = 2.35. They did this because Marais and Ekama (1976) observed an increase in effluent ammonia concentration as the reactor pH decreased with increasing sludge age. It is simple to include this additional effect into the model, but it was omitted because very little data could be found in the literature on the effect of pH on K_n to support the observation of Marais and Ekama (1976), probably because the effect of pH on nitrification was observed as an effect on μ_A, rather than an effect on μ_A and K_n individually. WRC (1984) did not consider cases where pH>8.5. Declining μ_A values at pH>8.5 have been observed and it has been noted that nitrification effectively ceases at a pH of about 9.5 (Malan and Gouws, 1966; Wild *et al.*, 1971; Antoniou *et al.*, 1990). Accordingly, for pH>7.2 an additional formulation is proposed to model the decline in the maximum specific growth rate from pH >7.2 to 9.5 as a function of $\mu_{A7.2}$ using inhibition kinetics as follows:

$$\mu_{ApH} = \mu_{A7.2}\, K_I\, \frac{K_{max} - pH}{K_{max} + K_{II} - pH} \qquad (3.30)$$

where

$K_I = 1.13$, $K_{max} = 9.5$, $K_{II} \approx 0.3$.

The overall effect of pH on μ_A is modelled by combining Eqs 3.29 and 3.30, giving the maximum specific growth rate at any pH between 5.5 and 9.5 as a fraction of the maximum rate at pH = 7.2, Eq 3.31, which is shown graphically in Fig 3.3. It can be seen that in the range pH = 7.2 to 8.3,

the change in μ_{ApH} is small, with $\mu_{ApH}/\mu_{A7.2} > 0.9$.

$$\mu_{ApH} = \mu_{A7.2}\, 2.35^{(pH-7.2)}\, K_I \frac{K_{max} - pH}{K_{max} + K_{II} - pH} \qquad (3.31)$$

where the term $2.35^{(pH-7.2)}$ is set = 1 for pH > 7.2, the term $K_I \frac{K_{max} - pH}{K_{max} + K_{II} - pH} = 1$ for pH < 7.2 and $\mu_{ApH} = 0$ for pH > 9.5.

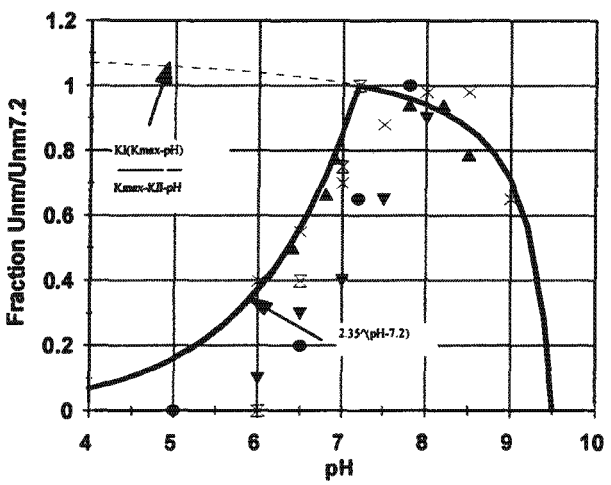

Fig 3.3: The effect of pH on the maximum specific growth rate of autotrophic nitrifying organisms (ANOs) μ_{nm}.
– Model (Eqs 3.29-3.31), • Malan & Gouws (1966)
▾ Sawyer *et al.* (1973), ⧗ Downing *et al.* (1966)
× Wild *et al.* (1971), ▲ Antoniou *et al.* (1990).

Experimental data from the literature are also shown in Fig 3.3 to provide some quantitative support for Eq 3.31. At low pH (<7.2) data from Wild *et al.* (1971) and Antoniou *et al.* (1990) fit the equation reasonably well. Very little data are available for pH>8.5, but the few points from Antoniou *et al.* (1990) show reasonable agreement with Eq 3.31. Accordingly, Eq 3.31 was accepted to calculate μ_{ApH} in the integrated model in the pH range 5.5 to 9.5. From Eq 3.31 the minimum sludge age for nitrification (R_{sm}) at different pH and temperature (T) and unaerated mass fraction (f_{xm}) is given by

$$R_{sm} = 1 / [\mu_{ApHT}(1 - f_{xm}) - b_{nT}] \quad \text{days} \qquad (3.32)$$

The problem with nitrification in low alkalinity wastewater is that the pH obtained is not known, because it is interactively established between the degree of nitrification, loss of alkalinity, pH and μ_{ApHT} (see below).

3.5 MODELLING GAS EXCHANGE IN THE INTEGRATED MODEL

3.5.1 Modelling Approach

In the three phase carbonate system weak acid/base model of Musvoto *et al.* (1997), the physical (P) processes of carbon dioxide gas exchange (passive) with the atmosphere were included. They did this by modelling the expulsion (reverse, K'_{rCO2}) and dissolution (forward, K'_{fCO2}) rates of diffusion separately and linking the two rates through the Henry's law constant for CO_2 (K_{HCO2}), i.e. $K'_{fCO2} = K'_{rCO2}\ K'_{HCO2}/RT$. They showed this approach yielded identical results to the usual interphase gas mass transfer equation with an overall liquid phase mass transfer rate coefficient K_{LaCO2}, where $K_{LaCO2} = K'_{rCO2}$. In their model application, the actual CO_2 expulsion rate constant value (K'_{rCO2}) was not important, because they considered final steady state conditions only, not the transient dynamic conditions to the final steady state.

Musvoto *et al.* (2000a) and van Rensburg *et al.* (2003) extended this chemical physical (CP) model to include three phase mixed weak acid/base systems to simulate multiple mineral precipitation and active gas exchange of CO_2 and NH_3 during aeration of anaerobic digester liquor and swinery wastewater. Because they simulated transient (dynamic) conditions, the gas exchange and mineral precipitation rates were important and these were determined from the experimental batch test results.

In this integrated CPB processes model of the activated sludge system, four gases need to be considered, viz. ammonia, carbon dioxide, nitrogen and oxygen. Because measurements of pH and $H_2CO_3^*$ alkalinity in aerobic reactors of full-scale activated sludge systems showed that equilibrium between the aqueous and gas (atmosphere) CO_2 phases is not reached during aeration in the aerobic reactor, the gas exchange (active) rates of the first three gases and the dissolution rate of oxygen by aeration are important for the simulation results, so that the K_{La} rate constants for the four gases had to be determined (Table 3.3).

For active gas exchange (stripping or dissolution), if the dimensionless Henry's law constant of a gas, H_c [$=1/(K_H RT)$] is > 0.55, then oxygen can be used as a reference gas and the overall liquid phase mass transfer (expulsion/dissolution) rate coefficient K_{La} ($= K'_r$) for the other gases can be accepted to be in a fixed relationship to the K_{La} rate for oxygen (K_{LaO2}) dependent on the relative magnitudes of the diffusivity of the other gases to oxygen (see Eq 3.33) (Munz and Roberts, 1989). Of the four gases, only ammonia has a $H_c < 0.55$ (= 0.011 at 20 °C, Table 3.6), so the K_{LaNH3} ($= K'_{rNH3}$, Musvoto *et al.*, 2000a) needs to be determined independently of the K_{La} rate of oxygen. However, because negligibly little ammonia is expelled from the aqueous phase with aeration in the pH range 6.5 to 8 for activated sludge systems, ammonia expulsion could have been omitted from the integrated model without loss of accuracy.

In the CP model of Musvoto *et al.* (2000a), the concentration of *non-dissolved* CO_2 gas, CO_2g, was essentially kept constant; CO_2g was included as a compound in the model only for continuity. In this integrated CPB model, CO_2g is not constant because dynamic variation in CO_2 production and consumption are considered. In implementation of the integrated CPB model, the CO_2g and the other gas compounds can be dealt with as part of the bulk liquid or as in a separate gaseous phase. Since the gas exchanges occur with the atmosphere where the partial pressures of the gases are essentially constant, and the head-space above activated sludge systems usually are not

confined, both approaches should lead to near identical simulations, provided the gas exchange rates are independent of the corresponding gas concentration e.g. CO_2g. Because the former approach is simpler to implement in the computer programme AQUASIM (Reichart, 1998), this approach was followed here. To ensure that the gas exchange rates are independent of the corresponding gas concentration, the original gas exchange dissolution formulation of Musvoto *et al.* (1997) was changed, with the gas species (e.g. CO_2g) concentration substituted for the relevant gas partial pressure and Henry's law constant (e.g. p_{CO2} K_{HCO2}, see Table 3.6). In effect this allows the gas species concentrations to vary and these are removed from the reactor hydraulically, i.e. with the effluent flow. If a separate gas phase implementation is required in AQUASIM, the diffusive link can be used for the gas exchange equations in Table 3.6. This would be necessary in anaerobic digestion (Batstone *et al.*, 2002).

Table 3.6: Dimensionless Henry's Law constants (H_c) at 20°C, liquid phase diffusion coefficient (D_L) at 20°C and liquid phase mass transfer rate coefficient (K_{La}) for oxygen, the reference gas, nitrogen, carbon dioxide and ammonia.

Gas	**Diffusivity at 20°C cm^2/s**	**Dimensionless Henry's law constant H_c**	**Overall liquid phase mass transfer rate coefficient K_{La}**
Oxygen, O_2	202500	32.54	600/d *1
Nitrogen, N_2	190000	64.2	Based on O_2 (Eq 3.33)
Carbon Dioxide CO_2	175300	1.06	Based on O_2 (Eq 3.33)
Ammonia, NH_3	-	0.011	3.2 /d*2

Note *1: Model fitted value to obtain 20% CO_2 super-saturation in the aerobic reactor bulk liquid, i.e. partial pressure of CO_2 20% higher than in the atmosphere (p_{CO2} atmosphere = 0.00035 atm).
Note *2: Arbitrary low value - actual low value not important because effectively zero ammonia gas strips from the aeration reactor by aeration.

$$K_{HCO_2} = 10^{-pK_{HCO2}} \text{ mol/(ℓ.atm)}; \quad pK_{HCO_2} = -\frac{2025.3}{T_K} - 0.0104\,T_K + 11.365;$$

$$H_{cCO_2} = \frac{1}{K_{HCO_2} R\,T_K}$$

$$K_{HN_{2T}} = K_{HN_{2\,25}} \exp\left[1300\left(\frac{1}{T_K} - \frac{1}{289.15}\right)\right] \quad \text{where} \quad K_{HN_{2\,25}} = 0.000661 \text{ mol/(ℓ.atm)}$$

$$r_{dissO2} = K_{LaO2}\left[O_{2\,sat} - O_{2\,reactor}\right] \quad \text{where } O_{2\,sat} = 8.9 \text{ mgO/ℓ (0.000278 mol/ℓ) at 20 °C and 1 atm,}$$

$O_{2\,reactor}$ = ~2.0 mgO/ℓ (0.000063 mol/ℓ) and K_{LaO2} = 600 /d.

Therefore, for CO_2, N_2 and NH_3 gas exchange from the anoxic and aerobic reactors, the following approach was adopted (using CO_2 as example):

Transfer from dissolved form $[H_2CO_3^*]$ to non-dissolved form CO_2g is the sum of processes P6 and P7 in Table 3.3.

$$r_{gmtCO2} = K_{LaCO2} \left[[H_2CO_3*] - p_{CO2} K_{HCO2} \right] \text{ molCO}_2/(\text{m}^3\text{d}) \text{ (see Table 3.6)} \qquad (3.33a)$$

where

r_{gmt} = rate of gas mass transfer (mol gas/(m^3d))
$[H_2CO_3^*]$ = concentration of dissolved CO_2 in aqueous phase (mol/ℓ)
p_{CO2} = partial pressure of CO_2 in the bulk liquid (atm)
K_{HCO2} = Henry's law constant for CO_2 (Table 3.6)
K_{LaCO2} = Overall liquid phase mass transfer rate coefficient for CO_2 (/d)

where

$$K_{LaCO2} = K_{LaO2} \left[\frac{D_{LCO2}}{D_{LO2}} \right]^n \left[1 + \frac{1}{\frac{k_G}{k_L} H_{cCO2}} \right]^{-1} \text{ (/d)} \qquad (3.33b)$$

where

K_{La} = Overall liquid phase mass transfer rate coefficient for CO_2 and O_2 (/d)
D_L = Liquid phase molecular diffusion coefficient for CO_2 and O_2 (cm^2/s) (Table 3.6)
k_G, k_L = Gas (k_G) and liquid (k_L) phase individual mass transfer coefficients (m/s)
H_{cCO2} = Dimensionless Henry's constant for CO_2 (Table 3.6)
n = Diffusivity coefficient = 0.50

In Eq 3.33, the ratio k_G/k_L represents the relative contribution of the gas and liquid phases mass transfer resistance under turbulent mixing conditions. A value of 30 to 40 is recommended by Munz and Roberts (1989) for the high turbulent mixing conditions created by power inputs (P/V) greater than 70 W/m^3 characteristic of aerated activated sludge reactors. In the simulations the k_G/k_L ratio was set to 40. From simulation, it was found that the K_{LaO2} rate affected the aerobic reactor dissolved oxygen (DO) and CO_2 ($H_2CO_3^*$) concentrations, but not the pH. As the K_{LaO2} rate was decreased from 600/d to 100/d, the DO decreased from close to saturation (~7 mgO/ℓ) to ~3.0 mgO/ℓ and CO_2 ($H_2CO_3^*$) concentration increased from 1.7 mgCO_2/ℓ (~3x saturated at p_{CO2} = 0.00035) to 6.2 mgCO_2/ℓ (~10 saturated) but the pH remained around 7.0. However, the anoxic reactor pH increased from 7.7 to 8.0 as the K_{LaO2} rate decreased due to increasing denitrification and greater alkalinity generation resulting from recycling less DO to the anoxic reactor (at a mixed liquor recycle ratio of 1:1). Tests at 2 full-scale activated sludge plants with fine bubble aeration indicated the aerobic reactor effluents were about 20% supersaturated with dissolved CO_2. So to get low dissolved CO_2 concentrations the K_{LaO2} rate was set at 600/d. Since the H_c for NH_3 is <0.55, the above equations cannot be applied for NH_3. The mass transfer coefficient for ammonia (K_{LaNH3}, Table 3.3) was set at a very low value of 3.2/d to ensure an extremely low loss of ammonia by aeration stripping. The partial pressure of the three gases in Table 3.3 were set at the standard atmospheric values i.e. p_{N2} = 0.79165, p_{O2} = 0.20800 and p_{CO2} = 0.00035 atmospheres.

3.6 THE INTEGRATED TWO PHASE MIXED WEAK ACID/BASE CHEMICAL, PHYSICAL AND BIOLOGICAL PROCESSES ACTIVATED SLUDGE MODEL

All the changes to the processes of growth for the heterotrophs and autotrophs discussed above were made to ASM1. The amended biological model was combined with the two phase (aqueous-gas) mixed weak acid/base subset model (Musvoto *et al.*, 2000), to give the integrated two phase mixed weak acid/base chemical, physical and biological processes (CPB) activated sludge model shown in matrix form in Tables 3.2 and 3.3. This model was incorporated into the AQUASIM computer programme (Reichart, 1998).

A number of simulations were done to verify the integrated CPB model, one of which, the aerobic batch test of Still *et al.* (1996), is shown in Fig 3.4 as illustration. Additional details such as kinetic and stoichiometric constants, are given by Dold *et al.* (1991). Because the total species concentrations of the carbonate, phosphate and SCFA systems were not measured by Still *et al.* (1996), values for these parameters had to be estimated for input to the model - values for the SCFA concentration were accepted to be zero as discussed above. All the remaining input information was taken from Dold *et al.* (1991). The predicted oxygen utilization rate (OUR), nitrate and TKN concentrations by the integrated model are compared with those predicted by the ASM1 (as given by Dold *et al.*, 1991) and the experimental data in Figs 3.4a, b and c. The predictions of the two models are identical and both compare very well with the experimental data. However, the integrated model predictions for the chemical physical processes could not be compared because ASM1 does not consider these processes, nor were they monitored experimentally in the batch test. Close correlation between predictions of the two models is expected because the simulations are for a municipal wastewater where the pH remained essentially constant so that, despite their inclusion in the integrated model, the weak acid/base systems (pH) have no significant effect on the biological processes. No suitable data on activated sludge treatment of municipal wastewaters where the weak acid/base systems and pH play a significant role could be found in the literature to directly validate the model. Because the chemical-physical and biological processes parts of the integrated model had been validated independently, rigorous validation of the integrated model was deemed not to be required except where the chemical physical processes affect the biological processes. In this regard, the principal interaction is the effect of pH on nitrification and this interaction was based and calibrated on literature information (Eqs 3.29 to 3.31, Fig 3.3).

3.6.1 A Note on the COD Mass Balance of the Model

Material mass balances (COD, C, N and P) are performed on model outputs and experimental systems to check model and data accuracy. Strictly, COD mass balances cannot be applied to the integrated model because inorganic C (CO_2) is changed to organic nitrifier (ANO) VSS (COD) mass, unless this contribution to the calculated VSS (COD) is specifically excluded. Theoretically, this contribution to the VSS (COD) is large enough (2-4%) to indicate a modelling error (>0.5%), but practically, remains small enough to be considered negligible for normal domestic wastewater where the mass of ANOs is very small compared with the mass of OHOs. However, for wastewaters which have a high TKN/COD ratio, such as sludge treatment liquors, the mass of ANOs will be significant compared with the mass of OHOs and COD mass balances much greater than 100% will be obtained if the ANO VSS (COD) is not excluded from the

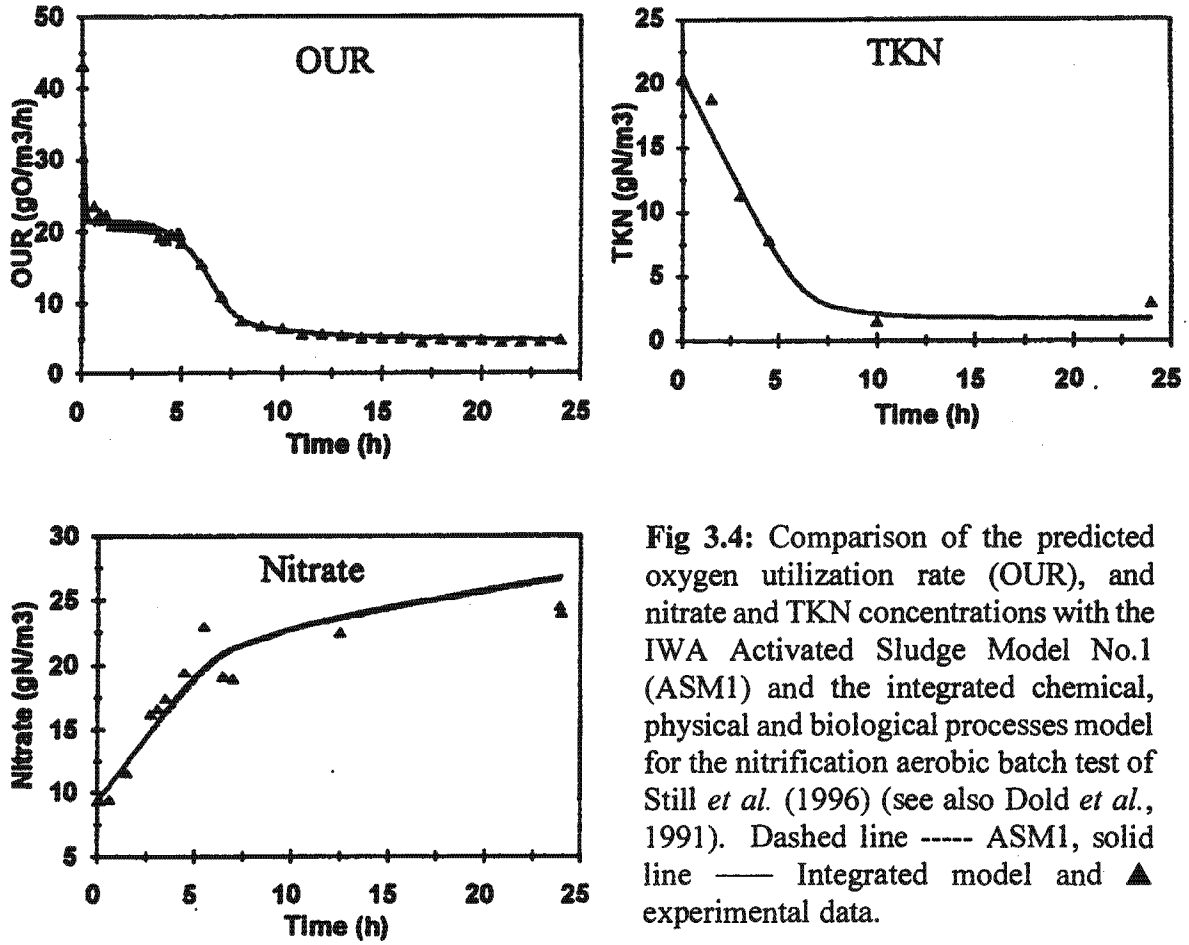

Fig 3.4: Comparison of the predicted oxygen utilization rate (OUR), and nitrate and TKN concentrations with the IWA Activated Sludge Model No.1 (ASM1) and the integrated chemical, physical and biological processes model for the nitrification aerobic batch test of Still *et al.* (1996) (see also Dold *et al.*, 1991). Dashed line ----- ASM1, solid line —— Integrated model and ▲ experimental data.

sludge mass in the COD mass balance. For the C mass balance, the COD/TOC ratio of the influent organics need to be known and was accepted at 3.0 (see above). Similarly, the COD/TOC ratios of the OHO and ANO active masses and their endogenous mass need to be known. For these, the active and endogenous masses were accepted to have the same stoichiometric formulation of $C_5H_7O_2N$ (WRC, 1984) which gives a COD/TOC of 2.67 mgCOD/mgC.

3.7 LOW ALKALINITY NITRIFYING / DENITRIFYING (ND) SYSTEM

To evaluate the performance of the integrated CPB model and illustrate the behaviour of ND activated sludge systems with low influent alkalinity, a Modified Ludzack Ettinger (MLE) anoxic -aerobic system was simulated. The influent wastewater characteristics (raw wastewater, COD=750mgCOD/ℓ, TKN=60mgN/ℓ, FSA=45mgN/ℓ, TP=11.27 mgP/ℓ, SCFA=0 mg/ℓ pH=7.3) and the system design and operating conditions (sludge age 30d, temperature 22°C, anoxic and aerobic mass fractions 0.35 and 0.65 and mixed liquor and sludge return recycles 3:1 and 1:1) were the same for each simulation. Also K_{LaO2} was set at 600/d to maintain low dissolved CO_2 concentrations (see above). Only the influent $H_2CO_3^*$ alkalinity was varied from 500 down to 15 mg/ℓ as $CaCO_3$. Effluent free and saline ammonia (FSA), nitrate (NO_3), total nitrogen (TN=FSA+NO_3) and $H_2CO_3^*$ alkalinity (as $CaCO_3$) concentrations and anoxic and aerobic reactor pH versus influent $H_2CO_3^*$ alkalinity are shown in Fig 3.5.

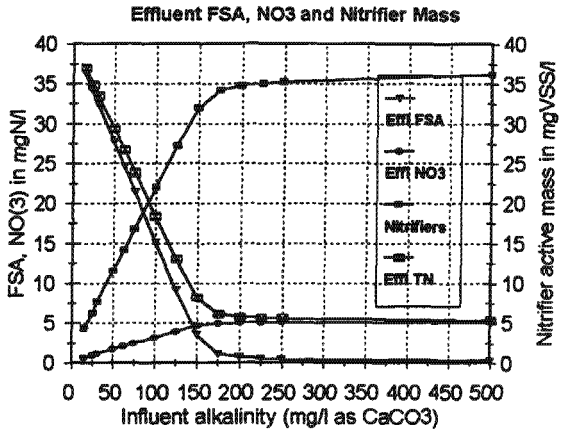

Fig 3.5a: Effluent free and saline ammonia (FSA), nitrate (NO_3) total nitrogen (TN= FSA+NO_3) and aerobic reactor autotrophic nitrifier organism (ANO) concentration versus influent $H_2CO_3^*$ alkalinity.

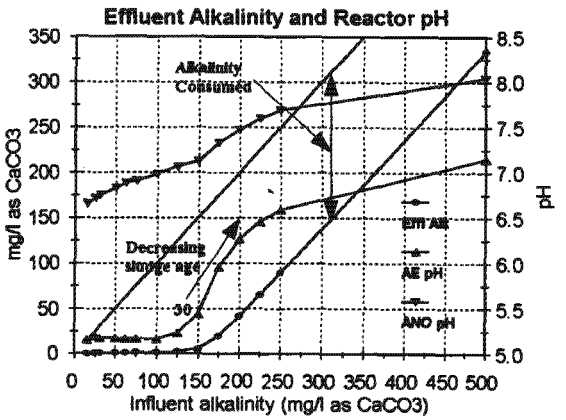

Fig 3.5b: Influent (diagonal) and effluent $H_2CO_3^*$ alkalinity and aerobic and anoxic reactor pH versus influent $H_2CO_3^*$ alkalinity.

The ND system delivers < 1 mgFSA-N/ℓ, ~5 mgNO_3-N/ℓ and ~5 mgTN-N/ℓ for influent $H_2CO_3^*$ alkalinity > 200 mg/ℓ (all alkalinities as $CaCO_3$) (Fig 3.5a). Although the pH in the aerobic reactor (which is about 1 pH unit below that in the anoxic reactor due to the CO_2 stripping by aeration) decreases with decreasing influent $H_2CO_3^*$ alkalinity, it remains above 6.3 (Fig 3.5b), at which pH the growth rate of the nitrifiers is still high enough for the long sludge age (30d) to achieve complete nitrification. The difference between the influent and effluent $H_2CO_3^*$ alkalinity is the $H_2CO_3^*$ alkalinity consumed by the system and from Fig 3.5b this is about 150 mg/ℓ when the influent $H_2CO_3^*$ alkalinity is >200 mg/ℓ. Once the influent $H_2CO_3^*$ alkalinity decreases below 200 mg/ℓ, the effluent $H_2CO_3^*$ alkalinity drops below 50 mg/ℓ and the aerobic reactor pH declines rapidly from 6.3 to below 5.5 for an influent $H_2CO_3^*$ alkalinity of <150 mg/ℓ. At pH 5.5 (influent $H_2CO_3^*$ alkalinity = 150 mg/ℓ), nitrification is at the point of failure and for lower influent alkalinities, the effluent FSA and TN concentrations begin to increase sharply and the effluent nitrate concentration decreases due to the lower concentration of nitrate generated by nitrification. Thus in general, if the effluent $H_2CO_3^*$ alkalinity from an activated sludge system, whether fully aerobic or ND, drops below 50 mg/ℓ, the reactor pH will fall below 5.5, which will inhibit nitrification and consequently compromise N removal. This conclusion is not new - WRC (1984) stated the same conclusion and recommended that when the effluent $H_2CO_3^*$ alkalinity falls below 50 mg/ℓ, lime dosing should be considered to raise the aerobic reactor pH, or, for fully aerobic systems, denitrification in anoxic zones be introduced to decrease the overall $H_2CO_3^*$ alkalinity consumption.

In this example, nitrification fails at the low pH of around 5.5 because the sludge age is very long (30d). At this pH, the maximum specific growth rate of the ANOs (μ_A) is depressed so low that an operating sludge age of 30 days becomes lower than the minimum sludge age for nitrification (R_{sm}) and the nitrifiers are washed out of the system. At shorter operating sludge ages, the pH at which nitrification fails will be higher (as indicated in Fig 3.5b). So at low influent $H_2CO_3^*$

alkalinity (<100 mg/ℓ), the pH declines, μ_A (Eq 3.31) decreases and R_{sm} increases (Eq 3.32). Once R_{sm} approaches the operating sludge age of the system (R_s), nitrification becomes unstable and the effluent FSA begins to increase, particularly under cyclic loading conditions.

3.8 CLOSURE

The biological processes of the nitrification-denitrification (ND) activated sludge model No 1 (ASM1, Henze *et al.*, 1987) were integrated into a two phase (aqueous-gas) subset of the three phase mixed weak acid/base chemical-physical kinetic model of Musvoto *et al.* (2000). In this integration, a number of additions were made to ASM1, such as (1) production and/or utilization of CO_2, H^+, NH_3, and H_3PO_4 in heterotrophic (OHO) and autotrophic (ANO) growth and death (endogenous respiration) and (2) the effect of pH (i.e. H^+) on the biological processes, in particular on the autotrophic nitrifiers (ANOs).

The integrated chemical, physical and biological (CPB) processes activated sludge model simulations were compared with those of ASM1 (Dold *et al.*, 1991) and experimental data in the literature. Identical simulation results were obtained with both models and the correlation of both models with experimental data was good. Strictly, these comparisons serve only as model verification because, although included, the weak acid/bases and pH have no significant effect on the biological processes in the cases considered. However, because the CPB model was developed by integrating previously individually validated models, rigorous independent experimental validation of the integrated model was not deemed necessary, except where the chemical-physical processes interact strongly with the biological processes. The principal interaction is the effect of pH on nitrification and this interaction was based on literature information and so is calibrated as best as possible. It is concluded from this integration that (i) the total organic carbon (TOC) to chemical oxygen demand (COD) ratio of the wastewater does not significantly influence the reactor pH, but (ii) the free and saline ammonia (FSA) to total Kjeldahl nitrogen (TKN) ratio and concentrations, (iii) nitrate uptake for OHO growth once ammonia is depleted (assimilative denitrification) and (iv) extent of denitrification and (v) the extent of CO_2 stripping from the aerobic reactor by aeration do affect reactor pH. Experimental determination of the inorganic carbon concentration (C_T) in effluents from full scale N removal activated sludge plants indicated that the effluents were about 20% supersaturated with CO_2 gas so that CO_2 gas exchange by aeration in the aerobic reactor does not yield CO_2 equilibrium with the atmosphere.

From simulation of long sludge age nitrification-denitrification (ND) activated sludge systems with incrementally decreasing influent $H_2CO_3^*$ alkalinity, when the effluent $H_2CO_3^*$ alkalinity falls below about 50 mg/ℓ as $CaCO_3$, the aerobic reactor pH drops below 6.3, which severely retards nitrification and causes the minimum sludge age for nitrification (R_{sm}) to increase up to the operating sludge age of the system. Therefore, when treating low $H_2CO_3^*$ alkalinity wastewaters, such as those from the Western and Southern coastal areas of South Africa, the minimum sludge age for nitrification (R_{sm}) varies with temperature and reactor pH and for low effluent $H_2CO_3^*$ alkalinity (< 50 mg/ℓ as $CaCO_3$), nitrification becomes unstable and sensitive to dynamic loading conditions resulting in increases in effluent ammonia concentration and reduced N removal. For effluent $H_2CO_3^*$ alkalinity < 50 mg/ℓ, lime should be dosed raise the aerobic reactor pH and stabilize nitrification.

In the next Chapter (Chapter 4), a model for the anaerobic digestion of wastewater sludges will be developed, also in two phases, so that it can be incorporated into this two phase biological, chemical and physical processes model to provide a kinetic model for the anaerobic digestion of wastewater sludges as well as the activated sludge system. Such a model will represent a significant step towards achieving an integrated kinetic model for an entire wastewater treatment system.

CHAPTER 4

INTEGRATED CHEMICAL/PHYSICAL AND BIOLOGICAL PROCESSES MODELLING: ANAEROBIC DIGESTION OF SEWAGE SLUDGES

4.1 INTRODUCTION

Anaerobic digestion (AD) is one of the oldest biological waste treatment processes, dating back more than a century. With the development of digester heating and mixing, AD has established itself as the most common method of sludge stabilization, and has proven to be effective also in reducing the volumes of sludge with the production of energy rich bio-gas. It has been shown that AD is an effective process for the treatment of a number of types of organic sludges, ranging from municipal waste activated (WAS) and primary sludges (Kayhanian and Tchobanoglous, 1992; Cout *et al.* 1994) to industrial organic sludges and agricultural slurries (Hill and Barth, 1977). In particular, the application of AD to the stabilization of sewage sludges (primary, WAS and humus) is widespread, and this chapter focuses on this application.

Despite its widespread application, the design, operation and control of anaerobic digesters treating sewage sludges are still based largely on experience or empirical guidelines. To aid the design, operation and control of (and research into) AD, a mathematical model would be an invaluable process evaluation tool. Mathematical models provide quantitative descriptions of the treatment system of interest that allow predictions of the system response and performance to be made. From these predictions, design and operational criteria can be identified to optimize the system performance. Mathematical models provide an integrated framework for the system which can give guidance to design, operation and research.

Recognising the potential usefulness of mathematical models, various researchers have developed such models to describe AD (e.g. McCarty, 1974, Hill and Barth, 1977; Gujer and Zehnder, 1983; Sam-Soon *et al.*, 1991; Kiely *et al.*, 1997, Batstone *et al.*, 2002). The early models focussed primarily on the biological processes operating in an anaerobic digester. Although the importance of the interaction between the biological processes and the weak acid/base chemistry environment in which they operate was recognised early on, because of the effect of pH on the biological processes, modelling this interaction proved to be a more complex problem than delineating the biological processes themselves. Initially the impact of the biological processes on pH was assessed graphically based on equilibrium chemistry principles of the carbonate weak acid/base system (e.g. Capri and Marais, 1975). The advent of computers and development of numerical algorithms made it easier to model the interaction based on single or two phase (aqueous-gas) weak acid/base chemistry equilibrium equations to estimate the pH in anaerobic digesters. The approach of Loewenthal *et al.* (1989, 1991) made it possible to include multiple mixed weak acid/base systems, both for estimating the digester pH and in the determination and interpretation of the commonly measured digester control parameters, short chain (volatile) fatty acids (SCFA) and alkalinity (Moosbrugger *et al.*, 1992; Lahav and

Loewenthal, 2000). The latest AD model (IWAADM1, Batstone *et al.*, 2002) includes algebraic algorithms, based on equilibrium weak acid/base chemistry and continuity of charge balances, that seek to model the environment in which the biological processes operate, to predict the pH. These algebraic algorithms and calculation of pH operate externally to the kinetic model structure. As alternative, dynamic equilibria equations for the weak acid/base systems are described (similar to the approach of Musvoto *et al.*, 1997, 2000a). However, the weak acid/base water is not included so that pH is again algebraically calculated externally to the kinetic model, via the charge balance. Calculation of pH externally via the charge balance cannot deal simply with multiple weak acid/base systems in three phases (aqueous/gas/solid), where several minerals competing for the same species may precipitate simultaneously or sequentially (Musvoto *et al.*, 2000a,c): In some anaerobic digestion systems precipitation of minerals is significant, either within the digester itself or in pipework leading from the digester so that the relevant chemical precipitation processes would require inclusion. For such situations, the biological processes and multiple weak acid/base systems in three phases should be modelled in an integrated way within the same kinetic model structure.

In Chapter 3, an integrated chemical (C), physical (P) and biological (B) processes kinetic model for the N removal activated sludge system was presented. This model was developed by integrating the biological processes of the International Water Association (IWA) Activated Sludge Model No 1 (ASM1, Henze *et al.*, 1987) into a two phase (aqueous-gas) subset of the three phase mixed weak acid/base C-P model of Musvoto *et al.* (1997, 2000a,b,c), and included additionally gas exchange of N_2. This chapter describes the development of an integrated two phase (aqueous-gas) chemical (C), physical (P) and biological (B) processes AD model for sewage sludges, by integrating the biological processes for AD with the same two phase subset of the three phase CP model of Musvoto *et al.* (1997, 2000a,b,c). In fact, the N removal activated sludge and AD models are two parts of a single larger model being developed for simulating the entire wastewater treatment plant (WWTP) on materials mass balance and continuity principles. It is planned to also include biological excess P removal (BEPR) and AD of P rich waste activated sludges in the WWTP model.

After reviewing ADM1 (Batstone *et al.*, 2002), which is a synthesis and refinement of many years of research and modelling of AD systems, the integrated chemical, physical and biological AD model is built up in stages. First, the biological processes are defined and then these are integrated into the mixed weak acid/base model of Musvoto *et al.* (1997, 2000a,b,c). For ease of cross-referencing to the source chapters, the same process and compound numbering system described in Chapter 3 will be used in this Chapter (see Table 3.1, Chapter 3).

4.2 LITERATURE REVIEW

4.2.1 Anaerobic Digestion Model No.1 (ADM1)

The IWA task group for mathematical modelling of anaerobic digestion processes developed the anaerobic digestion model no.1 (ADM1, Batstone *et al.*, 2002) through collaboration between many international experts in anaerobic digestion process analysis, modelling and simulation. The final model was presented at the 9th IWA Anaerobic Digestion Conference in Antwerpen, Belgium, in September 2001. A short review of the ADM1 model (Batstone *et al.*, 2002) is presented below.

4.2.1.1 Biochemical processes

Batstone *et al.* (2002) agreed on a structural model, because the inclusion of processes and components maximized the models applicability while still retaining a reasonably simple structure. The model that they implemented is shown in Figure 4.1 below. The model includes three overall biochemical processes (acidogenesis, acetogenesis and methanogenesis), an extracellular disintegration step (i.e. the influent organic material is split into carbohydrate, protein, lipid and inert material fractions) and an extracellular hydrolysis step - see Figure 4.1. They described cellular kinetics by three expressions: Uptake, growth and decay. They based the substrate uptake on substrate level Monod-type kinetics, and they chose substrate uptake related kinetics rather than growth kinetics to decouple growth from substrate uptake, and hence allow for a variable organism yield. Organism growth is implicit in substrate uptake, and they described biomass decay using first order kinetics with an independent set of expressions. The 'dead' cell matter contributes to the composite particulate waste pool, and therefore it undergoes disintegration and hydrolysis with the influent substrate to become soluble substrate for the remaining organisms.

Hydrolysis:
Batstone *et al.* (2002) split the process of hydrolysing the influent complex mixed organics into two distinct steps, (i) the disintegration of the mixed substrate into carbohydrates, proteins and lipids and (ii) the hydrolysis of the carbohydrates, proteins and lipids into monosaccharides, amino acids and long chain fatty acids respectively. They described the disintegration step as a non-biological process, and they included it as the first process so that ADM No.1 could be applied to diverse influents, including complex organic material (e.g. primary sludge) as well as waste activated sludge (from the waste stream of an activated sludge process), where the disintegration of the former (complex organic material) represents the separation of composite material while the disintegration of the latter (waste activated sludge) represents the lysis of cell material. Together, the separation and lysis represent the disintegration of a pool of composite organic material. Batstone *et al.* (2002) termed the subsequent degradation of the disintegrated and now defined particulate or macromolecular substrate into its soluble monomers as hydrolysis. They identified carbohydrates, proteins and lipids as the most significant substrates to undergo hydrolysis, and for these substrates, the depolymerisation process matches the formal definition of hydrolysis.

They assumed that the hydrolysis of carbohydrates, proteins and lipids is mediated extra cellularly by enzymes that are produced directly by the organism groups that utilize the soluble products of the hydrolysis process. Further, they agreed that in anaerobic mixed cultures, the organisms attach to the particulate substrate and produce the enzymes required for hydrolysis in close proximity to this substrate, rather than secreting the enzymes to the bulk liquid, so that the organisms can benefit directly from the soluble substrate produced by the hydrolysis. They concluded that the organisms growing on the surface of the particulate substrate should therefore be regarded as the catalyst for hydrolysis, rather than the enzymes excreted by the organisms. To describe the kinetics of the disintegration and hydrolysis steps, Batstone *et al.* (2002) recommend that first order kinetics should be used by default, because all models in literature that use a disintegration term as opposed to a hydrolysis term have used first order kinetics. They reasoned that the complete enzymatic hydrolysis of carbohydrates, proteins and lipids is a complex multi-step process that may include multiple enzyme production, diffusion, adsorption, reaction and

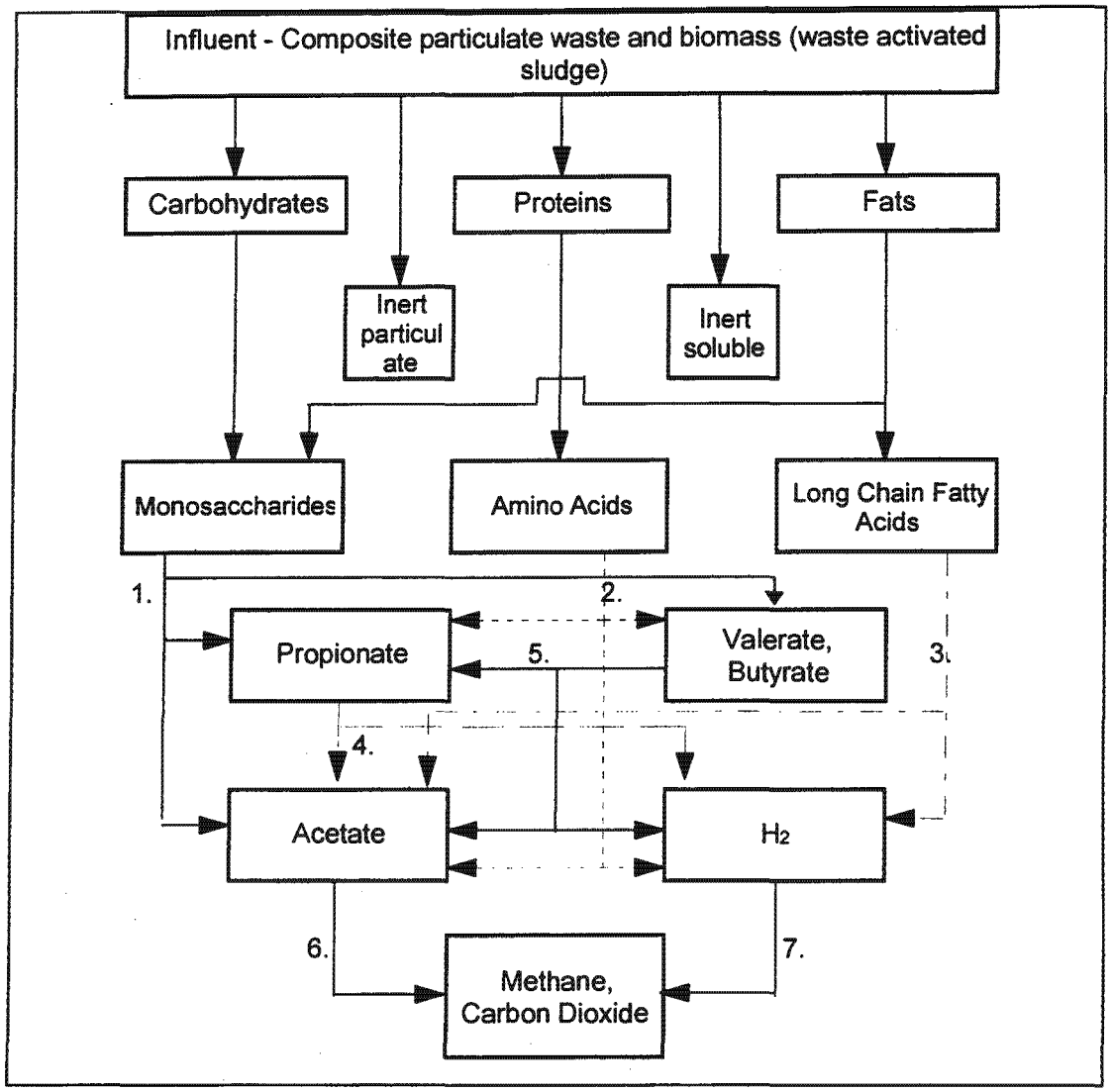

Fig. 4.1: The ADM No.1 model (Batstone *et al.*, 2002) including biochemical processes: (1.) Acidogenesis from sugars, (2.) acidogenesis from amino acids, (3.) acetogenesis from long chain fatty acids, (4.) acetogenesis from propionate, (5.) acetogenesis from butyrate and valerate, (6.) acetoclastic methanogenesis and (7.) hydrogenotrophic methanogenesis.

enzyme deactivation steps, and the most commonly used kinetic relationship to describe these processes is the first order relationship, because it is an empirical expression that reflects the cumulative effect of all microscopic processes occurring in hydrolysis (Eastman and Ferguson, 1981).

Acidogenesis:
For the acidogenesis of monosaccharides, Batstone *et al.* (2002) decided to use glucose as the model monomer. Further, they included acetate (Eq 4.1 and 4.2)), butyrate (Eq 4.3) and propionate as end products from monosaccharide (glucose) acidogenesis, while lactate (which should not be present in a normally operating anaerobic digester, because it is an intermediate in glucose fermentation and degrades very rapidly) and ethanol (which is produced as an

alternative to acetate at pH<5.0) were not included. The stoichiometric reactions from glucose that were included in ADM1 are given below:

$$C_6H_{12}O_6 \rightarrow 2CH_3COOH + 2CO_2 + 4H_2 \quad (4.1)$$

$$3C_6H_{12}O_6 \rightarrow 4CH_3CH_2COOH + 2CH_3COOH + 2CO_2 + 2H_2O \quad (4.2)$$

$$C_6H_{12}O_6 \rightarrow CH_3CH_2CH_2COOH + 2CO_2 + 2H_2 \quad (4.3)$$

Batstone *et al.* (2002) used a modified version of the uncoupled reaction of glucose to propionate (Eq 4.2), which converts glucose to both propionate and acetate. They used Eq 4.2 rather than the true uncoupled reaction of glucose to propionate because (i) no organism producing propionate only has been cultured and (ii) oxidising formate or elemental hydrogen is thermodynamically unfavourable except at high hydrogen partial pressure and is therefore inconsistent with the release of formate or hydrogen by organisms fermenting monosaccharides to butyrate or acetate.
The organism group that mediates acidogenesis of monosaccharides was modelled as a single group of organisms with lumped parameters, and no hydrogen regulation function was included in ADM1.

For modelling the acidogenesis from amino acids, Batstone *et al.* (2002) recognized that there are two two main pathways for the anaerobic digestion of amino acids: (i) Stickland oxidation-reducing paired fermentation and (ii) oxidation of a single amino acid with hydrogen ions or carbon dioxide as the external electron acceptor. They chose the Stickland oxidation-reduction paired fermentation to model the acidogenesis of amino acids, and some characteristics of the Stickland oxidation-reduction paired fermentation are:

(i) Amino acids can act as electron donors, acceptors or both.
(ii) The electron donor loses one carbon to carbon dioxide and forms a carboxylic acid with one carbon shorter than the original amino acid.
(iii) The electron acceptor retains carbon atoms to form a carboxylic acid with the same chain length as the original amino acid.
(iv) Only histidine cannot be degraded via the Stickland reactions.
(v) Around 10% of total amino acids are degraded by uncoupled oxidation because of a shortfall in electron acceptors, and this results in hydrogen or formate production.

Batstone *et al.* (2002) regarded these characteristics as important for modelling amino acid acidogenesis because the source proteins are likely to contain a mixture of amino acids and the stoichiometric yields of products can be predicted. They argued that the Stickland spreadsheet, which is a compilation of yields from amino acids to estimate the yields from the amino acid content of a protein substrate, offers a reasonable initial estimate of the product yields for the modelling of amino acid fermentation. Because the Stickland reactions are not inhibited by hydrogen, they excluded hydrogen regulation or inhibition functions from ADM1.

Acetogenesis and methanogenesis:
Batstone *et al.* (2002) describe the degradation of higher organic acids to acetate as an oxidation step, with no internal electron acceptor. Therefore, the organisms are required to utilize an additional electron acceptor such as the hydrogen ion or carbon dioxide to produce hydrogen gas or formate respectively. The electron acceptors must however be present at low concentration for the oxidation reaction to be thermodynamically possible and hydrogen and formate are consumed by methanogenic organisms. They stated further that the thermodynamics of acetogenesis and hydrogen utilizing methanogenesis reactions are only possible in a narrow range of hydrogen or formate concentrations. They considered this important for modelling, because the thermodynamic limitations largely determine the parameter for hydrogen inhibition, as well as half saturation coefficients and yields.

The electron acceptor can be either hydrogen, formate or carbon dioxide. Batstone *et al.* (2002) decided to implement hydrogen as the only electron acceptor here, because (i) hydrogen transfer is faster for short interspecies distances, (ii) model implementation is assumed unaffected as the stoichiometry and thermodynamics are virtually identical for hydrogen and formate and (iii) acetogens can utilize either and hydrogenotrophic methanogens can accept either hydrogen or formate.

Batstone *et al.* (2002) incorporated three acetogenic bacterial groups into ADM1: One for propionate, one for butyrate and valerate and one for the long chain fatty acids. A single group of organisms was included for hydrogen utilizing methanogenesis. A standard non-competitive inhibition function was included in ADM1 for hydrogen regulation.

Acetoclastic methanogenesis:
In acetoclastic methanogenesis, acetate is cleaved to form methane:

$$CH_3COOH \rightarrow CH_4 + CO_2 \tag{4.4}$$

Batstone *et al.* (2002) included a single group of acetoclastic methanogenic organisms in ADM1. They state that two organism groups are known to utilize acetate to produce methane, but it has been found that the presence of two different organism populations in anaerobic digesters is usually mutually exclusive, therefore they included only one acetoclastic methanogen organism group into ADM1.

Inhibition functions:
Batstone *et al.* (2002) considered several mechanisms of modelling inhibition in ADM1. They argued that because the inhibition forms in anaerobic digestion are varied and extensive, Eq 4.5 below expresses the inhibition forms most suitably and it allows for easy substitution or addition of inhibition terms:

$$\rho_j = \frac{k_m S}{K_s + S} X \cdot I_1 \cdot I_2 \cdots I_n \tag{4.5}$$

where the first part of Eq 4.5 is the uninhibited Monod-type uptake and $I_{1...n}$ are the inhibition functions.

They included the following inhibition functions in ADM1:

(i) pH inhibition of all intracellular processes, with different parameters for each organism group (acidogens, acetogens, hydrogenotrophic methanogens and acetoclastic methanogens). pH inhibition for hydrolysis was not included, but Batstone *et al.* (2002) argued that if a user does require pH inhibition for hydrolysis, functions are readily available in the literature and can easily be added to ADM1.

(ii) Hydrogen inhibition of the acetogens.

(iii) Free ammonia inhibition of the acetoclastic methanogens.

4.2.1.2 Physio-chemical processes

Batstone *et al.* (2002) defined the physio-chemical processes as non-biologically mediated processes that commonly occur in anaerobic digesters. There are three types of chemical/physical processes, namely (i) liquid-liquid processes which are usually fast (e.g. ion dissociation/association), (ii) liquid-gas processes which are fast to medium speed (e.g. carbon dioxide expulsion/dissolution) and (iii) liquid-solid processes which are medium speed to slow reactions (e.g. precipitation/solubilization). Liquid-liquid and liquid-gas processes were included in ADM1. Batstone *et al.* (2002) excluded the liquid-solid processes from ADM1, because of the complexity of the process, the range of different cations and because systems which have high calcium and magnesium levels are relatively limited.

Liquid-liquid processes:

The following acid/base pairs were included in ADM1: $CO_2(aq)/HCO_3^-$ (carbonate), NH_4^+/NH_3 (ammonia), H_2S/HS (Sulphide), OH^-/H^+ (water), HAc/Ac^- (acetate), HPr/Pr^- (propionate), HBu/Bu^- (butyrate), HVa/Va^- (valerate). The equations describing acid/base reactions can be formulated and solved as differential equations or as an implicit algebraic set of equations. Batstone *et al.* (2002) stated that either of two approaches can be taken to formulate the acid/base reaction equations, either (i) the charge balance, or (ii) the tableau method (Morel and Hering, 1993). For ADM1, they chose to use the charge balance, as they considered it easier to understand and of greater educational value. The charge balance can be expressed as:

$$\sum S_{C^+} - \sum S_{A^-} = 0 \tag{4.6}$$

where S_{C+} represents the cation equivalents and S_{A-} the anion equivalents. As implemented in ADM1, Batstone *et al.* (2002) give the charge balance as follows:

$$S_{Cat^+} + S_{NH4^+} + S_{H^+} - S_{HCO3^-} - \frac{S_{AC^-}}{64} - \frac{S_{Pr^-}}{112} - \frac{S_{Bu^-}}{160} - \frac{S_{Va^-}}{208} - S_{OH^-} - S_{An^-} = 0 \tag{4.7}$$

where S_{Ca+} and S_{An-} represent metallic ions and are included to represent strong bases and acids respectively. They did not include the long chain fatty acids, because the number of charged sites per COD is very small. Further, they did not include the amino acids, because of their low concentrations as well as the wide range of amino acid pK values which would complicate the model unnecessarily. When they implemented the acid/base equations as an algebraic set, the combined concentration of each acid/base pair was expressed as a dynamic state variable, and

the remaining algebraic equations were formed from the respective acid/base equilibria equations.

Liquid-gas processes:
Batstone *et al.* (2002) considered the following gas components as significant intermediates that have a strong effect on the biological processes or their outputs: (i) hydrogen gas, (ii) methane gas and (iii) carbon dioxide gas. These three gases where incorporated into ADM1. They also considered hydrogen sulphide gas as important, but they did not include it in ADM1 because sulphate reduction was not included as a biological process. Ammonia gas was considered equally important, but they considered the mass flux to gas as negligible compared to that in the effluent, and hence they did not include ammonia gas in ADM1.

Batstone *et al.* (2002) used dynamic gas transfer equations to describe the liquid-gas transfer, because they believed that the gases in the liquid phase in anaerobic digestion are usually significantly supersaturated, and therefore Henry's law does not apply, as it is only valid when the liquid phase is relatively dilute. Therefore they decided to use the most common dynamic transfer equations, which follow the two-film theory:

$$\rho_{T,j} = k_{La}\left(S_{liq,i} - K_H \rho_{gas,i}\right) \tag{4.8}$$

where k_{La} is the overall mass transfer coefficient multiplied by the specific transfer area and $p_{T,i}$ is the specific mass transfer rate of gas i. They further stated that because all three gases (hydrogen, methane and carbon dioxide) included in ADM1 are liquid film controlled, and the diffusivities are similar, they should have k_{La} values of similar order of magnitude.

4.2.1.3 The complete model
Batstone *et al.* (2002) present the complete model, ADM1 in four matrices: (i) The biochemical rate coefficients and kinetic rate equations for soluble components, (ii) the biochemical rate coefficients and kinetic rate equations for particulate components, (iii) gas transfer and (iv) acid/ base equilibrium.

They chose COD units as the chemical component base unit, because of its use as a wastewater characterization measure, its use in upstream and gas utilization industries, the implicit balancing of carbon oxidation state and to enable compatibility with the IWA Activated Sludge Models. They used molar units for components with no COD, such as carbon dioxide. The complete model contains 26 state variables and they suggest values for all required kinetic and stoichiometric constants.

4.3 BIOLOGICAL PROCESSES OF ANAEROBIC DIGESTION

4.3.1 Conceptual Model

In the literature there is considerable variation in conceptual schemes for describing the biological processes of AD with sewage sludge as influent, from simple two stage reaction schemes including only hydrolysis/acidogenesis and methanogenesis (Kiely *et al.*, 1997) to the most commonly used six step reaction scheme as proposed by Gujer and Zehnder (1983).

In the reaction scheme of Gujer and Zehnder (1983) (Fig 4.2), the hydrolysis process acts separately on three main groups of complex organics, viz (i) proteins, (ii) carbohydrates and (iii) lipids. These complex polymeric materials are hydrolysed by extracellular enzymes to soluble products that are small enough to allow their transport across the cell membrane. The products of the separate hydrolysis processes are amino acids, sugars and fatty acids respectively. These relatively simple, soluble compounds are fermented (acidogenesis) or anaerobically oxidised to short chain fatty acids (SCFAs) (acetate), alcohols, CO_2, hydrogen and ammonia. A portion of the hydrolysis products are also converted to intermediate products (propionate, butyrate, etc.), which are then converted to acetate, hydrogen gas and CO_2 through a process called acetogenesis. Lastly, methanogenesis occurs by hydrogen reduction with CO_2 (hydrogenotrophic methanogenesis) and from acetate cleavage (acetoclastic methanogenesis).

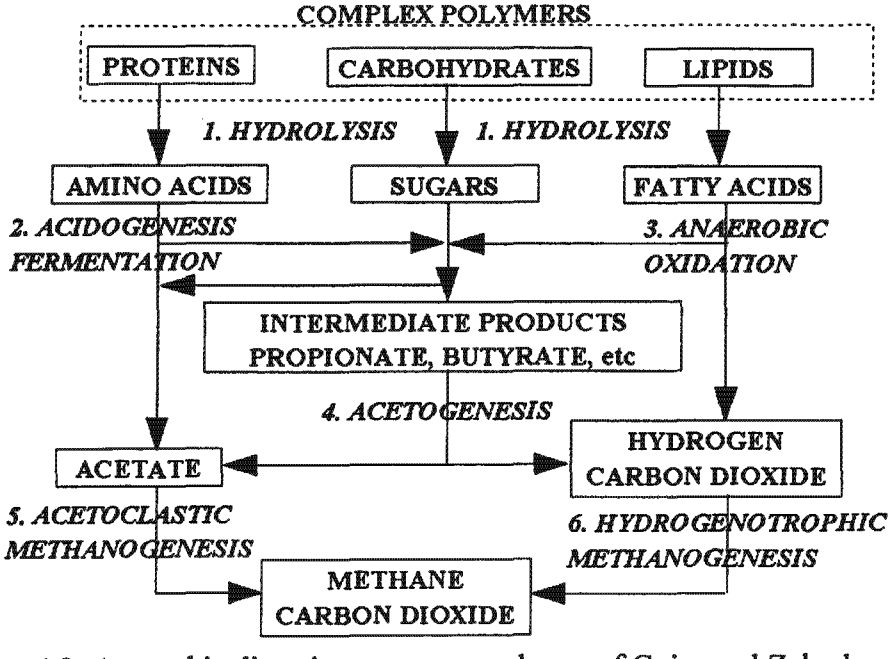

Fig 4.2: Anaerobic digestion processes scheme of Gujer and Zehnder (1983)

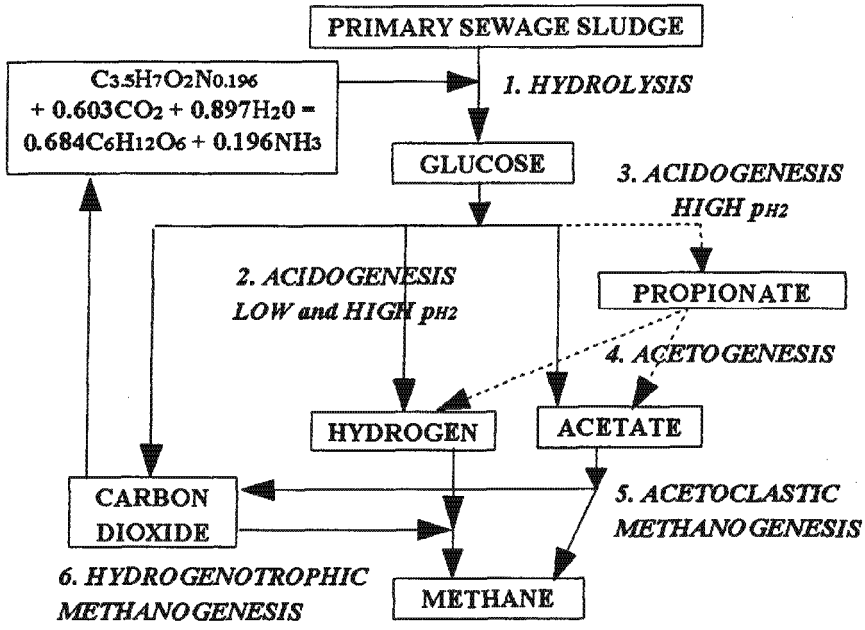

Fig 4.3: Anaerobic digestion processes scheme of University of Cape Town Anaerobic Digestion Model No 1 (UCTADM1) including (i) the effect of high hydrogen partial pressure on acidogenesis and (ii) COD, carbon and nitrogen mass balances with a generic CHON sludge composition.

The Gujer and Zehnder (1983) reaction scheme formed the basis for the AD model developed here, but with four main modifications (Fig 4.3), viz:

(1) Recognising that carbohydrate, protein and lipid measurements on sewage sludges are unlikely to be routinely available and indeed are difficult to do, the hydrolysis of the three separate organic materials was modified to a single hydrolysis process acting on a generic organic material representing sewage sludge ($C_XH_YO_ZN_A$, McCarty, 1974). This simplification is not unreasonable since the end products of hydrolysis and subsequent acidogenesis of the three organic groups are essentially the same, namely SCFAs. In this approach, the C, H, O and N contents of sewage sludges are needed to determine the X, Y, Z and A values in $C_XH_YO_ZN_A$; These were determined by simulation of measured data and direct measurement, see below. In follow-up work, which is beyond the scope of this thesis project report, it is envisaged to extend the model to AD of waste activated sludges (including biological excess P removal sludges) in 3 phases (liquid-gas-solid), i.e. including mineral precipitation, the P content of sewage sludges will be added to this formulation (i.e. $C_XH_YO_ZN_AP_B$).

(2) With the proposed single hydrolysis process, recognition of three separate hydrolysis products was no longer necessary. Accordingly, a single hydrolysis process and end product were included. This end product was chosen to be the idealised carbohydrate 'glucose' for a number of reasons: The subsequent biological processes on 'glucose' are well established and the acidogenic/fermentation process acting on 'glucose' to convert it to SCFAs is unlikely ever to be rate limiting. Accordingly, in model application accumulation of 'glucose' will not occur, even under digester failure conditions. This implies that the 'glucose' acts merely as an

intermediate compound, which is acidified to SCFAs as soon as it is produced. In any event, because the end products of hydrolysis and acidogenesis in the scheme of Gujer and Zehnder (1983) (Fig 4.2) are the same as in the revised scheme (Fig 4.3), the net result is the same in both schemes. In order to maintain the COD, C, H, O and N balances, water and carbon dioxide are taken up from the bulk liquid to generate the glucose from the sewage sludge (Fig 4.3), and ammonia is released.

(3) As a consequence of accepting a single hydrolysis process, separate anaerobic oxidation of fatty acids does not need to be included.

(4) In the reaction scheme of Gujer and Zehnder (1983), a fixed proportion of hydrolysis end products are converted to intermediate SCFA (propionate, butyrate, etc.) and the balance directly to acetate. As an alternative, the influence of the hydrogen partial pressure (p_{H2}) on acidogenesis of glucose to acetate and propionate as proposed by Sam - Soon *et al.* (1991) was included in the revised scheme. This provides a better description of AD behaviour under failure conditions. To include the proposals of Sam - Soon *et al.* (1991), the acidogenesis was divided into two processes - (i) under high p_{H2} conditions, acetic and propionic acids are generated together with H_2 and CO_2 and (ii) under low p_{H2} conditions, acetic acid only is generated together with H_2 and CO_2. In this revised scheme, generation of butyrate and higher SCFAs was not considered, because with sewage sludge as influent these usually are only found in minor concentrations, even under digester failure conditions.

4.3.2 Mathematical Model - UCTADM1

Accepting the revised reaction scheme (Fig 4.3), the biological processes mediated by the four recognized AD organism groups were included in the two phase (aqueous-gas) chemical (C), physical (P) and biological (B) anaerobic digestion model (UCTADM1, see Table 4.1). Following ASM1 for activated sludge systems (Henze *et al.*, 1987), the processes were formulated either as hydrolysis or organism group growth processes. All four organism groups were accepted to be subject to endogenous respiration and so an endogenous mass loss process was included in the model for each group. It is recognised that the organism groups are not representative of a single organism species, but rather are 'surrogates' representing all organism species performing a particular function of interest; This is similar to the approach followed for modelling of activated sludge systems (e.g. Dold *et al.*, 1980, Henze *et al.*, 1987). In formulating the model, since weak acid/base chemistry is included directly, all biological processes that act on weak acid/base species needed to be formulated in terms of the relevant dissociated or undissociated species (see below). This included both the stoichiometric consumption or production of weak acid/base species by the processes, and the formulation of the kinetic rate expressions. Whichever species is selected, in the production or consumption of weak acid/base species, because the weak acid/base chemistry is included directly, the model will automatically redistribute the weak acid/base species including the hydrogen ion (H^+) and establish a new pH.

Table 4.1: Biological processes included in the two phase anaerobic digestion model.

PROCESS	SPECIFIC BIOLOGICAL PROCESS	ORGANISM GROUP
Hydrolysis	D1. Hydrolysis of $C_XH_YO_ZN_A$ to 'glucose'	Acidogens, Z_{AD}
Growth	D2. Acidogens on 'glucose' under low p_{H2}	Acidogens, Z_{AD}
	D3. Acidogens on 'glucose' under high p_{H2}	Acidogens, Z_{AD}
	D5. Acetogens on propionic acid	Acetogens, Z_{AC}
	D7. Acetoclastic methanogens on acetic acid	Acetoclastic methanogens, Z_{AM}
	D9. Hydrogenotrophic methanogens on H_2	Hydrogenotrophic methanogens, Z_{HM}
Death / Endogenous decay	D4. Acidogens	Acidogens, Z_{AD}
	D6. Acetogens	Acetogens, Z_{AC}
	D8. Acetoclastic methanogens	Acetoclastic methanogens, Z_{AM}
	D10. Hydrogenotrophic methanogens	Hydrogenotrophic methanogens, Z_{HM}

The 10 biological processes listed in Table 4.1 act on 14 compounds and cause changes in their concentrations. The changes in some compound concentrations may be directly measurable, but the changes in the non-measurable compound concentrations are inferred from the conceptual model of the processes (Fig 4.3) and mass balance requirements. The compounds and processes of AD based on the reaction scheme of Fig 4.3 are shown in the Petersen matrix format in Table 4.2, in which each row represents a biological process and each column a compound, and the stoichiometric relationships between the compounds and processes are listed at their intersection blocks, the process kinetic rates on the right hand side and the units of the compounds along the bottom. Note that all the compounds in Table 4.2 are specified as mol/ℓ, including the sewage sludge. The mol/ℓ of the sewage sludge is calculated from its measured COD concentration and its gCOD/mol, which is calculated from its known composition, i.e. known X, Y, Z and A in $C_XH_YO_ZN_A$ (see below). The AD organism concentrations for all four organism groups are also specified as mol/ℓ based on a formulation of $C_5H_7O_2N$, which has a molar mass of 113g/mol and a COD/VSS ratio of 1.42 mgCOD/mgVSS (McCarty, 1964). The gCOD, gN or $gH_2CO_3^*$ Alk per mol of the compounds as appropriate are also given along the bottom of the matrix. If the gCOD/mol ratios are multiplied by the corresponding stoichiometric value in the matrix and summed across a process, it will be found that these sums are zero, i.e. the COD mass balance applies across each process. The requirement to express the model compounds in mole units arises from the requirement to model CO_2 production/utilisation (zero COD), which is essential for the weak acid/base chemistry part of the model.

Table 4.2: Petersen matrix representation of the biological processes and associated compounds of the University of Cape Town Anaerobic Digestion Model No 1 (UCTADM1). Influent sewage sludge concentration is in mol/ℓ. This concentration is calculated from the measured COD concentration of the sludge and the sludge composition formula $C_XH_YO_ZN_A$ with measured values of X, Y, Z and A.

	Number	C1	C2	C3	C7	C13	C28	C29	P1†	P4	D1	D2	D3	D4	D5	D6	D7	
	Compounds	NH_4^+	NH_3	$H_2CO_3^*$	H^+	HAc	HPr	Pr^-	CO_2	CH_4	$C_XH_YO_ZN_A$	$C_6H_{12}O_6$	H_2	Z_{AD}	Z_{AC}	Z_{AM}	Z_{HM}	
No	Processes		Dslvd	Dslvd					Gas	Gas	S_{bp}	S_{baf}	Dslvd	Acido gens	Aceto gens	AMs	HMs	Process rates
C46	Forward dissociation of HPr				1		-1	1										$K_{PrC}[HPr]$
C47	Reverse dissociation of HPr				-1		1	-1										$K_{PrC}[Pr^-][H^+]$
P6†	Dissolution of CO_2 gas			1					-1									$K_{rCO2}(pCO_2)(K_{HCO2})$
P7†	Expulsion of CO_2 gas			-1					1									$K_{rCO2}[H_2CO_3^*]$
P8†	Expulsion of NH_3 gas		-1															$K_{rNH3}[NH_3]$
D1	Hydrolysis		S1	S2							-1	S3						Eq 4.16d
D2	Acidogenesis (low pH_2)	-1		S4	1	S5						$-1/Y_{AB}$	S6	1				Eq 4.17
D3	Acidogenesis (high pH_2)	-1		S7	1	S8	S9					$-1/Y_{AD}$	S10	1				Eq 4.18
D4	Acidogen endogenous decay		S11	S12							S13			-1				$b_{AD}[Z_{AD}]$
D5	Acetogenesis	-1		S14	1	S15	$-1/Y_{AC}$						S16		1			Eq 4.19
D6	Acetogen endogenous decay		S11	S12							S13				-1			$b_{AC}[Z_{AC}]$
D7	Acetoclastic methanogenisis	-1		S17	1	$-1/Y_{AM}$				S18						1		Eq 4.20
D8	Acetoclastic methanogen endogenous decay		S11	S12							S13					-1		$b_{AM}[Z_{AM}]$
D9	Hydrogenotrophic methanogenesis	-1		S19	1					S20			$-1/Y_{HM}$				1	Eq 4.21
D10	Hydrogenotrophic methanogen endogenous decay		S11	S12							S13						-1	$b_{HM}[Z_{HM}]$
	Units	mol/ℓ	mol/ℓ	mol/ℓ	mol/ℓ	mol/ℓ	mol/ℓ	mol/ℓ	mol/ℓ	mol/ℓ	mol/ℓ	mol/ℓ	mol/ℓ	mol/ℓ	mol/ℓ	mol/ℓ	mol/ℓ	
	g COD/mol	-	-	-	-	64	112	112	0	64	131.3‡	192	16	160	160	160	160	
	g N/mol	14	14	-	-	-	-	-	-	-	2.744	-	-	-	-	-	-	
	g H_2CO_3* as $CaCO_3$ /mol	-	-	0	-50	-	-	-	-	-	-	-	-	-	-	-	-	

† These processes and compound were included in the models of Musvoto *et al.* (1997, 2000a) as follows: Processes P6 was C7, P7 was C8, and P8 was C46 and compound P1 was C6.
Because the matrix units are mol/ℓ summing the stoichiometry across each process does not yield zero. However, if each stoichiometric value is multiplied by the compounds' gCOD/mol ratio and then summed across the process, zero is obtained, i.e. COD balances across each process. Also, C, N, O and H mass balances across each process.
‡ This is the g COD/mol for the primary sludge CHON content measured and predicted in this investigation, i.e. $C_{3.5}H_7O_2N_{0.196}$

4.3.3 Stoichiometry of the Biological Processes

The stoichiometry in the model was deduced directly from the biochemical stoichiometric equations of the processes. The metabolic pathways used by fermentative organisms for the degradation of carbohydrates to SCFAs are well defined. As noted above, for this reason amongst others, the biodegradable particulate COD entering the system was directly hydrolysed to the intermediate 'glucose', from which the remainder of the products were formed. As an example for calculating the stoichiometry, consider the process of acetogenesis:

Acetogenesis (Process D5, Table 4.2) is the process whereby under low hydrogen partial pressure (p_{H2}) the acetogens convert propionic acid (HPr) (generated by acidogenesis under high p_{H2}) to acetic acid (HAc). The stoichiometric equation for the acetogenesis reaction is:

$$CH_3CH_2COOH + 2H_2O \rightarrow CH_3COOH + CO_2 + 3H_2 \tag{4.9}$$

During acetogenesis, growth of acetogenic organisms (Z_{AC}) takes place which can be stoichiometrically represented by:

$$3CH_3CH_2COOH + CO_2 + 2NH_4^+ \rightarrow 2C_5H_7O_2N + 4H_2O + H_2 + 2H^+ \tag{4.10}$$

Note that in Eqs 4.9 and 4.10 (i) CO_2 is utilised as an additional carbon source - in all CO_2 consumption/production the undissociated carbonate species $H_2CO_3^*$ acts as source/sink respectively, (ii) ammonium is the nitrogen source for organism growth - under normal operating conditions and pH ($6.5<pH<7.5$) of an anaerobic digester, the ammonium species (NH_4^+) dominates over the ammonia species (NH_3) so that using ammonia as the N species for organism growth can cause numerical instability in solution procedures for the model, (iii) the undissociated propionic acid species is used as substrate source, in agreement with observations in the literature, and (iv) the chemical formulation for organisms is assumed to be $C_5H_7O_2N$, which is the formulation generally accepted to represent organism active mass in activated sludge (WRC, 1984).

Accepting that Y_{ac} mol of acetogen organisms are formed (i.e. the anabolic yield of acetogens), Eq 4.10 can be rewritten as:

$$\frac{3Y_{ac}}{2}CH_3CH_2COOH + \frac{Y_{ac}}{2}CO_2 + Y_{ac}NH_4^+ \rightarrow Y_{ac}C_5H_7O_2N + 2Y_{ac}H_2O + \frac{Y_{ac}}{2}H_2 + Y_{ac}H^+ \tag{4.11}$$

Adding Eqs 4.9 and 4.11 and dividing by Y_{ac} yields:

$$\frac{1+\frac{3Y_{ac}}{2}}{Y_{ac}}CH_3CH_2COOH + \frac{2(1-Y_{ac})}{Y_{ac}}H_2O + NH_4^+ \rightarrow \frac{1}{Y_{ac}}CH_3COOH + C_5H_7O_2N + \frac{1-\frac{Y_{ac}}{2}}{Y_{ac}}CO_2 + \frac{3+\frac{Y_{ac}}{2}}{Y_{ac}}H_2 + H^+ \tag{4.12}$$

Recognising that in Eq 4.12 the 'true' acetogen yield (Y_{AC}, mole organism/mole propionate) is $Y_{ac}/(1+3/2Y_{ac})$, and substituting Y_{AC} into Eq 4.12 and solving gives:

$$\frac{1}{Y_{AC}}CH_3CH_2COOH + \frac{(2-5Y_{AC})}{Y_{AC}}H_2O + NH_4^+$$

$$\Rightarrow \frac{1-\frac{3}{2}Y_{AC}}{Y_{AC}}CH_3COOH + C_5H_7O_2N + \frac{1-2Y_{AC}}{Y_{AC}}CO_2 + \frac{3-4Y_{AC}}{Y_{AC}}H_2 + H^+ \qquad (4.13)$$

The stoichiometry for acetogenesis and acetogen growth was extracted from Eq 4.13 directly, and is summarised in Table 4.3. Note that compounds that are utilised (reactants, left hand side of Eq 4.13) are negative (reduction), while compounds produced (products, right hand side of Eq 4.13) are positive (production), that H_2O has been included in Eq 4.13 for an element balance, but is not included directly in Table 4.3, and that there is a net production of CO_2 expressed as $H_2CO_3^*$ in the kinetic model ($1/Y_{AC}$ >2). Following this procedure, the stoichiometries for the remaining processes were derived and are summarised in Table 4.4.

Table 4.3: Stoichiometry for acetogenesis and acetogen growth (Process D5 in Table 4.2). The S numbers in brackets cross reference to the model Petersen matrix (Table 4.2).

C1/B10 NH_4^+	C3 (S14) H_2CO^{3*}	C7 H^+	C13 (S15) HAc	C28 HPr	D3 (S16) H_2	D5 Z_{AC}
moles	moles	moles	moles	moles	moles	moles
-1	$\frac{1-2Y_{AC}}{Y_{AC}}$	1	$\frac{1-\frac{3}{2}Y_{AC}}{Y_{AC}}$	$-\frac{1}{Y_{AC}}$	$\frac{3-4Y_{AC}}{Y_{AC}}$	1

In the hydrolysis process, the biodegradable particulate organics measured as COD (S_{bp}) in the sewage sludge are first changed to mole units 'outside' of the kinetic model, i.e. matrix, by dividing by the COD/mol ratio = $\{(Y + 4X - 2Z - 3A)\cdot MW_{O2}/4\}$, with MW_{O2} being the molecular weight of O_2 = 32 g/mol. Thereafter, the sewage sludge biodegradable particulate organics measured as moles (S_{bp}) are transformed to the intermediate organic 'glucose' also as moles (S_{bs}). This process is crucial in anaerobic digestion modelling, as the amount of 'glucose' formed will determine the amount of the end products (CH_4, CO_2 and biomass) in a stable digester. To develop the stoichiometry for the hydrolysis process, the stoichiometric reaction was separated into two half reactions, effectively the redox half reactions, which were added based on an electron (COD) balance. In setting up the conversion of the primary sludge COD to mole units and the two subsequent half reactions in the transformation to the intermediate 'glucose', the chemical formulation for the sewage sludge was kept as a variable, i.e. $C_XH_YO_ZN_A$, to allow the composition of the influent sewage sludge to the AD to be easily changed (McCarty, 1974). The formulation for the sewage sludge was assumed to be the same for all sewage sludge fractions (i.e. biodegradable and unbiodegradable), and to remain constant with degradation. In subsequent refinements of the model, different stoichiometric compositions can be assigned to the biodegradable and unbiodegradable organics, if necessary. This gives the stoichiometric reaction for sewage sludge hydrolysis as:

$$C_XH_YO_ZN_A \rightarrow \frac{Y+4X-2Z-3A}{24}C_6H_{12}O_6 + ANH_3 + \frac{Y-4X+2Z-3A}{4}H_2O + \frac{2Z+3A-Y}{4}CO_2 \qquad (4.14)$$

In the death / endogenous decay processes for the four organism groups (Table 4.4), it was accepted that the organisms die releasing biodegradable particulate organics (S_{bp}), which are assumed to have the same formulation as the sewage sludge, i.e. $C_XH_YO_ZN_A$ with CO_2, H_2O and NH_3 released or taken up

from the bulk liquid as required to maintain the C, H, O and N mass balances. Due to the low organism yields and relatively low death rates, and the relatively large fraction of unbiodegradable particulate organics in the influent, generation of endogenous residue (Dold *et al.*, 1980) was not included, but this can be done relatively simply if required. Hence, the stoichiometric reaction for organism death is (Table 4.4):

$$C_5H_7O_2N + \frac{4(2Y-2X-6A+Z)}{Y+4X-2Z-3A}H_2O \Rightarrow \frac{20}{Y+4X-2Z-3A}C_XH_YO_ZN_A + \frac{Y+4X-2Z-23A}{Y+4X-2Z-3A}NH_3 + \frac{5(Y-2Z-3A)}{Y+4X-2Z-3A}CO_2 \qquad (4.15)$$

Table 4.4: Stoichiometry for of the AD processes hydrolysis (D1), acidogenesis (D2, D3), acetoclastic methanogenesis (D7), hydrogenotrophic methanogenesis (D9) and endogenous respiration of the four organism species (D4, D6, D8 and D10). The S1 to S13 numbers cross-reference to the stoichiometry in the Petersen matrix (Table 4.2). Stoichiometry of process D5 is given in Table 4.3.

Hydrolysis (Process D1)						
C2 - NH_3 (S1)	C3 - $H_2CO_3^*$ (S2)		D1 - S_{bp}		D2/B2 - S_{bs} (S3)	
moles	moles		moles		moles	
$+A$	$\frac{2Z+3A-Y}{4}$		-1		$\frac{Y+4X-2Z-3A}{24}$	
Acidogenesis for low pH2 (Process D2)						
C1/B10 NH_4^+	C3 (S4) $H_2CO_3^*$	C7 H^+	C13 (S5) HAc	D2/B2 S_{bsf}	D3 (S6) H_2	D4 Z_{AD}
moles	moles	moles	moles	moles	moles	moles
-1	$\frac{2(1-\frac{5}{6}Y_{AD})}{Y_{AD}}$	1	$\frac{2(1-\frac{5}{6}Y_{AD})}{Y_{AD}}$	$-\frac{1}{Y_{AD}}$	$\frac{4(1-\frac{5}{6}Y_{AD})}{Y_{AD}}$	1
Acidogenesis for high pH2 only (Process D3)						
C1/B10 NH_4^+	C3 (S7) $H_2CO_3^*$	C7 H^+	C13 (S8) HAc	C28 (S9) HPr	D2/B2 S_{bsf}	D3 (S10) H_2	D4 Z_{AD}
moles	moles	moles	moles	moles	moles	moles	moles
-1	$\frac{(1-\frac{5}{6}Y_{AD})}{Y_{AD}}$	1	$\frac{(1-\frac{5}{6}Y_{AD})}{Y_{AD}}$	$\frac{(1-\frac{5}{6}Y_{AD})}{Y_{AD}}$	$-\frac{1}{Y_{AD}}$	$\frac{(1-\frac{5}{6}Y_{AD})}{Y_{AD}}$	1
Acetoclastic methanogenesis (Process D7)						
C1/B10 NH_4^+	C3 - $H_2CO_3^*$ (S17)	C7 - H^+	C13 - HAc	P4 - CH_4 (S18)	D6 - Z_{AM}	
moles	moles	moles	moles	moles	moles	

-1	$\frac{(1-\frac{5}{2}Y_{AM})}{Y_{AM}}$	1	$-\frac{1}{Y_{AM}}$	$\frac{(1-\frac{5}{2}Y_{AM})}{Y_{AM}}$	1
Hydrogenotrophic methanogenesis (Process D9)					
C1/B10 - NH_4^+	C3 - $H_2CO_3^*$ (S19)	C7 - H^+	P4 - CH_4 (S20)	D3 - H_2	D7 - Z_{HM}
moles	moles	moles	moles	moles	moles
-1	$-\frac{(1+10Y_{HM})}{4Y_{HM}}$	1	$\frac{(1-10Y_{HM})}{4Y_{HM}}$	$-\frac{1}{Y_{HM}}$	1
Death / Endogenous respiration Processes (D4, D6, D8, D10)					
C2/B10 NH_3 (S11)	C3 $H_2CO_3^*$ (S12)	D1 S_{bp} (S13)	D4, D6, D8, D10 Z_{AC}, Z_{AD}, Z_{AM}, Z_{HM}		
moles	moles	moles	moles		
$\frac{Y+4X-2Z-23A}{Y+4X-2Z-3A}$	$\frac{5(Y-2Z-3A)}{Y+4X-2Z-3A}$	$\frac{20}{Y+4X-2Z-3A}$	-1		

The position of the stoichiometric formulae of Tables 4.3 and 4.4 are shown in the Petersen matrix in Table 4.2. By tracking through with defined organism yield values (Table 4.5) the stoichiometric sequence of AD processes (ignoring high p_{H2} conditions, which has no effect under stable steady state conditions, and endogenous respiration processes, which have a very small effect, <3%), degradation of 100 gCOD biodegradable particulate sewage sludge of composition $C_{3.5}H_7O_2N_{0.196}$ (see below) produces 88.3 g COD methane and 11.7 gCOD biomass (Fig 4.4). Also the 100 gCOD contains 2.67 mol carbon (32.0 gC). Stoichiometrically 88.3 gCOD methane contains 1.38 molC (16.5 gC) and the 11.7 gCOD biomass of composition $C_5H_7O_2N$ contains 0.37 molC (4.4 gC). The difference between the input and output molC is the molC CO_2 produced, viz. 2.67- (1.38 + 0.37) = 0.92 molC (11.0 gC), which is equal to the model predicted net CO_2 production. This CO_2 production exits the digester as CO_2 gas and dissolved CO_2 in the effluent flow. The split between the gaseous and dissolved CO_2, or equivalently the partial pressure of CO_2 in the gas phase, is governed by the sludge feed COD concentration, i.e. the influent (and effluent) flow with which the 100 gCOD enters the digester, and the digester pH through the mixed weak acid/base chemistry of the system. This calculation is complex because the digester pH is unknown. The pH is affected by the mol N released as ammonia in the breakdown of the sludge organics (0.15 molN from the 100gCOD $C_{3.5}H_7O_2N_{0.196}$ sewage sludge) and the partial pressure of CO_2 in the gas phase (p_{CO2}). While estimates of the p_{CO2} and digester pH can be obtained iteratively manually (see Chapter 5), the usefulness of the integrated two phase weak acid/base chemistry and biological processes kinetic model is that this calculation of the effluent gas p_{CO2} and digester pH is done seamlessly within the model structure including all the weak acid/bases in the digester influencing pH (not only the inorganic C system) and the measured (or estimated) dissolved constituents in the sludge feed as a result of prior acidogenesis. Also, while not validated for this yet, the integrated AD model can deal with cyclic flow and load conditions.

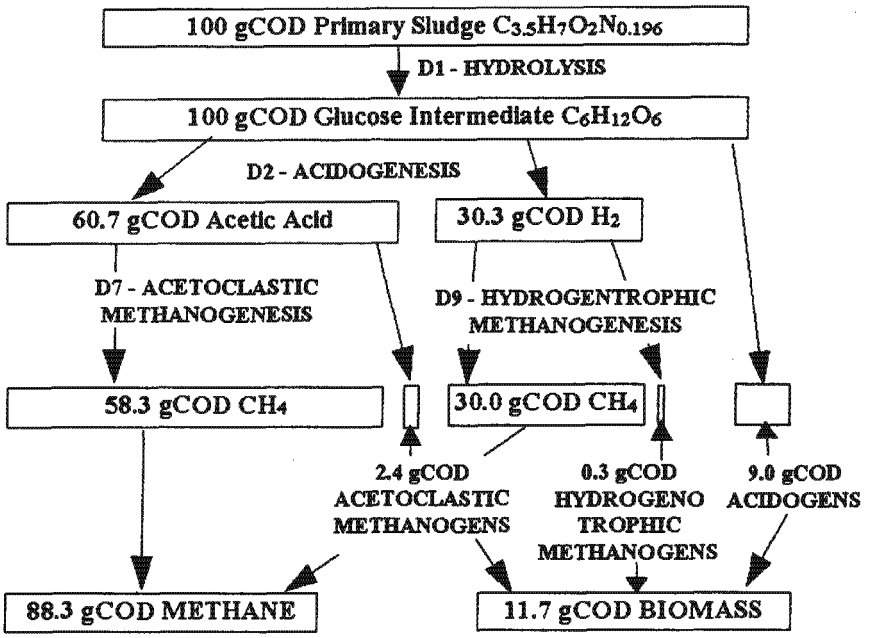

Fig 4.4: Stoichiometry of anaerobic digestion 100 gCOD primary sludge ignoring high partial pressure of hydrogen and endogenous respiration.

Table 4.5: Kinetic and stoichiometric constants at 37 °C for the four anaerobic digestion organism groups. The Y, μ_{max}, K_S and b values were obtained from Sam-soon et al. (1991); the $K_{max,HYD}$ and $K_{S,HYD}$ values by calibration in this application.

Organism group	Y	μ_{max}	K_S	b
Acidogens (subscript AD)	0.1074	0.8	7.8×10^{-4}	0.041
Acetogens (subscript AC)	0.0278	1.15	8.9×10^{-5}	0.015
Acetoclastic methanogens (subscript AM)	0.0157	4.39	1.3×10^{-5}	0.037
Hydrogenotrophic methanogens (subscript HM)	0.0040	1.2	1.56×10^{-4}	0.01
Hydrogen inhibition coefficient for high p_{H2}	$K_{H2} = 6.25\times10^{-4}$ molH_2/ℓ			
Acidogenic hydrolysis of biodeg particulate organics				
First order	$K_h = 0.381$			
First order specific	$K_H = 40$			
Monod	$\mu_{max,HYD} = 4.529$		$K_{SM,HYD} = 0.0486$	
Surface mediated reaction (Contois)	$K_{max,HYD} = 6.797$		$K_{SS,HYD} = 10.829$	

Y= yield coefficient (mol organism/mol substrate); μ_{max} = maximum specific growth rate (/d);
K_S = half saturation coefficient (mol/ℓ); b = endogenous respiration rate (/d);
K_h = first order hydrolysis rate constant (/d)
K_H = first order specific hydrolysis rate constant (ℓ/mol Z_{AD}.d)
$\mu_{max,HYD}$ = Monod kinetics maximum specific hydrolysis rate (mol S_{bp}/mol Z_{AD}.d)
$K_{SM,HYD}$ = Monod kinetics hydrolysis half saturation coefficient (mol S_{bp}/ℓ)
$k_{max,HYD}$ = surface mediated reaction kinetics maximum specific hydrolysis rate (mol S_{bp}/mol Z_{AD}.d);
$K_{SS,HYD}$ = surface mediated reaction kinetics half saturation coefficient (mol S_{bp} /mol Z_{AD})

4.3.4 Kinetic Equations of the Biological Processes

The rate equations for the 10 biological processes (Table 4.2) were obtained from various literature sources, where possible, and modified to describe the reactions as realistically and accurately as possible. The rate equations chosen for each of the biological processes included in the two phase CPB processes AD model are briefly described below.

4.3.4.1 Hydrolysis process (D1)

A number of different kinetic formulations for the hydrolysis process were investigated:

(i) First order kinetics:

The most common way of modelling the rate of hydrolysis of particulate organic material (process D1) has been to use first order kinetics. A number of researchers (e.g. Eastman and Ferguson, 1981; Gujer and Zehnder, 1983; Pavlostathis and Giraldo-Gomaz, 1991) used simple first order equations, dependent only on the biodegradable substrate (as COD) concentration:

$$r_{HYD} = K_h\ [S_{bp}] \tag{4.16a}$$

where:

r_{HYD} = hydrolysis rate (mol S_{bp}/ℓ.d)
K_H = first order hydrolysis kinetic rate constant (/d)
$[S_{bp}]$ = biodegradable particulate organics concentration (mol/ℓ).

Application of the first order kinetics has been found to result in values for the first order rate constant (K_H) that are situation specific, varying with, for example, sludge age or equivalently hydraulic retention time (e.g. Henze and Harremoës, 1983; Bryers, 1985; Pavlostathis and Giraldo-Gomez, 1991). Because the objective is to develop a kinetic model for anaerobic digestion that would be applicable over a range of sludge ages, alternative more general approaches were investigated. It is well known that the rate of hydrolysis is affected by temperature, pH, acidogen organism concentration, and type, particle size and concentration of organics. Among these, intuitively at least the acidogen organism concentration plays a major role in regulating the rate of hydrolysis and should be included in the kinetic rate expression in some way. Eliosov and Argaman (1995) included the acidogen active biomass directly into the first order kinetics:

$$r_{HYD} = K_H\ [S_{bp}][Z_{AD}] \tag{4.16b}$$

where:

K_H = first order specific hydrolysis kinetic rate constant (ℓ/mol Z_{AD}.d)
$[Z_{AD}]$ = acidogen active biomass concentration (mol/ℓ)

(ii) Monod kinetics:

Monod kinetics are commonly used in modelling biological wastewater treatment processes (e.g. McCarty, 1974; Dold *et al.*, 1980, Henze *et al.*, 1987):

$$r_{HYD} = \left[\frac{\mu_{max,HYD}\ [S_{bp}]}{K_{SM,HYD} + [S_{bp}]}\right] [Z_{AD}] \tag{4.16c}$$

where:

$\mu_{max,HYD}$ = maximum specific hydrolysis rate constant (mol S_{bp}/(mol Z_{AD}.d))
$K_{SM,HYD}$ = Monod half saturation constant for hydrolysis (mol S_{bp}/ℓ)

(iii) Surface mediated reaction (or Contois) kinetics:
To model the hydrolysis of particulate slowly biodegradable COD in activated sludge systems, Dold *et al.* (1980) used Levenspiel (1972) planar surface mediated reaction kinetics (also known as Contois kinetics, Vavilin *et al.*, 1996). With a single set of constant values, these kinetics gave reasonable predictions over a wide range of activated sludge system conditions including sludge age. Since the hydrolysis processes in activated sludge and anaerobic digestion could be regarded as similar and operate on the same organics (present in raw sewage), this approach also was investigated for the AD model:

$$r_{HYD} = \left[\frac{k_{max,HYD} \dfrac{[S_{bp}]}{[Z_{AD}]}}{K_{SS,HYD} + \dfrac{[S_{bp}]}{[Z_{AD}]}} \right] [Z_{AD}] \qquad (4.16d)$$

where

$k_{max,HYD}$ = Maximum specific hydrolysis rate constant [mol S_{bp}/(mol Z_{AD} .d)]
$K_{SS,HYD}$ = Half saturation constant for hydrolysis (mol S_{bp}/mol Z_{AD})

Selection of the most suitable hydrolysis kinetic formulation is investigated later in this chapter. Irrespective of the hydrolysis formulation used, no acidogen biomass growth takes place in this hydrolysis process, and 1 gCOD sewage sludge forms 1 gCOD 'glucose' intermediate (Fig 4.4, Eq 4.14). Growth of acidogens arises from the acidogenic conversion of the glucose intermediate to SCFA and hydrogen, which, relative to the rate of hydrolysis, is immediate resulting in zero accumulation of glucose in the AD system.

4.3.4.2 Acidogenesis process (D2 and D3)

As noted above, acidogenesis refers to the utilization of the model intermediate 'glucose' (S_{bs}) by the acidogenic organisms, producing propionic acid, acetic acid, hydrogen, carbon dioxide and protons. Under conditions of low hydrogen partial pressure (p_{H2}), the acidogenic reaction (process D2) produces only acetic acid, hydrogen and CO_2. The process is formulated in terms of the growth rate of acidogens (r_{ZAD}), which is modelled with a Monod equation (Gujer and Zehnder, 1983; Pavlostathis and Giraldo-Gomez, 1991), as follows:

$$r_{Z_{AD}} = \frac{\mu_{max,AD} [S_{bsf}]}{K_{S,AD} + [S_{bsf}]} \left\{ 1 - \frac{[H_2]}{k_{H2} + [H_2]} \right\} [Z_{AD}] \qquad (4.17)$$

where:

$\mu_{max,AD}$ = Maximum specific growth rate constant for the acidogens (/d)
$K_{S,AD}$ = Half saturation concentration for acidogens (mol/ℓ)
$[S_{bsf}]$ = Biodegradable soluble (glucose) substrate concentration (mol/ℓ)
$[H_2]$ = Hydrogen concentration (mol/ℓ)
k_{H2} = Hydrogen inhibition constant for high p_{H2} (mol/ℓ)

The second part of the term in { } brackets in Eq 4.17, called a non-competitive inhibition function, takes account of the reduction in rate when the p_{H2} is high. At high p_{H2}, in addition to acetic acid,

hydrogen and CO_2, propionic acid also is produced (process D3). For the production of propionic acid under high p_{H2}, the growth rate of the acidogens (r_{ZAD}) is based on the same Monod kinetic equation (Eq 4.17) as for low p_{H2}, viz.:

$$r_{Z_{AD}} = \frac{\mu_{max,AD}\,[S_{bsf}]}{K_{S,AD} + [S_{bsf}]} \left\{ \frac{[H_2]}{k_{H2} + [H_2]} \right\} [Z_{AD}] \qquad (4.18)$$

To ensure that this process only operates when the p_{H2} is high, the non-competitive inhibition function in { } switches the process 'on' under conditions of high p_{H2} and 'off' under conditions of low p_{H2}, controlled by switching constant k_{H2}. Additionally, to ensure that the rate of glucose (S_{bsf}) utilisation is the same under both conditions and in the intermediate condition, the rate of acetate production (Eq 4.17) is reduced by subtracting the inhibition function value from 1 in Eq 4.17.

4.3.4.3 Acetogenesis process (D5)

In the process of acetogenesis, the propionic acid produced under high p_{H2} conditions is degraded under low p_{H2} by acetogenic organisms to produce acetate (Eq 4.9). This rate was modelled in terms of the acetogen growth rate (r_{ZAC}), also with a Monod equation for the specific growth rate:

$$r_{Z_{AC}} = \frac{\mu_{max,AC}\,[HPr]}{K_{S,AC} + [HPr]} \left\{ 1 - \frac{[H_2]}{k_{H2} + [H_2]} \right\} [Z_{AC}] \qquad (4.19)$$

where:

$\mu_{max,AC}$	= Maximum specific growth rate constant for the acetogens (/d)
$K_{S,AC}$	= Half saturation concentration for acetogens (mol/ℓ)
[HPr]	= Undissociated propionic acid concentration (mol/ℓ)
$[Z_{AC}]$	= Acetogenic organism concentration (mol/ℓ)

Since the weak acid/base chemistry is being modelled, both the undissociated and dissociated species of propionic acid are included as compounds, and the growth rate needs to be formulated in terms of the appropriate species. In Eq 4.19, the specific growth rate is a Monod function in terms of the undissociated propionic acid species, and not the more abundant dissociated species, in agreement with observations. Also, in the stoichiometry (Table 4.2) the undissociated propionic acid species (HPr) is used as substrate source. Should this approach lead to numerical instability in solution procedures (due to the low concentrations of HPr), the dissociated species (Pr^-) can be used instead without undue difficulty, but taking due cognisance of the concentration effects in the Monod expression and the requirement of the charge balance in the stoichiometric equations.

The same non-competitive inhibition function in the { } brackets of Eq 4.17 appears in Eq 4.19, because the acetogenesis process is sensitive to p_{H2}, decreasing as p_{H2} increases. This means that as p_{H2} increases, not only do acidogens begin to produce propionic acid (process D3), but also the rate of propionic acid utilization by acetogens (process D5) decreases. This causes a progressive build up of propionic acid as p_{H2} increases and contributes to the decrease in pH when the hydrogen consuming hydrogenotrophic methanogen growth rate (D9) decreases for some reason (see below).

4.3.4.4 Acetoclastic methanogenesis process (D7)

Acetoclastic methanogenesis (or acetate cleavage) is the process whereby acetic acid is converted to methane and CO_2 ($CH_3COOH \rightarrow CO_2 + CH_4$), and growth of acetoclastic methanogens takes place. As for processes D2 and D3, the rate is modelled in terms of the rate of growth of the acetoclastic

methanogens (r_{ZAM}) with a Monod equation, viz.:

$$r_{Z_{AM}} = \frac{\mu_{max,AM}\,[HAc]}{K_{S,AM} + [HAc]}\,[Z_{AM}] \qquad (4.20)$$

where:

$\mu_{max,AM}$	=	Acetoclastic methanogens maximum specific growth rate constant (/d)
$K_{S,AM}$	=	Half saturation concentration of acetoclastic methanogens growth on acetic acid (mol/ℓ)
[HAc]	=	Undissociated acetic acid concentration (mol/ℓ)
$[Z_{AM}]$	=	Acetoclastic methanogen organism concentration (mol/ℓ)

As for the acetogens, the specific growth rate of the acetoclastic methanogens is a function of the undissociated acetic acid species (HAc). Also, in the stoichiometry acetic acid uptake is via the undissociated species, and CO_2 production via $H_2CO_3^*$.

4.3.4.5 Hydrogenotrophic methanogenesis process (D9)

Hydrogenotrophic methanogenic organisms use H_2 and CO_2 to form methane and water ($CO_2 + 4H_2 \rightarrow CH_4 + 2H_2O$). This process (D9) is also modelled in terms of the rate of growth of the hydrogenotrophic methanogens (r_{ZHM}), with a Monod equation:

$$r_{Z_{HM}} = \frac{\mu_{max,HM}\,[H_2]}{K_{S,HM} + [H_2]}\,[Z_{HM}] \qquad (4.21)$$

where:

$\mu_{max,HM}$	=	Maximum specific growth rate of hydrogenotrophic methanogens (/d)
$K_{S,HM}$	=	Half saturation concentration of hydrogenotrophic methanogens growth on hydrogen (mol/ℓ)
$[H_2]$	=	Molecular hydrogen concentration (mol/ℓ)
$[Z_{HM}]$	=	Hydrogenotrophic methanogen organism concentration (mol/ℓ)

In agreement with the other processes, CO_2 uptake for hydrogenotrophic methanogenesis is via the $H_2CO_3^*$ species.

4.3.4.6 Death/endogenous respiration of the four organism groups (processes D4, D6, D8 and D10)

Organism death in AD consists of endogenous respiration/death only, since predation apparently does not occur under anaerobic conditions. Hence, for each organism group the organism death rate is modelled with first order kinetics, viz.:

$$-r_Z = b_Z\,[Z] \qquad (4.22)$$

where:

b_Z = the death/endogenous mass loss rate unique for a specific organism group (/d)
[Z] = specific organism group concentration (mol/ℓ)

The organism mass that dies adds to the slowly biodegradable organics (S_{bp}) of the influent (Table 4.4, Eq 4.15), which passes through the same hydrolysis, acidogenesis and subsequent processes as the influent biodegradable organics. Because the organism yields and endogenous respiration rates of the AD organisms are relatively very low, it was accepted that no endogenous residue (particulate

unbiodegradable organics) forms and no COD (electrons) is utilized by the AD organisms for maintenance.

The stoichiometric and kinetic constants for the four organism groups (yield coefficients, maximum specific growth rates, half saturation concentrations, endogenous mass loss rates) were obtained from the literature and are listed in Table 4.5.

4.4 AQUEOUS CHEMICAL PROCESSES

The reaction scheme for the weak acid/base part of this two phase AD model was taken unchanged from Musvoto *et al.* (1997, 2000a,b,c). The 16 chemical equilibrium dissociation (CED) processes (C1-C6 and C9- C18) of the ammonia, carbonate, phosphate, short chain (volatile) fatty acid (SCFA, acetate) and water weak acid/base systems and their 13 associated compounds (C1-C5 and C7-C14) were included in the AD model (Tables 1 of Musvoto *et al.*, 1997 and Table 3.1 Chapter 3). Only the five chemical (C) and one physical (P) compounds directly associated with the 10 biological (B) and 3 physical (P) processes of AD (D1-D10 and P6-P8) are shown in the Petersen matrix in Table 4.2, i.e. NH_4^+ (C1/B10), NH_3 (C2), $H_2CO_3^*$ (C3), H^+ (C7), HAc (C13) and CO_2 gas (P1/C6). Two additional CED processes had to be added, viz. the reverse and forward dissociation processes for the propionate weak acid/base system (C46 and C47), together with its two associated compounds propionic acid (HPr, C28) and propionate (Pr^-, C29). The 22 chemical ion pairing processes (CIP, C20-C41) with their 13 associated chemical compounds (C15-C27) were not included in this two phase AD model, because mineral precipitation (3rd phase) is not yet included (Table 3.1, Chapter 3).

4.5 PHYSICAL PROCESSES - GAS EXCHANGE

In the three phase carbonate system weak acid/base model of Musvoto *et al.* (1997), the physical (P) processes for carbon dioxide gas exchange (PGE) with the atmosphere were included, by modelling the expulsion (reverse, K'_{rCO2}) and dissolution (forward, K'_{fCO2}) processes separately and linking the rates for these two processes through the Henry's law constant for CO_2 (K_{HCO2}), i.e. $K'_{fCO2} = K'_{rCO2} K'_{HCO2} \bullet RT$. Musvoto *et al.* showed that this approach yielded identical results to the usual interphase gas mass transfer equation with an overall liquid phase mass transfer rate coefficient K_{LaCO2}, where $K_{La,CO2} = K'_{rCO2}$. In their model application, the actual CO_2 expulsion rate constant value (K'_{rCO2}) was not important because they considered initial and final steady state conditions only, not the transient dynamic conditions to the final steady state. Also, the CO_2 gas concentration ($CO_2(g)$) was kept constant as calculated from a selected partial pressure of CO_2 ($CO_2(g) = p_{CO2}/RT$), since gain or loss of $CO_2(g)$ did not need to be determined.

Musvoto *et al.* (2000a) and van Rensburg *et al.* (2003) extended this model to include three phase mixed weak acid/base systems to simulate multiple mineral precipitation and active gas exchange of CO_2 and NH_3 during aeration of anaerobic digester liquor and swine wastewater. For CO_2, they followed the approach of Musvoto *et al.* (1997) above. For the NH_3, they noted that the atmospheric concentration of NH_3 is negligible (i.e. acts as an infinite sink), so that only NH_3 expulsion need be included, and dissolution could be neglected. Because they simulated transient (dynamic) conditions, the CO_2 gas exchange (as above) and NH_3 gas expulsion (stripping) (and mineral precipitation) rates were important and these were determined from the experimental results. In determining the rates for the gas exchanges, Musvoto *et al.* (2000a) noted that, if the dimensionless Henry's law constant of a gas, H_c [$=\{1/(K_H R T)\}$] is > 0.55, then O_2 can be used as a reference gas and the expulsion rate constant K'_r ($= K_{La}$) for the individual gases will be in the same proportion to the rate for O_2 ($K'_{rO2} = K_{LaO2}$) as their diffusivity is to the diffusivity of O_2. Of the two gases they considered, only NH_3 has a

$H_c < 0.55$ (= 0.011 at 20 °C), so the value for K'_{rNH3} had to be determined independently of the values for K'_{rO2}, by calibration. For CO_2 $H_c = 0.95$ at 20°C (Katehis *et al.*, 1998) and accordingly they defined K_{LaCO2} in terms of K_{LaO2}. However, since the compound oxygen was not included in their model, in effect only K_{LaCO2} was determined by calibration against measured data.

In Chapter 3 the biological processes of IWA Activated Sludge Model No 1 were integrated into the two phase (aqueous-gas) mixed weak acid/base chemistry model of Musvoto *et al.* (2000a) allowing the reactor pH to become a model predicted parameter. Four gases were considered, viz. O_2, N_2, CO_2 and NH_3. For CO_2 and NH_3, the formulations of Musvoto *et al.* and van Rensberg *et al.* above were accepted. However, since gas production was of interest, for CO_2 they substituted $K'_{rCO2} \bullet K'_{HCO2} \bullet p_{CO2}$ for $K'_{fCO2} \bullet [CO_2(g)]$ (Table 3.3, Chapter 3). This allows the $CO_2(g)$ concentration to vary without influencing the rate of CO_2 gas exchange, of importance in their implementation of the model in Aquasim (Reichert, 1998), where for simplicity the gas compounds were considered part of the bulk liquid. This approach for CO_2 was adopted for N_2 gas also. For O_2, the more conventional approach for aeration transfer to the bulk liquid was followed (Process P11 in Table 3.3, Chapter 3). In their application, because equilibrium between the aqueous and gas (atmosphere) phases is not reached during aeration in the aerobic reactor, the expulsion rates of the four gases were important for the simulation results and so values for K'_r (= K_{La}) for the four gases had to be determined. For the K_{La} values for the gases, they followed the approach of Musvoto *et al.* (2000a) above. The K_{La} for CO_2 and N_2 were linked to the K_{La} for O_2 through the diffusivities. The K_{LaO2} was calibrated to reflect the CO_2 supersaturation observed on samples from the aerobic reactor of full-scale plants (~20%), and cross-checked against the model determined dissolved O_2 concentration. For K'_{rNH3} (= K_{LaNH3}), this was calibrated independently. However, because negligibly little NH_3 actually strips out of the aqueous phase with aeration in the usual pH range of 6.5 to 8 for activated sludge systems, the actual NH_3 stripping rate, and hence the value for K'_{rNH3}, was of little consequence (provided it is not excessively large) and in fact the process itself could have been omitted from the integrated model without loss in accuracy.

In the application here of integrating the biological processes of AD into the two phase (aqueous-gas) mixed weak acid/base chemistry model of Musvoto *et al.* (2000a), four gases also need to be considered, i.e. CO_2, CH_4, H_2 and NH_3. Of these four, only CO_2 needs to be modelled with both expulsion and dissolution processes, because this gas is significantly soluble. Hence, both dissolved and gaseous CO_2 compounds are included (compounds C3 and P1, Table 4.2) and the process scheme of Chapter 3 above was followed. CH_4 is (i) very insoluble and (ii) not utilized in the biological or chemical processes, so it's dissolved (aqueous) phase is bypassed and only a gas phase CH_4 compound is included (compound P4, Table 4.2). It is therefore assumed that the acetoclastic and hydrogenotrophic methanogenesis processes (D7 and D9) produce CH_4 gas directly and no CH_4 expulsion and dissolution processes need to be included in the model. Although H_2 also is very insoluble, it is utilized at an interspecies level in the hydrogenotrophic methanogenesis process (D9) and so it cannot be transferred instantaneously to the gas phase. H_2 is therefore modelled as a dissolved compound (D3, Table 4.2), but because it is utilized so rapidly and at an inter-organism species level, it's residual concentration is extremely small; From a gas production perspective, it can be ignored. Hence, expulsion and dissolution processes for H_2 are not included in the model. NH_3 is readily soluble and its production from organically bound N in the sewage sludge is one of the processes governing the pH in the digester. It can diffuse from the dissolved (aqueous) to the gas phases and so a process for expulsion of NH_3 is included in the model. However, because the rate and quantity of NH_3 expulsion into the gas phase are so slow and low respectively with respect to the total gas production of the digester, in particular in the digester pH range 6.8 to 8, the gas phase is assumed to maintain a negligible NH_3 partial pressure. An NH_3 dissolution process is therefore not included in the model, only an

expulsion process (in agreement with Musvoto *et al.*, 2000a, van Rensberg *et al.*, 2003 and Chapter 3). The expulsion and dissolution processes for CO_2 and the expulsion process for NH_3 are shown in the Petersen matrix of the AD model (processes P6 - P8, Table 4.2). Thus, only the K_T' (=K_{La}) values for these two gases need to be considered. However, because transient conditions are not being modelled in this particular application, but only the final steady state, the expulsion rates of the gases are not important provided the simulation run times are long enough to reach steady state. From the above it is clear that the gas phase partial pressure required in the rate formulations for CO_2 gas exchange need be calculated only from the CO_2 and CH_4 gas concentrations.

4.6 INFLUENT SEWAGE SLUDGE CHARACTERISATION

In terms of the structure of the UCTADM1 above, in addition to requiring as input the influent concentrations of the various inorganic compounds (e.g. total inorganic carbon, C_T, speciated into $H_2CO_3^*$, HCO_3^- and CO_3^{2-} for the relevant pH), various sewage sludge organic compounds need to be specified. For UCTADM1, the sewage sludge characterisation into its constituent fractions is shown in Fig 4.5; The characterisation structure adopted is near identical to that for sewage in activated sludge modelling (ASM2, Henze *et al.*, 1995). For undigested pristine sewage sludges, the two particulate fractions (biodegradable and unbiodegradable) can be expected to dominate to the extent that the other fractions can be neglected (this is evident from a mass balance around the primary settling tank for primary sludges, and simulation of activated sludge systems for waste activated sludges). However, primary sewage sludges are seldom in the pristine state, having undergone hydrolysis and acidogenesis within the primary settling tank (e.g. Barnard, 1984 measured SCFA concentrations in primary settling tank underflows in the range 1 700 to 2 700 mg/ℓ at various treatment plants in South Africa), and in transport and storage for laboratory investigations. The SCFA thus produced (and equal concentrations

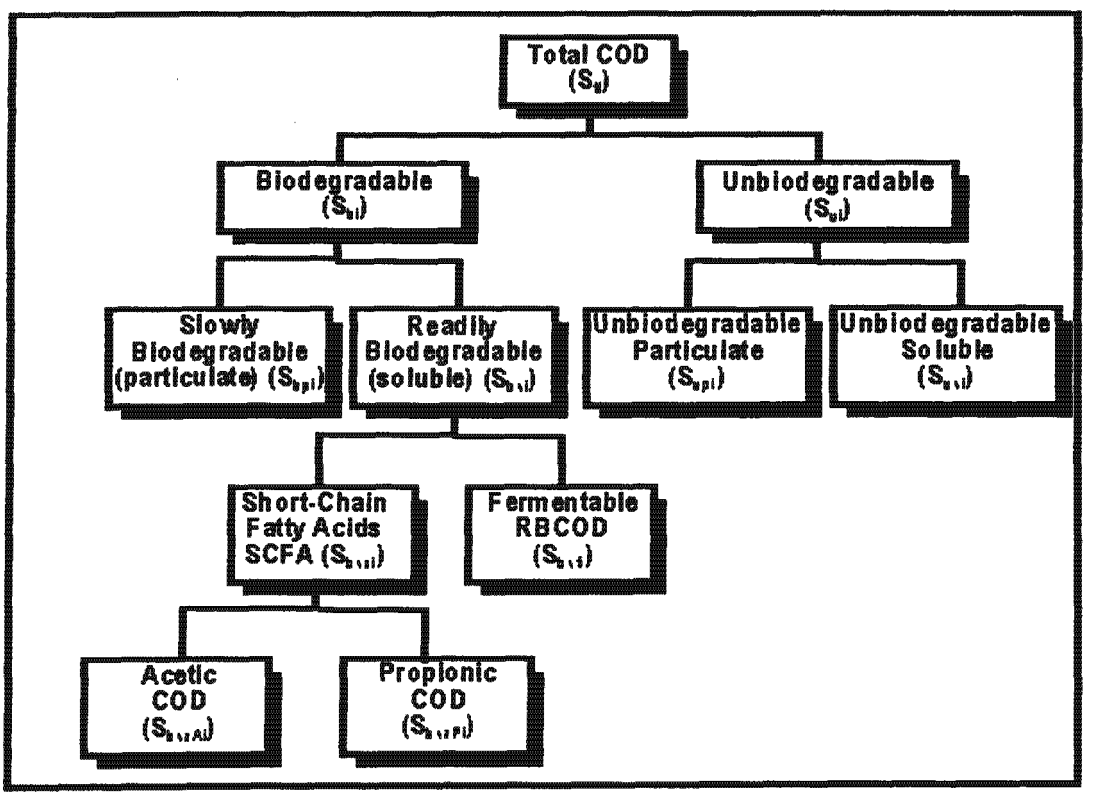

Fig 4.5: Schematic showing characterization of the influent sewage sludge organics, required as input to the model; the acetic and propionic require speciation for the influent pH.

of non-SCFA soluble COD, Lilley *et al.*, 1990) have a significant influence on the predicted pH in simulating anaerobic digesters, since uptake and utilisation of dissociated SCFA generates significant alkalinity (see Chapter 5). Furthermore, the SCFAs influence the hydrolysis rate constants in model calibration (Ristow *et al.*, 2004a,b). Thus, quantifying and specifying the influent sludge organic fractions are essential both in model calibration and simulation. Of the sewage sludge fractions (Fig 4.5), the unbiodegradable and biodegradable particulate (S_{upi} and S_{bpi}) and the two readily biodegradable fractions (S_{bsai} and S_{bsfi}) are of importance - the unbiodegradable soluble organics (S_{usi}) usually are present in such low concentrations that they can be neglected. For S_{bsai}, two SCFA types are recognised in the model, acetic and propionic, and hence these form two subfractions of the S_{bsai}.

The characterisation structure is based on COD units, which are widely applied to quantify wastes. Since the kinetic model is based on mole units, conversion between the COD and mole units would be needed to generate the input for the model. For the two readily biodegradable fractions, the S_{bsai} usually are measured directly, while in terms of the model presented here, the S_{bsfi} is 'idealised' glucose so that conversion of these to mole units is relatively simple. For the particulate fractions, the conversion to mole units requires that the stoichiometric formulation for these sewage sludge fractions be specified, i.e. X, Y, Z and A in $C_XH_YO_ZN_A$. This is discussed in more detail below.

4.7 MODEL CALIBRATION

From the above model development, the integrated two phase (aqueous-gas) chemical (C), physical (P) biological (B) processes AD model comprises (Table 4.2): (1) the 16 forward and reverse chemical equilibrium dissociation (CED) processes (C1-C6, C9-C18) and their 13 associated compounds (C1-C2, C4-C14) - Table 1 in Musvoto *et al.* (1997); (2) The two forward and reverse CED processes for propionic acid (C47-C48) and their two associated compounds (C28-C29), (3) the three physical gas exchange processes of dissolution of CO_2 (P6) and its associated compound CO_2 gas (P1) and expulsion of CO_2 (P7) and NH_3 (P8) and, (4) the 10 biological processes for AD (D1-D10) and their 8 associated compounds (P4 and D1-D7). The model was implemented in the computer programme AQUASIM (Reichert, 1998).

Omitted from this AD model are the five mineral precipitation processes (P1/C19 - Musvoto *et al.*, 1997 and P2/C42-P5/C45 - Musvoto *et al.*, 2000a), because mineral precipitation is not included in this two phase AD model. Also omitted are the 22 chemical iron pairing (CIP) processes (C20-C41) and their 13 associated compounds (C15-C27), because these processes are important mainly for multiple mineral precipitation modelling, which is beyond the scope of this thesis project report and will be included in the next phase of the AD and wastewater treatment plant model development.

In implementation of the model in AQUASIM, since initial simulations were of steady state anaerobic digesters, the gas compounds were accepted to remain part of the bulk liquid and to leave the digester with the effluent flow. This is possible because at steady state the gas composition does not change. For dynamic simulations, the gas composition may change significantly and this may influence the dissolved species bulk liquid concentrations through the gas exchange processes, and hence a separate gas stream may need to be included (see later).

4.7.1 Kinetics and Stoichiometric Constants

The kinetic constants required for the C and P processes part of the model are the equilibrium constants (pK) of the six weak acid/base systems, Henry's law constant for CO_2 ($K'_{H,CO2}$), and the apparent reverse dissociation and expulsion rate constants (K'_r) respectively for these processes. The equilibrium

constants (pK) and Henry's law constant for CO_2 ($K'_{H,CO2}$), and their temperature sensitivity equations were obtained from the literature (see Table 2c of Musvoto *et al.*, 1997 - 1940s database). The pK value for propionic acid (pK_{Pr}) was accepted to be the same as for acetic acid, and is given by $pK_{Pr} = 1170.5/T_k - 3.165 + 0.0134T_k$, where T_k = temperature in Kelvin. The weak acid/base apparent reverse dissociation rate constants (K'_r) were set at very high values to ensure that aqueous chemical equilibrium conditions are established very rapidly at every time step (< 2 sec), e.g. ammonia $K'_{rN} = 10^{12}$/d, see Table 2a in Musvoto *et al.* (1997). The weak acid/base apparent forward (K'_f) dissociation rate constants are linked to the apparent reverse rate constants (K'_r) and the equilibrium constants (pK) appropriately adjusted for ionic strength effects, e.g. $K'_{fCl} = K'_{rCl}\ 10^{-pKCl}/\ f_m^2$, where f_m is the mono-valent ion activity coefficient (Loewenthal *et al.*, 1989), see Table 2a, Musvoto *et al.* (1997). For the expulsion rate constants of the CO_2 and NH_3 gases modelled ($K'_r = K_{La}$), for CO_2 the K_{LaCO2} was assumed to have a high value (1000/d) since only the steady state was initially simulated, while for NH_3 the K'_{rNH3} was accepted to have a low value (1/d). As noted above, the value for K'_{rNH3} does not influence the simulations provided it is not too high, since little NH_3 is lost at the pH < 7.5.

In the biological digestion processes part of the model, the kinetic and stoichiometric constants are required (Y, μ_{max}, K_S and b) for the four AD organism groups (Table 4.5). In the literature there is considerable variation and hence uncertainty in these values. Accepting this uncertainty, values for these constants were taken from Sam-Soon *et al.* (1991), who obtained their values from a survey of the literature. Where specific weak acid/base species are included in the rate formulation (e.g. acetoclastic methanogenesis), the rate constants (e.g. Monod half saturation coefficients) had to be appropriately adjusted to take into account weak acid/base speciation.This was done via the relevant pK values and pH. In application, the maximum specific growth rate of the acetoclastic methanogens ($\mu_{max,AM}$ in Eq 4.20) was increased from the range of 0.3 - 0.5/d used by Sam-Soon *et al.* (1991) to 4.39/d, to reproduce the observation of low HAc/Ac^- residual concentrations; due to the low HAc/Ac^- concentrations, decreasing the intuitively more satisfying half saturation constant ($K_{S,AM}$ in Eq 4.20) as alternative caused instability in solution procedures. This aspect requires further investigation.

This left two parts of the AD model that required calibration against experimental data, viz, (i) the kinetic constants for the various hydrolysis rate expressions, e.g. maximum specific hydrolysis rate ($k_{max,HYD}$) and half saturation coefficient ($K_{S,HYD}$) in Eq 4.16d, and selection of the most appropriate kinetic formulation, and (ii) the sewage sludge CHON composition, i.e. the X, Y, Z and A values in $C_XH_YO_ZN_A$. Additionally, in model application the sewage sludge constituent fractions and the input concentrations of the various compounds needed to be quantified. Values for all these parameters were obtained interactively through analysis of and model application to the experimental data set of Izzett *et al.* (1992), as described below.

4.7.2 Experimental Anaerobic Digester Systems

In any calibration and validation exercise, the measured parameters must conform to the same mass balance and continuity principles as in the model, and hence (i) must be sufficient to be able to calculate the material mass balances and (ii) the mass balances must be as close as possible to 100%. The data of Izzett *et al.* (1992) appeared to conform reasonably well to these criteria. They conducted a series of experiments aimed at identifying the effects of thermophyllic heat pre-treatment on the anaerobic digestibility of a mixture of primary and humus sewage sludges. In this investigation four laboratory scale anaerobic digesters were operated at a controlled temperature of 37 °C, two of which were fed heat pre-treated (70°C for 24h) sludge while the other two were fed untreated sludge. The digesters were run in parallel, and the retention times were progressively reduced to observe possible differences in digestibility (fraction unbiodegradable and rate of hydrolysis) between the heat pre-treated and untreated

sludges. The digester fed untreated sludge was operated for a period of 211 days, during which time the retention time was reduced from 20 to 15, then 12, 10 and finally 7 days after the system had run at steady state for two to three retention times at each retention time. The data collected from this AD system (influent and effluent COD, VSS, TSS, TKN, FSA, SCFA, pH, $H_2CO_3^*$ alkalinity and gas production and CO_2 composition) at a particular retention time were averaged over the final two to three steady state retention times (Table 4.6). The averages were used to check the N and COD mass balances. The N and COD balances obtained at the 20, 15, 12, 10 and 7 day retention times were 91 to 99% and 107 to 109% respectively (Table 4.6), indicating that the measured parameters conformed closely to the mass balance requirement. The measured averages therefore could be accepted to represent the behavioural characteristics of the digester under stable operating conditions at the different retention times.

Table 4.6: Experimental results for Izzett et al. (1992) 14ℓ flow though mesophilic (37°C) anaerobic digesters operated from 20 to 7 days retention time on primary sewage sludge.

Retention time (d)	20	15	12	10	7
Feed rate (ℓ/d)	0.7	0.93	1.17	1.4	2
Feed COD (mgCOD/ℓ)	42595	42367	39222	40721	43286
Feed VFA (mgCOD/ℓ as HAc)	2249	1824	2872	1961	1871
Feed TKN (mgN/ℓ)	1171	1075	1028	1100	1105
Feed FSA (mgN/ℓ)	244	221	235	203	196
Feed VSS (mgVSS/ℓ)	25690	25863	24727	25768	25971
Feed $H_2CO_3^*$ Alk (mg/ℓ as $CaCO_3$)	56	82	90	81	80
Feed pH	5.28	5.42	5.2	5.34	5.34
Effluent COD (mgCOD/ℓ)	19005	19969	18678	20521	23637
Effluent VFA (mgCOD/ℓ as HAc)	23	27	28	28	50
Effluent TKN (mgN/ℓ)	1157	976	992	1039	1041
Effluent FSA (mgN/ℓ)	511	404	430	404	511
Effluent $H_2CO_3^*$ Alk (mg/ℓ as $CaCO_3$)	2066	1994	2072	1951	1882
Effluent pH	7.15	7.14	7.2	7.11	7.12
Gas production (ℓ/d at 20°C)	11.053	13.958	16.696	20.07	27.932
Gas composition (% methane)	63.3	63.6	63.3	62.1	63.2
COD balance (%)	107.3	106.9	109.1	108.6	108.4
N balances (%)	98.8	90.8	96.5	94.5	94.2

Model COD and N balances at all retention times 100.0053% and 99.999% respectively.

As input to the various simulations and calculations below, the influent inorganic and organic constituent fractions need to be specified. A number of these were available from direct measurements, or could be derived directly. For the inorganic concentrations, the inorganic carbon and nitrogen weak acid/base species are required. The total inorganic nitrogen (free and saline ammonia, FSA, Table 4.6) was measured directly and the total inorganic carbon (C_T) could be calculated from the measured influent $H_2CO_3^*$ alkalinity and pH (Loewenthal *et al.*, 1986). From the influent total species concentrations, pH, temperature and relevant pK values adjusted for ionic strength effects, the influent inorganic carbon and nitrogen weak acid/base species concentrations could be calculated, as required for the simulations.

For the organic concentrations (Fig 4.5), the total COD (S_{ti}) and SCFA (S_{bsai}) concentrations were

available from direct measurement (Table 4.6). For the simulations, all S_{bsai} were accepted to be HAc/Ac^- and this weak acid/base was speciated from the influent total species concentration, pH, temperature and relevant pK value adjusted for ionic strength effects (see Chapter 3). Further, from the experimental work of Lilley *et al.* (1990) and Ristow *et al.* (2004a), the non-SCFA fermentable biodegradable soluble COD concentration (S_{bsfi}) was accepted to be equal to the S_{bsai} concentration. The unbiodegradable soluble COD (S_{usi}) was accepted to be so low as to be negligible. This left two COD fractions to be quantified, the unbiodegradable and biodegradable particulates (S_{upi} and S_{bpi}). In the calculations and simulation below, the S_{upi} was determined, and hence S_{bpi} was calculated by difference.

Thus, the Izzett *et al.* (1992) data set was used to calibrate three parts of the model; (i) hydrolysis process kinetic formulation and associated rate constants, (ii) sewage sludge CHON composition, and (iii) the unbiodegradable particulate fraction of the sewage sludge. The three parts were determined interactively and iteratively through calculation and simulation of the experimental systems.

4.7.3 Sewage Sludge Stoichiometric Formula

In the model, the biodegradable sewage sludge is hydrolysed to the intermediary compound 'glucose' (Fig 4.3). Since the stoichiometry of the subsequent products for complete anaerobic oxidation of the intermediate 'glucose' is well established and essentially fixed (see above), the stoichiometric transformation of the sewage sludge to the intermediate 'glucose' is crucial to predict the observed digester effluent and gas compositions. This is directly influenced by the CHON stoichiometric composition for the sewage sludge, Eq 4.15. Furthermore, the carbonate weak acid/base species play an important role in fixing digester pH, $H_2CO_3^*$ alkalinity, CO_2 and CH_4 gas produced, and it is therefore necessary to establish the correct C content of the influent sewage sludge to correctly predict these parameters also.

As a starting point, the sewage sludge composition was assumed to be the same as the generally accepted stoichiometric formula for activated sludge: $C_5H_7O_2N$ (WRC, 1984). However, $C_5H_7O_2N$ could not correctly predict the digester output (pH, gas flow and composition) as measured by Izzett *et al.* (1992) and therefore needed to be changed. Accordingly an improved estimate was derived from the measurements made on the influent.

Since influent TKN and FSA measurements were available (Table 4.6), the organic nitrogen (OrgN) in the feed was calculated for the different retention times. The result was expressed as a ratio of the measured COD and remained fairly constant during the investigation, ranging between 0.0201 and 0.0220 gN/gCOD for the different retention times. VSS measurements on the influent were also available (Table 4.6). Recognising that the VSS represents particulate organics, the equivalent particulate COD was determined as (total COD -2·SCFA COD, i.e. S_{ti} - 2·S_{bsai}). The particulate COD/VSS ratio at each retention time was calculated, and ranged from 1.36 to 1.52 gCOD/gVSS. Additionally the organic N/VSS ratios were calculated and ranged from 0.032 to 0.036 gN/gVSS. From these ratios and accepting the H:O ratio in $C_XH_YO_ZN_A$ as 7:2 (from $C_5H_7O_2N$ above), X and A could be calculated for each retention time, from:

$$\frac{COD}{orgN} = \frac{(Y + 4X - 2Z - 3A)\cdot MW_{O2}}{4\cdot A\cdot MW_N} \tag{4.23}$$

$$\frac{COD}{VSS} = \frac{(Y + 4X - 2Z - 3A)\cdot MW_{O2}}{4(MW_C\cdot X + MW_H\cdot Y + MW_O\cdot Z + MW_N\cdot A)} \tag{4.24}$$

$$\frac{orgN}{VSS} = \frac{A \cdot MW_N}{(MW_C \cdot X + MW_H \cdot Y + MW_O \cdot Z + MW_N \cdot A)} \quad (4.25)$$

where:

MW_X = molecular weight of compound X

In Eqs 4.23 to 4.25 above, accepting Y = 7 and Z = 2, from the different pairings of equations (Eqs 4.23 and 4.25, and Eqs 4.23 and 4.24) two sets of (X; A) data pairs could be calculated for each retention time. The (X; A) pairs at the different retention times were all averaged, to give X = 3.4 and A = 0.192, giving a stoichiometric formulation for the sewage sludge of $C_{3.4}H_7O_2N_{0.192}$. These calculations did not require *a priori* information on the hydrolysis kinetics and S_{upi} and hence this formulation formed the starting point for the simulations, which were used to refine the stoichiometry (in conjunction with the hydrolysis kinetics and S_{upi}).

In the simulations the parameters that were targeted for improved estimation of the sewage sludge formulation were the gas flow and composition, which requires a carbon (C) balance over the digester. Izzett *et al.* (1992) did not measure the C content of the sewage sludge, so the influent C was calculated from an assumed 100% C balance over the digester (Fig 4.4), through combined use of measured and predicted C output values. This was reasonable because the COD balances were good (107-109%). Essentially, the C content of the influent sewage sludge appears in the outputs, as gaseous CO_2 and CH_4, dissolved inorganic carbon weak acid/base species and effluent soluble and particulate organic C, the particulate organic C being made up of biomass, S_{up} and undegraded S_{bp}.

By tracking all the measured C in CO_2 (gaseous and dissolved) and CH_4 and the simulated organic C exiting the digester at different retention times and ensuring that the predicted and measured effluent CODs corresponded, the C content of the influent could be equated to the C exiting the digester. Subtracting the influent inorganic C (calculated from the measured influent $H_2CO_3^*$ and pH) gave the influent organic C. This was expressed as an influent organic C/COD ratio for the different retention times. Like the OrgN/COD ratio, the organic C/COD ratios also varied in a narrow band for the different retention times. The average organic C/COD ratio was therefore used to calculate the C content (X) in the sewage sludge feed. Taking due consideration that the influent OrgN/COD ratio must also remain at the measured value, a sewage sludge composition formula of $C_{3.5}H_7O_2N_{0.196}$ was determined, very close to the stoichiometry calculated above from the available influent measurements. This formulation was accepted for all subsequent calculations on and simulations of the Izzett *et al.* (1992) data. In the simulations, to derive the organic C/COD ratio the hydrolysis kinetics and S_{upi} needed to be correctly specified, and hence the requirement for interactive calculations and simulations.

To check how the model sewage sludge composition compares with real sludges, primary sludge from two different full-scale wastewater treatment plants (WWTP) around Cape Town (South Africa) were analysed for VSS, TSS, COD and their organic C, H, N and phosphorus (P) contents (see Appendix A). From the measured data, the CHON composition of the primary sludge was calculated (P was omitted because it was not measured by Izzett *et al.*, 1992). The average measured composition was $C_{3.65}H_7O_{1.97}N_{0.19}$. The model C, H, O, N content and molar mass of primary sludge are 95.9%, 100%, 98.5%, 94.5% and 98.7% of the measured values. This provides powerful validation of the UCTADM1 model. Appendix A provides more detail on how the sludge stoichiometric formulae were calculated.

4.7.4 Estimating the Unbiodegradable Fraction of Sewage Sludge and Hydrolysis Kinetics and Constants

Before an even remotely reasonable correspondence could be obtained between model predicted and measured effluent parameters and gas composition and production, the fraction of unbiodegradable particulate COD of the sewage sludge ($f_{PSup} = S_{upi}/S_{ti}$) and the hydrolysis rate kinetics and constants needed to be determined. These were determined interactively between mass balance based calculations and simulations on the Izzett *et al.* data set. Initially, a value for the f_{PSup} was estimated and then the various kinetic formulations evaluated, and thereafter the estimate for f_{PSup} improved. In the mass balance based calculations below, COD units are used. The calculated values for the various parameters can be readily converted to the mole units required in the model, see below.

For the Izzett *et al.* data set, the influent sewage sludge is characterised by (Fig 4.5):

$$S_{ti} = S_{bpi} + S_{bsfi} + S_{bsai} + S_{usi} + S_{upi} \qquad \text{(mgCOD/}\ell\text{)} \qquad (4.26)$$

In Eq 4.26 as noted above, S_{ti} and S_{bsai} were directly available from measurement (Table 4.6); S_{usi} could be accepted to be negligible, and S_{bsfi} could be accepted to be equal to S_{bsai}. This left two unknowns, S_{bpi} and S_{upi}. Letting $S_{upi} = f_{PSup} \cdot S_{ti}$, then S_{bpi} could be found by difference and hence f_{PSup} was the only unknown.

For the effluent:

$$S_{te} = S_{bpe} + S_{bsfe} + S_{bsae} + S_{use} + S_{upe} + biomass \qquad \text{(mgCOD/}\ell\text{)} \qquad (4.27)$$

In Eq 4.27, S_{te} and S_{bsae} were available from direct measurement and it could be accepted that $S_{bsfe} = S_{bsae}$ (the values are very low due to stable digester operation and hence do not influence the analysis significantly). Accepting negligible generation of unbiodegradable material in the anaerobic digester, then $S_{use} = S_{usi} = 0$ and $S_{upe} = S_{upi}$. With regard to the biomass, under stable digester operation three organism groups are generated, acidogens (Z_{AD}), acetoclastic methanogens (Z_{AM}) and hydrogenotrophic methanogens (Z_{HM}). Of these, the mass of Z_{HM} developed is very much smaller than that of Z_{AD} and Z_{AM}, and accordingly can be neglected in an initial steady state analysis. Thus Eq 4.27 reduces to:

$$S_{te} = S_{bpe} + S_{bsfe} + S_{bsae} + S_{use} + S_{upe} + Z_{AD} + Z_{AM} \qquad \text{(mgCOD/}\ell\text{)} \qquad (4.28)$$

Developing mass balances around the digester (Ristow *et al.*, 2004a,b) and recognising from Table 4.2 that in the death of biomass the released organics add to the sewage sludge, for biodegradable particulate COD (S_{bp}) :

$$V \cdot S_{bp} = Q_i \cdot S_{bpi} \cdot dt - Q_e \cdot S_{bpe} \cdot dt - r^*_{HYD} \cdot V \cdot dt + (b_{AD} \cdot Z_{AD} + b_{AM} \cdot Z_{AM}) \cdot V \cdot dt \quad \text{(mgCOD/}\ell\text{)} \qquad (4.29)$$

where:

r^*_{HYD} = volumetric hydrolysis rate, COD units (mgCOD/ℓ.d)
V_d = digester volume (ℓ)
$Q_i = Q_e$ = influent and effluent flow rate respectively (ℓ/d)

At steady state, solving for r^*_{HYD} :

$$r^*_{HYD} = \frac{1}{R_h}(S_{bpi} - S_{bpe}) + b_{AD} \cdot Z_{AD} + b_{AM} \cdot Z_{AM} \qquad \text{(mgCOD/}\ell\text{.d)} \qquad (4.30)$$

where:

R_h = V_d/Q_i = hydraulic retention time (d)

Similarly for S_{bsf} and S_{bsa} with r^*_{AD} and r^*_{AM} as the volumetric rates in COD units of acidogenesis and acetoclastic methanogenesis respectively:

$$r^*_{AD} = \frac{1}{R_h}(S_{bsfi} - S_{bsfe}) + r^*_{HYD} \qquad \text{(mgCOD/ℓ.d)} \qquad (4.31)$$

$$r^*_{AM} = \frac{1}{R_h}(S_{bsai} - S_{bsae}) + f_{Sbsa/Sbsf} \cdot r^*_{AD} \qquad \text{(mgCOD/ℓ.d)} \qquad (4.32)$$

where:

$f_{Sbsa/Sbsf}$ = fraction of S_{bsf} appearing as S_{bsa} in the acidogenesis reaction (Table 4.4)
= 0.607 (mgCOD/mgCOD)

Developing similar mass balances for the biomass concentrations:

$$Z_{AD} = \frac{r^*_{AD} \cdot Y^*_{AD} \cdot R_h}{(1 + b_{AD} \cdot R_h)} \qquad \text{(mgCOD/ℓ)} \qquad (4.33)$$

$$Z_{AM} = \frac{r^*_{AM} \cdot Y^*_{AM} \cdot R_h}{(1 + b_{AM} \cdot R_h)} \qquad \text{(mgCOD/ℓ)} \qquad (4.34)$$

where:

Y^*_{AD} = acidogen yield (mg COD/mg COD)
Y^*_{AM} = acetoclastic methanogen yield (mg COD/mg COD)

Recognising that from Eq 4.28:

$$S_{bpe} = S_{te} - S_{bsfe} - S_{bsae} - f_{PSup} \cdot S_{ti} - Z_{AD} - Z_{AM} \qquad \text{(mg COD/ℓ)} \qquad (4.35)$$

In the set of equations above, f_{PSup}, S_{bpe}, Z_{AD} and Z_{AM} are the principal unknowns. If an estimate for f_{PSup} is available, then S_{bpe}, Z_{AD} and Z_{AM} can be calculated through iteration. However, f_{PSup} is not known for the Izzett *et al.* data set, and would need to be determined via some other technique, see later.

4.7.5 Determining Hydrolysis Rate Constants

In the section above, for any selected f_{PSup}, the volumetric rate of hydrolysis (r^*_{HYD}) can be calculated, as well as Z_{AD}, Z_{AM} and S_{bpe}, all in COD units. Converting these values to mole units:

$$r_{HYD} = r^*_{HYD} \Big/ \left(\frac{COD}{mol}\right)_{S_{bp}} \qquad \text{(mol } S_{bp}\text{/ℓ.d)} \qquad (4.36)$$

$$[S_{bpe}] = S_{bpe} \Big/ \left(\frac{COD}{mol}\right)_{S_{bp}} \qquad \text{(mol } S_{bp}\text{/ℓ)} \qquad (4.37)$$

$$[Z] = Z \Big/ \left(\frac{COD}{mol}\right)_{Z} \qquad \text{(mol Z/ℓ)} \qquad (4.38)$$

where:

$\left(\frac{COD}{mol}\right)_{S_{bp}}$ = COD/mol ratio for S_{bp}
= 131.3 gCOD/mol for $C_{3.5}H_7O_2N_{0.196}$

$\left(\frac{COD}{mol}\right)_{Z}$ = COD/mol ratio for biomass
= 160 gCOD/mol for $C_5H_7O_2N$

[ ] = mole concentration

Equating this r_{HYD} with the first order and first order specific kinetic expressions for the hydrolysis (Eqs 4.16a and 4.16b respectively), and solving for K_h and K_H yields:

$K_h = r_{HYD}/[S_{bpe}]$ (/d) (4.39)

$K_H = r_{HYD}/([S_{bpe}][Z_{AD}])$ (ℓ/mol Z_{AD}.d) (4.40)

Thus, from Eqs 4.39 and 4.40 above, values for K_h and K_H could be determined, provided f_{PSup} was known.

Similarly, for the Monod (Eq 4.16c) and surface mediated reaction (Contois, Eq 4.16d) kinetics:

$$r_{HYD} = \left[\frac{\mu_{max,HYD}\ [S_{bp}]}{K_{SM,HYD} + [S_{bp}]}\right][Z_{AD}] \tag{4.41}$$

$$r_{HYD} = \left[\frac{k_{max,HYD}\ \frac{[S_{bp}]}{[Z_{AD}]}}{K_{SS,HYD} + \frac{[S_{bp}]}{[Z_{AD}]}}\right][Z_{AD}] \tag{4.42}$$

In each of Eqs 4.41 and 4.42 above, the values for the two constants needed to be determined, namely $\mu_{max,HYD}$ and $K_{SM,HYD}$ and $k_{max,HYD}$ and $K_{SS,HYD}$ respectively. To determine these constants, the equations were linearized by three different methods, i.e. (i) Lineweaver-Burke, (ii) inversion and (iii) Eadie-Hofstee (Lehninger, 1977). For the Monod kinetics for example, these yielded respectively:

(i) $$\frac{[Z_{AD}]}{r_{HYD}} = \frac{K_{SM,HYD}}{\mu_{max,HYD}} \cdot \frac{1}{[S_{bpe}]} + \frac{1}{\mu_{max,HYD}} \tag{4.43a}$$

(ii) $$\frac{[S_{bpe}]}{r_{HYD}} = \frac{K_{SM,HYD}}{\mu_{max,HYD}} + [S_{bpe}] \cdot \frac{1}{\mu_{max,HYD}} \tag{4.43b}$$

(iii) $$\frac{r_{HYD}}{[Z_{AD}]} = -K_{SM,HYD} \cdot \frac{r_{HYD}}{[S_{bpe}] \cdot [Z_{AD}]} + \mu_{max,HYD} \tag{4.43c}$$

Linear regression was fitted to the Izzett *et al.* experimental data plotted according to the three linearization methods, for example see Figs 4.6a, b and c respectively for Monod kinetics. From the slopes and y-intercepts of the fitted lines, the appropriate pair of kinetic constants was determined. Again these calculations required that the value for f_{PSup} was known.

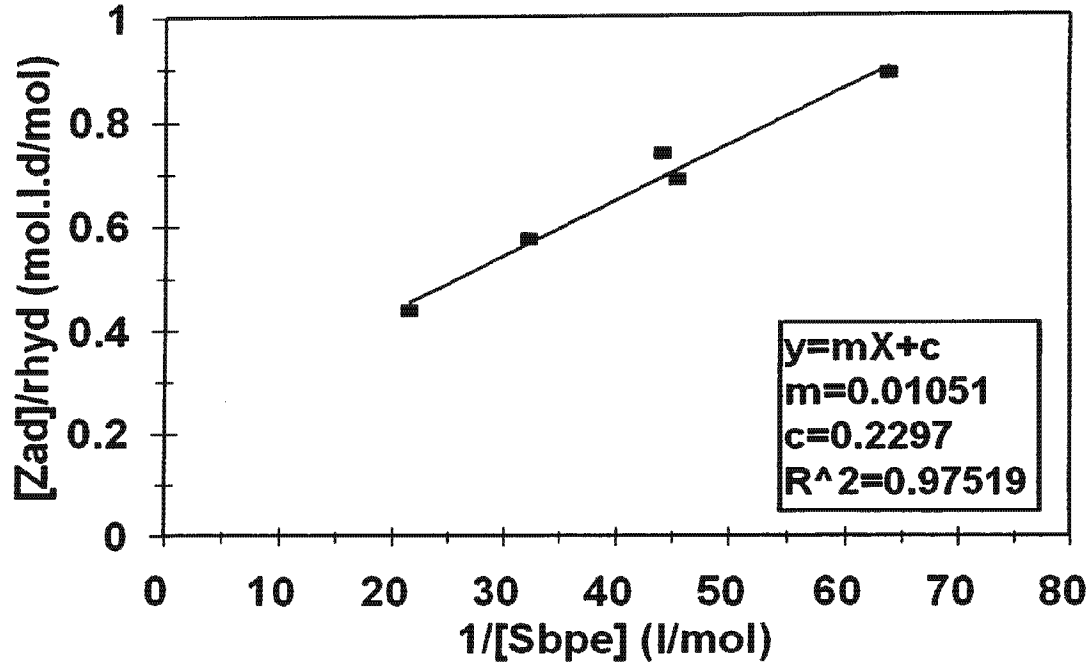

Fig 4.6a: Linearisation by Lineweaver-Burke of Monod kinetics for hydrolysis of sewage sludge for the data of Izzet *et al* (1992) at retention times of 7, 10, 12, 15 and 20d, with linear regression fit of straight line to data.

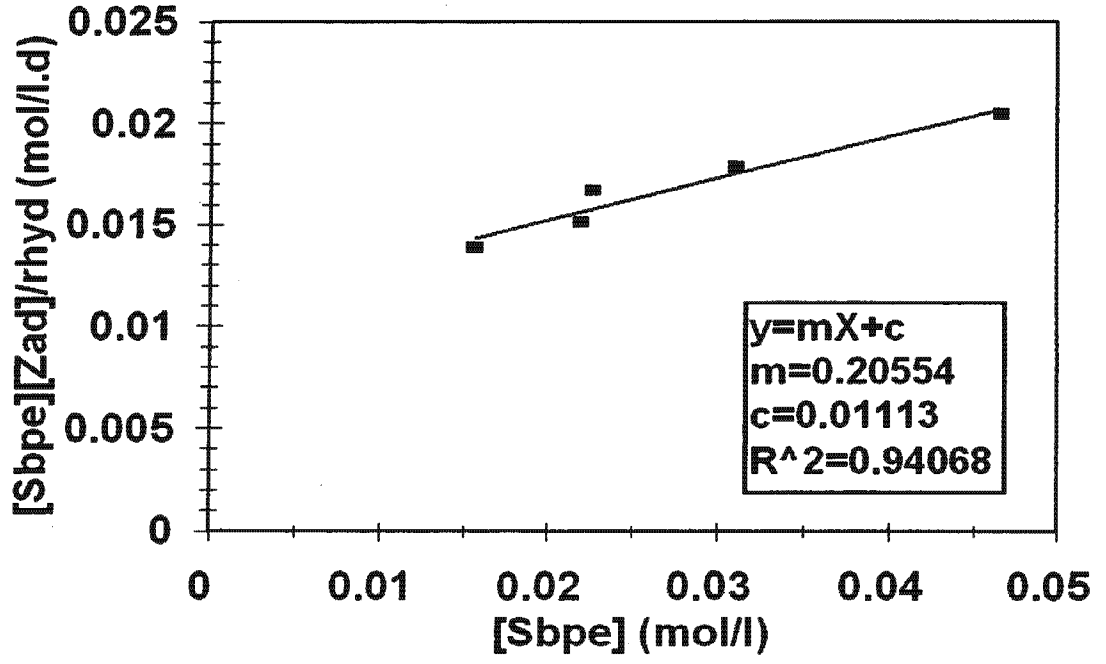

Fig 4.6b: Linearisation by inversion of Monod kinetics for hydrolysis of sewage sludge for the data of Izzet *et al* (1992) at retention times of 7, 10, 12, 15 and 20d, with linear regression fit of straight line to data.

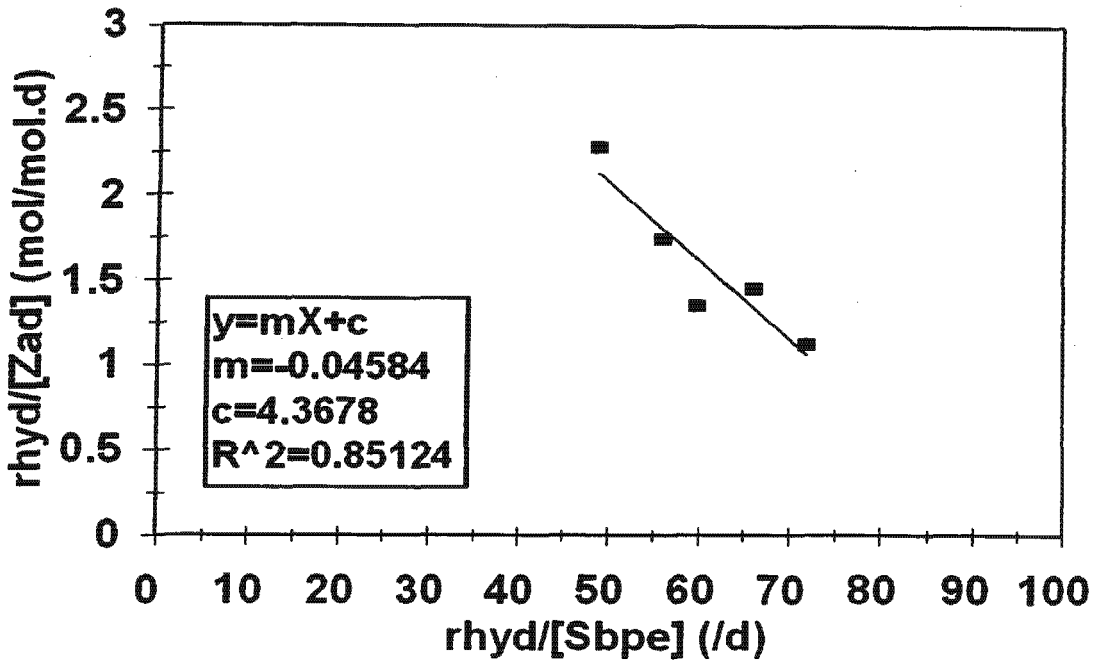

Fig 4.6c: Linearisation by Eadie-Hofstee of Monod kinetics for hydrolysis of sewage sludge for the data of Izzet *et al* (1992) at retention times of 7, 10, 12, 15 and 20d, with linear regression fit of straight line to data.

4.7.6 Determining the Sewage Sludge Unbiodegradable Particulate Fraction (f_{PSup})

In all the calculations above, a value for f_{PSup} needed to be known. However, this value was not directly available from the Izzett *et al.* data set. In the calculations, for each value of f_{PSup} selected, a different set of kinetic constants was obtained for the different kinetic formulations.

Working on the principle that the most appropriate set of kinetic constants would be the one that provides the greatest consistency between predicted and measured values for all retention times of the Izzett *et al.* data set, techniques were devised to identify these constants and the corresponding f_{PSup} value. For the first order and first order specific kinetic formulations, the value for f_{PSup} was varied and the coefficient of variation (standard deviation/average) calculated for the relevant K rates for the four retention times, for each f_{Psup} value. The coefficients of variation were then plotted against f_{PSup}, see Fig 4.7. From Fig 4.7, the coefficients of variation for first order and first order specific kinetics both exhibit minima; For the first order kinetics this is at $f_{PSup} = 0.34$, and for the first order specific kinetics at $f_{PSup} = 0.32$. In effect these values of f_{PSup} are the ones that give the least variation in the relevant kinetic rate constants across the four retention times. Since the Izzett *et al.* systems were operated on the same source sewage sludge, these values would provide the most suitable estimate for f_{PSup} and the kinetic constants. Furthermore, these values for f_{PSup} are very similar to that determined by O'Rourke (1968) of 0.36, and that expected (0.32 or 0.36) from a mass balance around the primary settling tank with typical South African raw and settled wastewater characteristics, i.e. raw ($f_{S,upR}$) and settled ($f_{S,upS}$) wastewater unbiodegradable particulate COD fractions of 0.15 and 0.04 and a COD removal (f_{PSR}) of 40% or 35% respectively in primary sedimentation (WRC, 1984), where (see Chapter 3):

$$f_{PSup} = f_{S,upS} + (f_{S,upR} - f_{S,upS}) / f_{PSR} \quad (4.44)$$

Thus, accepting that for the first order kinetics $f_{PSup} = 0.34$, then $K_h = 0.381$ /d ± 0.0066, and for first order specific kinetics that $f_{PSup} = 0.32$, then $K_H = 40$ ℓ/mol Z_{AD}/d ± 2.0.

For the Monod and surface mediated reaction kinetics, in the three linearization techniques, least squares linear regression was used to fit a straight line to the data, and the correlation coefficients (R^2) of these lines calculated. Thus, for each selected value of f_{PSup} three correlation coefficients were obtained for each of Monod and surface mediated reaction kinetics. These correlation coefficients were plotted against f_{PSup}, see Figs 4.8 and 4.9 for Monod and surface mediated reaction kinetics respectively. Both sets of R^2 values exhibit maximum values at $f_{PSup} = 0.36$, and hence this value was selected for these kinetics. Averaging the values for the three linearizations gives $\mu_{max,HYD} = 4.529$ mol S_{bp}/(mol Z_{AD}.d) and $K_{SM,HYD} = 0.0486$ mol S_{bp}/ℓ for Monod kinetics and $k_{max,HYD} = 6.797$ mol S_{bp}/(mol Z_{AD}.d) and $K_{SS,HYD} = 10.829$ mol S_{bp}/mol Z_{AD} for surface mediated reaction kinetics. To confirm the values determined with this method, the experimental data and predicted lines were plotted on the Monod type plot for both Monod kinetics (Fig 4.10) and surface saturation kinetics (Fig 4.11); In both cases a close fit to the data is obtained.

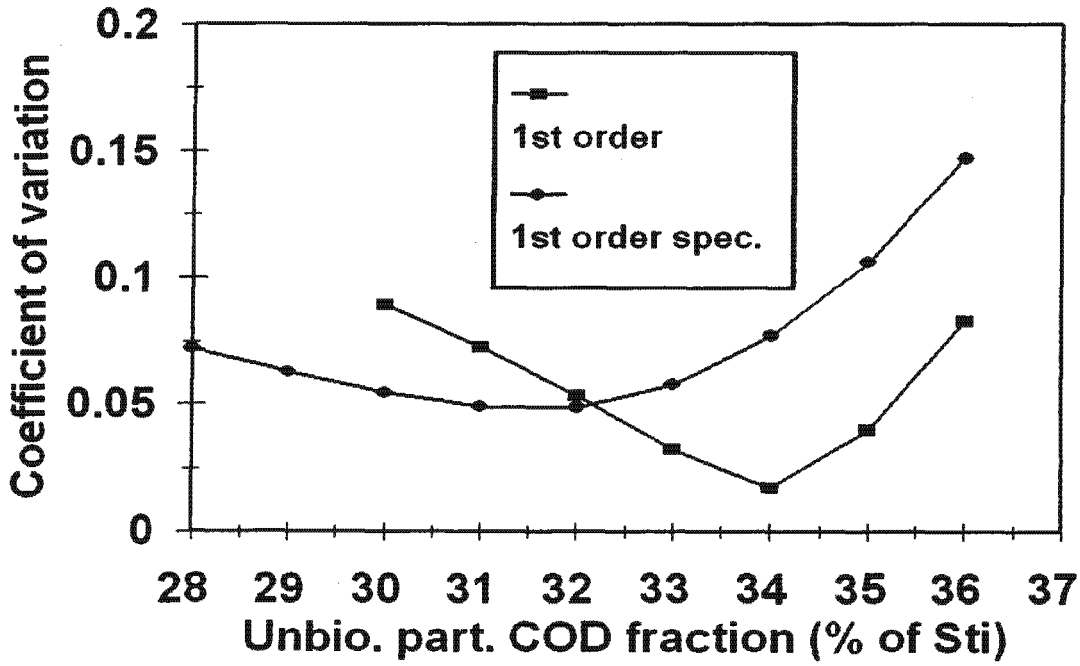

Fig 4.7: Coefficient of variation in the kinetic constants for 1st order and 1st order specific kinetics for sewage sludge hydrolysis, for the data of Izzet *et al.* (1992) at retention times of 7, 10, 12, 15 and 20d.

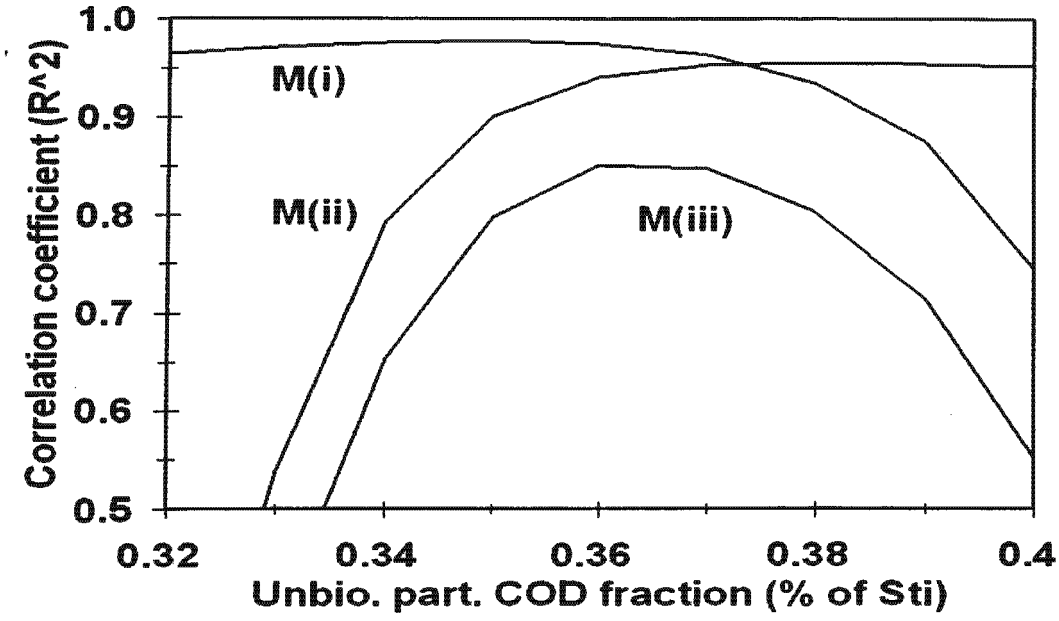

Fig 4.8: Correlation coefficients versus unbiodegradable particulate COD fraction for linear fits to Monod hydrolysis kinetics, for the data of Izzet et al. (1992) at retention times of 7, 10, 12, 15 and 20d: M(i) Lineweaver-Burke, M(ii) inversion, M(iii) Eadie-Hofstee linearisations (see Fig 4.6a to c).

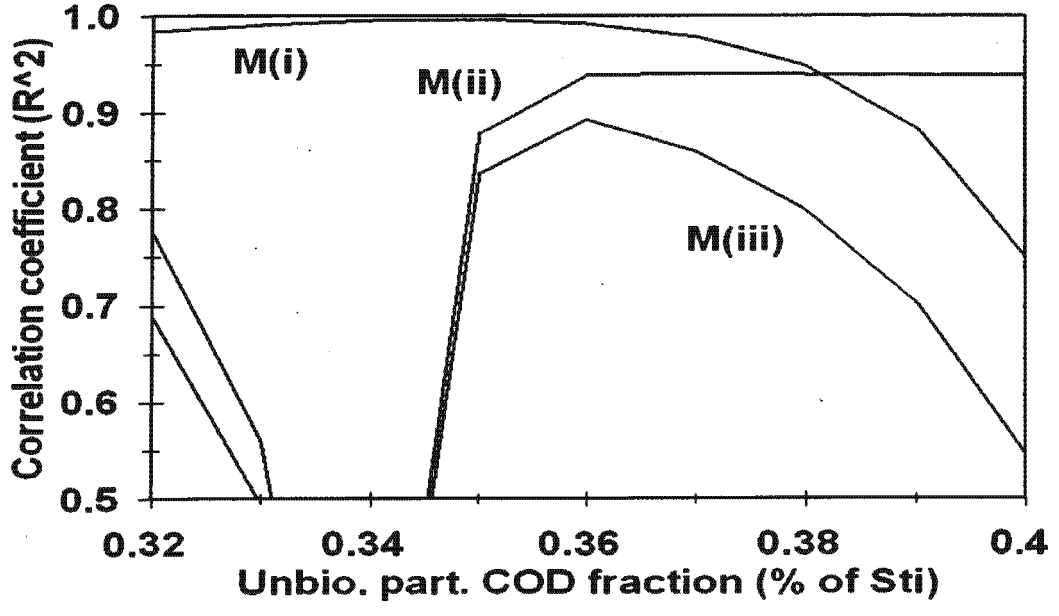

Fig 4.9: Correlation coefficients versus unbiodegradable particulate COD fraction for linear fits to surface mediated reaction hydrolysis kinetics, for the data of Izzet *et al.* (1992) at retention times of 7, 10, 12, 15 and 20d: M(i) Lineweaver-Burke, M(ii) inversion, M(iii) Eadie-Hofstee linearisations.

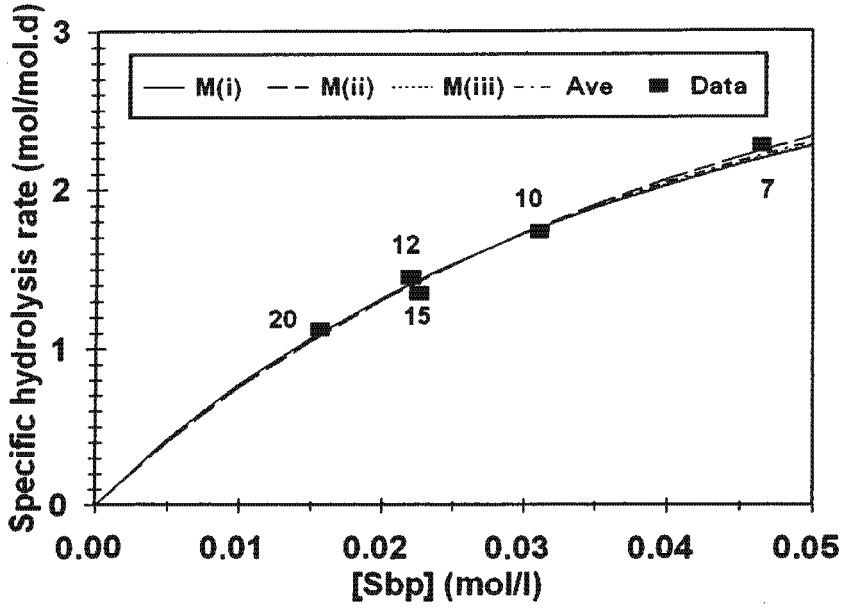

Fig 4.10: Monod specific hydrolysis rate versus biodegradable particulate organics (S_{bp}, mole/ℓ) for the Izzet *et al.* (1992) data at 7, 10, 12, 15 and 20d retention time: M(i) Lineweaver-Burke, M(ii) inversion, M(iii) Eadie-Hofstee linearisations, see Fig 4.6.

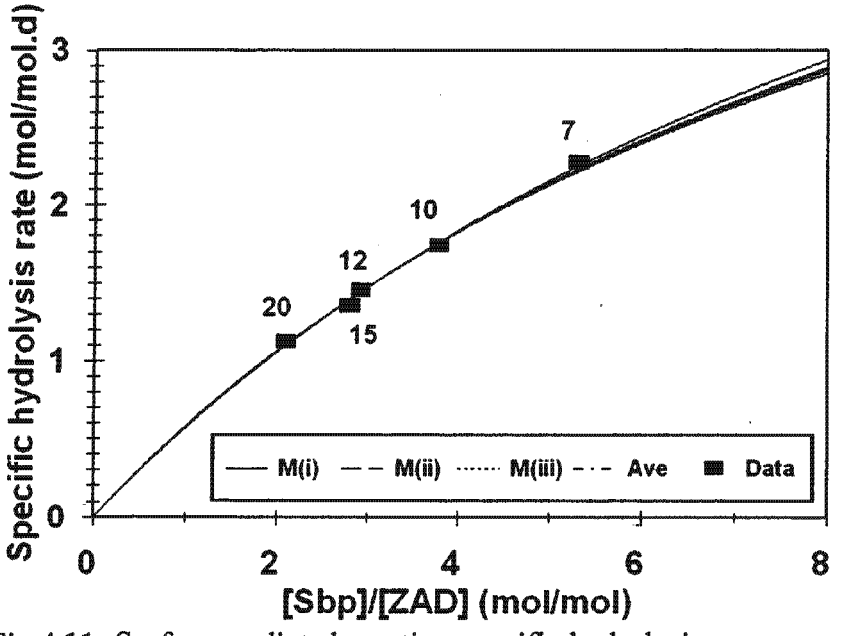

Fig 4.11: Surface mediated reaction specific hydrolysis rate versus biodegradable particulate organics (S_{bp}, mole/ℓ) to acidogen biomass (Z_{AD}, mole/ℓ) ratio for the Izzet *et al.* (1992) data at 7, 10, 12, 15 and 20d retention time: M(i) Lineweaver-Burke, M(ii) inversion, M(iii) Eadie-Hofstee linearisations, see Fig 4.6.

4.7.7 Selection of Hydrolysis Kinetics

In the section above, the data set of Izzett *et al.* was used to calibrate the constants for the four hydrolysis kinetic equations, first order (Eq 4.16a), first order specific (Eq 4.16b), Monod (Eq 4.16c) and surface mediated reaction or Contois (Eq 4.16d). In this exercise, measures of variability were derived for the various kinetic equations, namely coefficient of variation for the first two formulations and correlation coefficients (R^2) for the second two. Comparing the coefficients of variation (Fig 4.7), the minimum value for the first order kinetics is smaller than that for the first order specific, which would suggest that the former describes this data set marginally better. Comparing the R^2 values (Figs 4.8 and 4.9), the values for surface mediated reaction kinetics are higher than those for Monod kinetics, also suggesting that the latter kinetics describes the data set marginally better. With regard to first order versus surface mediated reaction kinetics, the data set cannot provide guidance as to which is superior, i.e. both kinetic formulations with the appropriate constants provide equally acceptable descriptions of the hydrolysis process for the Izzett *et al.* data set. However, since this process is mediated by the acidogens, the surface mediated reaction kinetics which includes this organism group intuitively would appear more reasonable and from a modelling perspective, it is also easier to use. Furthermore, this kinetic formulation has been applied with considerable success in activated sludge system models (e.g. ASM1, Henze *et al.*, 1987), in which the organisms act on the same biodegradable particulate substrate. Accordingly, the surface mediated reaction kinetics were accepted for incorporation in UCTADM1.

4.7.8 Refinement of Values for Sewage Sludge Composition, and Model Validation

Accepting the surface mediated reaction kinetics for hydrolysis and the estimates for the various constants (f_{PSup}, $k_{max,HYD}$ and $K_{SS,HYD}$) as determined above, the averages of the Izzett *et al.* measured influent parameters were set as input to AD model, with the influent weak acid/bases (NH_3/NH_4^+; HAc/Ac^-; $H_2CO_3^*/HCO_3^-/CO_3^{2-}$; phosphorus not included as measurements not available). The model predictions for the effluent parameters and gas streams compositions and flows were compared with the corresponding measured averages at the different retention times. Only one part of the model required refinement (sewage sludge CHON composition) and this was then adjusted iteratively until the best correspondence between predicted and measured results at all retention times was obtained, to give $C_{3.5}H_7O_2N_{0.196}$; because the model is internally consistent and fixed by the kinetic and stoichiometric equations and determined constants, the only way a different effluent pH or gas composition can be predicted by the model is by changing the influent composition of the feed sludge. As noted above, independent validation was obtained by comparing the determined primary sludge composition with measured values. The model predicted parameters are compared with the corresponding measured values for all retention times in Fig 4.12 a to f. The predicted COD removal (Fig 4.12a) and gas composition (Fig 4.12c) correspond very well to those measured. The gas production (Fig 4.12b) is under predicted, because the model is based on 100% COD balance and the experimental data COD balances range from 107 to 109% (Table 4.6) - model calibration was on COD removal and hence the COD over recovery manifests in the gas production. The predicted effluent free and saline ammonia (FSA) concentration is generally higher than that measured, because the model is based on 100% N mass balance and the experimental mass balances were 91 to 99% (Table 4.6). By decreasing the N content of the influent organics (A in $C_XH_YO_ZN_A$) by a small amount (5% to 0.186), the predicted effluent FSA could be made to closely match the measured values, but this would cause the influent organic N concentration to be in error. The effluent $H_2CO_3^*$ alkalinity is over predicted, and this prediction can be improved by decreasing the N content of the organics or including some of the influent SCFA as propionic. However, both these would cause the predicted pH to decrease causing it to deviate from the measured value. Since insufficient experimental data are available to resolve this, these changes were not implemented. The experimentally measured pH, $H_2CO_3^*$ alkalinity and p_{CO2}

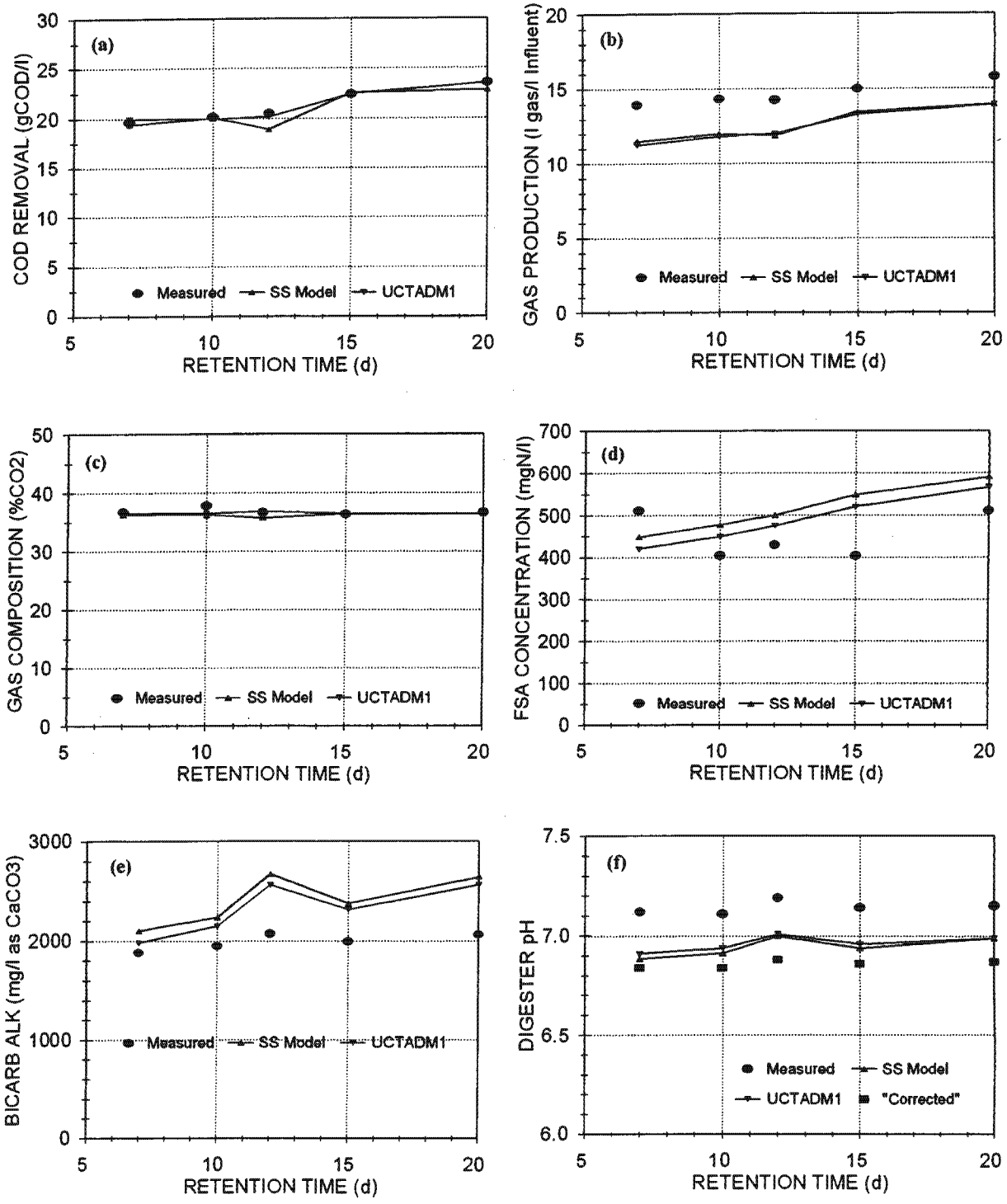

Fig 4.12: Comparison between kinetic simulation model (UCTADM1) predicted (lines) and measured (points) (a) COD removal, (b) gas production, (c) gas composition, (d) free and saline ammonia, (e) $H_2CO_3^*$ alkalinity and (f) digester pH versus retention time for the Izzett *et al.* (1992) data set; also shown are the predictions of the steady state AD model presented in Chapter 5.

show inconsistency in that these are not in equilibrium. Accepting the gas composition and $H_2CO_3^*$ alkalinity as the most reliable measurements (CO_2 loss on sampling would influence pH but not $H_2CO_3^*$ alkalinity, Loewenthal *et al.*, 1991), the equilibrium 'corrected' pH was calculated. Both experimentally measured and 'corrected' pH are shown in Fig 4.12f together with the predicted pH values; The predicted and 'corrected' pH values correspond closely. Overall, accepting the margin for error in the experimental measurements, good correlation between measured and predicted parameters was obtained. More extensive simulations with the model of a wider range of experimental systems are required for further model validation.

4.8 FURTHER MODEL VALIDATION

Ristow *et al.* (2004a) studied the rate of hydrolysis of primary sewage sludge under methanogenic, acidogenic and sulfate reducing conditions and the influence of system physical constraints on the hydrolysis rate. The aims of their research were to (i) determine the rate of hydrolysis of primary sludge under methanogenic conditions, (ii) determine the effects of feed COD concentration, hydraulic retention time and pH on the rate of hydrolysis under methanogenic conditions, (iii) develop a mathematical model for the biological processes mediating the hydrolysis of primary sludge in methanogenic systems, so that the hydrolysis rate can be predicted for various feed COD concentrations, hydraulic retention times and operating pH, based only on the feed characterization and system operation, (iv) evaluate the various rate formulations for the primary sludge hydrolysis, also at varying operating conditions, to identify the most appropriate rate formulation for hydrolysis of primary sludge under methanogenic conditions, (v) determine the rate of primary sludge hydrolysis under acidogenic conditions (i.e. to repeat i to iii above for acidogenic conditions), (vi) appropriately modify the mathematical model selected in iv above to predict the rate of hydrolysis under acidogenic conditions, (vii) predict the rate of primary sludge hydrolysis under sulfate reducing conditions and (viii) determine the effects of sulfate reduction on the rate of hydrolysis of primary sludge.

The research approach adopted by Ristow *et al.* (2004a) was to operate parallel laboratory scale, completely mixed anaerobic digesters with primary sewage sludge as influent, and to monitor the behaviour of these systems under a range of feed COD concentrations, retention times, pH and feed sulfate conditions under stable methanogenic, acidogenic and sulfate reducing conditions. To further validate the anaerobic model developed in this Chapter, the methanogenic experimental laboratory scale completely mixed anaerobic digesters operated by Ristow *et al.* (2004a) were simulated with the anaerobic model developed here.

4.8.1 Modelling the Laboratory Scale Completely Mixed Methanogenic Anaerobic Digesters Operated by Ristow *et al.* (2004a)

During their research, Ristow *et al.* (2004a) operated 21 methanogenic laboratory scale completely mixed anaerobic digesters at a controlled temperature of 35°C at various hydraulic retention times between 5 and 60 days. They were fed primary sewage sludge at varying concentrations, from 1.950 gCOD/ℓ up to 41.441gCOD/ℓ. The feed primary sewage sludge originated from the primary settling tanks at the Athlone Wastewater Treatment Works (City of Cape Town, South Africa), which treats municipal wastewater of mainly domestic origin, but with a significant mixed industrial component. The primary sludge was collected in batches using a number of 25 ℓ plastic drums, and each batch of feed was given a feed batch number (for details see Ristow *et al.*, 2004a). Table 4.7 gives a summary of the 21 digesters operated by Ristow *et al.* (2004a), where FB is the feed batch number for the digester.

Table 4.7: Laboratory scale, completely mixed methanogenic anaerobic digesters operated by Ristow *et al.* (2004).

Feed COD Concentraion gCOD/ℓ	Hydraulic Retention Time (days)							
	60	20	15	10	8	6.67	5.71	5
40			FB13	FB13	FB14	FB14	FB15	
25		FB12	FB12	FB12	FB12	FB13	FB13	FB13
13			FB12	FB13	FB13	FB14	FB15	
9	FB12							
1.95				FB14	FB14			

4.8.2 Feed Characterization and Effluent Experimental Data

Ristow *et al.* (2004a) give the unbiodegradable particulate and unbiodegradable soluble fractions for all the feed batches as 0.3345 and 0.008 respectively. The unbiodegradable particulate fraction was derived from the 60 day experimental unit. Ristow *et al.* (2004a) argued that 60 days are sufficient time for all the biodegradable organic material to be utilized, and therefore the effluent particulate COD (that is not organism mass) can be assumed to be unbiodegradable particulate organic material only. The unbiodegradable soluble fraction was calculated from the measured dissolved effluent COD of all the systems.

Unfortunately, Ristow *et al.* (2004a) did not measure the influent alkalinity and pH on the diluted feed. They only measured alkalinity and pH on the undiluted feed for feed batches 12 and 13, but they did not measure any alkalinity and pH for feed batches 14 and 15. The alkalinity and pH data collected on the undiluted influent primary sludge is given in Table 4.8. Included in Table 4.8 is the data for feed batches 9 and 10, which was not used for the methanogenic systems in the research of Ristow *et al.* (2004a), but is used here, together with the measured data from feed batches 12 and 13 to estimate values for the influent (alkalinity and pH) that was not measured on feed batches 13 and 14. The primary sludge stoichiometric formulations are also given in Table 4.8; These were calculated in the same way as those for the data set of Izzett *et al.* (1992) described above (see Chapter 4.7.3 and Appendix A).

Table 4.8: Sludge stoichiometric formula, alkalinity and pH data for feed batches 9, 10, 12, 13, 14 and 15 from Ristow *et al.* (2004).

Feed Batch No.	Sludge Stoichiometric Formula	Alkalinity mg/l as $CaCO_3$	pH
9	-	86.7	5.35
10	-	75.52	5.54
12	$C_{4.15}H_7O_{2.42}N_{0.22}$	47.3	4.91
13	$C_{4.17}H_7O_{2.63}N_{0.22}$	151.6	5.73
14	$C_{4.31}H_7O3.03N_{0.24}$	90.28*	5.38*
15	$C_{4.06}H_7O2.43N_{0.19}$	90.28*	5.38*

* Calculated averages from feed batches 9,10,12 and 13.

When tap water is added to the raw primary sludge to dilute it to the required feed concentration, the alkalinity and pH values are not merely diluted by volume, they change in a complex manner, dependent on the aquatic chemistry of the primary sludge/tap water blend. Therefore, the alkalinity and pH measurements on the diluted feeds cannot be calculated by multiplying the measured undiluted feed values with the corresponding dilution factor. To obtain a more accurate estimate of the alkalinity and pH values of the diluted feeds, the primary sludge fraction and the corresponding fraction of tap water (alkalinity and pH assumed to be 35.0 mg/ℓ as $CaCO_3$ and 7.0 respectively) were entered into the computer program STASOFT version 2.4 (Loewenthal *et al.*, 1988) to obtain the estimated primary sludge/tap water blend alkalinity and pH. These alkalinity and pH values were used as input to the anaerobic model developed in this Chapter.

All influent data for the feed to each experimental methanogenic system are listed in Table 4.9. Ristow *et al.* (2004a) measured the total COD (S_{ti}), soluble COD (S_{bsi}), VFA (S_{bsai}) and FSA (N_{ai}) on the undiluted primary sludge. These values were multiplied by their corresponding dilution factors to calculate the corresponding diluted values. All data listed in Table 4.9 refers to the diluted influent that was fed to the anaerobic digesters.

Table 4.9: Feed data for the methanogenic laboratory scale, completely mixed anaerobic digesters operated by Ristow *et al.* (2004).

Ret. Time days	Feed Rate ℓ/d	React. Vol. ℓ	Feed Batch No.	S_{ti} mgCOD/ℓ	S_{bsi} mgCOD/ℓ	S_{bsai} mgCOD/ℓ as HAc	S_{usi} mgCOD/ℓ	N_{ai} mgN/ℓ	Alkalinity mg/ℓ as $CaCO_3$	pH
60	0.33	20	12	9810	1204	528	78	15	37.3	5.55
20	1	20	12	25953	2327	994	208	39	41.1	5.16
15	1.33	20	13	39790	3550	1516	318	180	139.9	5.74
15	1.33	20	12	25953	2647	1145	208	39	41.1	5.16
15	1.33	20	12	13618	1432	621	109	20	38.2	5.42
10	2	20	13	39810	4446	1937	318	214	139.9	5.74
10	1.6	16	12	25953	2331	996	208	39	41.1	5.16
10	2	20	13	13270	1164	496	106	59	70	5.93
10	2	20	14	1950	254	112	16	5	38.1	6.24
8	2.5	20	14	34818	3828	1665	279	44	90.28	5.38
8	2	16	12	25953	2675	1158	208	39	41.1	5.16
8	2.5	20	13	13270	1525	666	106	73	70	5.93
8	2.5	20	14	1950	284	126	16	7	38.1	6.24
6.67	3	20	14	34818	4354	1912	279	70	90.28	5.38
6.67	2.4	16	13	24818	2038	863	199	106	100.6	5.81
6.67	3	20	14	13579	1845	815	109	37	56.6	5.6
5.71	3.5	20	15	41441	2583	1056	332	40	69.7	5.48
5.71	2.8	16	13	24960	2516	1087	200	124	100.6	5.81
5.71	3.5	20	15	13186	957	400	105	18	46.1	5.81
5	3.2	16	13	24881	2703	1175	199	131	100.6	5.81

After startup of each digester, Ristow *et al.* (2004a) operated it for three full sludge ages to allow it to reach steady state. Once steady state was reached, daily data collection commenced for at least 20 days. The average effluent data measured by Ristow *et al.* (2004a) for each steady state is given in Table 4.10.

Table 4.10: Effluent data for the methanogenic laboratory scale completely mixed anaerobic digesters operated by Ristow *et al.* (2004).

Ret. Time days	Effluent total COD mgCOD/ℓ	Effluent total soluble COD mgCOD/ℓ	Effluent VFA mgCOD/ℓ as HAc	Effluent FSA mgN/ℓ	Effluent Alk mg/ℓ as $CaCO_3$	pH	Methane Volume l/d	Gas Comp. % Methane	COD Bal. %	N Bal %
60	3590	88	5	101	775	6.74	0.78	66.51	100.0	103.0
20	10525	179	11	231	1577	6.89	5.41	63.11	96.0	107.5
15	16972	250	28	347	2446	6.98	12.12	61.40	103.4	86.9
15	10212	157	17	212	1539	6.85	7.71	63.08	98.6	108.3
15	5751	97	6	114	845	6.80	3.95	63.26	100.1	116.4
10	18085	256	27	260	2362	6.92	17.33	62.73	103.4	78.3
10	10849	178	24	208	2424	7.00	10.69	63.24	110.3	107.5
10	6249	108	8	127	854	6.69	5.00	60.98	97.2	92.2
10	905	32	0	19	170	6.59	0.62	53.20	88.4	92.8
8	15094	205	22	258	1868	6.90	19.39	58.85	102.7	84.5
8	11299	168	21	186	1394	6.80	10.94	63.24	99.6	113.3
8	6299	104	7	112	863	6.78	6.40	63.06	98.8	43.7
8	892	51	10	15	144	6.38	0.84	59.30	91.9	83.5
6.67	14984	207	12	255	1821	6.83	22.71	59.32	100.9	75.1
6.67	12595	200	19	196	1504	6.86	11.66	60.98	102.6	94.6
6.67	5944	96	5	104	789	6.57	8.74	60.95	100.9	81.9
5.71	19737	295	26	183	1612	6.75	30.32	63.76	103.3	81.8
5.71	12729	205	32	200	1463	6.93	13.24	61.67	101.4	93.2
5.71	6757	120	19	63	564	6.45	9.23	65.70	104.5	81.7
5	12610	301	87	193	1359	6.78	13.57	65.70	96.0	74.1

4.8.3 Modelling the Ristow *et al.* (2004a) Methanogenic Laboratory Scale Completely Mixed Anaerobic Digesters

The data listed in Table 4.9, together with the unbiodegradable particulate and soluble fractions, the operating temperature of the digesters and the hydrolysis rate constants are required as input to the anaerobic model. Ristow *et al.* (2004a) concluded that the first order kinetics and surface mediated reaction kinetics most accurately predict the rate of primary sewage sludge hydrolysis under methanogenic conditions for all hydraulic retention times and feed COD concentrations. They concluded that since first order kinetics are (i) a simplification of the hydrolysis process (ii) do not explicitly include the acidogenic biomass and (iii) does not set an upper limit to the rate, surface mediated reaction kinetics are the most appropriate rate formulation to model primary sewage sludge hydrolysis. Ristow *et al.* (2004a) found the $k_{max,HYD}$ and $K_{SS,HYD}$ rate constants for the surface mediated reaction kinetics for their methanogenic systems to be 12.32 mol S_{bp}/(mol Z_{AD}.d) and 14.30 mol S_{bp}/mol Z_{AD}. These are higher than the values calculated for the data of Izzett *et al.* (1992) above ($k_{max,HYD}$ = 6.797 mol S_{bp}/(mol Z_{AD}.d) and $K_{SS,HYD}$ = 10.829 mol S_{bp}/mol Z_{AD}), which is reasonable, because the influent sludge used by Izzett *et al.* (1992) was a mixture of primary sewage and humus sludges, while Ristow *et al.* (2004a) used pure primary sewage sludge. It was therefore decided to use the hydrolysis rate constants for the surface mediated reaction kinetics calculated by Ristow *et al.* (2004a) to model their methanogenic anaerobic digesters.

Figures 4.13 (for feed concentrations 9 to 13 gCOD/ℓ), 4.14 (for feed concentrations 24 to 26 gCOD/ℓ) and 4.15 (for feed concentrations 34 to 42 gCOD/ℓ) show the results simulated by the anaerobic model, together with the experimental results measured by Ristow *et al.* (2004a).

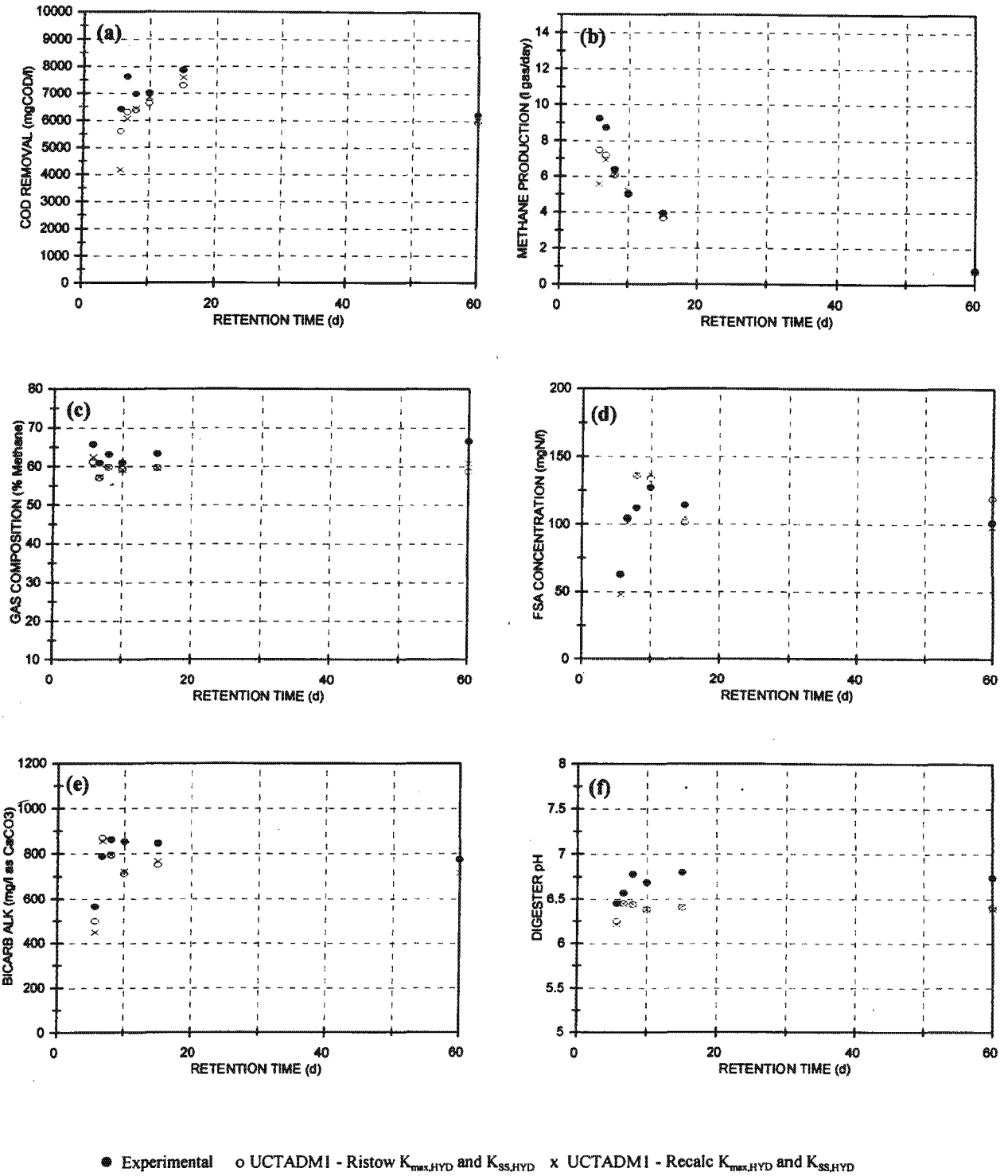

Fig 4.13: Comparison between kinetic simulation model (UCTADM1) predicted and measured (a) COD removal, (b) gas production, (c) gas composition, (d) free and saline ammonia, (e) $H_2CO_3^*$ alkalinity and (f) digester pH versus retention time for the Ristow *et al.* (2004a) data set for feed COD concentrations between 9 and 13 gCOD/ℓ.

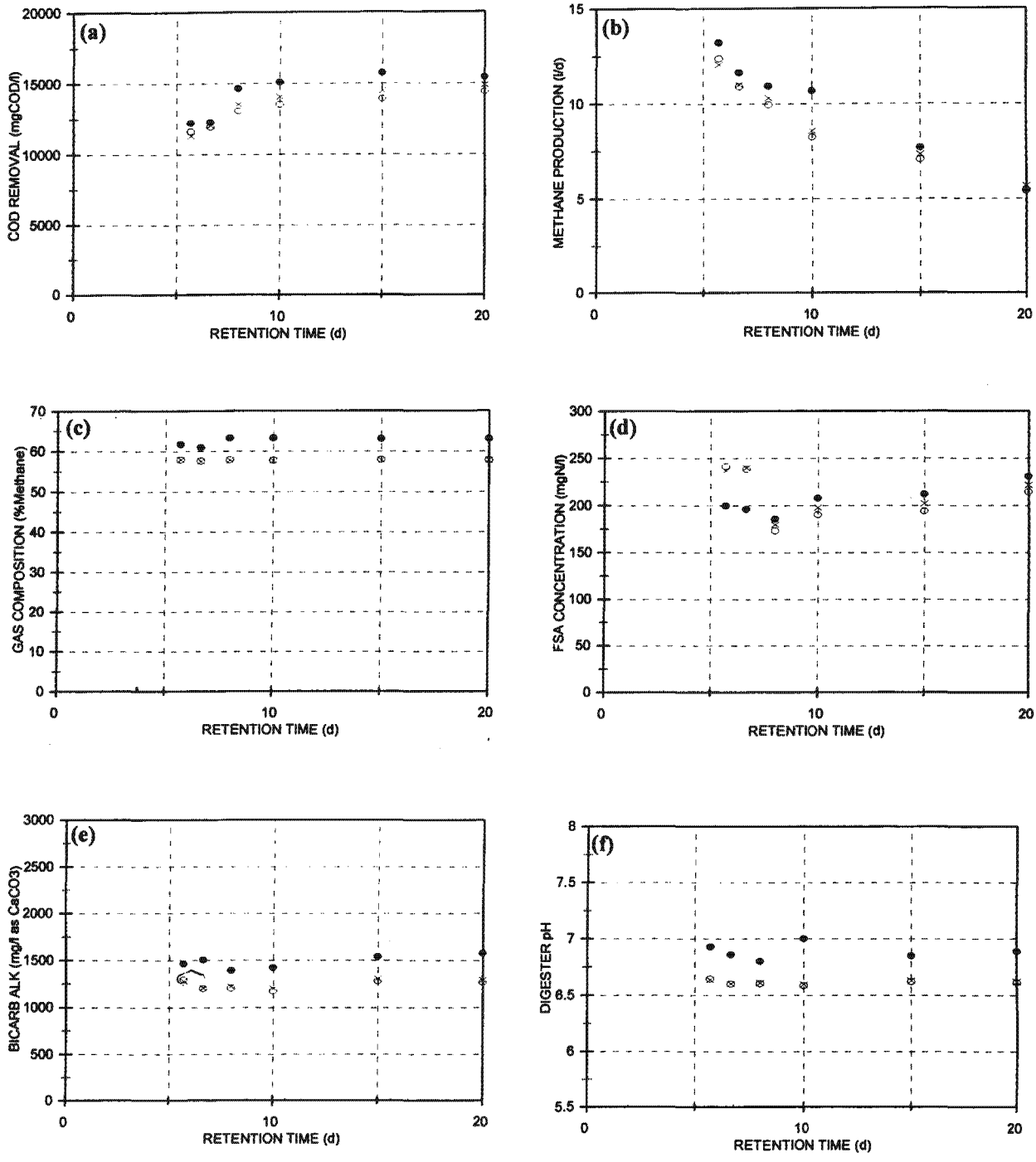

Fig 4.14: Comparison between kinetic simulation model (UCTADM1) predicted and measured (a) COD removal, (b) gas production, (c) gas composition, (d) free and saline ammonia, (e) $H_2CO_3^*$ alkalinity and (f) digester pH versus retention time for the Ristow *et al.* (2004a) data set for feed COD concentrations between 24 and 26 gCOD/*ℓ*.

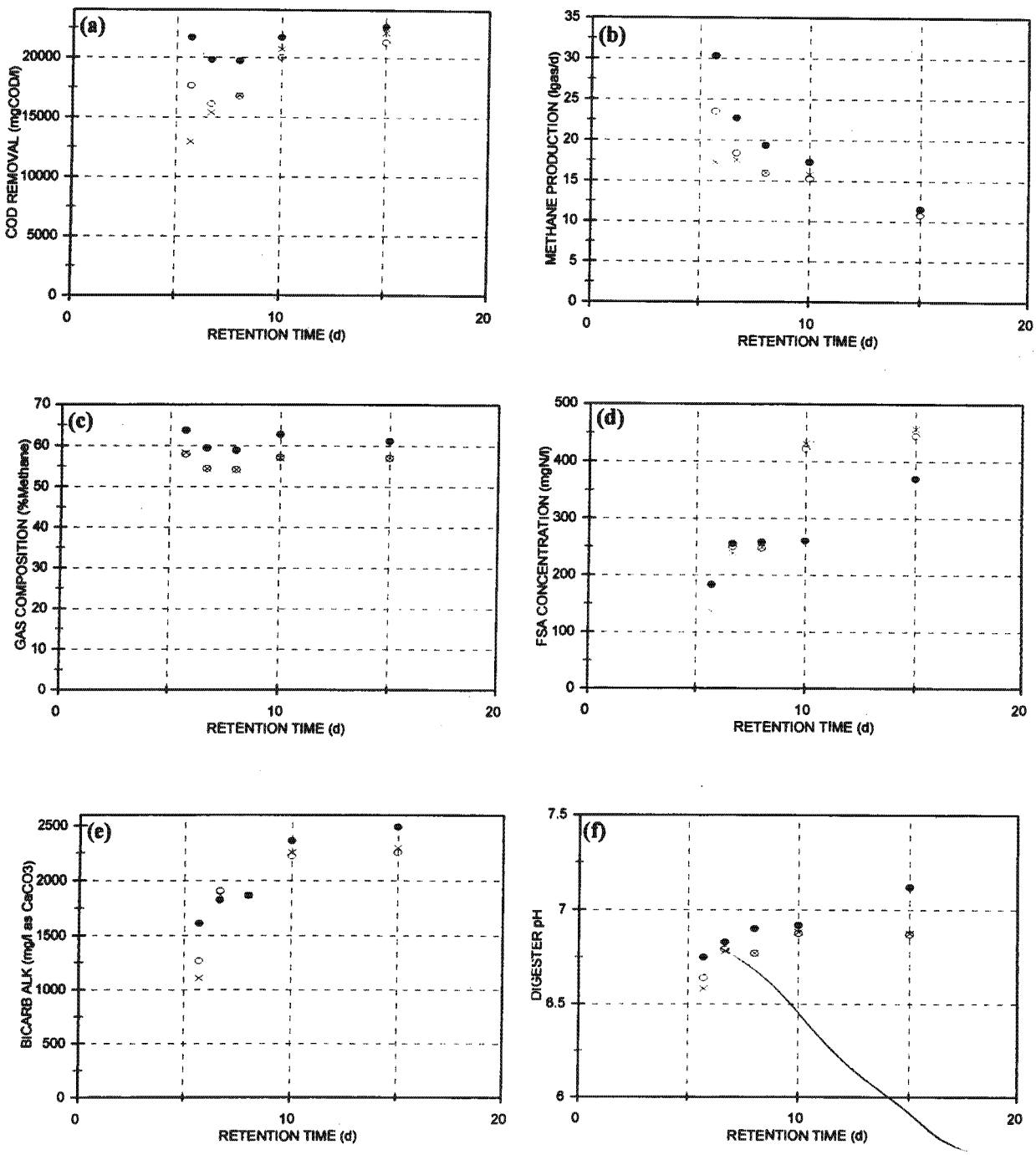

Fig 4.15: Comparison between kinetic simulation model (UCTADM1) predicted and measured (a) COD removal, (b) gas production, (c) gas composition, (d) free and saline ammonia, (e) $H_2CO_3^*$ alkalinity and (f) digester pH versus retention time for the Ristow *et al.* (2004a) data set for feed COD concentrations between 34 and 42 gCOD/ℓ.

In Figures 4.13, 4.14 and 4.15 the solid circles represent the experimental data measured by Ristow *et al.* (2004a) and the open circles show the anaerobic model predictions using the hydrolysis rate constants calculated by Ristow *et al.* (2004a). The crosses show the anaerobic model predictions using recalculated hydrolysis rate constants (see below); These will be discussed in 4.8.4 below.

Comparing the COD removal measured by Ristow *et al.* (2004a) with the predictions by UCTADM1 using the hydrolysis rate constants calculated by Ristow *et al.* (2004a) (Figs. 4.13a, 4.14a and 4.15a) it can be seen that for the systems receiving low feed COD concentrations (9 to 13 g COD/ℓ) and high feed COD concentrations (34 to 42 gCOD/ℓ) the simulated results for the higher sludge ages (>= 10d) compare well, with the simulated COD removal always lower than the experimental COD removal. For the lower sludge ages (< 10d) the simulated COD removals correspond less well, being significantly lower than the experimental results in some cases. This worsening correlation between simulated and measured COD removal at the low sludge ages is thought to be a result of a combination of (i) the hydrolysis rate constants chosen by Ristow *et al.* (2004a) and (ii) the experimental outliers mentioned by Ristow *et al.* (2004a). The hydrolysis rate constants are considered further in 4.8.4 below. For the systems with an influent COD concentration between 24 and 26 COD/ℓ, the simulated and measured COD removals correspond well throughout the range of sludge ages, with the simulated COD removals under predicted, as was the case for the other feed COD concentrations.

The simulated and measured methane production (Figs. 4.13b, 4.14b and 4.15b) mirror the COD removal, which is expected, because the methane production is proportional to the COD removal. For the low and high feed COD concentration and low (<10d) sludge ages, the simulated methane production is substantially lower than the experimental methane production, but this is a direct consequence of the lower COD removal mentioned above. The simulated methane production for the higher sludge ages (>= 10d) corresponds well with the measured methane production, with the simulated results always lower than the measured values, as for the COD removal. For the influent COD concentrations between 24 and 26 gCOD/ℓ the simulated methane productions correspond closely to the measured values for all sludge ages, except for the 10 day system, however, this 10 day system has the poorest COD balance (110%, see Table 4.10), which explains why it is an outlier here. The simulated and measured gas compositions (Figs. 4.13c, 4.14c and 4.15c) correspond equally well for all feed COD concentrations and sludge ages, but the simulated gas compositions are consistently lower than those measured by Ristow *et al.* (2004a). This results from a combination of factors, namely (i) the lower COD removals predicted by UCTADM1, (ii) and the resulting lower methane production, (iii) the measured and calculated influent sludge stoichiometric formulae and (iv) the estimated influent pH and alkalinity parameters (that were not measured by Ristow *et al.*, 2004a). It may however also indicate that in UCTADM1 less CO_2 is expelled, which would show in lower simulated bulk liquid pH values. In the comparison of the experimental and simulated Izzett *et al.* (1992) data, the simulated and measured gas compositions corresponded more closely, but that may merely indicate that the Izzett *et al.* (1992) data is of better quality.

The measured and simulated effluent FSA concentrations (Figs. 4.13d, 4.14d and 4.15d) again mirror the COD removal, the lower retention times effluent FSA corresponding less well with the measured values. This is again mainly due to the fact of the lower COD removal in these cases, lower COD removal equating to less biodegradable particulate organics hydrolysed and therefore less organic N released as FSA. In some cases the predicted effluent FSA is substantially higher than the measured values (e.g. 5.71 and 6.67 day systems for 24 to 26 gCOD/ℓ feed COD concentrations and 10 and 15 day systems for 34 to 42 gCOD/ℓ feed COD concentrations), however these all correspond to the systems with the lowest N balances (81.7, 81.9 and 78.3 and 85.5% respectively, see Table 4.10) which explains why the predicted effluent FSA is so much higher than the measured values for these cases.

The measured and predicted alkalinities (Figs. 4.13e, 4.14e and 4.15e) correspond better than the alkalinities in the comparison of the experimental and simulated Izzett *et al.* (1992) data. The simulated alkalinities are all lower than the measured values, with the difference between the simulated and measured values worsening at lower sludge ages. However, this is expected, because these are the systems with the markedly lower COD reduction, which in part explains the greater difference in simulated and measured COD values. Also, the influent alkalinity and pH values were estimated, because they were not directly measured by Ristow *et al.* (2004a). Had more accurate influent and alkalinity data been available, the simulated effluent alkalinity results would most likely have corresponded even better to the measured values. The simulated and measured pH values (Figs. 4.13f, 4.14f and 4.15f) correspond in the same way as those from the comparison of the simulated and measured data of Izzett *et al.* (1992) above. The simulated pH's are all lower than the measured values. For the data of Ristow *et al.* (2004a), the influent pH values were estimated, which will have had an effect on the simulated values. Further, the simulated alkalinities are all lower and less CO_2 was expelled in the simulations, which also had an effect on the pH values. However, the trend of lower simulated pH values observed with the data of Izzett *et al.* (1992) clearly also applies here.

Considering (i) that the influent alkalinity and pH values were estimated, (ii) the low N mass balances of the Ristow *et al.* (2004a) data and (iii) the experimental outliers, the simulated data as a whole compares reasonably well with the experimental results of Ristow *et al.* (2004a) and provides further validation of the UCTADM1 anaerobic model developed in this Chapter.

4.8.4 The Hydrolysis Rate Constants

The above comparison indicates that the hydrolysis rate constants calculated by Ristow *et al.* (2004a)($k_{max,HYD}$ and $K_{SS,HYD}$ rate constants for the surface mediated reaction kinetics for the methanogenic experimental systems of 12.32 mol S_{bp}/(mol Z_{AD}.d) and 14.30 mol S_{bp}/mol Z_{AD}) seem not to describe the lower sludge age experimental systems very well and may require re-calibration.

Figure 4.16 shows the hydrolysis rate vs the biodegradable COD/acidogen ratio for the methanogenic systems of Ristow *et al.* (2004a) for the surface mediated reaction kinetics. The data (each laboratory scale system) is represented by a solid dot (•) or a cross (X). The crosses show the five systems that Ristow *et al.* (2004a) used to calculate their hydrolysis rate constants ('Ristow' on the graph, see Ristow *et al.*, 2004a for details). The lines represent the hydrolysis rate constants calculated by the Lineweaver-Burke (L-B), Double-reciprocal (DR) and Eadie-Hofstee (E-H) and the average of all three methods (Avg) with all the data points (excluding the 60 day system) as was done above for the Izzett *et al.* (1992) data set. All concentrations are in COD units.

From Fig. 4.16 it can be seen that there is appreciable scatter in the experimental data, with two discernable bands of data, one higher band lying above the other. This shows that obtaining good estimates of the hydrolysis rate constants from this experimental data is difficult. Ristow *et al.* (2004a) chose the five systems (crosses on Fig. 4.16) for their hydrolysis rate constant estimation, because they represent the five systems with the lowest sludge ages. They reasoned that the low sludge ages dictate the hydrolysis rate constants, and therefore chose the sludge ages below 8d, without outliers, to calculate their hydrolysis rate constants. However, from the comparison of measured and simulated results above, those low sludge ages are the sludge ages where the simulated results deviate the furthest from the measured results.

The hydrolysis rate constants calculated from the Lineweaver-Burke, Double-reciprocal and Eadie-Hofstee methods ($k_{max,HYD}$ and $K_{SS,HYD}$ of 1.63 S_{bp}/(Z_{AD}.d) and 0.057 S_{bp}/Z_{AD}, 2.43 S_{bp}/(Z_{AD}.d) and 0.736

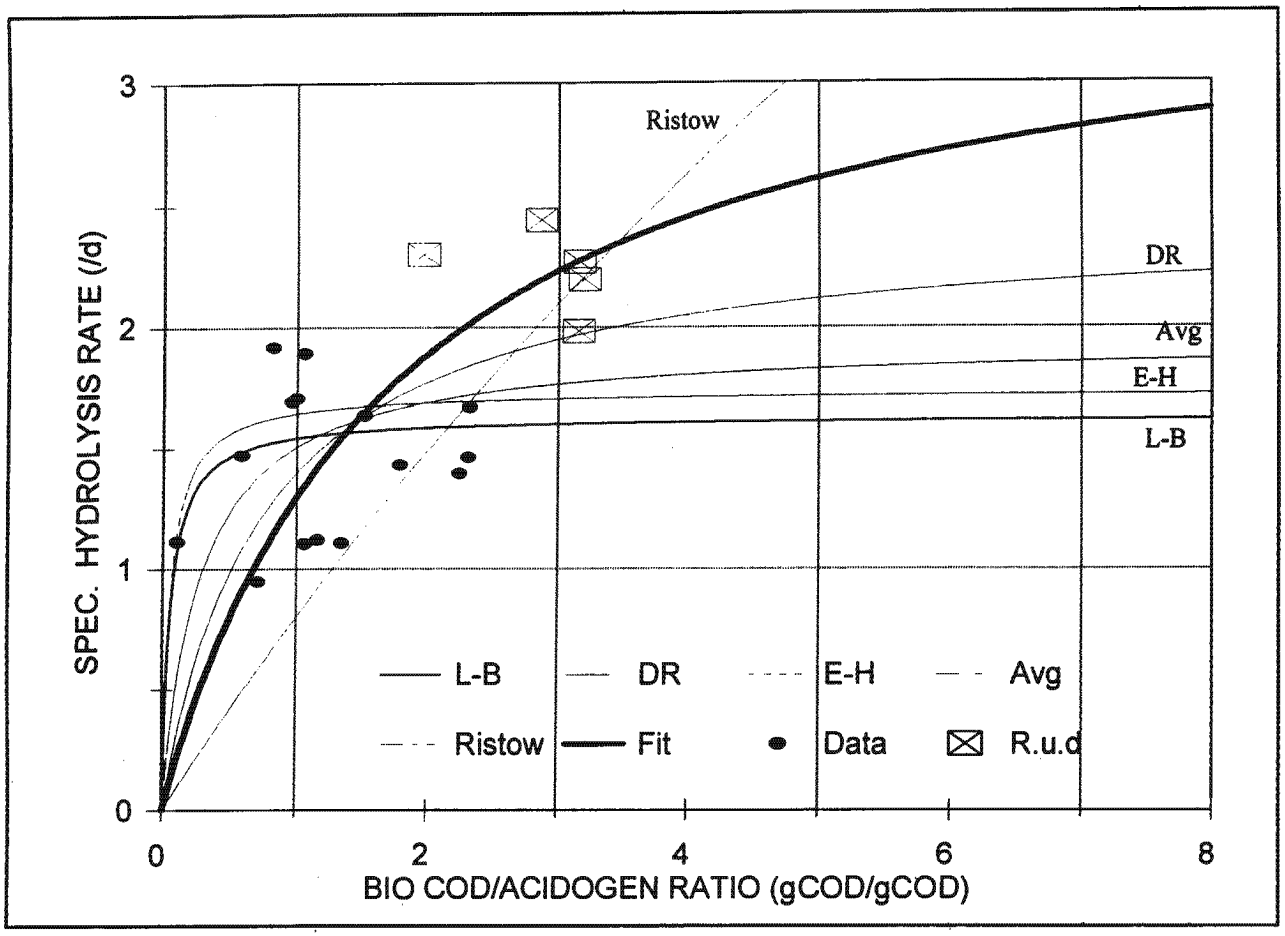

Fig. 4.16: Specific hydrolysis rate vs. biodegradable COD/acidogen ratio for the methanogenic laboratory scale completely mixed anaerobic digesters of Ristow *et al.* (2004a).

S_{bp}/Z_{AD}, 1.74 $S_{bp}/(Z_{AD}.d)$ and 0.055 S_{bp}/Z_{AD} respectively, all in COD units) seem very low, and therefore it seems that for this data set, there is too much scatter to obtain a reasonable estimate of the hydrolysis rate constants by this method. A further set of hydrolysis rate constants were obtained by fitting a line through the data by eye ('Fit' on Fig. 4.16). This resulted in the following hydrolysis rate constants: $k_{max,HYD} = 3.5\ S_{bp}/(Z_{AD}.d)$ and $K_{SS,HYD} = 1.7\ S_{bp}/Z_{AD}$ in COD units.

The Ristow *et al.* (2004a) methanogenic systems were simulated again, with the hydrolysis rate constants obtained by the fit, converted to mole units. The results are shown on Figs. 4.13, 4.14 and 4.15 as crosses. From Figs. 4.13, 4.14 and 4.15 it can be seen that this change improved the simulated results marginally for the higher sludge ages, but exacerbated the bad correlations for the low sludge ages, showing that the hydrolysis rate values chosen by Ristow *et al.* (2004a) give a better fit for the lower sludge ages.

From Fig. 4.16 it can be seen that because of the amount of scatter in the experimental data, many different lines could be fitted and as a result many different combinations of hydrolysis rate constants could be calculated. To obtain a few other hydrolysis rate constant combinations, the data were grouped by (i) influent COD concentration and (ii) sludge age, and the hydrolysis rate constants recalculated for each group. Simulations with these recalculated hydrolysis rate constants were performed, but no discernible improvement was achieved; The results for the low sludge age systems would either marginally improve or deteriorate, with an opposite but equally small deterioration or improvement for

the simulated results of the higher sludge age systems. It therefore seems reasonable to assume that given the scatter in the experimental data (see Fig. 4.16), the hydrolysis rate constants calculated by Ristow *et al.* (2004a) are as good as any other combination that can be obtained from their methanogenic data set.

4.9 MODELLING DIGESTER FAILURE

The model applications above are all to stable anaerobic digesters operating at steady state. Under such conditions the rate limiting process is the hydrolysis, so that the other processes are essentially stoichiometric. This precluded assessment of the ability of the model to predict dynamic variations (except for hydrolysis). Very little quantitative information is available in the literature on the dynamics of anaerobic digestion. Accordingly, a theoretical simulation exercise was undertaken to evaluate dynamics, namely anaerobic digester failure. Acetoclastic methanogens are probably the most sensitive organisms in anaerobic digesters (Gujer and Zehnder, 1983) and so are strongly influenced by their surrounding environment. It is commonly accepted that failure of anaerobic digesters usually starts with the inhibition of acetoclastic methanogens. This can happen by an inhibitor or toxin in the influent, a shock load on the digester and/or a sudden drop in temperature because the acetoclastic methanogens (e.g. *Methanothrix soehngenii)* have been reported to show extreme temperature sensitivity (Zehnder *et al.*, 1980). Any of these factors will slow down or inhibit the growth rate of the acetoclastic methanogens, resulting in an increase in acetic acid concentration in the digester. This increase causes a decrease in pH. Both acetoclastic methanogens and hydrogenotrophic methanogens (e.g. *Methanobrevibacter arboriphilus*) are pH sensitive, the latter also showing some sensitivity to temperature changes. Thus, the drop in pH will slow down their rates of growth, resulting in a further increase in acetic acid and an increase in hydrogen partial pressure p_{H2}. The increase in p_{H2} affects the acidogenesis process as described above (Eqs 4.17 and 4.18) and instead of producing only acetic acid, also produce propionic acid. The increase in p_{H2} also slows the acetogenesis process (Eq 4.19) so that the propionic acid concentration increases, causing a further decrease in pH. Clearly, anaerobic digestion is a poised system and even a small disturbance in one of the methanogenic processes causes irreversible system collapse. Such a collapse, called digester souring, is characterized by increases in acetic and propionic acid concentrations and hydrogen partial pressure and decreases in pH and gas production. The digester pH should not drop below 6.6 to maintain methanogenesis processes uninhibited by pH (Moosbrugger *et al.*, 1993). The AD kinetic model was extended to include the above failure condition.

4.9.1 Inhibition of Acetoclastic Methanogens (Process 7)

These organisms are inhibited by the hydrogen ion concentration (pH). To include this, the inhibition term commonly used with Monod kinetics of $(1+ I/K_I)$, where I is the aqueous inhibitor compound concentration and K_I the concentration at which the growth rate is half the normal rate (Batstone *et al.*, 2002), was introduced into the growth rate equation (Eq 4.20) i.e.:

$$r_{Z_{AM}} = \frac{\mu_{max,AM}\,[HAc]}{\left(K_{S,AM} + [HAc]\right)\left(1+\frac{[H^+]}{K_{I,AM}}\right)}\,[Z_{AM}] \qquad (4.45)$$

where:

$K_{I,AM}$ = Inhibition constant i.e. the hydrogen ion concentration at which the growth of acetoclastic methanogens is half the normal rate (mol/ℓ)

$[H^+]$ = Hydrogen ion concentration (mol/ℓ) from which pH = -log (H^+)

4.9.2 Inhibition of Hydrogenotrophic Methanogens (Process 9)

Hydrogenotrophic methanogens function to keep the hydrogen partial pressure p_{H2} low, and like the acetoclastic methanogens, they are also neutrophiles and are inhibited at pH values below 6.6 (Gujer and Zehnder, 1983, Zehnder and Wuhrmann, 1977). Hence, an inhibition term was also introduced into the growth rate equation for this organism group (Eq 4.21) i.e.:

$$r_{Z_{HM}} = \frac{\mu_{max,HM}\,[H_2]}{\left(K_{S,HM} + [H_2]\right)\left(1 + \frac{[H^+]}{K_{I,HM}}\right)}\,[Z_{HM}] \qquad (4.46)$$

4.9.3 Inhibition of Acetogens (Process 5)

Due to the thermodynamics of the acetogenic process, the growth of acetogens decreases when the hydrogen partial pressure p_{H2} increases. This reduces the rate of propionic acid conversion to acetic acid and hydrogen. This reduction in growth rate at elevated p_{H2} has already been included in the acetogen growth process (Eq 4.19). The inhibition constants for the above are listed in Table 4.11.

Table 4.11: Inhibition constants for the different organism groups in anaerobic digestion.

Organism group	Process	Compound	Symbol	Value	Units
Acetoclastic methanogens	D7	Hydrogen ion	$K_{I,AM}$	1.15×10^{-6}	mol/ℓ
Hydrogenotrophic methanogens	D9	Hydrogen ion	$K_{I,HM}$	530×10^{-6}	mol/ℓ
Acetogens	D5	Hydrogen gas	$K_{I,AC}$	0.45×10^{-6}	mol/ℓ

4.9.4 Gas Expulsion from Aqueous to Head Space Gas Phases

In the implementation above of the kinetic model in AQUASIM, the exchange of gases between the aqueous and gas (head-space) phases was not specifically modelled; The dissolved and non-dissolved gases were accepted to be part of the bulk liquid and hence flow out of the digester with the effluent, which is equivalent to a zero volume head-space. For steady state conditions this is acceptable, because the molar gas composition remains constant with time. Under digester failure conditions, the molar composition of the gas phase may not remain constant with time and hence have an influence on the dissolved gas concentrations. To ensure a more realistic AD system under failure conditions, a head-space compartment was added to the model in AQUASIM, with a diffusive link to the reactor aqueous phase. The dissolved gaseous compounds CO_2 (as $H_2CO_3^*$), CH_4 and H_2 diffuse from the aqueous phase to the gas phase in the head-space, in accordance with the usual diffusion gas exchange equations (Batstone *et al.*, 2002), i.e. the gas exchange equations are applied across the diffusive link. In such an implementation, due cognizance must be taken of the different forms of the Henry's law constant and its dimensions. In AQUASIM, the diffusive link is modelled as:

$$r_{gas} = K_{La\,gas}\left(K_{c\,gas}C_{hsgas} - C_{disgas}\right) \qquad \text{mol gas/d} \qquad (4.47)$$

where:

r_{gas} = Rate of gas diffusion across head-space - bioreactor link
$K_{LA\ gas}$ = Specific gas mass transfer rate (/d)
K_{cgas} = Constant for the phase change from liquid to gas
= K_{Hgas} or $1/K_{Hgas}$ depending on the form of the Henry's law constant
K_{Hgas} = *Dimensionless* Henry's law constant for the gas
C_{disgas} = Dissolved (aqueous) gas concentration in reactor liquid (mol/ℓ)
C_{hsgas} = Concentration of gas in the headspace (mol/ℓ)
p_{gas} = Partial pressure of the gas
= $C_{hsgas} \times RT_k$
R = Universal gas constant = 8.206×10^{-2} (ℓ.atm)/(mol.K)
T_k = Temperature in Kelvin = (T in °C +273).

In modeling this gas exchange ammonia was omitted, because with its high pK value (9.1), negligibly little diffuses into the gas phase for pH < 8. The partial pressure of the three gases were calculated from the head-space gas concentrations (C_{hsgas}) using Dalton's law of partial pressures ($p_{gas} = [C_{hsgas}]\ RT$) and the total gas pressure in head-space (P_{tot}) is sum of the partial pressures. The vent gas flow rate from the head-space (q_{gas}) was calculated from a proportional control loop with respect to atmospheric pressure (P_{atm}), which was accepted to be 101.3 kPa, viz.

$$q_{gas} = K_p \frac{(P_{tot} - P_{atm})}{P_{atm}} V_h \quad \ell/d \tag{4.48}$$

where:

K_p = Gas vent rate constant (/d)
V_h = Volume of head space (1ℓ for Izzett *et al.* digesters)

One constant in Eq 4.47 has an important influence on the dynamics of the head-space gas concentrations, i.e. the specific gas mass transfer rate ($K_{La\ gas}$). If this rate is very rapid, then the head-space concentrations respond very quickly to the dissolved gas concentrations. The actual rate would be situation specific, depending on the mixing regime in the anaerobic digester, and would be faster with gas recirculation mixing than with mechanical mixing. Since no guidance in the literature could be found for this value, a fast rate of 1000 /d was selected for all $K_{La\ gas}$ so that the head-space gas concentrations rapidly respond to the dissolved gas concentrations. To provide a sense of the magnitude of this value, Musvoto *et al.* (2000a) observed K_{La} values between 200 and 600 /d for CO_2 stripping in their anaerobic digester liquor aeration batch tests. The value for this constant requires further investigation.

4.9.5 Simulating Digester Failure

With the model set up as described, digester failure was simulated by halving the maximum specific growth rate of the acetoclastic methanogens ($\mu_{max,AM}$) for three days (72h) in the middle of a 60 day simulation. The anaerobic digester at 15d retention time in Table 4.6 was simulated for sufficient time to ensure steady state - very low effluent SCFA concentrations and hydrogen partial pressure were obtained and the pH was about 6.9. Failure was then artificially induced by temporarily halving the $\mu_{max,AM}$ value for the period of 3 days, and thereafter restoring it to its original value.

Immediately after halving $\mu_{max,AM}$, the acetic acid concentration increased sharply to reach a maximum of 0.14 mol/ℓ (8 400 mgHAc/ℓ) after 15h. This increase caused the pH to decrease from 6.9 to 4.5 in 4h.

The reduction in pH caused (i) the acetoclastic methanogen growth rate to reduce further, contributing to the sharp increase in acetic acid concentration and (ii) the hydrogenotrophic methanogen growth rate to reduce causing the hydrogen concentration to increase to a maximum of 0.00012 mol/ℓ (0.24 mgH_2/ℓ) after 22h. The increased H_2 concentration raised the p_{H2} which caused the acidogens to produce also propionic acid, which increased from a very low concentration at around 5h to a maximum concentration of 0.15 mol/ℓ (11 100 mgHPr/ℓ) at 55h. Immediately after halving $\mu_{max,AM}$ of the acetoclastic methanogens, their concentration decreased sharply to reach 10% of its initial value after 15h. The hydrogenotrophic methanogen organism concentration also decreased rapidly after about 4h to less than 10% of its initial value after 40h. Concomitantly with the decrease in methanogen biomass concentrations, the CO_2 and CH_4 gas production rates decreased rapidly, reaching 10% of their original rates at 20 and 28h respectively. Restoring the $\mu_{max,AM}$ of the acetoclastic methanogens to its original rate after 72h had no affect on the results indicating that the failure was irreversible. Also, simulating this digester failure situation with and without the head-space gas dynamics made negligibly little difference to the results.

This simulation of AD failure by halving temporarily the acetoclastic methanogen growth rate indicates that (i) the AD model correctly reflects the qualitatively observed digester failure behaviour and (ii) even a short (3 days) inhibition of these species causes irreversible failure (pH<5.5) within 4h. The % decrease in acetoclastic methanogen growth rate from which the digester can recover without intervention was not determined. Because the conceptual AD model (Fig 4.3) is similar to that developed for UASB digesters (Sam-Soon *et al.*, 1991), the simulation model shows the same progression to failure as the lower bed volume of an upflow anaerobic sludge bed (UASB) digester, except that in the UASB system, collapse of the methanogens does not take place because the pH is maintained above 6.6 in the high SCFA concentration region (Moosbrugger *et al.*, 1993). From the UASB digester behaviour and practical experience, anaerobic digestion failure due to a reduction in methanogen activity can be averted if the pH can be maintained above 6.6. This may require dosing lime which needs to be carefully controlled to avoid calcium carbonate precipitation (Capri and Marais, 1974). Digester failure and recovery is a dynamic modelling problem and will be examined in further research.

4.10 CLOSURE

An integrated two phase (aqueous-gas) mixed weak acid/base chemistry and biological processes anaerobic digester kinetic model for sewage sludge is presented. The salient features of this model are:

(i) As an alternative to characterizing the sewage sludge feed into carbohydrates, proteins and lipids, as is done in IWA ADM1 (Batstone *et al.*, 2002), it is characterized in terms of total COD, its particulate unbiodegradable COD fraction (f_{PSup}), the short chain fatty acid (SCFA) COD and the CHON content of the particulate organics, i.e. X, Y, Z and A in $C_XH_YO_ZN_A$. This approach characterizes the sludge in terms of measurable parameters and allows COD, C and N mass balances to be set up over the anaerobic digestion system. With this approach, the interactions between the biological processes and weak acid/base chemistry could be correctly predicted for stable steady state operation of anaerobic digesters. While not validated for dynamic flow and load conditions, the model has the capability of being applied to such conditions.

(ii) The COD, C and N mass balances and continuity basis of the model fixes quantitatively, via the interrelated chemical, physical and biological processes, the relationship between all the compounds of the system so that for a given biodegradation the digester outputs (i.e. effluent COD, TKN, FSA, SCFA, $H_2CO_3^*$ Alk, pH, gaseous CO_2 and CH_4 production and partial

pressures) are governed completely by the input sludge (and aqueous) characteristics. All the kinetic and stoichiometric constants in the model, except those for hydrolysis, were obtained from the literature so that model calibration reduced to determining (i) the unbiodegradable particulate COD fraction of the sewage sludge (f_{PSup}), (ii) the hydrolysis kinetics formulation and associated constants and (iii) the sewage sludge CHON composition, i.e. the X, Y, Z and A values in $C_XH_YO_ZN_A$.

(iii) Interactively with determining the hydrolysis kinetics ((4) below), the unbiodegradable particulate fraction of the sewage sludge was estimated at 0.32 - 0.36 for the sewage sludge fed to the mesophilic anaerobic digesters of Izzett *et al.* (1992) ranging over 7 - 20 days retention time, depending on the type of hydrolysis kinetics selected. These values are very close to the values of 0.36 determined by O'Rourke (1968) and 0.33 by Ristow *et al.* (2004), and estimated from a COD mass balance around the primary settling tank from typical raw and settled wastewater characteristics (0.32 - 0.36 for COD removals of 40 - 35%).

(iv) Various formulations for the hydrolysis rate of sewage sludge particulate biodegradable organics were evaluated, see below. Surface mediated reaction (Contois) kinetics similar to that used by Dold *et al.* (1980) and IWA Activated Sludge Model 1 (Henze *et al.*, 1987) for slowly biodegradable organics in activated sludge systems, were selected. Once calibrated against the Izzett *et al.* (1992) data, this formulation showed the required sensitivity of gas production and unfiltered effluent COD concentration to variation in retention time, without changing the constants in the hydrolysis rate equation. In their study, Ristow *et al.* (2004a) also concluded that the surface reaction kinetics most accurately predict the rate of primary sewage sludge under methanogenic conditions for all hydraulic retention times and feed COD concentrations of their experimental methanogenic anaerobic digesters, further justifying the selection of surface mediated reaction (Contois) kinetics to describe the hydrolysis rate of sewage sludge particulate biodegradable organics for the UCTADM1 model.

(v) From the influent COD, organic N and VSS measurements of Izzett *et al.*, the stoichiometric formulation of the influent sewage sludge was estimated to be $C_{3.4}H_7O_2N_{0.192}$. With the sludge biodegradability and hydrolysis process rate defined, to match the anaerobic digester performance data of Izzett *et al.* (1992) ranging over 7 - 20 days retention time, (i.e. effluent COD, TKN, FSA, SCFA, $H_2CO_3^*$, Alk, pH, gaseous CO_2 and CH_4 production and partial pressures), the sewage sludge composition was refined to $C_{3.5}H_7O_2N_{0.196}$ to conform to the COD, C and N mass balances of the model. This formulation was confirmed with primary sludge CHON composition tests, the average of which was $C_{3.65}H_7O_{1.97}N_{0.19}$. The model predicted CHON content and molar mass of the PS was therefore 95.9%, 100%, 98.5%, 94.5% and 98.7% of the measured values. This provides persuasive validation of the UCTADM1 model. For the Ristow *et al.* (2004a) data, the sewage sludge formulation was not estimated because the CHON composition test results were used directly to further validate the model. The average sewage sludge formulation for the Ristow *et al.* (2004a) 'pure' primary sludge feed was $C_{4.17}H_7O_{2.63}N_{0.22}$. The C, O and N content of this 'pure' primary sludge is higher than that of the Izzett *et al.* (1992) feed, however they used a mixture of primary and humus sludge and hence a minor difference in composition is not unexpected.

(vi) Validation of the AD model under steady state conditions validates only its stoichiometry and the system rate limiting process, which is hydrolysis. However, the model, which includes the influence of high hydrogen partial pressure on the acidogenesis and acetogenesis processes, showed the expected sensitivity to a digester upset initiated by temporary inhibition of the acetoclastic methanogens, which is the usual cause in practise. The model demonstrated that even a brief inhibition of this organism group causes an irreversible failure of the digester (pH < 6.6).

The proposed surface mediated reaction (or Contois kinetic) hydrolysis rate equation reproduced the observed change in biodegradable particulate COD acidified versus retention time with the same kinetic constants. Based on the Izzett *et al.* anaerobic digester data, a Monod type hydrolysis rate equation also showed consistency of constants over 7 to 20 d retention time, but simple first order and first order specific hydrolysis rate equations yielded different rate constants at different retention times. However, by changing the unbiodegradable particulate COD fraction of the sewage sludge (f_{PSup}) the fit of both the first order and first order specific hydrolysis rate equations to the experimental data of Izzett *et al.* (1992) could be significantly improved (with concomitant deterioration in the fit with Contois and Monod kinetics). In their study, Ristow *et al.* (2004a) concluded that the first order kinetics and surface reaction kinetics most accurately predict the rate of primary sewage sludge under methanogenic conditions for all hydraulic retention times and feed COD concentrations of their experimental methanogenic anaerobic digesters. Modelling the Ristow *et al.* (2004a) experimental data with their unbiodegradable particulate COD fraction and hydrolysis rate constants and a surface mediated reaction (or Contois kinetic) hydrolysis rate equation resulted in a reasonable correlation between the experimental and simulated data. However, because of considerable scatter in the Ristow *et al.* (2004a) experimental data, it proved difficult to derive hydrolysis rate constants that would result in a better fit of the experimental and simulated data. Hence, the Izzet *et al.* anaerobic digester data set is too limited and the Ristow *et al.* (2004a) data too variable to make a definitive conclusion as to which is the best equation to model the hydrolysis process, and what the best value for f_{PSup} is. Intuitively and based on its widespread application in activated sludge systems acting on the same biodegradable particulates, the surface mediated reaction (Contois) kinetics has been selected for hydrolysis.

The characterisation of sewage sludge in terms of its CHON(P) contents appears a sound approach. While testing primary sludges for the UCTADM1 model validation, a range of other sewage sludges were also tested, such as waste activated, anaerobic digested and mixtures of primary and waste activated. From the tests done to date, it seems that the CHON contents of sludges are consistent and grouped approximately in conformity with type. It appears likely, therefore, that typical CHON(P) contents of the different sludges may be selected, and that the standard characterisation tests such as COD, TKN and VSS, are sufficiently discerning and accurate for modelling AD of sewage sludges. Measurement of sewage sludge composition is continuing and its effect on digester pH and gas composition will be evaluated when more information has been collected.

The successful integration in a kinetic way of the two phase mixed weak acid/base chemistry and biological processes of AD has provided a sound basis for further model development. Still to be included in the AD model are mineral precipitation and the P content of sewage sludges. This will extend the model to digestion of biological excess P removal waste activated sludges and provide a direct and quantitative link between feed sludge composition and mineral precipitation problems in digesters.

The integrated physical, chemical and biological processes kinetic modelling approach, applied in this thesis project report to biological N removal activated sludge systems and anaerobic digesters, has opened the way to develop a kinetic simulation model for the entire wastewater treatment plant on a materials mass balance and continuity basis. The plant would comprise selected unit operations such as primary settling, biological N and/or P removal activated sludge and anaerobic or aerobic digestion of waste sludges. With such a model, the impact of wastewater characteristics and type and upstream unit operations performance on downstream unit operations, and the recycling of liquors from downstream unit operations to upstream unit operations, can be assessed for improved and more economical design and operation.

CHAPTER 5

A STEADY STATE MODEL FOR ANAEROBIC DIGESTION OF SEWAGE SLUDGES

5.1 INTRODUCTION

In Chapter 4, an integrated two phase (aqueous-gas) mixed weak acid base chemical, physical and biological processes kinetic model for anaerobic digestion (AD) of sewage sludge was developed. The COD, C and N mass balances and continuity basis of this model fixes quantitatively, via the interrelated chemical, physical and biological processes, the relationship between all the compounds of the system. Thus for a given sewage sludge COD removal, the digester outputs (i.e. effluent COD, TKN, FSA, SCFA, $H_2CO_3^*$ Alk, pH, gaseous CO_2 and CH_4 production and partial pressures) are governed completely by the input sludge solids (and dissolved) constituents. In this model, the sewage sludge feed is characterized in terms of total COD, its particulate unbiodegradable COD fraction ($f_{PS'up}$), the short chain fatty acid (SCFA) COD and the CHON content, i.e. X, Y, Z and A in $C_XH_YO_ZN_A$ of the particulate organics. This approach characterizes the sludge in terms of measurable parameters in conformity with the COD, C and N mass balances approach. With this approach, the interactions between the biological processes and weak acid/base chemistry could be correctly predicted for stable steady state operation of anaerobic digesters. While not validated for dynamic flow and load conditions, the model has the capability of being applied to such conditions. In this chapter this complex dynamic simulation model is simplified to a steady state one for integration into a steady state mass balance model of the whole wastewater treatment plant (see Chapter 2).

Steady state models are based on the slowest process kinetic rate that governs the overall behaviour of the system and relates this process rate to the system design and operating parameters. Therefore, steady state models allow the system design and operating parameters, such as reactor volume and recycle ratios, to be estimated reasonably simply and quickly from system performance criteria specified for the design, such as effluent quality. Once approximate design and operating parameters are known, these can serve as input to the more complex simulation models to investigate dynamic behaviour of the system and refine the design and operating parameters. A steady state AD model is therefore useful to (i) estimate retention time, reactor volume, gas production and composition for a required system performance like COD (or VSS) removal, (ii) investigate the sensitivity of the system performance to the design and operation parameters, (iii) provide a basis for cross-checking simulation model results, and (iv) estimate product stream concentrations for design of down- (or up-) stream unit operations of the wastewater treatment plant.

Anaerobic digestion of organics require a consortium of four organism groups (see Chapter 4) viz. (i) acidogens, which convert complex organics to SCFA (acetic, Hac and propionic, HPr), carbon dioxide (CO_2) and hydrogen (H_2), (ii) acetogens, which convert HPr to HAc and H_2, (iii) acetoclastic methanogens, which convert HAc to CO_2 and methane (CH_4) and (iv)

hydrogenotrophic methanogens, which convert H_2 and CO_2 to CH_4 and water. The two methanogenic groups are very sensitive to pH and so the acetogens and acetoclastic methanogens must utilize the HAc and HPr respectively as soon as they are produced to maintain a near neutral pH for optimal operation. Because the hydrolysis/acidogenesis process mediated by the acidogens ((i) above) is the slowest process in the system, high SCFA concentrations and therefore low pH, arise only under unstable and digester upset operating conditions caused by a shock load in organics, a rapid decrease in temperature or a methanogen inhibitor in the influent. A steady state model, therefore, need only consider the kinetics of this process. The processes following hydrolysis/acidogenesis, being much more rapid (usually), can be accepted to reach completion. This implies that in stable AD systems the intermediate products of the processes following after hydrolysis/acidogenesis such as SCFAs and H_2, do not build up in the system and their concentrations are sufficiently low to be considered negligible. Consequently, in the steady state AD model, the products of hydrolysis/acidogenesis can be dealt with stoichiometrically and converted to digester end products. In effect, it can be assumed that the hydrolysis/ acidogenesis process generates directly the digester end-products biomass, CH_4, CO_2 and water. Thus the steady state anaerobic digester model developed below considers three aspects: (i) The kinetics of the hydrolysis/acidogenesis process (ii) stoichiometric conversion of the products from (i) to digester end-products, free and saline ammonia, methane and CO_2 gas, alkalinity and (iii) weak acid/base chemistry which fixes the digester pH from the alkalinity and CO_2 partial pressure of the gas generated.

5.2 LITERATURE REVIEW

5.2.1 Anaerobic Processes by McCarty (1974)

5.2.1.1 Chemistry and microbiology

McCarty (1974) described the general anaerobic process as an overall methane fermentation process which requires a variety of anaerobic and facultative bacteria. The complex materials in the influent (e.g. protein and cellulose) undergo extracellular hydrolysis, and the hydrolysed organics are then fermented by acid forming bacteria to simple organic acids (e.g. acetic, propionic, butyric acids). These acids are then fermented by methane producing bacteria to produce methane and carbon dioxide. The pathways for anaerobic digestion described by McCarty (1974) are illustrated in Fig. 5.1 below.

The percentages in Fig. 5.1 show the portions of the organic COD which are converted via the various routes. McCarty (1974) did not indicate the portion of COD that is converted to cell mass, however he states that the percentage COD converted to cell mass can be between 4 and 20%, depending on the organic compounds fermented and the retention time of the digester.

Process chemistry:

McCarty (1974) proposed a generalized reaction for the overall methane fermentation of a organic waste with an empirical formulation of $C_nH_aO_bN_c$ to methane, carbon dioxide and bacterial cells ($C_5H_7O_2N$):

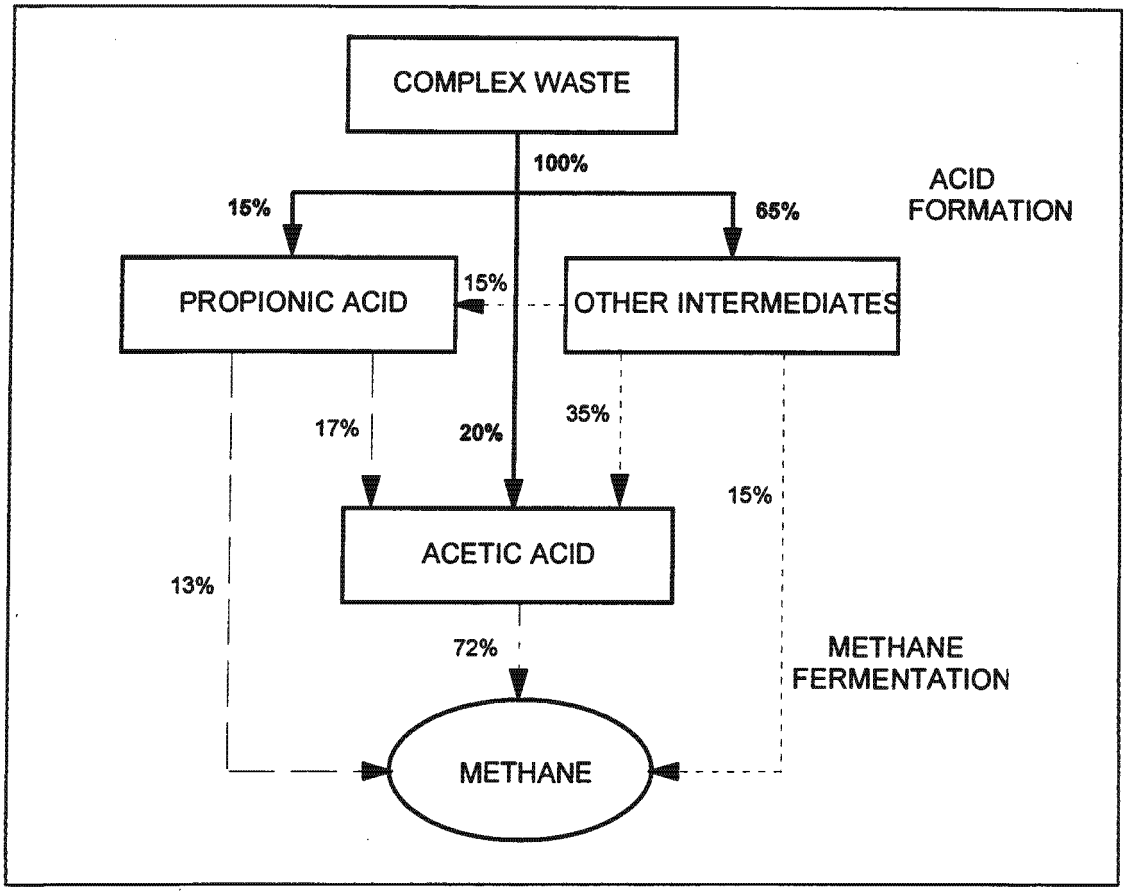

Fig. 5.1: Pathways for anaerobic digestion, McCarty (1974).

$$C_nH_aO_bN_c + \left(2n + c - b - \frac{9sd}{20} - \frac{ed}{4}\right) H_2O \rightarrow \frac{de}{8} CH_4$$
$$+ \left(n - c - \frac{sd}{5} - \frac{de}{8}\right) CO_2 + \frac{sd}{20} C_5H_7O_2N + \left(c - \frac{sd}{20}\right) NH_4^+ + \left(c - \frac{sd}{20}\right) HCO_3^- \qquad (5.1)$$

where $d = 4n + a - 2b - 3c$.

In Eq 5.1, s represents the fraction of COD synthesized to cell mass and e represents the fraction converted to methane gas for energy, where $s + e = 1$. McCarty (1974) stated further, that the value of s is related to the solids retention time (R_s) and the organism decay rate (b) as follows:

$$s = a_e \cdot \frac{1 + 0.2 \cdot b \cdot R_s}{1 + b \cdot R_s} \qquad (5.2)$$

where the value 0.2 represents the unbiodegradable fraction of the organism cell mass during

endogenous respiration, and a_e represents the maximum value for s when R_s equals zero. McCarty (1974) calculated values for a_e for various compounds (e.g. carbohydrates, proteins, fatty acids, domestic sludge) where carbohydrates give the maximum yields and fatty acids, on the other end of the scale, the minimum yields.

pH and alkalinity requirements:
McCarty (1974) stated that the optimum pH for the methane producing organisms is between 7.0 and 8.0, although most methane producing organisms are not harmed unless the pH drops below 6.0. When a digester begins to fail, the volatile fatty acid concentration increases, because the methane producing organisms no longer utilize the volatile fatty acids, and the acids accumulate in the bulk liquid causing a drop in the pH. The pH will continue to drop as long as volatile fatty acids are produced and continue to accumulate in the bulk liquid. As the volatile fatty acid concentration increases, the bicarbonate alkalinity decreases according to the following:

$$HCO_3^- + HAc \rightarrow H_2O + CO_2 + Ac^- \qquad (5.3)$$

This results in a pH decrease, however the total alkalinity does not change significantly because Ac^- forms part of the alkalinity measurement. McCarty (1974) stated further, that the bicarbonate alkalinity can be calculated when the volatile fatty acid concentration and the total alkalinity are known, by the following relationship:

$$BA = TA - (0.71 \cdot VA) \qquad (5.4)$$

where BA = bicarbonate alkalinity, mg/l as $CaCO_3$
TA = total alkalinity, mg/l as $CaCO_3$
VA = volatile acid concentration, mg/l as acetic acid.

Furthermore, the ammonia released into the bulk liquid during the hydrolysis of the organic material produces alkalinity, and this helps in maintaining a near neutral pH. If the influent organics do not contain organic nitrogen, or contain only little organic nitrogen, alkalinity may have to be dosed to maintain optimum pH levels in the bulk liquid.

Process kinetics:
McCarty (1974) developed a model to describe the rate of substrate utilization in a digester. He started with two basic equations describing organism growth (Eq 5.5) and substrate utilization (Eq 5.6). The first equation, describing the rate of growth of organisms during the process of COD reduction and methane production, is given by:

$$\frac{dX}{dt} = Y\left(\frac{dS_d}{dt}\right) - bX \qquad (5.5)$$

where X = organism concentration, mgCOD/l
Y = organism yield, g cells/g COD consumed
S_d = substrate concentration, mgCOD/l
b = organism decay coefficient, /d

The second equation, describing the rate at which the substrate is consumed by the organisms is given by:

$$\frac{dF}{dt} = \frac{k \cdot S_d \cdot X}{K_S + S_d} = -\frac{dS}{dt} \tag{5.6}$$

where k = rate of substrate utilization, gCOD/l.d
K_S = half saturation coefficient, g/l

Using Eqs 5.5 and 5.6, McCarty (1974) considered a completely mixed reactor with Q (in l/d) as the influent flow and S_T (as gCOD/l) as the influent substrate concentration. S_T consists of a biodegradable fraction (S_d) and an unbiodegradable fraction (S_r). He determined the relationship between the reactor substrate concentration (biodegradable and unbiodegradable), reactor organism concentration, the flow rate and the influent substrate concentration from mass balances around the reactor. In this way McCarty (1974) formulated expressions for the active organism concentration (Eq 5.7), influent unbiodegradable and endogenous residue COD concentration (Eq 5.8) and residual biodegradable substrate concentration (Eq 5.9) in the reactor:

$$X_a = \frac{Y(S_d^\circ - S_d)}{1 + bR_s} \tag{5.7}$$

$$X_I = 0.2b \cdot X_a \cdot R_s + S_r \tag{5.8}$$

$$S_d = \frac{K_s(1 + bR_s)}{R_s(Yk - b) - 1} \tag{5.9}$$

where X_a = active organism concentration (mgCOD/l)
X_I = unbiodegradable COD concentration (mgCOD/l)
S_d°, S_d = Influent (initial) and residual biodegradable substrate concentration (mgCOD/l)

Furthermore, McCarty (1974) stated that the methane production can be directly linked to the COD reduction (COD utilized by the organisms). He argued that since there is no external electron acceptor present in anaerobic digestion, the only way that a COD reduction can occur is by the removal of the organic material from the bulk liquid, i.e through the production of methane. Other ways of reducing the COD are through (i) the reduction of sulfates to hydrogen sulfide gas and (ii) the production of hydrogen gas. McCarty (1974) determined the methane production from the following balanced equation:

$$CH_4 + 2O_2 \rightarrow CO_2 + 2H_2O \tag{5.10}$$

One mole (or 22.4 litres at 0°C and 1atm pressure) of methane is equivalent to 2 moles of oxygen, or 64 grams of COD. Therefore, a reduction of 1 gram of COD is equivalent to the production of 0.35 litres of methane gas, using the following relationship:

$$G = 0.35 \cdot Q \cdot (S_T^{\circ} - S_T) \tag{5.11}$$

where G is the rate of gas production in litres per day.

5.2.1.2 Closure

McCarty (1974) developed a generalized reaction for the overall anaerobic digestion of a waste with an empirical formula (Eq 5.1) as well as a kinetic model to describe the rate of waste utilization in a completely mixed reactor. His model demonstrates that anaerobic digestion has certain advantages over aerobic processes. For example, anaerobic digestion produces usable energy (methane gas), while aerobic degradation requires the input of energy (in the form of dissolved oxygen) to function optimally and further, the anaerobic digestion produces significantly less sludge than an aerobic treatment process, which results in significantly less solids to dispose. This model provides a sound basis from which to develop a steady sate model for anaerobic digestion, which is described in this Chapter.

5.3 HYDROLYSIS/ACIDOGENESIS KINETICS

5.3.1 Hydrolysis Rate Equations

Since the hydrolysis/acidogenesis process is the slowest one in the sewage sludge anaerobic digester and does not reach completion within the normal range of the principal digester design parameter of hydraulic retention time, a kinetic expression describing this process rate is required for the steady state model. In Chapter 4, four kinetic equations for this process were considered, viz. (1) first order with respect to the residual biodegradable particulate organic (COD) concentration S_{bp}, (2) first order with respect to S_{bp} and the acidogen biomass concentration (Z_{AD}) which mediates this process, (3) Monod kinetics and (4) saturation (or Contois) kinetics (see Eqs 5.12 to 5.15 in Table 5.1). All these equations have been used to model various biological processes for many years; the first to describe the hydrolysis/acidogenesis of sewage sludge solids in AD (e.g. Henze and Harremoës, 1983, Bryers, 1985), the second for modelling the conversion of readily biodegradable organics to short chain fatty acids in the anaerobic reactor of biological P removal systems (e.g. Wentzel *et al.*, 1985), and the last two for the utilization of soluble readily and particulate slowly biodegradable organics respectively in activated sludge models (Dold *et al.*, 1980; Henze *et al.*, 1987) and hydrolysis of sewage sludge (McCarty, 1974). From Chapter 4 it can be seen that it cannot be determined which equation was superior for modelling hydrolysis/acidogenesis process in AD because for the experimental data evaluated, the unbiodegradable particulate COD fraction ($f_{PS'up}$) of the sewage sludge (primary+humus) organics was not sufficiently well known - by changing $f_{PS'up}$ in a fairly narrow range from 0.32 to 0.36, each of the equations gave a better correlation coefficient than the other equations at different specific $f_{PS'up}$ values. It was accepted that the saturation kinetics were satisfactory for the integrated model (UCTADM1), because this equation (i) gave a similar $f_{PS'up}$ value (0.36) to O'Rourke (1968) (0.34) working with AD of 'pure' primary sludge (no trickling filter humus or waste activated sludge) and (ii) has been successfully used to model hydrolysis/utilization of the same particulate biodegradable organics in activated sludge kinetic models. In the evaluation of the four hydrolysis/acidogenesis equations in Chapter 4, the effect of the acidogen (Z_{AD}) and acetoclastic methanogen (Z_{AM}) biomass formation was included, because these two organism groups have the highest yield coefficients and so contribute to the effluent organics (COD) concentration and decrease the gas production.

In steady state models, detail is not required - in fact, it is undesirable. From the simulation model, sufficient accuracy for a steady state model is obtained by selecting any of the four hydrolysis/acidogenesis equations and increasing the acidogen biomass yield to include the acetoclastic methanogens. The acidogens have the highest yield coefficient (Y_{AC}=0.089 gCOD biomass/gCOD substrate hydrolysed) and make up more than 77% of the total biomass formed. Increasing Y_{AD} from 0.089 to 0.113 very closely takes into account the biomass formation of the other organism groups. A consequence of accepting this approach is that in kinetic rate formulations that include the acidogen biomass concentration (first order specific, Monod and saturation), the specific rate constants in the steady state model here will be lower compared with the corresponding values in the dynamic model discussed in Chapter 4, but the predicted performances (e.g. %COD removal) will be the same.

Table 5.1: Steady state anaerobic digester kinetic equations for the residual biodegradable particulate organics concentration (S_{bp}), acidogen biomass concentration (Z_{AD}), unbiodegradable organics concentration (S_{up}) and methane production in gCOD/ℓ influent (S_m) for four different hydrolysis kinetic rate equations. Kinetic constants of the four hydrolysis equations for unbiodegradable particulate COD fraction ($f_{PS,up}$) = 0.36.

Hydrolysis kinetic equation	1st order with respect to (wrt) S_{bp}	1st order specific (wrt to S_{bp} & Z_{ad})	Monod kinetics	Saturation kinetics
Hydrolysis rate r_h gCOD/(ℓ.d)	$r_h = K_h S_{bp}$ .....1 Eq 5.12	$r_h = K_H S_{bp} Z_{AD}$..2 Eq 5.13	$r_h = \frac{K_m S_{bp}}{(K_s + S_{bp})} Z_{AD}$..3 Eq 5.14	$r_h = \frac{K_M (S_{bp}/Z_{AD})}{[K_S + (S_{bp}/Z_{AD})]} Z_{AD}$....4 Eq 5.15
Residual biodegradable organics concentration gCOD/ℓ S_{bp}	$S_{bp} = \frac{S_{bpi}}{\left\{1 + K_h R \frac{[1 + b_{AD} R(1 - Y_{AD})]}{(1 + b_{AD} R)}\right\}}$	$S_{bp} = \frac{1/R + b_{AD}}{Y_{AD} K_H}$	$S_{bp} = \frac{K_s (1/R + b_{AD})}{Y_{AD} K_m - (1/R + b_{AD})}$	$S_{bp} = \frac{S_{bpi}}{\left\{1 + \frac{[Y_{AD} K_M - (1/R + b_{AD})]\,[1 + b_{AD} R(1 - Y_{AD})]}{Y_{AD} K_S (1/R + b_{AD})}\right\}}$
Acidogen biomass concentration Z_{ad} gCOD/ℓ	$Z_{AD} = \frac{Y_{AD}(S_{bpi} - S_{bp})}{[1 + b_{AD} R(1 - Y_{ad})]}$			
Unbiodegradable organics concentration S_{up} gCOD/ℓ	$S_{up} = S_{upi}$			
Methane production concentration S_m gCOD/ℓ	$S_m = (1 - Y_{AD}) R r_h$			
Kinetic constants (Izzett et al., 1992 data)	K_h = 0.515±0.041 /d *K_h = 0.481±0.040 /d	K_H = 0.322±0.047 *K_H = 0.379±0.056 ℓ/(gCOD biomass.d)	K_m = 3.34 (*3.72) gCOD organics/(gCOD biomass.d) K_s = 6.76 (*6.38) gCOD/ℓ	K_M = 5.27 (*5.58) gCOD organics/ (gCOD biomass.d); K_S = 7.98 (*8.89) gCOD/ℓ
COD balance	$S_{ti} = S_{te} + S_m = S_{bp} + Z_{AD} + S_{up} + S_m$; S_{ti} = COD in; $S_{te} = S_{bp} + Z_{AD} + S_{up}$ = COD out as sludge solids; S_m = COD out as methane gas			

*Determined with the more complex hydrolysis model described in Chapter 4 at $f_{PS',up}$ = 0.36.

The steady state AD model will be derived using the COD to quantify the organics and biomass concentrations and the Monod equation for the hydrolysis/acidogenesis rate. However, the model equations for all four hydrolysis kinetics rate expressions have been derived and are summarized in Table 5.1.

5.4 STEADY STATE MODEL DEVELOPMENT - HYDROLYSIS KINETICS

Consider a flow through digester of volume V and influent flow Q giving a hydraulic retention time or sludge age of R = V/Q days (Fig 5.2).

Defining the unbiodegradable fraction of the influent total particulate sewage sludge COD (S_{ti}) as $f_{PS'up}$, then the particulate biodegradable (S_{bpi}) and unbiodegradable (S_{upi}) COD concentrations in the influent are (see Fig 5.3)

$$S_{bpi} = (1 - f_{PS'up})\, S_{ti} - S_{bsai} \tag{5.16}$$

$$S_{upi} = f_{PS'up}\, S_{ti} \tag{5.17}$$

where

S_{bsai} = Influent volatile fatty acid (VFA) concentration (mgCOD/ℓ)

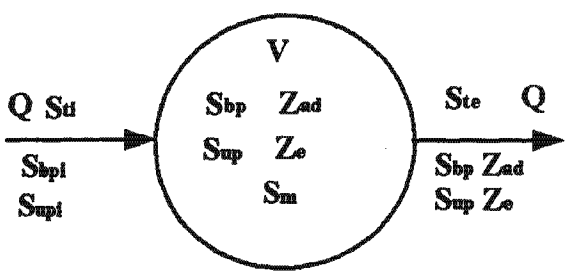

Fig 5.2: Schematic diagram of the flow through anaerobic digester of retention time R = V/Q showing symbols used in the steady state AD model.

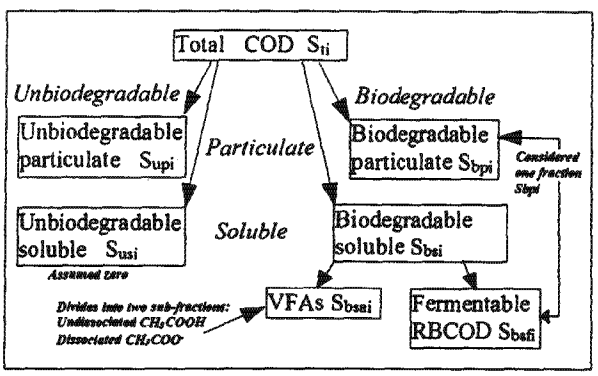

Fig 5.3: Influent primary sludge COD fractionation for the steady state anaerobic digestion model.

Sewage sludge comprises two additional dissolved COD fractions, i.e. the unbiodegradable soluble COD (S_{usi}) and the fermentable (non-VFA) readily biodegradable soluble COD (S_{bsfi}) (Fig 5.3). The S_{usi} is very low in relation to the S_{upi} and so can be assumed zero for the purposes of this steady state model. The S_{bsfi} goes through the same hydrolysis/acidogenesis processes as the particulate biodegradable COD (S_{bpi}) and so is included with the S_{bpi}. Because the steady state model is based on the hydrolysis process, the S_{bsai} is not included with the COD passing through this process. However, the S_{bsai} does generate methane and CO_2 (but negligible sludge mass)

mediated by the two methanogenic species. Hence S_{bsai} can be excluded in the hydrolysis part of the model, but needs to be included in the stoichiometry part of the model due to its effect on gas composition and digester pH. Hence S_{ti} is given by $S_{upi}+S_{bpi}+S_{bsai}$ (Fig 5.3).

The net acidogen growth rate from the hydrolysis/acidogenesis and endogenous processes is given by

$$\frac{dZ_{AD}}{dt} = Y_{AD}\, r_h - b_{AD} Z_{AD}$$

where r_h = volumetric hydrolysis/acidogenesis rate in gCOD/(ℓ.d) (Eqs 5.12 to 5.15 in Table 5.1)
Y_{AD} = pseudo acidogen yield coefficient (gCOD biomass/ gCOD organics hydrolysed)
b_{AD} = acidogen endogenous respiration rate (/d).

The steady state model is derived by applying the general mass balance equation (Eq 5.18) over the system (Fig 5.2) to the four system variable compound concentrations (all gCOD/ℓ), i.e. S_{bp}, S_{up}, Z_{AD} and methane (S_m) concentrations. For the flow through system, the effluent compound concentrations are equal to the reactor concentrations. For example, the mass balance for S_{bp} over a time interval dt is

$$\begin{bmatrix} Mass \\ change \\ in\ system \end{bmatrix} = \begin{bmatrix} Mass\ flow \\ into \\ system \end{bmatrix} - \begin{bmatrix} Mass\ flow \\ out\ of \\ system \end{bmatrix} - \begin{bmatrix} Mass\ loss \\ by\ bio- \\ process \end{bmatrix} + \begin{bmatrix} Mass\ gain \\ by\ bio- \\ process \end{bmatrix} \qquad (5.18)$$

$$dS_{bp}V = +QS_{bpi}dt - QS_{bp}dt - r_h V dt + b_{AD} Z_{AD} V dt \qquad (5.19)$$

In Eq 5.19, the first and second terms on the right hand side are the biodegradable organics flowing in and out of the digester, and the third and fourth terms the decrease in biodegradable organics due to hydrolysis and the increase from the biodegradable part of the acidogen biomass that dies. Dividing Eq 5.19 through by Vdt yields

$$\frac{dS_{bp}}{dt} = +\frac{S_{bpi} - S_{bp}}{R} - r_h + b_{AD} Z_{AD} \qquad \text{gCOD/(ℓ.d)} \qquad (5.20)$$

Similarly the mass balance on acidogen biomass concentration (Z_{AD}) yields

$$dZ_{AD}V = +0 - QZ_{AD}dt + Y_{AD} r_h V dt - b_{AD} Z_{AD} V dt$$

Again dividing through by Vdt yields

$$\frac{dZ_{AD}}{dt} = -\frac{Z_{AD}}{R} + Y_{AD} r_h - b_{AD} Z_{AD} \qquad (5.21)$$

At steady state the transient dZ_{AD}/dt in Eq 5.21 = 0 and solving for the hydrolysis rate r_h yields,

$$r_h = \frac{Z_{AD}}{Y_{AD}}\left(\frac{1}{R} + b_{AD}\right) \qquad \text{gCOD/(ℓ.d)} \qquad (5.22)$$

Setting Eq 5.20 = 0 for steady state and solving for r_h yields,

$$r_h = \frac{S_{bpi} - S_{bp}}{R} + b_{AD} Z_{AD} \qquad \text{gCOD/(ℓ.d)} \qquad (5.23)$$

Then substituting Eq 5.22 for r_h into Eq 5.23 and solving for Z_{AD} yields,

$$Z_{AD} = \frac{Y_{AD}(S_{bpi} - S_{bp})}{[1 + b_{AD} R(1 - Y_{AD})]} \qquad \text{gCOD/ℓ} \qquad (5.24)$$

Equation 5.24 seems to indicate that the acidogen biomass concentration (Z_{AD}) is independent of the hydrolysis kinetic rate (and hence its formulation) because r_h does not appear in it. However, it is implicitly dependent on r_h because S_{bp} appears in the equation and S_{bp} is dependent on the hydrolysis kinetic rate. Equation 5.24 does show that once S_{bp} is known, then Z_{AD} can be calculated for any hydrolysis rate equation.

Substituting the Monod equation (Eq 5.14 in Table 5.1) for r_h into Eq 5.22 and solving for S_{bp} yields

$$S_{bp} = \frac{K_s(1/R + b_{AD})}{Y_{AD} K_m - (1/R + b_{AD})} \qquad \text{gCOD/ℓ} \qquad (5.25)$$

Ignoring as negligible the formation of unbiodegradable organics from the acidogens that die (i.e. endogenous residue is zero), the total unbiodegradable organics concentration in the effluent (S_{up}) is equal to the influent, i.e.

$$S_{up} = S_{upi} \qquad \text{gCOD/ℓ} \qquad (5.26)$$

The methane production in COD units is directly related to the rate of hydrolysis of biodegradable organics. If the methane concentration in the effluent in COD units is S_m, a mass balance on S_m yields

$$dS_m V = 0 - Q S_m dt + (1 - Y_{AD}) r_h V dt \qquad (5.27)$$

where S_m = methane concentration in the effluent in gCOD/ℓ (if it were dissolved)

Dividing Eq 5.27 through by Vdt and setting $dS_m/dt = 0$ and solving for S_m yields

$$S_m = (1 - Y_{AD}) R r_h \qquad \text{gCOD/ℓ} \qquad (5.28)$$

Because methane has a COD 64 gCOD/mol and a gas volume at ambient temperature 20°C of

22.4 (293/273) = 24.0 ℓ/mole, the methane gas production Q_m is

$$Q_m = (1-Y_{AD})\,R\,r_h\,24.0/64 \quad (\ell \text{ methane/d})/(\ell \text{ influent flow/d}) \tag{5.29}$$

The partial pressure of CO_2 in the gas (p_{CO2}) and the CO_2 composition of the gas are numerically equal. Hence, if the partial pressure of CO_2 or the CO_2 gas composition are known (in atmospheres, or volume or mole fractions), then the total gas production at 20°C (Q_{gas}) is

$$Q_{gas} = \frac{Q_m}{(1-p_{CO2})} = \frac{(1-Y_{AD})\,R\,r_h\,24.0}{(1-p_{CO2})64} \quad (\ell \text{ gas/d})/(\ell \text{ influent flow/d}) \tag{5.30}$$

A COD mass balance over the digester system (Fig 5.2) yields

$$S_{ti} = S_{te} + S_m = S_{bp} + Z_{AD} + S_{up} + S_m \tag{5.31}$$

Equation 5.31 shows that COD exits the digester only as sludge mass in the effluent (S_{te}) and as methane gas (S_m). Substituting Eq 5.24 with S_{bp} as its subject for S_{bp}, Eq 5.26 for S_{up}, Eq 5.27 for S_m and Eq 5.14 for r_h into Eq 5.31 yields,

$$S_{ti} = S_{bpi} - \frac{Z_{AD}}{Y_{AD}}[1+b_{AD}R(1-Y_{AD})] + Z_{AD} + S_{upi} + (1-Y_{AD})R\frac{K_m S_{bp}}{K_s + S_{bp}}Z_{AD}$$

which on simplifying gives Eq 5.25 for S_{bp}, and therefore proves the input and output COD masses balance exactly.

The total (S_{tr}) and biodegradable (S_{bpr}) COD removals and methane production (S_m) are given by

$$S_{tr} = S_{ti} - S_{te} = S_m \tag{5.32}$$

$$S_{bpr} = S_{bpi} - S_{bp} \tag{5.33}$$

The equations for the biodegradable organics (S_{bp}), acidogen (Z_{AD}), unbiodegradable (S_{up}) and methane (S_m) concentrations for all four hydrolysis rate formulations are given in Table 5.1.

5.5 CALIBRATION OF HYDROLYSIS KINETICS

The equations developed above were evaluated and calibrated against data from steady state anaerobic digesters.

5.5.1 Calculating the Effluent COD Concentration (S_{te})

From the steady state COD mass balance equation (Eq 5.31), the effluent total particulate COD concentration, S_{te} is given by

$$S_{te} = S_{up} + S_{bp} + Z_{AD} \qquad \text{gCOD}/\ell \tag{5.34}$$

Substituting Eq 5.26 for S_{up}, Eq 5.17 for S_{upi} and Eq 5.24 for Z_{AD} in Eq 5.34 yields,

$$S_{te} = f_{PS'up}S_{ti} + S_{bp} + \frac{Y_{AD}[(1-f_{PS'up})S_{ti} - S_{bp}]}{[1+b_{AD}R(1-Y_{AD})]} \qquad \text{gCOD}/\ell \tag{5.35}$$

Solving Eq 5.35 for S_{bp} yields,

$$S_{bp} = \frac{S_{ti}[f_{PS'up} + E(1-f_{PS'up})] - S_{te}}{[E-1]} \qquad \text{gCOD}/\ell \tag{5.36a}$$

$$\text{where } E = \frac{Y_{AD}}{1+b_{AD}R(1-Y_{AD})} \tag{5.36b}$$

With S_{te} and S_{ti} known from measurement, Eq 5.36 defines S_{bp} in terms of the unbiodegradable fraction of the primary sludge ($f_{PS'up}$), the retention time of the digester (R) and the acidogen constants (Y_{AD}, b_{AD}). By estimating an unbiodegradable fraction of the primary sludge ($f_{PS'up}$) and selecting acidogen biomass constants (i.e. Y_{AD} = 0.113 gCOD biomass/ gCOD organics, b_{AD} = 0.041 /d), S_{bp} can be calculated with Eq 5.36 from experimental data. The yield coefficient of the acidogens (Y_{AD}) has been increased from 0.089 to 0.113 to take account of the acetoclastic methanogen biomass that grows in the system. Because acidogenesis produces 61% acetic acid (and 39% hydrogen), 61% of the acetoclastic methanogen yield coefficient (Y_{AM} = 0.040) was added to Y_{AD}. This simplification is acceptable because the endogenous respiration rate is closely the same for these two organism groups (b_{AD} = 0.041 /d and b_{AM} = 0.037 /d). However, as noted above this simplification does influence the values of the constants in the hydrolysis rate equations. The hydrogenotrophic methanogen yield (Y_{HM}) is low enough (0.01 gCODbiomass/gCOD H_2) to be ignored.

5.5.2 Estimating the Unbiodegradable COD Fraction of Primary Sludge

For wastewater treatment plant design, the primary sludge (PS) unbiodegradable COD fraction ($f_{PS,up}$) is entirely dependent on the unbiodegradable particulate COD fractions ($f_{S'up}$) selected for the raw and settled wastewaters and the fraction of COD removed by primary sedimentation (f_{psr}). From a COD mass balance around the primary settling tank (PST), the $f_{PS'up}$ in terms of the raw and settled wastewater $f_{S'up}$ values and the PST f_{psr} is

$$f_{PS'up} = f_{S'up\,Set} + \frac{1}{f_{psr}}(f_{S'up\,Raw} - f_{S'up\,Set}) \tag{5.37}$$

where

$f_{PS'up}$ = unbiodegradable COD fraction of primary sludge (PS)
$f_{S'up\ Set}$ = Settled wastewater unbiodegradable particulate COD fraction
$f_{S'up\ Raw}$ = Raw wastewater unbiodegradable particulate COD fraction
f_{psr} = fraction of COD removed in the primary settling tank (PST)

Equation 5.37 has been simplified and is not strictly in conformity with a water flow balance over the PST. In Eq 5.37, it has been assumed that the raw and settled wastewater flows entering and exiting the PST are equal. In practice, this is not true due to the low PST underflow, typically between 0.5 and 2% of average dry weather flow (ADWF). The error is very small on $f_{PS'up}$, but large enough to cause an error of ~1% on the COD mass balance around the whole WWTP. Mass balances are used wherever possible to verify the mathematical equations in models and errors > 1% are signals of possible errors in logic and formulae.

A graphical representation of Eq 5.37 is given in Fig 5.4. For the typical South African raw and settled municipal wastewaters, $f_{S'up}$ fractions of 0.15 and 0.04 respectively (WRC, 1984) and 35% COD removal (f_{psr} = 0.35), the $f_{PS'up}$ is 0.36. Literature on full-scale AD of primary sludge (PS) give maximum VS removals at long retention times at around 0.60 (Eckenfelder, 1980), suggesting an unbiodegradable fraction of around 0.35. O'Rourke (1968) determined a $f_{PS'up}$ of 0.36 in their investigation into AD of PS.

Incidently, Eq 5.37 shows that (i) the $f_{S'up}$ values selected for the raw and settled wastewaters must be consistent with observed PS characteristics and (ii) the % removal of unbiodegradable organics (COD) in PSTs is apparently much higher (83% for the selected $f_{S'up}$ values above) than that of biodegradable organics (38%). The latter has been of significant economic benefit for the activated sludge system because a large mass of unbiodegradable organics from the influent do not accumulate in the reactor. In some wastewater treatment plant simulation models, equal proportions of biodegradable and unbiodegradable particulate organics are removed in the PST. This leads to settled wastewater and PS characteristics that deviate significantly from observed values, e.g. if equal proportions of the raw wastewater biodegradable and unbiodegradable particulate COD are removed and the %COD removal remains at 35%, then the settled wastewater $f_{S'up}$ would have to be 0.12 and $f_{PS'up}$ = 0.20. Both these values are considerably different to those observed.

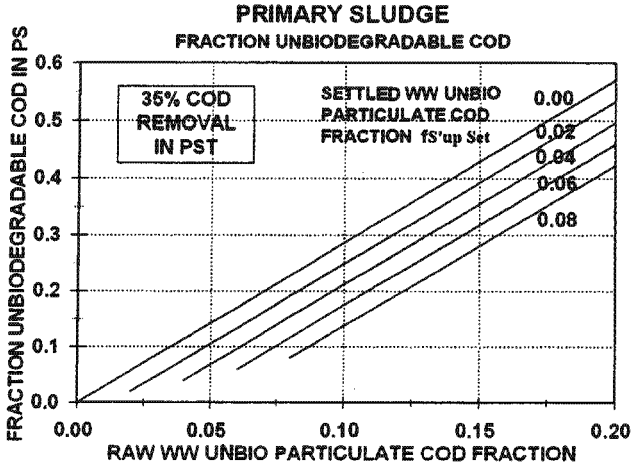

Fig 5.4: Fraction of unbiodegradable COD in primary sludge versus raw wastewater unbiodegradable particulate COD fraction for different settled wastewater unbiodegradable particulate COD fraction.

5.5.3 Calculating the Constants in the Hydrolysis Kinetic Equations - Izzett *et al.* (1992) Results

Izzett *et al.* (1992) operated two laboratory-scale mesophilic (37°C) anaerobic digesters fed a mixture of primary and humus (trickling filter) sludge from the Potsdam wastewater treatment plant (Milnerton, Cape, South Africa) at 7, 10, 12, 15 and 20 days retention time. The steady state experimental results measured on the systems are listed in Table 5.2.

Accepting $f_{PS'up} = 0.36$ from Chapter 4 for the Izzett data, the calculated S_{bp} concentrations from Eq 5.36 are listed in Table 5.3. With S_{bp} known, Z_{AD} and ΔS_{bp} ($= S_{bpi}-S_{bp}$) can be calculated from the measured results (Table 5.3). Because the hydrolysis process does not reach completion in the digester, the observed hydrolysis rate r_h is given by Eq 5.23 and the calculated values are listed in Table 5.3. With the hydrolysis rate known, the kinetic constants in the various hydrolysis rate equations can be calculated, i.e. for the first order rate with respect to S_{bp} only (Eq 5.12), $K_h = r_h / S_{bp}$ (/d) and for the first order specific rate with respect to S_{bp} and Z_{AD} (Eq 5.13), $K_H = r_h / (S_{bp} Z_{AD})$ [ℓ/(gCOD biomass.d)].

Table 5.2: Experimental data measured by Izzett *et al.* (1992) on 14ℓ completely mixed mesophilic (37°C) anaerobic digesters at 7 to 20 days retention time fed a mixture of primary and humus (trickling filter) sludge from the Potsdam wastewater treatment plant (Milnerton, Cape, South Africa).

Retention time (d)	7	10	12	15	20
Influent flow ℓ/d	2	1.4	1.17	0.93	0.7
Influent COD gCOD/ℓ	43.286	40.721	39.222	42.367	42.595
Influent VFA gCOD/ℓ	1871	1961	2872	1824	2249
Influent TKN mgN/ℓ	1105	1100	1028	1075	1171
Influent FSA mgN/ℓ	196	203	235	221	244
Influent Alk mg/ℓ as $CaCO_3$	80	81	90	82	56
Influent pH	5.34	5.34	5.2	5.42	5.28
Effluent COD gCOD/ℓ	23.637	20.521	18.678	19.969	19.005
Effluent VFA mgCOD/ℓ	50	28	28	27	23
Effluent TKN mgN/ℓ	1041	1039	992	976	1157
Effluent FSA mgN/ℓ	511	404	430	404	511
Effluent Alk mg/ℓ as $CaCO_3$	1882	1951	2072	1994	2066
Gas Composition %CH_4	63.2	62.1	63.3	63.6	63.3
COD removal	19.649	20.2	20.544	22.398	23.59
Gas prod ℓ gas/ℓ influent	13.97	14.33	14.27	15.01	15.79
Gas Composition %CO_2	36.8	37.9	36.7	36.4	36.7
FSA released	315	201	195	183	267
Measured digester pH	7.12	7.11	7.19	7.14	7.15
'Corrected' digester pH	6.84	6.84	6.88	6.86	6.87
COD balance (%)	108.4	108.6	109.1	106.9	107.3
Nitrogen Balance (%)	94.2	94.5	96.5	90.8	98.8
Carbon Balance (%)*	99	100	99.5	101.3	101.4

*Based on a sludge composition of $C_{3.5}H_7O_2N_{0.196}$ calculated from the influent COD and N masses and effluent C mass in the gas and liquid streams.

The calculated K_h and K_H rates for the different retention times are listed in Table 5.3 and plotted versus R in Fig 5.5. For a hydrolysis rate equation to be reasonably general, it should take into account the major factors that influence the rate. If it achieves this, then the K constants in the rate equation will not change with the principal design parameters, in this case, hydraulic retention time (or sludge age). For the first order and the first order specific hydrolysis rate equations (Eqs 5.12 and 5.13 in Table 5.1), it can be seen that this would not appear to be the case (Fig 5.5) - both K_h and K_H increase with increasing retention time. The average K_h and K_H rates over the five retention times are 0.515 /d and 0.322 ℓ/(gCOD biomass.d) respectively (Table 5.3, see also Table 5.1). Although these rate equations do not appear to be sufficiently general to describe the change in hydrolysis rate with retention time, the difference in predicted %COD removal based on the average K_h and K_H rates compared with experimental results is very small.

Determination of the K constants in the Monod and saturation kinetic rate equations require linearization of these rate equations and linear regression over the retention time range of the experimental results, as described in Chapter 4. For the Monod equation, the hydrolysis rate r_h is given by Eq 5.14 in Table 5.1, where r_h, S_{bp} and Z_{AD} are calculated from experimental data (Table 5.3). The linearization can be done by three methods, viz. (i) Lineweaver-Burke, (ii) inversion and (iii) Eadie-Hofstee, each giving different K values, because each method emphasizes different aspects of the Monod equation.

The specific hydrolysis rate (r_h / Z_{AD}) versus S_{bp} graphs obtained for the Monod rate equation with constants derived from the three linearization methods (listed in Table 5.4) are shown in Fig 5.6, together with the Izzett experimental data. Although method (i) gives the best fit with the data (highest correlation coefficient $R^2 = 0.948$), method (ii) gives marginally the best fit at the short retention time (7d). Linearization method (iii) showed that the 15d retention time data is an outlier and is the reason for the low R^2 value (0.688) for all five retention time data. Excluding the 15d data significantly improved the R^2 value for method (iii) (0.888). The average K_m and K_s values obtained from the three methods, with the 15d retention time data excluded for method (iii), are given in Table 5.4 (see also Table 5.1). Figure 5.6 shows that even though different K values are obtained with the three different methods, the specific hydrolysis rate (r_h/Z_{AD}) versus biodegradable COD concentration (S_{bp}) curves obtained from each and the average are virtually the same and plot very closely to one another.

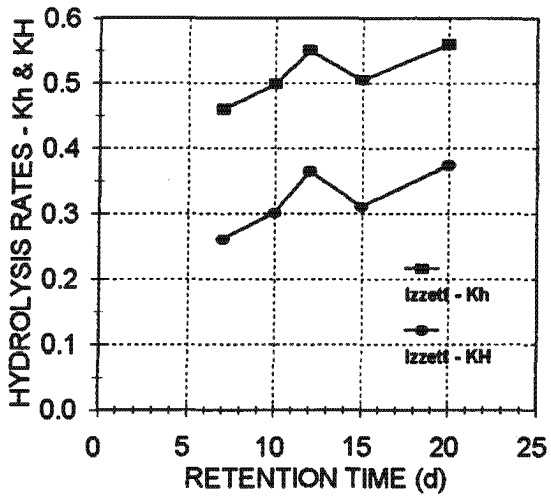

Fig 5.5: Hydrolysis rate constants for the 1st order (K_h, /d) and 1st order specific [K_H, ℓ/(gCOD biomass.d)] hydrolysis kinetic rate equations versus retention time for the Izzett *et al.* (1992) anaerobic digester data set.

The K_M and K_S values for the saturation hydrolysis rate equation (Eq 5.15 in Table 5.1) are found by the same linearization methods, the only difference being that for saturation kinetics, the concentration variable is S_{bp}/Z_{AD} instead of S_{bp}. The K_M and K_S values so obtained are listed in Table 5.4. The specific hydrolysis rate, r_h/Z_{AD} (gCOD organics/ gCOD biomass.d) versus the saturation ratio S_{bp}/Z_{AD} (gCOD organics/ gCD biomass) graphs obtained for the saturation rate equation from the three linearization methods are shown in Fig 5.7 with the Izzett experimental data. As with the Monod kinetics, although method (i) gives the highest R^2 (0.979), method (ii) fits the experimental data marginally best at the shortest retention time (7d). For saturation kinetics also, linearization method (iii) showed that the 15d retention time data is an outlier and is the reason for the low R^2 value (0.699) for all five retention time data. Excluding the 15d data significantly improved the R^2 value for method (iii) (0.897). The average K_M and K_S values obtained from the three methods, with the 15d retention time data excluded for method (iii), are given in Table 5.4. As with the Monod equations, Fig 5.7 shows that even though different K values are obtained with the three different methods, the specific hydrolysis rate (r_h/Z_{AD}) versus saturation ratio (S_{bp}/Z_{AD}) curves obtained from each and the average are virtually the same and plot very closely to one another. Moreover, each of the four different hydrolysis kinetics equations yield near identical specific hydrolysis rate (r_h/Z_{AD}) versus biodegradable COD acidogen biomass concentration ratio (S_{bp}/Z_{AD}) curves.

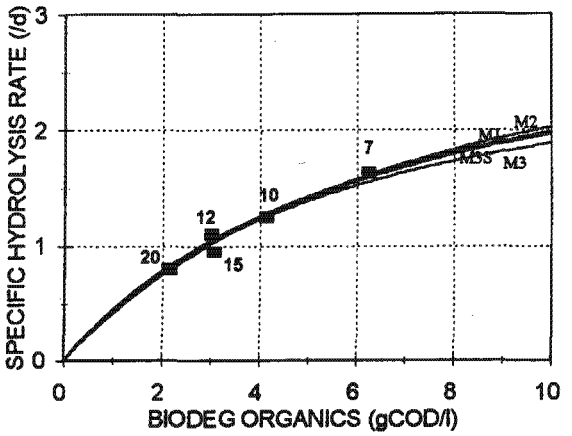

Fig 5.6: Specific hydrolysis rate [r_h/Z_{ad}, gCOD organics/(g COD biomass .d)] versus residual biodegradable organics concentration (S_{bp}, gCOD/ℓ) calculated for Monod hydrolysis kinetic rate equation with constants determined from the Lineweaver-Burke (M1), inversion (M2) and Eadie-Hofstee (M3) linearization and regression methods for the Izzett *et al* (1992) anaerobic digester data from 7 to 20 days retention time; experimental data (■) also shown.

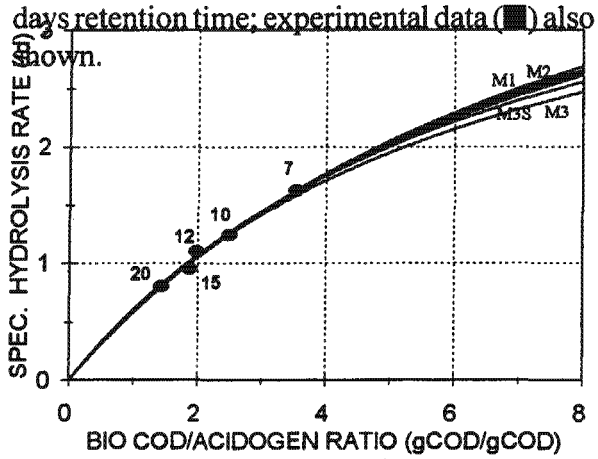

Fig 5.7: Specific hydrolysis rate [r_h/Z_{ad}, gCOD organics/(g COD biomass .d)] versus residual biodegradable organics to acidogen biomass concentration ratio (S_{bp}/Z_{ad} , gCOD/gCOD) calculated for saturation hydrolysis kinetic rate equation with constants determined from the Lineweaver-Burke (M1), inversion (M2) and Eadie-Hofstee (M3) linearization and regression methods for the *Izzett et al* (1992) anaerobic digester data from 7 to 20 days retention time; experimental data (●) also shown.

Table 5.3: Izzett *et al.* (1992) 7 to 20 d retention time (R) anaerobic digester measured influent* (S_{ti}) and effluent* (S_{te}) COD concentrations, influent unbiodegradable (S_{upi}) and biodegradable COD (S_{bpi}) concentrations for an unbiodegradable COD fraction ($f_{PS'up}$) of 0.36, calculated residual biodegradable COD concentration (S_{bp}) (Eq 5.34), change in biodegradable concentration across digester (ΔS_{bp}), observed hydrolysis rate ($r_h = dS_{bp}/R + b_{AD}Z_{AD}$, Eq5.23), acidogen biomass concentration (Z_{AD}), specific hydrolysis rate [r_h/Z_{AD})] and the 1st order and 1st order specific hydrolysis rate constants (K_h and K_H). All mass units in gCOD.

R	$^*S_{ti}$	$^*S_{te}$	S_{upi}	S_{bpi}	S_{bp}	ΔS_{bp}	r_h	Z_{AD}	r_h/Z_{AD}	K_h	K_H
d	g/ℓ	g/ℓ	g/ℓ	g/ℓ	g/ℓ	g/ℓ	g/(ℓ.d)	g/ℓ	gCOD S_{bp}/(gCOD Z_{AD}.d)	/d	ℓ/(gCOD Z_{AD}.d)
7	43.3	23.637	15.58	25.83	6.24	19.59	2.871	1.765	1.586	0.46	0.261
10	40.7	20.521	14.66	24.1	4.142	19.96	2.064	1.654	1.207	0.498	0.301
12	39.2	18.678	14.12	22.23	3.018	19.21	1.663	1.511	1.059	0.551	0.365
15	42.4	19.969	15.25	25.29	3.065	22.23	1.548	1.625	0.912	0.505	0.311
20	42.6	19.005	15.33	25.01	2.151	22.86	1.204	1.495	0.764	0.56	0.374
									Mean**	0.515	0.322

* Measured total unfiltered COD. The VFA concentration was subtracted from this in conformity with Eq 5.16 when calculating the Z_{AD} because this concentration is already hydrolysed and produces negligible biomass in the digester. The unbiodegradable soluble COD concentration was assumed zero. The fermentable (non-VFA) soluble COD (Fig 5.3) was included in the S_{bpi} (in conformity with Eq 5.16) because these organics pass through the hydrolysis process like the S_{bpi}. The unbiodegradable COD concentration (S_{upi}) of the sludge was calculated from the influent total unfiltered COD as listed and therefore included the soluble COD. This was done to approximate the unbiodegradable COD concentration of the 'pristine' sewage sludge before any acidogenesis commenced. This is approximate because hydrogen is generated and lost in the acidogenesis that takes place in the sludge before feeding to the digester. ** Mean of all five retention time values.

Table 5.4: Monod and saturation kinetics K constants and correlation coefficients (R^2) for the anaerobic digester data of Izzett *et al.* (1992) obtained from Lineweaver-Burke (M1), inversion (M2) and Eadie-Hofstee (M3) linearization and regression methods, for the Eadie-Hofstee (M3) method without the 15 day retention time data (M3S), and the averages of the M1, M2 and M3 and the M1, M2, and M3S methods for unbiodegradable fraction ($f_{Sps'up}$) of 0.36.

Kinetic rate	Monod kinetics			Saturation kinetics		
Linearization Method	K_m	K_s	R^2	K_M	K_S	R^2
Units	g organics/(g biomass.d)	g organics/ℓ	-	g organics/(g biomass.d)	g organics/g biomass	-
Method 1 (M1)	3.33	6.81	0.948	5.44	8.35	0.979
Method 2 (M2)	3.55	7.49	0.876	5.61	8.69	0.823
Method 3 (M3)	2.94	5.55	0.688	4.46	6.44	0.699
Method 3S (M3S)	3.14	5.98	0.888	4.77	6.91	0.897
Average M1, M2, M3	3.27	6.62	-	5.17	7.82	-
Average M1, M2, M3S	3.34	6.76	-	5.27	7.98	-

The unbiodegradable fraction of sludge ($f_{PS'up}$) influences the calibration results of the different hydrolysis/acidogenesis rate equations. For the more complex approach in Chapter 4, it was found that the lowest coefficient of variation (C_{var}, standard deviation/mean) for the first order (C_{var} = 0.017) and first order specific (C_{var} = 0.049) hydrolysis equations at $f_{PS'up}$ = 0.34 and 0.32 respectively and the highest correlation coefficient (R^2) for the Monod (R^2=0.98) and saturation (R^2=0.99) equations at $f_{PS'up}$ = 0.36. For this simpler steady state model the results are virtually the same. For the first order and first order specific hydrolysis equations, the lowest coefficient of variation (C_{var}) is at $f_{PS'up}$ = 0.34 (C_{var} = 0.040) and 0.32 (C_{var} = 0.074) respectively (Fig 5.8a) and the highest correlation coefficient (R^2) for the Monod (R^2=0.945) and saturation (R^2=0.972) equations at $f_{PS'up}$ = 0.37 (Fig 5.8b). It is clear that the steady state model gives almost the same results as the more complex hydrolysis model derived for UCTADM1. Even though this simpler steady state model yields different K values to the more complex model for reasons described above, the specific hydrolysis rate (r_h/Z_{AD}) versus biodegradable COD concentration (S_{bp}) curves obtained from the model are virtually the same as for the more complex model, and similarly for the saturation kinetics.

With the hydrolysis rate kinetic constants determined from the Izzett *et al.* (1992) experimental results for the four different kinetic hydrolysis rate equations, plots of the %COD removal (i.e. %COD converted to methane, Eq 5.32) versus retention time (R) calculated from the four hydrolysis rate equations are shown in Fig 5.9. It is clear that the different rate equations give virtually identical results at long retention times (>10d), but that critical differences between them arise at short retention times (<10d). It seems, therefore, that different digester failure retention times are predicted by different hydrolysis rate equations. However, this is not so because the hydrolysis process is not the one that causes digester failure - it is loss of methanogen species activity, usually the acetoclastic methanogens, that causes the digester pH to decrease that leads to failure. The low pH and high volatile fatty acid (VFA) concentration reduces the hydrolysis rate but does not cause it to stop (O'Rourke, 1968, Ristow *et al.*, 2004).

From the above evaluation and Fig 5.9, it can be concluded that the mixture of primary and humus sludge tested by Izzett *et al.* (1992) conforms very closely to both the Monod and saturation kinetics, because the % COD removal increases gradually with increasing retention time. From the Fig 5.9 it can be seen that digesters at very long retention times (>60d) are required to determine the $f_{PS'up}$ and at short retention times (<15d) to calibrate and determine the best hydrolysis rate equation.

5.5.4 Calculating the Constants in the Hydrolysis Kinetic Equations - O'Rourke (1968) Results

O'Rourke (1968) studied the kinetics of anaerobic sludge treatment at ambient temperatures,since at the time, most AD systems were operated at 35°C, and little was known about the performance of the systems at ambient temperatures. To determine the kinetics of AD at the ambient temperatures and the influence of temperature, digesters were fed a primary sludge concentration of 28.4 gCOD/ℓ and operated at 35, 25, 20 and 15°C and hydraulic retention times from 60 days to as low as 2.75 days, in which methanogenesis had failed. For this evaluation, only the methanogenic systems operated at 35°C are considered, of which there were five, i.e. 7.5, 10, 15, 30 and 60d systems. The experimental results of these five systems are listed in Table 5.5.

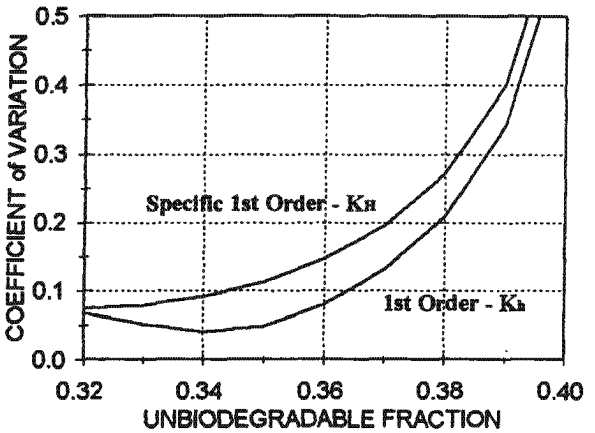

Fig 5.8a: Coefficient of variation versus unbiodegradable COD fraction of the primary sludge ($f_{PS'up}$) for the 1st order and 1st order specific hydrolysis equations for the Izzett *et al.* digester data set.

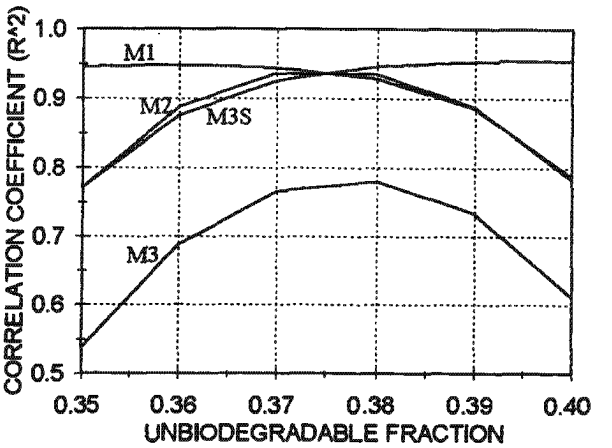

Fig 5.8b: Regression correlation coefficient (R^2) versus unbiodegradable COD fraction of the primary sludge ($f_{PS'up}$) for the Lineweaver-Burke (M1), inversion (M2) and Eadie-Hofstee linearization methods, with (M3) and without (M3S) the 15 day retention time data, with the Monod hydrolysis rate equation for the Izzett *et al.* digester data set.

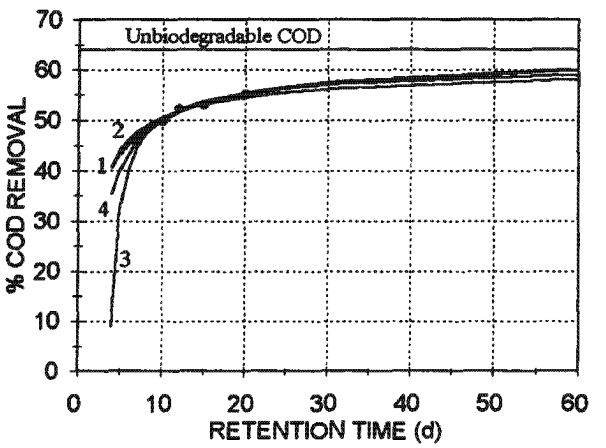

Fig 5.9: Percentage COD removal versus retention time for the 1st order (1), 1st order specific (2), Monod (3) and saturation (4) hydrolysis rate equations showing also the Izzett *et al.* experimental data at 7, 10, 12, 15 and 20 days.

Table 5.5: Experimental data measured by O'Rourke (1968) on completely mixed mesophilic (37°C) anaerobic digesters at 7 to 60 days retention time fed primary sludge.

Retention time (d)	7.5	10	15	30	60
Influent COD gCOD/ℓ	28.4	28.4	28.4	28.4	28.4
Influent VFA gCOD/ℓ	1020	1020	1020	1020	1020
Influent Lipids g/ℓ	12.6	12.6	12.6	12.6	12.6
Influent Cellulose g/ℓ	4.47	4.47	4.47	4.47	4.47
Influent Proteins g/ℓ	6.4	6.4	6.4	6.4	6.4
Influent VSS g/ℓ	18.4	18.4	18.4	18.4	18.4
Effluent COD gCOD/ℓ	12.4	11.7	11.8	11.8	10.3
Effluent VFA gCOD/ℓ	0.14	0.09	0.06	0.06	0.03
Effluent Lipids g/ℓ	5.05	4.66	40.7	4.45	3.52
Effluent Cellulose g/ℓ	0.41	0.34	0.44	0.36	0.33
Effluent Proteins g/ℓ	4.32	4.33	4.35	3.78	3.67
Effluent VSS g/ℓ	8.3	8.1	7.2	7.1	6.6
Gas Composition %CH_4	?	?	?	?	?
Gas prod mℓ CH_4/gCOD	308	328	330	350	347
COD balance (%)	99.7	100.9	101.6	105.3	99.4
FSA released	315	201	195	183	267
Effluent Alk mg/ℓ as CaCO3	1800	1600	1800	2000	2300
Digester pH	6.9-7.3	6.8-7.3	6.9-7.3	7.0-7.4	7.0-7.4

Initially, all five retention time data were analysed in the identical way as the five retention time data of Izzett *et al.* (1992). From this analysis it was found that the validity of the hydrolysis kinetic constants obtained was very sensitive to the unbiodegradable COD fraction ($f_{PS'up}$). Values higher than 0.338 yielded negative effluent biodegradable COD concentrations (S_{bp}). This set an upper limit of 0.338 on the $f_{PS'up}$ value. A lower $f_{PS,up}$ for primary sludge seems reasonable in comparison with the 0.36 value obtained for the mixture of primary and humus sludge. Furthermore, the R^2 values for the Monod and saturation models were very low (<0.60) for all reasonable $f_{PS,up}$ from 0.32 to 0.34 and $f_{PS,up} > 0.336$ yielded negative K_s values with linearization method (iii) (because $S_{bp} < 0$). The best $f_{PS,up}$ value was 0.334 - it yielded the lowest C_{var} for the first order and first order specific hydrolysis equations and the highest R^2 values (0.54 - 0.60) for the Monod and saturation equations. The calculated K_h and K_H rates and the Monod and saturation kinetics constants for all five retention times for $f_{PS'up} = 0.334$ are listed in Tables 5.6 and 5.7 respectively. The average K_h and K_H rates over the five retention times are 1.591 /d and 1.538 ℓ/(gCOD biomass.d) respectively. The K_h and K_H rates are plotted versus R in Fig 5.10 together with the Izzett *et al.* data K_h and K_H rates. The O'Rourke K rates are significantly higher and vary widely over 7.5 to 60 days retention time. Higher K rates are expected from the O'Rourke data, because 'pure' primary sludge would be expected to hydrolyse faster than a mixture of primary and humus sludge. The large variation of the K values is due to the sensitivity of the hydrolysis equations to the measured effluent total COD concentration (see Table 5.6), which do not decrease consistently with retention time (as anticipated by the hydrolysis equations). This is also the reason for the low correlation coefficients (R^2) obtained from the three linearization methods for the Monod and saturation equations (Table 5.7).

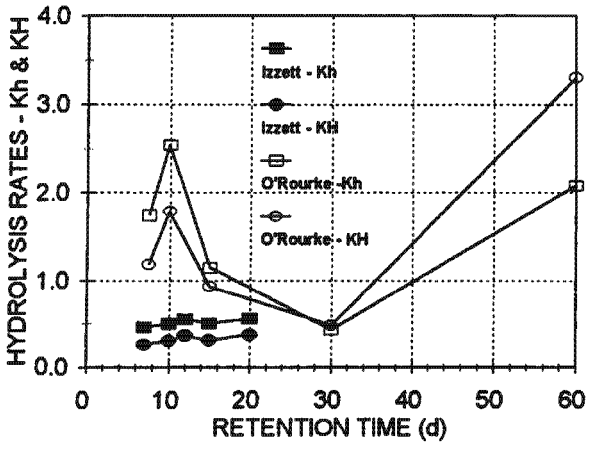

Fig 5.10: Hydrolysis rate constants for the 1st order (K_h, /d) and 1st order specific [K_H, ℓ/(gCOD biomass.d)] hydrolysis kinetic rate equations versus retention time for the Izzett *et al.* and O'Rourke anaerobic digester data sets.

To try to bring some consistency to the K rates obtained from the O'Rourke data, the 60 day retention time system was used to determine the $f_{PS'up}$ and the three shortest retention time systems (7.5, 10 and 15d) to determine the K rates, i.e. the 30d system was omitted from the analysis, which seems reasonable from Fig 5.10. For the 60d system, a $f_{PS'up}$ = 0.338 yielded a very low effluent biodegradable COD, i.e. S_{bp} = 0.041 gCOD/ℓ (0.340 makes it -ve). For this $f_{PS'up}$, determining the hydrolysis rate r_h and K rates with the 7.5, 10 and 15d retention time systems yielded (i) the same r_h rates determined previously for these retention times with $f_{PS'up}$ = 0.334 (see Table 5.6 and 5.8), (ii) the K_h and K_H rates still varied considerably, from 1.296 to 3.034 /d and 1.050 to 2.129 ℓ/(gCOD.d) at 15 and 10 days retention time respectively (Table 5.8) with little improvement in the coefficient of variation (C_{var}), and (iii) lower R^2 values for the Monod and saturation kinetics (Table 5.9). The reason for (ii) and (iii) for the three retention time systems compared with the five retention time systems is because the measured effluent COD concentration from the 15d system is higher than that from the 10d system, which is contrary to the functional form of the hydrolysis equations. Furthermore, while the K_m and K_M rates increased, the increase was not large enough to indicate that primary sludge hydrolysed faster than a mixture of primary and humus sludges. Accordingly, the 15 day system data was also removed from the data set and the K rates calculated with only the 7.5 and 10d system data (see Tables 5.8 and 5.10). The calculated K_h and K_H rates at 7.5 and 10d retention time do not change, only the average changes because it is based on only the 7.5 and 10d system K rates (Table 5.8). The average 1st order K_h rate and 1st order specific K_H rate constants obtained are 2.474 /d and 1.714 ℓ/(mgCOD.d) respectively (Table 5.8). Because there are only two systems and 2 degrees of freedom (i.e. 2 unknowns), the R^2 values for the Monod and saturation equations are 1.00 (i.e. perfect fit, Table 5.10). The percentage COD removal versus retention time calculated from the four calibrated hydrolysis equations for the 7.5 and 10d system data only is shown in Fig 5.11.

Table 5.6: O'Rourke (1968) 7.5 to 60 d retention time (R) anaerobic digester measured influent* (S_{ti}) and effluent* (S_{te}) COD concentrations, influent unbiodegradable (S_{upi}) and biodegradable COD (S_{bpi}) concentrations for an unbiodegradable COD fraction ($f_{PS'up}$) of 0.334, calculated biodegradable COD concentration (S_{bp}) (Eq 5.36), change in biodegradable concentration across digester (ΔS_{bp}), observed hydrolysis rate ($r_h = dS_{bp}/R+b_{AD}Z_{AD}$, Eq 5.23), acidogen biomass concentration (Z_{AD}), specific hydrolysis rate [r_h/Z_{AD})] and the 1st order and 1st order specific hydrolysis rate constants (K_h and K_H). All mass units in gCOD.

R	$^*S_{ti}$	$^*S_{te}$	S_{upi}	S_{bpi}	S_{bp}	ΔS_{bp}	r_h	Z_{AD}	r_h/Z_{AD}	K_h	K_H
d	g/ℓ	g/ℓ	g/ℓ	g/ℓ	g/ℓ	g/ℓ	g/(ℓ.d)	g/ℓ	gCOD S_{bp}/ (gCOD Z_{AD}.d)	/d	ℓ/ (gCOD Z_{AD}.d)
7.5	28.4	12.4	9.486	17.894	1.301	16.593	2.273	1.473	1.543	1.746	1.186
10	28.4	11.7	9.486	17.894	0.7	17.195	1.778	1.425	1.248	2.541	1.784
15	28.4	11.8	9.486	17.894	1.021	16.874	1.175	1.234	0.953	1.152	0.934
30	28.4	11.8	9.486	17.894	1.361	16.533	0.588	0.893	0.658	0.432	0.483
60	28.4	10.3	9.486	17.894	0.154	17.74	0.321	0.63	0.51	2.082	3.305
									Mean**	1.591	1.538

* See note on Table 5.3.
**Mean of all five retention time values.

Table 5.7: Monod and saturation kinetics K constants and correlation coefficients (R^2) for the 7.5 to 60d anaerobic digester data of O'Rourke (1968) obtained from Lineweaver-Burke (M1), inversion (M2) and Eadie-Hofstee (M3) linearization and regression methods and the mean values of the three methods for unbiodegradable fraction ($f_{PS'up}$) of 0.334.

Kinetic rate	Monod kinetics			Saturation kinetics		
Linearization Method	K_m	K_s	R^2	K_M	K_S	R^2
Units	g organics/ (g biomass.d)	g organics/ℓ	-	g organics/ (g biomass.d)	g organics/ g biomass	-
Method 1 (M1)	1.174	0.195	0.577	1.303	0.306	0.349
Method 2 (M2)	0.939	0.003	0.604	0.674	-0.17	0.809
Method 3 (M3)	1.177	0.127	0.108	0.69	-0.184	0.128
Average M1, M2, M3	1.097	0.108	-	0.889	-0.016	-

Table 5.8: O'Rourke (1968) 7.5 to 60d retention time (R) anaerobic digester measured influent* (S_{ti}) and effluent* (S_{te}) COD concentrations, influent unbiodegradable (S_{upi}) and biodegradable COD (S_{bpi}) concentrations for an unbiodegradable COD fraction ($f_{PS'up}$) of 0.338, calculated residual biodegradable COD concentration (S_{bp}) (Eq 5.36), change in biodegradable concentration across digester (ΔS_{bp}), observed hydrolysis rate ($r_h = dS_{bp}/R+b_{AD}Z_{AD}$, Eq5.23), acidogen biomass concentration (Z_{AD}), specific hydrolysis rate [r_h/Z_{AD})] and the 1st order and 1st order specific hydrolysis rate constants (K_h and K_H). All mass units in gCOD. Note that r_h, Z_{AD} and r_h/Z_{AD} are identical to the values calculated in Table 5.4 for $f_{PS'up}$ of 0.334.

R	S_{ti}	S_{te}	S_{upi}	S_{bpi}	S_{bp}	ΔS_{bp}	r_h	Z_{AD}	r_h/Z_{AD}	K_h	K_H
d	g/ℓ	g/ℓ	g/ℓ	g/ℓ	g/ℓ	g/ℓ	g/(ℓ.d)	g/ℓ	gCOD S_{bp}/ (gCOD Z_{AD}.d)	/d	ℓ/ (gCOD Z_{AD}.d)
7.5	28.4	12.4	9.599	17.781	1.188	16.593	2.273	1.473	1.543	1.914	1.299
10	28.4	11.7	9.599	17.781	0.586	17.195	1.778	1.425	1.248	3.034	2.129
15	28.4	11.8	9.599	17.781	0.907	16.874	1.175	1.234	0.953	1.296	1.05
30	28.4	11.8	9.599	17.781	1.247	16.553	0.588	0.893	0.658	0.471	0.527
60	28.4	10.3	9.599	17.781	0.04	17.74	0.321	0.63	0.51	7.876	12.503
									Mean**	2.081	1.493
									Mean***	2.474	1.714

* See note on Table 5.3. **Mean of 7.5, 10 and 15d retention time values.
***Mean of 7.5 and 10d retention time values only.

Table 5.9: Monod and saturation kinetics K constants and correlation coefficients (R^2) for the O'Rourke 7.5, 10 and 15 d retention time data obtained from Lineweaver-Burke (M1), inversion (M2) and Eadie-Hofstee (M3) linearization and regression methods for unbiodegradable fraction ($f_{PS'up}$) of 0.338.

Kinetic rate	Monod kinetics			Saturation kinetics		
Linearization Method	K_m	K_s	R^2	K_M	K_S	R^2
Units	g organics/ (g biomass.d)	g organics/ℓ	-	g organics/ (g biomass.d)	g organics/ g biomass	-
Method 1 (M1)	1.35	0.1	0.026	1.17	-0.016	0
Method 2 (M2)	1.91	0.5	0.418	1.32	0.063	0.519
Method 3 (M3)	1.08	-0.12	0.048	1	-0.117	0.123

Table 5.10: Monod and saturation kinetics K constants and correlation coefficients (R^2) for the O'Rourke 7.5 and 10d retention time data for unbiodegradable fraction ($f_{PS'up}$) of 0.338. Note that all three linearization and regression methods give the same results and perfect correlation for a pair of results.

Kinetic rate	Monod kinetics			Saturation kinetics		
Linearization Method	K_m	K_s	R^2	K_M	K_S	R^2
Units	g organics/ (g biomass.d)	g organics/ℓ	-	g organics/ (g biomass.d)	g organics/ g biomass	-
Methods 1, 2 & 3	2.004	0.355	1	2.047	0.263	1

It can be seen that with primary sludge only, a high %COD removal (> 60%) is obtained even at short retention times (<10d). In contrast, because humus sludge in the primary and humus sludge mixture hydrolyses more slowly than primary sludge, the %COD removal is only 55% at significantly longer retention times (>20d) (Fig 5.9). A comparison between the Monod curves obtained for the primary sludge (O'Rourke data) and the primary and humus sludge mixture (Izzett *et al.* data) calculated from the respective Monod K_m and K_s values is shown in Fig 5.12 together with the experimental data. Figure 5.12 reinforces the conclusion above. because with its low K_s value, higher rates of hydrolysis are maintained with 'pure' primary sludge for much lower biodegradable COD concentrations, S_{bp} (and therefore shorter retention times) than for the primary and humus sludge mixture. Because such similar results were obtained for the steady

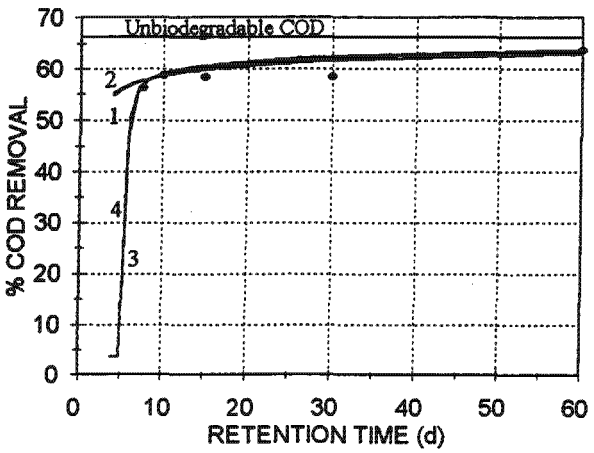

Fig 5.11: Percentage COD removal versus retention time for the 1st order (1), 1st order specific (2), Monod (3) and saturation (4) hydrolysis rate equations calibrated on the 7.5 and 10 day retention time systems of O'Rourke showing also the experimental data at 7.5, 10, 15, 30 and 60 days.

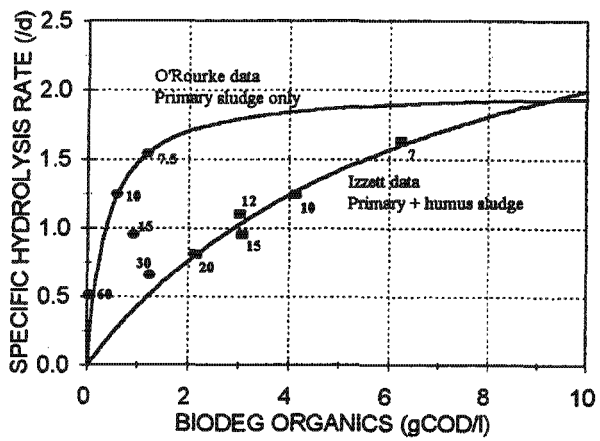

Fig 5.12: Specific hydrolysis rate [r_h/Z_{ad}, gCOD organics/(g COD biomass .d)] versus biodegradable organics concentration (S_{bp}, gCOD/ℓ) calculated for Monod hydrolysis kinetic rate equation for the Izzett *et al.* (1992) (all 5 retention times) and O'Rourke (1968) (7.5 and 10d retention times) anaerobic digester data showing also their experimental data (■, Izzett) and (●, O'Rouke) with retention time indicated.

state model for the Izzett *et al.* (1992) and O'Rourke data, the calibration of the hydrolysis equations with the Ristow *et al.* (2004a) data was not repeated - similar results would have been obtained as already presented in Chapter 4.

5.6 STEADY STATE MODEL DEVELOPMENT - STOICHIOMETRY

Once the concentration of hydrolysable organics utilized in the anaerobic digester is known from the hydrolysis kinetics, the sludge composition and stoichiometry of the biological processes following the hydrolysis process and the utilization of the influent VFA concentration (S_{bsai}), define the digester gas composition and pH.

McCarty (1974) gives the following general stoichiometric reaction for the overall AD system fed an organic waste of empirical composition $C_XH_YO_ZN_A$ to methane, carbon dioxide and biomass (of composition $C_5H_7O_2N$) as final end products:

$$C_XH_YO_ZN_A + \left(2X+A-Z-\frac{9ED}{20}-\frac{(1-E)D}{4}\right)H_2O \rightarrow \left(X-A-\frac{ED}{5}-\frac{(1-E)D}{8}\right)CO_2 + \left(\frac{(1-E)D}{8}\right)CH_4 + \left(\frac{ED}{20}\right)C_5H_7O_2N + \left(A-\frac{ED}{20}\right)NH_4^+ + \left(A-\frac{ED}{20}\right)HCO_3^- \quad (5.38a)$$

where D = $4X + Y - 2Z - 3A$ = the e^- donating capacity of biomass = $20e^-$/mol for $C_5H_7O_2N$

In Eq 5.38a, E is the fraction of hydrolysed COD utilized (ΔS_{bp}) that is converted to biomass (Z_{AD}), which from Eqs 5.24 or 5.36 is

$$E = \frac{Z_{AD}}{S_{bpi}-S_{bp}} = \frac{Y_{AD}}{[1+b_{AD}R(1-Y_{AD})]} \quad (5.38b)$$

The gCOD/mol and molar mass (MM) of the influent organics $C_XH_YO_ZN_A$ are given by:

$COD = 8[Y+2(2X-Z)-3A]$ gCOD/mol (5.39a)
$MM = 12X+Y+16Z+14A$ g drymass/mol or gVSS/mol (5.39b)

where VSS = volatile suspended solids

The influent VFA concentration are assumed to be acetate species with a MM = 60 g/mol and COD=64 gCOD/mol. The stoichiometry of utilization of the undissociated and dissociated acetate species by the methanogens, assuming zero sludge production (E=0 in Eq 5.38a), is

$CH_3COOH \rightarrow CH_4 + CO_2$ and (5.40a)
$CH_3COO^- + H_2O \rightarrow CH_4 + HCO_3^-$ (5.40b)

The total CH_4, CO_2 and HCO_3^- species produced is the sum of Eqs 5.38 and 5.40. The split between the undissociated and dissociated acetate species is governed by the influent pH (Eq

5.41). This split is shown versus pH in Fig 5.13 for a pK'$_a$ value for acetate of 4.68 obtained for an influent TDS concentration of 2500 mg/ℓ and a temperature of 37°C (Loewenthal *et al.*, 1989). Figure 5.13 shows that the higher influent pH, the higher the fraction of dissociated acetate species, the higher the alkalinity generation (Eq 5.40b) and therefore the higher the digester pH.

$$S_{bsHAci} = \frac{S_{bsai}}{\left(1 + 10^{pH_i - pK'_a}\right)} \quad \text{and} \quad S_{bsAci} = \frac{S_{bsai}}{\left(1 + 10^{pK'_a - pH_i}\right)} \quad \text{mgCOD/ℓ} \qquad (5.41)$$

where pH_i is the influent pH and S_{bsHAci} and S_{bsAci} the undissociated and dissociated acetate species concentration in the influent respectively.

For acidogen organism constants $Y_{AD} = 0.113$ mgCOD biomass/mg COD organics degraded and $b_{AD} = 0.041$ /d, the fraction of COD hydrolysed converted to sludge mass (E, Eq 5.38b) and methane (1-E) are shown as % in Fig 5.14. One of the major advantages of anaerobic treatment is evident in Fig 5.14, i.e. sludge production is extremely low compared with aerobic treatment - only 9 and 5% of COD degraded from 5 to 40 days retention time with practically all (91 to 95%) converted to useful methane gas.

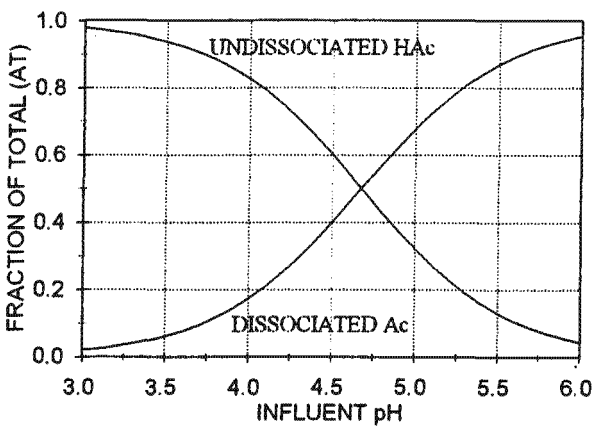

Fig 5.13: Fraction of undissociated and dissociated acetate species versus influent pH for a pK'$_a$ value of 4.68 for a TDS of 2500 mg/ℓ and temperature of 37°C.

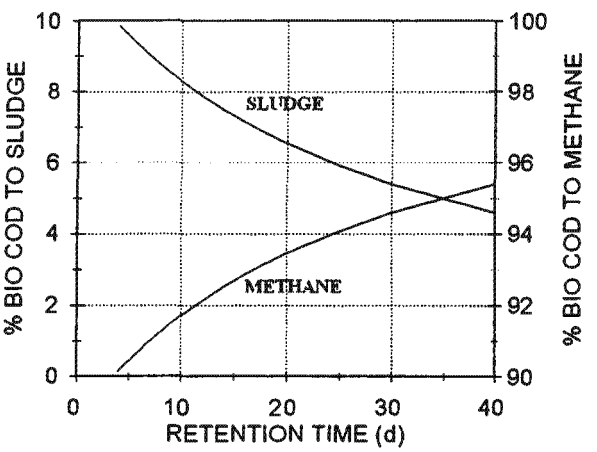

Fig 5.14: Percentage of biodegradable COD removed [$\Delta S_{bp}/S_{bpi} = (S_{bpi}-S_{bp})/S_{bpi}$] converted to sludge mass (E factor in Eq 5.38) and methane versus retention time. Although very slow, the endogenous process results in lower sludge and higher methane production at longer retention time.

5.7 STEADY STATE MODEL DEVELOPMENT - WEAK ACID/BASE CHEMISTRY

In Eqs 5.38 and 5.40, the total CO_2 produced is the sum of the gaseous CO_2 and the dissolved CO_2, which, at the near neutral pH of AD (6.5 to 7.5), is mostly in the bicarbonate (HCO_3^-) form. The proportion of the total CO_2 that is in the bicarbonate form is governed by (i) the ammonia released in the breakdown of the hydrolysable organics (Eq5.38a), which at neutral pH, picks up a proton from the dissolved CO_2 ($H_2CO_3^*$) to form saline ammonia (NH_4^+) and bicarbonate (HCO_3^-) according to $NH_3 + H_2CO_3^* \rightarrow NH_4^+ + HCO_3^-$ and (ii) the concentration of influent dissociated acetate species utilized in the digester (Eq 5.40b), which is governed by the degree of hydrolysis of the sludge prior to entry to the digester and the influent pH. The gaseous CO_2 and CH_4 produced define the gas composition, which sets the partial pressure of CO_2 (p_{CO2}). The pH of the digester is defined by the p_{CO2} and the bicarbonate concentration (HCO_3^-) generated, which is equal to the alkalinity generated. Clearly, the N content of the influent organics and the influent VFA concentration and pH are very important because these (i) define the HCO_3^- alkalinity concentration generated and p_{CO2} of the gas, both of which (ii) set the digester pH. If the N content of the influent organics is too low, lime may need to be dosed to augment the uptake of H^+ by the NH_3 released from the organics and establish the appropriate HCO_3^- concentration and p_{CO2} for the required digester pH (>6.5) (Capri and Marais, 1975). Accepting that (i) the pH is established predominantly by the carbonate weak acid/base system and (ii) the bicarbonate concentration ($[HCO_3^-]$, mol/ℓ) is generated principally from the ammonia released from the breakdown of the influent hydrolysable organics and the utilization of influent dissociated acetate species, (i.e. low influent alkalinity with respect to that generated, see Table 5.2) and (iii) equilibrium exists between the dissolved and gaseous inorganic carbon species (reasonable at long retention times), the relationship between the bicarbonate concentration, p_{CO2} and pH is given by,

$$p_{CO2} = \frac{[HCO_3^-]\left(1 + 10^{pK'_{c1}-pH} + 10^{pH-pK'_{c2}}\right)}{10^{-pK'_{HCO2}}\left(1 + 10^{pH-pK'_{c1}} + 10^{2pH-pK'_{c1}-pK'_{c2}}\right)} \quad \text{atm or mole fraction} \qquad (5.42)$$

where

$[HCO_3^-]$ = bicarbonate concentration ~ $H_2CO_3^*$ alkalinity (mol/ℓ) ~ Total alkalinity (mol/ℓ)
p_{CO2} = partial pressure of CO_2 in the gas phase
pH = -ve $\log_{10}$ of the (H^+) activity
pK'_{HCO2} = -ve $\log_{10}$ of the apparent Henry's law constant for CO_2
pK'_{C1}, pK'_{C2}, = -ve $\log_{10}$ of 1st and 2nd carbonate system apparent dissociation constants where apparent means corrected for ionic strength effects (see Loewenthal *et al.*, 1989).

Equation 5.42 is plotted in Fig 5.15 for a temperature of 37°C and a TDS of 2500 mg/ℓ at which $pK'_{C1} = 6.211$, $pK'_{C2} = 9.960$ and $pK'_{HCO2} = +1.609$ (Loewenthal *et al.*, 1989), together with the range of normal anaerobic digester operation.

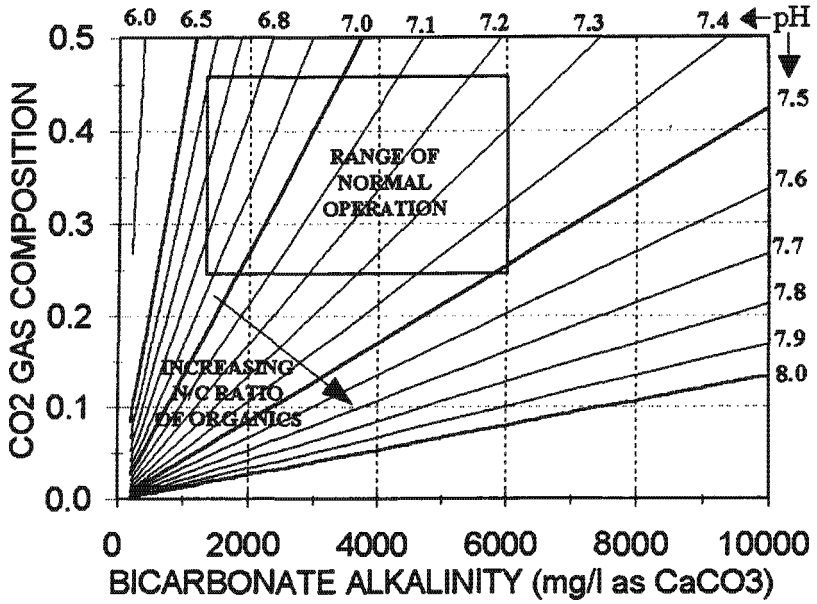

Fig 5.15: Fraction CO_2 gas composition versus reactor bicarbonate concentration (≈ alkalinity) for pH ranging from 6.5 to 8.0. Also shown is the range of normal anaerobic digester operation.

5.8 DESIGN EXAMPLE

The steady state model with the Monod hydrolysis rate equation and its associated kinetic constants (Table 5.1) are applied to the 20d retention time system of Izzett *et al.* (1992) (Table 5.2).

5.8.1 Calculating the COD Removal and Methane Production - Hydrolysis Kinetics

Total influent COD concentration (S_{ti}) = 42.59 gCOD/ℓ (measured)
Influent VFA concentration (S_{bsai}) = 2.24 gCOD/ℓ (measured)
Unbiodegradable fraction of the primary sludge ($f_{PS'up}$) = 0.36 (determined above)
Influent hydrolysable COD concentration (S_{bpi}) = (1-0.36)42.59 - 2.24 = 25.02 gCOD/ℓ (Eq 5.16)
Influent unbiodegradable COD concentration (S_{upi}) = 0.36x42.59 = 15.33 gCOD/ℓ (Eq 5.17)
Residual biodegradable COD concentration (S_{bp}) = 2.15 gCOD/ℓ (Eq 5.25)
Biodegradable COD concentration removed ($\Delta S_{bp} = S_{bpi} - S_{bp}$) = 22.87 gCOD/ℓ (Eq 5.33)
Acidogen biomass concentration (Z_{AD}) = 1.50 gCOD/ℓ (Eq 5.24)
Unbiodegradable COD concentration (S_{up}) = 15.33 gCOD/ℓ (Eq 5.26)
Total effluent COD concentration (S_{te}) = 15.33+2.15+1.50=18.98 gCOD/ℓ (Eq 5.34)
Methane production concentration (S_m) = 21.38 gCOD/ℓ influent (Eq 5.28)
Methane production from VFA = 2.24 gCOD/ℓ influent (Equal to VFA COD, Eq 5.40)
Total methane production concentration = 21.38+2.24= 23.62 gCOD/ℓ influent
Total COD concentration out ($S_{te} + S_m$) = 18.98+23.82= 42.60 gCOD/ℓ (Eq 5.31)

Hence COD balance $100(S_{te}+S_m)/S_{ti}$ = 100.0%
Methane production gas volume (Q_m) = 8.87 (ℓ methane/d)/(ℓ influent flow/d) (Eq 5.29).
Fraction of biodegradable COD removed converted to sludge mass (E) = 0.0654 (Eq 5.38b).
Fraction of biodegradable COD removed converted to methane (1-E) = 0.9346.

5.8.2 Calculating the Partial Pressure of CO_2, and the Ammonia and Alkalinity Concentrations Generated - Stoichiometry

The primary sludge composition was estimated as $C_{3.5}H_7O_2N_{0.196}$ (see Chapter 4). Hence the COD content of the sludge is 131.3 gCOD/mol (Eq 5.39a) and the hydrolysable COD concentration removed 22.87/131.3 = 0.1742 mol/ℓ. From Eq 5.38,with E=0.0654, the stoichiometric equation for the overall digestion process therefore is

$$0.1742\,C_{3.5}H_7O_2N_{0.196} + 0.1530\,H_2O \rightarrow 0.2042\,CO_2$$

$$+0.3340\,CH_4 + 0.0094\,C_5H_7O_2N + 0.0248\,NH_4^+ + 0.0248\,HCO_3^- \qquad (3.42a)$$

The influent VFA concentration was 2.240 gCOD/ℓ, which at an influent pH of 5.28 (Table 5.2) comprises 20% (0.4480 gCOD/ℓ = 0.4480/64=0.0070 mol/ℓ) undissociated (Eq 5.41a) and 80% (1.792 gCOD/ℓ=1.792/64=0.0280 mol/ℓ) dissociated acetate species (Eq 5.41b). From Eq 5.40, this yields

$$0.0070\,CH_3COOH \rightarrow 0.0070\,CH_4 + 0.0070\,CO_2 \quad \text{and} \qquad (5.43a)$$

$$0.0280\,CH_3COO^- + 0.00280\,H_2O \rightarrow 0.00280\,CH_4 + 0.00280\,HCO_3^- \qquad (5.43b)$$

Adding Eqs 5.42a, 5.43a and 5.43b yields for the total biodegradable COD utilized,

$$0.1742\,C_{3.5}H_7O_2N_{0.196} + 0.0070\,CH_3COOH + 0.0280\,CH_3COO^- + 0.1810\,H_2O \rightarrow 0.2112\,CO_2$$

$$+0.3690\,CH_4 + 0.0094\,C_5H_7O_2N + 0.0248\,NH_4^+ + 0.0528\,HCO_3^- \qquad (5.44)$$

Equation 5.44 shows that 0.0094 mol/ℓ biomass ($C_5H_7O_2N$) is formed, which is 0.0094x160gCOD/mol = 1.50 gCOD/ℓ and corresponds exactly with Eq 5.24. It also shows that 0.2112 and 0.3690 mols gaseous CO_2 and CH_4 are produced yielding a total gas volume 0.5802 mol/ℓ influent. At 24.0 ℓ gas/mol at 20°C and 1 atm pressure (Eq 5.30), this is 5.08, 8.87 and 13.95 ℓ CO_2, CH_4 and total gas volume per ℓ influent flow. It can be seen that the volume of methane production calculated from the kinetic part of the AD model is the same as that calculated from the stoichiometric part of the model, i.e. 8.87 ℓ methane/ℓ influent flow. This because the E value calculated from the kinetic model (fraction of COD removed converted to sludge mass = 0.0654, Eq 38b) was applied to the stoichiometric model. From the CO_2 and CH_4 gas production, the CO_2 gas composition (in mol fraction or partial pressure, p_{CO2}) is 5.08/13.95 = 0.364. From Eq 5.44, 0.0248 mol/ℓ ammonia and 0.0582 mol/ℓ bicarbonate alkalinity are generated. This is 0.0248x14000 = 347 mgN/ℓ and 0.0528x50000 = 2640 mg/ℓ as $CaCO_3$ respectively. Adding these generated ammonia and alkalinity concentrations to the influent concentrations (Table 5.2) yields the predicted effluent concentrations, i.e. 244+347=591 mgFSA-N/ℓ and 56+2640=2696 mg$CaCO_3$/ℓ.

5.8.3 Calculating the Digester pH - Weak Acid/Base Chemistry

With the p_{CO2} = 0.364 and HCO_3^- concentration = 2696 mg/ℓ as $CaCO_3$, the digester pH is 6.99 (Eq 5.42, Fig 5.15). Following the above procedure, a comparison between theoretically predicted and experimentally observed (i) COD removal (gCOD/ℓ) (ii) gas production (ℓ gas/d per ℓ influent/d), (iii) gas composition (%CO_2), (iv) effluent FSA concentration (mgN/ℓ), (v) alkalinity (mg/ℓ as $CaCO_3$) and (vi) digester pH are given in Figs 5.16a to f respectively for the Izzett *et al.* 7, 10, 12, 15 and 20 day retention time digesters.

5.8.4 Comparison Between Theoretically Predicted and Experimentally Observed Results

The predicted COD removal (Fig 5.16a) corresponds very well to those measured. The gas production (Fig 5.16b) is under predicted because the model is based on 100% COD balance and experimental data COD balances ranged between 107 and 109% (Table 5.2) and also due to uncertainty in the gas temperature (20°C was assumed but if it was 37°C to would be 6% higher). Because the steady state model was calibrated on COD removal (rather than on gas production, which can also be done depending on whether effluent COD or gas production data show the best consistency, i.e. sequentially decreasing or increasing respectively with retention time), the predicted COD removal conforms almost exactly to that measured (Fig 5.16a) and so the error in the experimental COD balance manifests in the gas production (Fig 5.16b). The gas composition (Fig 5.16c) corresponds very well to that measured. The predicted effluent FSA concentration (Fig 5.16d) is higher than that measured, because the model is based on 100% N balance and the N balance of experimental data range between 90 and 99% (Table 5.2). By decreasing the N content of the hydrolysable organics (A in $C_XH_YO_ZN_A$) by a small amount (5% to 0.186), the predicted effluent FSA can be made to closely fit the measured effluent FSA of the 10 to 20d retention time systems. This also will result in an improved correlation between predicted and measured alkalinity (Fig 5.16e), because with a lower N content in the sludge, less alkalinity is generated. The lower alkalinity will decrease the predicted digester pH causing it to deviate further (~0.3 pH units) from the actual measured pH, but closer to the 'corrected' measured pH (Fig 5.16f).The actual measured pH data (7.11 to 7.19) shows an inconsistency in that these pH values and the measured alkalinity and gas composition do not conform to Eq 5.42 - accepting the data that are most reliably measured, i.e. gas composition (Fig 5.16c) and alkalinity (Fig5.16e) with the five point titration method of Moosbrugger *et al.* (1992), the digester pH must be lower than that measured to conform to Eq 5.42 (see Table 5.2 and Fig 5.16f). A digester pH lower than that actually measured is quite likely, because CO_2 loss during sampling and testing will increase the pH. Despite the improvement between predicted and measured results that reducing the A value to 0.186 will yield to conform to the measured effluent N mass, the A=0.196 value in $C_XH_YO_ZN_A$ was retained because it is based in the influent N mass. Further, Chapter 4 shows that the $C_{3.5}H_7O_2N_{0.196}$ stoichiometry accepted for the primary and humus sludge composition, which was obtained from the COD, C and N mass balances over the Izzett *et al.* AD systems (Table 5.2), conforms very closely to independently measured CHON composition measurements on 'pure' primary sludge, i.e. within 96%, 100%, 95% and 99% respectively. Considering the complexity of the system and the margin of error in the experimental data, overall the steady state model predicts the anaerobic digester performance over the 7 to 20 d retention time satisfactorily for steady state design. The predictions of the more detailed two phase (aqueous-gas) integrated chemical, physical and biological processes anaerobic digester model (UCTADM1) presented in Chapter 4 are also shown in Figs 16a to f and the steady state

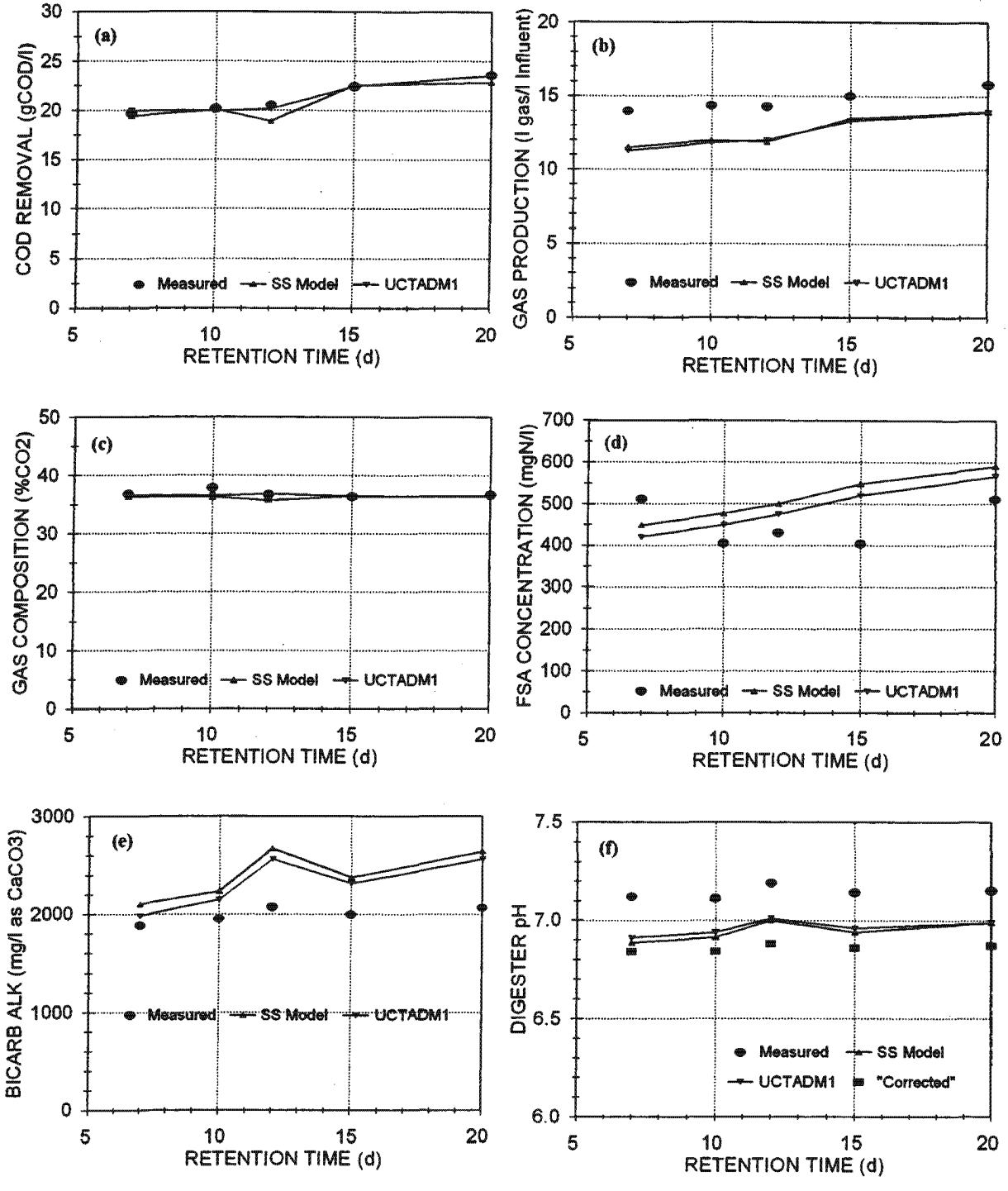

Fig 5.16: Comparison between steady state model and integrated simulation (UCTADM1) model predicted and measured COD removal (5.16a), gas production (5.16b), gas composition (5.16c), effluent FSA (5.16d), alkalinity (5.16e) and digester pH (5.16f) versus retention time for the Izzett *et al.* data set.

AD model can be seen to corelate very closely also with UCTADM1. Hence, the steady state AD model provides a reliable basis for cross-checking simulation model results.

5.9 CLOSURE

A steady state AD model for the treatment of sewage sludge has been developed. It comprises three sequential parts, (i) a kinetic part with which the influent COD hydrolysed/ utilized, gas and biomass production and effluent COD concentration are calculated for a given retention time, (ii) a stoichiometry part with which the gas composition (or partial pressure of CO_2), ammonia released and alkalinity generated are calculated from the COD utilized and the CHON composition of the hydrolysed COD and (iii) a carbonate system weak acid/base chemistry part with which the digester pH is calculated from the partial pressure of CO_2 and alkalinity generated. This model shows that for a given %COD removal, the partial pressure of CO_2 and alkalinity generated, and hence the digester pH, are governed entirely by the influent sludge composition, i.e. X, Y, Z and A in $C_XH_YO_ZN_A$ and the undissociated volatile fatty acids (VFA) species concentration of the influent.

The hydrolysis kinetic part of the model was calibrated against AD data for two types of sewage sludge, (i) a primary and humus sludge mixture extending over a retention time range of 7 to 20 days and (ii) a 'pure' primary sludge extending over a retention time range of 7.5 to 60 days. Also, four hydrolysis kinetic rate (r_h) equations were calibrated against both sludge types, viz. (i) first order ($r_h = K_h\ S_{bp}$), (ii) first order specific ($r_h = K_H\ S_{bp}\ Z_{AD}$), (iii) Monod [$r_h = K_m\ S_{bp}/(K_s + S_{bp})\ Z_{AD}$] and (iv) saturation [$r_h = K_M\ (S_{bp}/Z_{AD})/(K_S + S_{bp}/Z_{AD})\ Z_{AD}$]. Once calibrated against the particular sludge type and taking due account of experimental error, the %COD removals predicted by the four hydrolysis kinetic equations were closely similar, which made it difficult to select the best kinetic equation. Also, by varying the unbiodegradable COD fraction ($f_{PS'up}$) of the sewages sludges within a narrow range (~2%) changed the coefficient of variation (C_{var}) for the first order and first order specific kinetic equations, and the correlation coefficient (R^2) for the Monod and saturation kinetic equations. Within the 2% range in unbiodegradable COD fraction, the different hydrolysis kinetic equations yielded best statistical fits between theoretically predicted and experimentally measured COD removals (or gas production) at different $f_{PS'up}$ values. It is concluded that for both types of sewage sludge, taking due account of experimental error (i.e. COD mass balance errors) each calibrated kinetic equation is equally good for calculating the %COD removal and gas production versus retention time. For each sewage sludge type, different hydrolysis kinetic rates and unbiodegradable COD fractions were obtained which showed that the pure primary sludge hydrolysed significantly faster and had a lower unbiodegradable particulate COD fraction ($f_{PS'up} = 0.33$) than the primary and humus sludge mixture ($f_{PS'up} = 0.36$). Anaerobic digesters treating pure primary sludge therefore will achieve higher COD or VSS removals at shorter retention times than digesters treating a primary and humus sludge mixture.

Once the COD removal is known from the hydrolysis kinetics part of the model, the CHON composition of the COD removed and the dissociated acetate species concentration in the influent (all utilised in the digester) fixes the gas composition (or partial pressure of CO_2), the ammonia released and the bicarbonate generated (equal to alkalinity generated) through the C, H, O and N mass balances based stoichiometry part of the model. From the influent COD, C and N masses of the primary and humus sludge digesters, a sludge composition of $C_{3.5}H_7O_2N_{0.196}$ has been

determined (see Chapter 4). With this sludge composition and measured influent VFA concentration and pH, from which the dissociated acetate species concentration was calculated, the stoichiometry part of the model predicted the experimentally observed gas composition (or CO_2 partial pressure), ammonia released and alkalinity generated well, taking due account of experimental error. With the CO_2 partial pressure and alkalinity generated, the digester pH was calculated from the carbonate system weak acid/base chemistry part of the model. The model predicted pH was significantly lower (by ~0.30 pH units) than that experimentally measured. From the observed CO_2 partial pressure and alkalinity, which can be measured reliably, there is an error in the measured digester pH, probably due to CO_2 gas loss in sampling and measurement. The 'corrected' measured pH should be between 6.84 and 6.88 for the 7, 10, 12, 15 and 20 day retention time systems and the predicted pH is 0.08 to 0.12 pH units higher than these corrected values. A significantly closer correlation between theoretically calculated and experimentally measured digester effluent FSA, alkalinity and pH can be obtained if the N content of the feed sludge is decreased from 0.196 to 0.186 based on the measured N mass exiting the digesters rather than on that entering the digesters. Taking into consideration experimental error (C and N mass balances errors) it is concluded that the steady state model predicts very well the observed 7 to 20 day retention time primary and humus sludge digester performance. The stoichiometry and carbonate system weak acid/base chemistry part of the model could not be checked against the 'pure' primary sludge digester data set of O'Rourke (1968) because the N concentrations in the effluent were not measured for this data set. The steady state AD model also correlated very closely with the predictions of the two phase (aqueous-gas) integrated chemical, physical and biological processes dynamic simulation anaerobic digester model (UCTADM1) presented in Chapter 4. Provided the hydrolysis rate of the particulate biodegradable organics is known for a particular sewage sludge, the steady state model is useful to (i) estimate retention time, reactor volume, gas production and composition for a required system performance like COD (or VSS) removal, (ii) investigate the sensitivity of the system performance to the design and operation parameters, (iii) provide a basis for cross-checking simulation model results, and (iv) estimate product stream concentrations for design of down- (or up-) stream unit operations of the wastewater treatment plant.

CHAPTER 6

MODELLING PHYSICAL CHEMICAL PROCESS IN 3 PHASES - TOWARDS INCORPORATING THE SOLID PHASE IN THE KINETIC MODEL FOR ANAEROBIC DIGESTION (UCTADM1)

6.1 INTRODUCTION

Aeration of anaerobic digester liquor (ADL), either deliberate or inadvertent, strips CO_2 from the ADL resulting in an increase in pH. At higher pH various calcium and magnesium phosphates (and possibly carbonates) precipitate and NH_3 stripping occurs. Loss of CO_2 thus can be problematic, with magnesium phosphate precipitants such as struvite causing pipe blockages (e.g. Borgerding, 1972; Mohajit *et al.*, 1989; Mamais *et al.*, 1994). This process has been exploited as a treatment method for removal of the high concentrations of N and/or P commonly found in ADL, particularly in those from digestion of waste sludge from biological phosphorus removal activated sludge systems (Pitman *et al.*, 1989, 1995; Woods *et al.*, 1999; Stratful *et al.*, 1999). A model that can conveniently handle three phase mixed weak acid/base chemistry will be helpful to optimize the aeration treatment method for ADL and to develop and evaluate alternative treatment methods. Further, such a model will find potential application in a variety of other chemical treatment systems.

The three phase mixed weak acid/base chemistry, when integrated into the kinetic model for anaerobic digestion developed in Chapter 4, would provide a useful extension to the anaerobic digestion model, in that it would enable the anaerobic model to predict solids precipitation. This would be useful to the user, because it would show potential precipitation problems that can then be taken into account during the design stage, rather than addressing a precipitation problem after the design has been implemented. Further, it would also extend the troubleshooting capability of the anaerobic digestion model for existing treatment plants that include anaerobic digestion as a unit operation.

In Chapters 3 and 4, two phases (aqueous and gas) of the Musvoto *et al.* (1997) three phase weak acid/base chemical-physical kinetic model were integrated into the biological processes of C and N removal in activated sludge systems and into the biological processes of anaerobic digestion respectively. Musvoto *et al.* (1997) describe the development of an integrated mass balances based kinetic model to simulate the chemical-physical processes of (i) the carbonate[1] system in

---

[1] In this thesis project report, the term 'carbonate system' refers to the inorganic carbon system. The term 'carbonate system species' refers to all the species making up the total inorganic carbon (denoted C_T), viz. $H_2CO_3^*$ comprising dissolved CO_2 and H_2CO_3, bicarbonate HCO_3^- and carbonate CO_3^{2-}, and the term 'carbonate species' refers to the CO_3^{2-} species only. The same nomenclature applies to the term 'phosphate system', 'phosphate system species', denoted P_T, and 'phosphate species'.

three phases (solid-aqueous-gas) and (ii) the mixed water[2], carbonate, phosphate[1], short chain fatty acid (SCFA) and ammonia weak acid/base systems in single (aqueous) phase. The model was validated for the steady state (time independent) conditions by comparing predicted equilibrium results with predictions from well established equilibrium chemistry based models in the literature, such as (i) Stasoft I (Loewenthal *et al.*, 1988) and Stasoft III (Friend and Loewenthal, 1992) for the three phase carbonate system in pure water and (ii) Loewenthal *et al.* (1989, 1991) for the single aqueous phase behaviour of the water, carbonate, phosphate, SCFA and ammonia mixed weak acid/base systems.

The model includes H^+ as a compound (and therefore pH), and is based on the kinetics of the forward and reverse reactions for the dissociation of the weak acid/bases. The weak acid/bases included in the model are water, carbonate, ammonium, phosphate and short-chain fatty acids. However, the approach used to develop the model is general, and can be applied to include any other weak acid/bases of importance. Precipitation of $CaCO_3$ and gas exchange of CO_2 have also been included (see Chapter 3). The model and the approach on which it is based have been validated by comparing model predictions to those obtained from equilibrium chemistry-based models and good correlation was obtained. Compared to the traditional equilibrium chemistry approach to modelling aqueous mixtures of weak acid/bases, the kinetic approach offers several advantages. In particular, the kinetic approach expedites the integration of the weak acid/base model with other kinetic models (see Chapters 3 and 4). By providing an estimation for the pH, the weak acid/base model greatly simplified the inclusion of chemical (e.g. dissociation/association) and/or physical (e.g. CO_2 and NH_3 gas exchange) processes in both the C and N removal activated sludge and the anaerobic digestion models. It therefore seems reasonable to consider integrating the third (solid) phase of the Musvoto *et al.* (1997) three phase weak acid/base chemical-physical kinetic model in the anaerobic digestion kinetic model developed in Chapter 4, to extend it to include solids precipitation.

6.2 LITERATURE REVIEW

6.2.1 Solid/Aqueous System Model: Precipitation of Sparingly Soluble Salts

The precipitation of sparingly soluble salts has been extensively reviewed by Musvoto *et al.* (1998), and a brief description is given below.

6.2.1.1 The kinetics of sparingly soluble salt precipitation

The first requirement for a solid to form from a solution is supersaturation, and the degree of supersaturation is the main factor that controls whether a solid will precipitate or not. Precipitation occurs in three steps: (i) nucleation, (ii) crystal growth and (iii) ripening. Ideally, precipitation would occur in three distinct steps, however, in reality all three processes occur simultaneously.

---

[2] In aqueous single or mixed weak acid/base systems, the water always is present and acts as an additional weak acid/base system because of its dissociation to H^+ and OH^-. It is included here for completeness. In mixed weak acid/base systems, the water system is one of several weak acid/base systems that contribute to the Total Alkalinity and Acidity mass parameters (Loewenthal *et al.*, 1989).

Nucleation:
Supersaturation by itself is not sufficient for a solid to precipitate. Before any crystals can grow, the solution must contain minute solid bodies (known as centres of crystallisation, seed or nuclei) to act as a centre from which crystal growth can occur. Initially, bimolecular attraction and then addition of single molecules lead to formation of critical clusters. Further addition of molecules to the critical cluster results in nucleation. Once the nucleus grows beyond a certain critical size, it becomes stable and solids formation begins. If the nucleus remains smaller than the critical size, it will re-dissolve and no solids will form. The rate of nucleation is controlled by interfacial energy, the collision frequency and temperature, and it is critically dependent on the degree of supersaturation. A critical degree of supersaturation must be exceeded for nucleation to occur.

Growth of crystals:
Crystal growth is a process that takes place in the following steps: (i) Ions are transported to the crystal/liquid interface, (ii) adsorption of the ions onto the crystal surface and (iii) incorporation of the ion into the crystal lattice. Crystal growth kinetics depend on a rate limiting step and two rate limiting theories on crystal growth have been developed: Diffusion controlled growth and surface controlled growth. Diffusion controlled growth is represented by the following equation:

$$\frac{dc}{dt} = -k \cdot s \cdot (c - c_o) \qquad (6.1)$$

where c = solution concentration at time t (mol/ℓ)
c_o = equilibrium solution concentration of salt being precipitated (mol/ℓ)
s = surface area of the crystalline material present (m^2/mol)
k = rate constant which depends on the diffusion coefficient and the extent of turbulence in the solution (mol/m^2s).

Eq. 6.1 is valid only if the solution has equivalent concentrations of cations and anions of the salt. Surface controlled growth does not depend on the turbulence of the solution and the results can be fitted generally to rate laws of the type:

$$\frac{dc}{dt} = -k \cdot s \cdot (c - c_o)^n \qquad (6.2)$$

where n = order of the reaction (determined experimentally)
k = rate constant which is independent of solution turbulence (mol/m^2s).

As for Eq. 6.1, Eq. 6.2 is valid only if the solution has equivalent concentrations of cations and anions of the salt being precipitated. Equations 6.1 and 6.2 should not be accepted as defining a particular type of growth, other measurements such as temperature effects, ion concentrations and the degree of turbulence should be taken into account when deciding on the growth type.

For surface controlled growth of crystals from a solution containing non-equivalent concentrations of anions and cations, Nichollas and Purdie (1964, cited by Wiechers, 1978) showed that it may be expressed by an equation similar to Eq. 6.2, but taking account of the

individual cation and anion concentrations. Considering the general reaction:

$$xM^{y+} + yA^{x-} \rightarrow M_xA_y \tag{6.3}$$

where M = cation with the charge y^+
A = anion with the charge x^-.

Then Nichollas and Purdie (1964, cited by Wiechers, 1978) derived the crystal growth rate equation for this reaction as follows:

$$-\frac{dm}{dt} = k \cdot s \cdot \left\{ \left(\left[M^{y+}\right]^x \left[A^{x-}\right]^y \right)^{\frac{1}{x+y}} - K_{sp}^{\frac{1}{x+y}} \right\}^{x+y} \tag{6.4}$$

where m = mass of salt precipitated (mol/ℓ)
k = rate constant (mol/m^{2}s)
s = surface area of crystals (m^2/mol)
K_{sp} = solubility product of salt M_xA_y (molar form)

Ripening:
Ripening is the formation of large crystals from fine crystallites and occurs after crystal growth. Ripening only occurs if sufficient time is allowed after crystal growth. The speed at which ripening occurs depends to a large extent on the particle sizes as well as on the solubility of the salt. Smaller particles of a more soluble salt will ripen much faster than those of a sparingly soluble salt.

6.2.1.2 Kinetics of precipitation applied to the solid/aqueous model
In order for crystallization to occur, the solution must be supersaturated to a certain degree with respect to the particular salt. When small concentrations of seed crystals are present, both nucleation and crystal growth take place simultaneously. Musvoto *et al.* (1998) accepted that the crystal growth process is the rate limiting process and so limits the overall rate of precipitation. They stated that Eq. 6.4 best describes the crystal growth kinetics for sparingly soluble salts from solutions of unequal cation and anion concentration and accordingly can be used to describe the overall precipitation process. Koutsoukos *et al.* (1980) also accepted the validity of this equation to describe the rate of precipitation of sparingly soluble salts, i.e. for a salt $M_{v+}A_{v-}$ the rate of crystallization can be expressed by the following general equation:

$$\frac{d}{dt} M_{v+}A_{v-} = -k \cdot s \cdot \left[\left(\left[M^{m+}\right]^{v+} \left[A^{a-}\right]^{v-} \right)^{\frac{1}{v}} - \left(\left[M^{m+}\right]^{v+}{}_0 \left[A^{a-}\right]^{v-}{}_0 \right)^{\frac{1}{v}} \right]^n \tag{6.5}$$

where $[M^{m+}]$, $[A^{a-}]$ and $[M^{m+}]_0$, $[A^{a-}]_0$ are the concentrations (mol/ℓ) of crystal lattice ions in solution at time t and at equilibrium respectively. At equilibrium $[M^{m+}]_0[A^{a-}]_0 = K'_{sp}$ where K'_{sp} is the apparent solubility product of the salt.
k = the precipitation rate constant (mol/m^{2}s)

s = proportional to the total number of available growth sites on the added seed material (m^2/mol)
v^+ = number of cation species
v- = number of anion species
v = $v^+ + v^-$
n = determined experimentally.

The aim of Musvoto *et al.* (1998) was to develop a model that predicts the precipitation of solids from wastewaters. From the above they concluded that the crystal growth kinetics during the precipitation of sparingly soluble salts is mostly surface controlled and rate limiting in the overall precipitation so that the kinetics can be represented by Eq. 6.5.

6.2.1.3 Precipitation from solutions containing a mixture of ions

Magnesium phosphates:
The following species can precipitate from a solution containing Mg, N and P: (i) Magnesium ammonium phosphate (or struvite), (ii) magnesium hydrogen phosphate trihydrate (or newberyite) and (iii) trimagnesium phosphate in two states of hydration. For magnesium phosphate precipitates, in solutions containing a mixture of Mg, ammonia and P ions, newberyite precipitates only at low pH (<6.0) and at high solution concentrations. Struvite precipitates at neutral and higher pH and at Mg/Ca molar ratios > 0.6. If the pH is reduced, the struvite already formed transforms to newberyite. Trimagnesium phosphate, which has a low formation rate, is not observed in this pH range.

Calcium phosphates:
The following species can precipitate from a solution containing Calcium (Ca) and P: (i) Hydroxyapatite (HAP), (ii) Tricalcium phosphate or Whitlockite (TCP), (iii) Octacalcium phosphate (OCP), (iv) Monenite (DCP) and (v) Dicalcium phosphate dihydrate or Brushite (DCPD). It has been established that a number of species act as precursors to the precipitation of HAP. The precursor species can be amorphous calcium phosphate (ACP), OCP and DCPD.

In highly supersaturated solutions containing Ca, Mg and P, DCPD (at pH < 7.0) and ACP (at higher pH)are the phases that precipitate first. Musvoto *et al.* (1998) state that precipitation follows Ostwald's rule of stages, with the initially formed metastable species converting with time to the more thermodynamically stable species of Monenite or HAP:

low pH: OCP → DCPD → HAP
~ pH = 7.0: OCP + DCPD → HAP
high pH: ACP → OCP → HAP

The conversion from the initial to the final species occurs via a solution mediated species transition with the initial species dissolving first and the new species growing. The nucleation of the first species is relatively fast, however, the growth of the second species is very slow, resulting in the conversion process being a slow one (from months to years).

Calcium carbonates:
Three crystalline structure varieties of calcium carbonate can precipitate: (i) Calcite, (ii) Aragonite and (iii) Vaterite.

Musvoto *et al.* (1998) state that it has been shown that the precipitate depend on temperature, degree of supersaturation, presence of foreign ions as well as the nucleation and growth rates of the crystals: The presence of Mg^{2+} results in the distortion of the calcium carbonate species and the inhibition of calcium carbonate precipitation by the spontaneous precipitation of other calcium carbonate species, like Aragonite, instead of Calcite. High concentrations of Mg^{2+} favour Aragonite formation (Mg/Ca molar ratio > 4), while at low Mg^{2+} concentrations Calcite precipitates (Mg/Ca malar ratio <4). Mg^{2+} also reduces the rate of calcium carbonate precipitation as well as increases the solubility of calcium carbonate. Phosphates inhibit the precipitation of calcium carbonate through crystal poisoning or co-precipitation or adsorption of phosphate into the calcium carbonate crystal. As with the presence of Mg^{2+}, when phosphate is present, the precipitation rate of calcium carbonate is reduced and its solubility is increased. Fe^{2+} is one of the strongest inhibitors of calcium carbonate growth, even at very low Fe^{2+} concentrations.

Other salts:
Other salts which may precipitate from solutions containing a mixture of ions are magnesium carbonates (Magnesite and Nesquehonite) and calcium magnesium carbonates (dolomite and huntite). Magnesite is stable below a pH ~ 10, but Nesquehonite is not. The conditions under which Dolomite precipitates are not well understood and attempts to precipitate Dolomite from supersaturated solutions under atmospheric conditions have been unsuccessful.

6.2.1.4 Solubility products for sparingly soluble salts
Musvoto *et al.* (1998) estimated the extent of precipitation for systems that reach equilibrium by considering the equilibrium constant. As an example, the precipitation/dissolution of calcium carbonate can be represented by the following equation *at equilibrium*:

$$(CaCO_3)_{solid} \Leftrightarrow Ca^{2+} + CO_3^{2-} \qquad (6.6)$$

with the thermodynamic solubility product equation given by:

$$K_{sp} = (Ca^{2+})(CO_3^{2-}) \qquad (6.7)$$

where () = active concentration
K_{sp} = thermodynamic solubility product for $CaCO_3$.

The solubility product of salts is affected by the ionic strength of the liquid as well as other equilibria that occur in the same solution. To take account of these effects, Musvoto *et al.* (1998) used the Debye-Huckel theory to calculate the activity coefficients of the various ions. The solubility product equation for $CaCO_3$, taking into account the Debye-Huckel effects is then expressed as:

$$K_{sp} = \gamma_{Ca}[Ca^{2+}]\gamma_{CO_3}[CO_3^{2-}] = K'_{sp}\gamma_{Ca}\gamma_{CO_3} \qquad (6.8)$$

where γ_{Ca} = activity coefficient of Ca^{2+} calculated from the Debye-Huckel theory
γ_{CO3} = activity coefficient of CO_3^{2-} calculated from the Debye-Huckel theory
K'_{sp} = apparent solubility product of $CaCO_3$.

6.2.1.5 Ion pairing

Ion pairs are either positively or negatively charged, or neutral species that are formed between ions of the opposite charge. The ion pairs reduce the amount of free ions in solution, thereby reducing the availability of free ions to form precipitates. They also have an effect on the ionic strength of the solution, thus changing the theoretical activity coefficients of the free ions in solution. This effectively increases the solubility of a salt.Therefore Musvoto *et al.* (1998) considered ion pairing the most important equilibria in aqueous systems that affect the solubility of salts, and they therefore had to take account of ion pairing to accurately predict the amount of free ions in solution.

Ion pairs are temporary bonds between anions and cations and can therefore be regarded as being in a state of dynamic equilibrium with the associated free ions:

$$Ca^{2+} + HPO_4^{2-} \leftrightarrow CaHPO_4^{0} \tag{6.9}$$

and the ion pairing association equilibrium constant is:

$$K_{CaHPO_4^0} = \frac{(CaHPO_4^0)}{(Ca^{2+})(HPO_4^{2-})} \tag{6.10}$$

Musvoto *et al.* (1998) treated the ion pairing equations as forward and reverse kinetic reactions, due to the kinetic nature of their model, in the same manner as they did for the weak acid/base dissociation reactions (see Chapter 3). Considering the formation of the $CaHPO_4$(aq) ion pair represented by Eq. 6.9, the rate of the, or ion association, reaction is given by:

$$\begin{aligned} r_{fCaHPO_4} &= K_{fCaHPO_4}(Ca^{2+})(HPO_4^{2-}) \\ &= K_{fCaHPO_4}\gamma_{CA}[Ca^{2+}]\gamma_{HPO4}[HPO_4^{2-}] \\ &= K'_{fCaHPO_4}[Ca^{2+}][HPO_4^{2-}] \end{aligned} \tag{6.11}$$

where $r_{fCaHPO4}$ = rate of the ion association reaction for the formation of the ion pair $CaHPO_4^0$
$K_{fCaHPO4}$ = specific rate constant for the ion association reaction
() = activity
γ_{Ca} = activity coefficient for the Ca^{2+} ion
γ_{HPO4} = activity coefficient for the HPO_4^{2-} ion
[] = molar concentration
$K'_{fCaHPO4}$ = apparent specific rate constant for the ion association reaction

The rate of the reverse, or ion pair dissociation reaction is:

$$\begin{aligned} r_{rCaHPO4} &= K_{rCaHPO4}(CaPO_4^0) \\ &= K_{rCaHPO4}[CaPO_4^0] \quad \text{(Activity of unchanged species is 1)} \end{aligned} \tag{6.12}$$

$= K'_{rCaHPO4}[CaHPO_4^0]$

where $r_{rCaHPO4}$ = rate of dissociation of the $CaHPO_4^0$ pair
$K_{rCaHPO4}$ = specific rate constant for dissociation of the ion pair
$K'_{rCaHPO4}$ = apparent specific rate constant for dissociation of the ion pair.

From the law of mass action, at equilibrium the forward rate of the reaction is equal to the reverse rate of the reaction, so:

$$K'_{fCaHPO4}[Ca^{2+}][HPO_4^{2-}] = K'_{rCaHPO4}[CaHPO_4^0] \quad (6.13)$$

and therefore

$$\frac{K'_{fCaHPO4}}{K'_{rCaHPO4}} = \frac{[CaHPO_4^0]}{[Ca^{2+}][HPO_4^{2-}]} = K'_{CaHPO4} \quad (6.14)$$

where K'_{CaHPO4} = apparent equilibrium (or stability) constant for the formation of the ion pair.

The rate of the forward association and reverse dissociation reactions cannot be measured, because they are very rapid. However, Musvoto *et al.* (1998) state that from a practical point of view the exact values are of little consequence. They selected the values for the rate constants in a manner similar as for the rate constants for the weak acid/bases, i.e. to ensure that the reactions are effectively instantaneous, one of the rate constants (the reverse rate constant) is given a very high theoretical value. To ensure that the kinetically established equilibrium corresponds to observed equilibrium chemistry, the value of the forward rate constant is calculated through the relationship with the apparent stability constant (Eq. 6.11).

Musvoto *et al.* (1998) included the following ion pairs in their model, which can form in solution containing carbonate, Ca, Mg and P: Ca^{2+}/OH^-, Ca^{2+}/CO_3^{2-}, Ca^{2+}/HCO_3^-, Ca^{2+}/PO_4^{3-}, Ca^{2+}/HPO_4^{2-}, $Ca^{2+}/H_2PO_4^-$, Mg^{2+}/OH^-, Mg^{2+}/CO_3^{2-}, Mg^{2+}/HCO_3^-, Mg^{2+}/HPO_4^{2-}, Mg^{2+}/PO_4^{3-}.

6.2.1.6 Closure

Musvoto *et al.* (1998) developed a single phase aqueous system model for mixed weak acid/base chemistry and added the solid/aqueous phase discussed above and the gaseous/aqueous phase to give a combined three phase (aqueous/solid/gas) systems model. This Chapter revisits the solid/aqueous phase model of the Musvoto *et al.* (1998) and assesses its application to full scale systems and its suitability for inclusion in the anaerobic digestion model developed in Chapter 4, and indeed in a combined three phase (aqueous/solid/gas) kinetic model for an entire wastewater treatment plant including primary sedimentation, anaerobic and/or aerobic digestion of primary and/or waste activated sludge and an activated sludge process.

6.2.2 Integrated 3 Phase Chemical Physical Modelling of the Mixed Weak Acid/Base System

The three phase physical-chemical kinetic model developed for the carbonate system (Musvoto *et al.*, 1997) was extended by Musvoto *et al.* (2000) to include the phosphate, ammonia and short chain fatty acid weak acid/base systems in three phases with multi-mineral precipitation and multi-gas stripping. The specific kinetic model was developed to simulate the physical-chemical reactions which occur in the aeration treatment of anaerobic digester liquors (ADLs). The processes that occur under these conditions are the dissociation of the weak acid/bases, precipitation of solids (struvite, newberyite, amorphous calcium phosphate (ACP), magnesium and calcium carbonate) and stripping of CO_2 and NH_3 gases. Ion pairing effects were also included in the model because the ionic strength of the liquors tested was greater than 0.025. The resultant kinetic model was validated by comparing predictions with (i) equilibrium concentrations from (a) an equilibrium based struvite precipitation algorithm (Loewenthal *et al.*, 1994) coded into a computer program called Struvite 3.1 by Loewenthal and Morrison (1997) and (b) experimental data available in the literature (Ferguson and McCarty, 1971) and (ii) kinetic (time dependent) and equilibrium (time independent) data obtained from aeration batch tests on anaerobic digester liquors (ADL) from (a) a spent wine upflow anaerobic sludge bed (UASB) digester and (b) a sewage sludge anaerobic digester.

In the kinetic model the dissociation constants, ion pair stability constants and mineral solubility products were regarded as model constants and were not changed (except for ionic strength and temperature adjustments). The specific precipitation rates of the minerals and the specific stripping rates of the gases were regarded as calibration constants and changed to fit predicted experimental results. The calibration constants are important when simulating time dependent experimental results and when simulating the final equilibrium condition for a solution with precipitation of multiple minerals that compete for common species (e.g. ACP and $CaCO_3$ competing for Ca species). In these latter solutions the final equilibrium condition may be influenced by the relative rates of precipitation of the competing precipitating minerals. For time independent simulations with non-competing minerals precipitating, when comparing predicted with observed results of only the final steady state conditions, only the model constants are important, not the kinetic mineral precipitation and gas stripping rates.

To check the performance of the model with a single precipitating mineral under time independent conditions, predicted results were compared with the Struvite 3.1 equilibrium based computer program of Loewenthal and Morrison (1997). Since in this situation only a single mineral is precipitating (struvite), only the model constants are of importance. From this comparison it was concluded that the kinetic model can accurately predict equilibrium conditions for single mineral precipitation. To check the performance of the model for multiple mineral precipitation, the experimental results of Ferguson and McCarty (1971) were simulated. In the experiments of Ferguson and McCarty, although only initial and final conditions are available, because multiple minerals are precipitating competing for the same compounds both the model and calibration constants are of importance. From these simulations it was concluded that the model performed well and was sufficiently robust and stable to simulate multiple mineral precipitation.

To validate the time dependent performance of the model and determine the calibration

constants, batch experiments were conducted by aerating two ADLs, viz. three batch tests on liquor from a spent wine UASB digester (UASBDL) and four batch tests on liquor from an anaerobic digester treating a blended primary sludge and waste activated sludge (SSADL). In these batch tests, Ca, Mg, PO_4-P (P_T), inorganic C (C_T, via the $H_2CO_3^*$ Alk), free and saline ammonia (FSA, N_T) and pH were measured over 24 to 54h. After establishing (i) the minerals most likely to precipitate viz. struvite ($MgNH_4PO_4$), newberyite ($MgHPO_4$), amorphous calcium phosphate [ACP, $Ca_3(PO_4)_2$], $CaCO_3$ and $MgCO_3$ and (ii) their solubility products from the literature, the specific precipitation and gas stripping rate constants were determined by (i) trial and error visual fitting of predicted results to the experimental data and (ii) a parameter estimation facility which searches for the calibration constants that minimize the error between the model predictions and experimental results. A good correlation was obtained between model predictions and experimental results with both methods for six of the seven batch tests and while the second method may be superior, visually there was no discernable difference between the predicted results of the two methods. The good correlation indicated that no mineral that precipitated significantly in the ADL was omitted from the model.

The same minerals were found to precipitate in the two liquors and in similar proportions, viz. in decreasing proportion of precipitate mass formed struvite ($MgNH_4PO_4$) (82-89%), amorphous calcium phosphate (ACP) (5-15%), calcium carbonate ($CaCO_3$) (0-6%), magnesium carbonate ($MgCO_3$) (0-5%) and newberyite ($MgHPO_4$) (0.1-0.3%). Unfortunately, no experimental tests were conducted to measure the concentration of precipitate formed. Comparing the mineral precipitation rates in the UASBDL and SSADL, it was found that (i) the rates of struvite and ACP precipitation were 9 and 2 times faster respectively in the UASBDL than in the SSADL, (ii) in contrast, the rate of $CaCO_3$ precipitation was 140 times faster in the SSADL than in the UASBDL, (iii) the rates of $MgCO_3$ and $MgHPO_4$ precipitation were approximately the same in both liquors. No meaningful comparison could be made for the gas stripping rates because the aeration rate was different in each batch test and were not measured. This is the weakest part of the batch tests and is, in hindsight, an omission; If the aeration rate had been measured, a comparison could have been made between the airflow rate and CO_2 and NH_3 gas stripping rates.

From the simulations it was evident that the kinetic model offers considerable advantages over equilibrium based models. Not only can it predict time dependent data, but it can also predict the final equilibrium state (in terms of the duration of the tests) for situations with precipitation of multiple minerals which compete for the same species - equilibrium models are not capable of predicting either situation. Further, the kinetic modelling approach also allows the determination of the specific precipitation rates for a number of minerals simultaneously in an integrated manner from a single batch test. However, it should be noted that the kinetic model developed by Musvoto *et al.* (2000) is restricted to the precipitation of minerals and does not consider mineral dissolution. For the tests considered, dissolution was not significant compared to the precipitation. For situations where dissolution is significant, the kinetic model will predict neither the time dependent behaviour nor the final equilibrium state correctly. Attempts to include separate processes for dissolution in the model caused instability in model simulations in AQUASIM (Reichert, 1998). This aspect requires further investigation.

The three phase kinetic based weak acid/base chemistry model, and the approach on which it is based, proved to be a useful tool for research into and design of wastewater treatment systems in which several weak acid/bases influence the behaviour. For research, the model helps to focus

attention on issues not obvious from direct experiment and allows determination of mineral precipitation rates for a particular wastewater from a single batch test. Once calibrated with the precipitation (and gas stripping if included) rates, this kind of model can be used to predict the performance of different treatment systems to identify for investigation those that appear technically and economically viable. This 3 phase modelling approach can possibly be extended to include biological processes, such as those of the 2 phase biological nutrient removal activated sludge (Chapter 3) and anaerobic digestion of sewage sludges (Chapter 4).

6.2.3 Application of the 3 Phase Mixed Weak Acid/Base Model to a Fullscale WWTP.

At the Cape Flats (CF) Wastewater Treatment Plant (WWTP) (Cape Town, South Africa), waste activated sludge (WAS) and primary sludge (PS) are thickened separately, the WAS by dissolved air flotation and the PS by gravity thickening. The two thickened sludge streams are blended, thickened further with centrifuges and anaerobically digested in three high rate anaerobic digesters (sludge age ~ 10d). The anaerobically digested sludge is degritted mechanically and then passes to a collection sump. The sludge is drawn from the sump, dewatered in centrifuges and the dewatered sludge is passed to a thermal drying pelletization plant. In operation of this sludge treatment scheme, problems have been experienced with mineral precipitation in the post digestion centrifuges, and in the pipework leading from the centrifuges to the pelletization plant. Precipitation inside the centrifuges reduces the capacity of the centrifuges to lower the moisture content of the digested sludge; Precipitation within the pipe network causes pipe blockages and reduced maximum flow rates.

This section summarizes an experimental and theoretical modelling investigation into mineral precipitation in ADL from the CFWWTP, to determine which minerals precipitate, what conditions induce this precipitation, and what operational strategies can minimise the precipitation (for details, see van Rensburg *et al.*, 2001, 2003).

From the investigation, the following conclusions can be drawn with regard to mineral precipitation in the Cape Flats (CF) ADL, some of which apply to ADL in general:

(i) For the CF ADL, the dominant mineral that precipitates is struvite. For the batch test conducted, struvite was dominant (543 mg/ℓ as $MgNH_4PO_4 \cdot 6H_2O$ = 97% of mass of precipitant), followed by ACP (16.1 mg/ℓ as $Ca_3(PO_4)_2$ = 3% of the mass of precipitant), and negligible newberyite, calcite and magnesite precipitated. These observations are similar to those of the extended pH change test and Musvoto *et al.* (2000c). With the large volumes of ADL passing to the downstream processes, this is a substantial precipitation potential.

(ii) The precipitation of struvite is stimulated by the increase in pH when CO_2 is lost from the ADL. This increase in pH causes struvite to become supersaturated, and hence it precipitates. Increasing the pH by addition of NaOH also results in struvite precipitation, which confirms that the increase in pH is the primary process driving the struvite precipitation.

(iii) When the ADL exits the CF WWTP digesters, it is initially undersaturated with respect to struvite. Depending on the initial conditions in the ADL, significant struvite

precipitation starts only when the pH increases above pH = 7.3 to 7.7. This critical pH for struvite precipitation is reached after 0.67 to 1.0h aeration. However, this time will depend on a number of factors, including inter alia aeration rate, initial pH, buffer capacity, initial P and Mg concentrations, etc.

(iv) From the batch tests in which the pH was raised by NaOH addition, the struvite precipitation rate is extremely rapid. The first sample taken immediately after NaOH addition and filtered as soon as possible (~1 min) showed closely similar Mg and PO_4-P concentrations to those taken after 1h. Therefore with aeration of the CF ADL, struvite was at equilibrium between the precipitant and soluble species at all times. Thus, in this case the rate of struvite precipitation is not limited by the precipitation kinetics, but rather by the rate of increase in pH through aeration. With ADL aeration to increase the pH, the practical upper limit on the aeration (K_{La}) rate therefore generally will limit the struvite precipitation rate.

(v) The mass of struvite that precipitates is limited by two factors: With aeration to increase pH, the struvite precipitating is limited by the final pH reached and the initial Mg concentration present - if the initial Mg concentration is increased, then more struvite precipitates. With addition of NaOH, the struvite precipitating is limited by the initial Mg concentration present - after precipitation the Mg concentration is very low, while significant concentrations of P and N are still present.

(vi) The initial concentrations of P and Mg in the ADL were variable, with P ranging from 89 to 190 mgP/ℓ, and Mg from 29 to 67 mgMg/ℓ. This is probably indicative of a variable BEPR performance of the activated sludge system. The higher P concentrations are in agreement with values measured for other anaerobically digested BEPR sludges, at 150 to 250 mgP/ℓ (Pitman, 1995).

(vii) The increase in pH with aeration also stimulates precipitation of ACP. However, the mass of ACP precipitating is relatively small compared with struvite. The ADL is initially undersaturated with respect to ACP, and ACP precipitation initiates only after the pH increases above 7.7. At pH>7.7, ACP precipitates because the ionic product of the soluble Ca and PO_4-P concentrations exceeds the solubility product after significant struvite precipitation. Because struvite precipitates much faster and at lower pH than ACP, the Ca and PO_4-P ionic product remains low as PO_4-P is incorporated into struvite with increasing pH.

(viii) Ion pairing plays a significant role in the multiple mineral precipitation dynamics. As soluble ions are incorporated into the precipitating minerals, so ions are 'released ' from the ion pairs keeping the soluble concentrations higher for longer as pH increases.

(ix) In running experiments on the ADL, the solids concentrations were so high that the ADL could not be effectively filtered. Accordingly, the ADL was settled for 5 days and the supernatant used for the experiments. Thus, the effect of solids concentration on precipitation could not be evaluated, e.g. factors such as surface area for nucleation of minerals, inhibition or poisoning of crystal growth.

From the simulations it was evident that the kinetic model offered considerable advantages over equilibrium based models. Not only could it predict time dependent data, but also it could predict the final equilibrium state (in terms of the duration of the batch tests) for situations with precipitation of multiple minerals which compete for the same species - equilibrium models are not capable of predicting either situation. Further, the kinetic modelling approach also allowed the determination of the specific precipitation rates for a number of minerals simultaneously in an integrated manner from a single batch test. However, the kinetic model is restricted to the precipitation of minerals and does not consider dissolution. For the tests considered, dissolution was not significant compared to the precipitation. For situations where dissolution is significant, the kinetic model will predict neither the time dependent behaviour nor the final equilibrium state correctly. Attempts to include separate processes for dissolution in the model caused instability in model simulations in AQUASIM (Reichert, 1998). This aspect requires further investigation.

6.3 FURTHER VALIDATION OF THE MODEL - APPLICATION TO SWINERY WASTEWATER.

6.3.1 Introduction

Recovery of phosphorus (P) by means of struvite (magnesium ammonium phosphate) precipitation requires optimisation of the conditions favouring its precipitation. This in turn requires knowledge of the struvite precipitation chemistry and kinetics, and their interaction with imposed design conditions, e.g. aeration, retention time, pH adjustment. Further, the simultaneous and/or sequential precipitation of competing minerals and formation of competing ion pair complexes are often encountered in the treatment of and/or P recovery from wastes and wastewaters, for example, anaerobic digester liquors (ADL) and swinery wastewater (SWW). Such problems are complex, interactive multi-phase (aqueous/gas/solid), multi-mineral, mixed weak acid/base ones. The complex nature of these problems requires the development of models to describe the underlying processes, thereby to facilitate design and optimisation. Models based on traditional equilibrium chemistry cannot be applied, because of the inability to correctly predict the changes that take place with time and with competing or sequential mineral precipitations and ion pairing. As an alternative, Musvoto *et al.* (1997, 2000a,b,c) developed a kinetic based model to simulate the three phase chemical and physical reactions that occur on ADL aeration. This model incorporates kinetics for the chemical and physical processes of weak acid/base chemistry, ion pairing, precipitation and gas stripping and was reviewed above.

The model was calibrated and validated through application to aeration batch tests on UASB liquors and sewage sludge ADL. For the calibration, values for the constants in the model were obtained from the literature if available, except the mineral precipitation and gas stripping rates, which were obtained by curve fitting theoretical predictions to measured data. From this integrated kinetic approach, *inter alia,* the dominant precipitating minerals, the conditions that cause these minerals to precipitate and their rates of precipitation could be identified. Similarly, van Rensburg *et al.* (2003) applied the kinetic model to the aeration of ADL from the Cape Flats Wastewater Treatment Plant (CFWWTP) to resolve struvite precipitation problems being experienced at this treatment plant, and were able to successfully simulate batch aeration tests on the ADL. The simulations enabled strategies to be proposed for implementation at the CFWWTP to minimise problems caused by struvite precipitation, which have been successfully implemented, and to possibly implement struvite recovery. From their investigation, they concluded that the kinetic modelling approach offers major advantages over equilibrium based models. Not only can it predict time dependent data, but also it can predict the final equilibrium state for situations with precipitation of multiple minerals which compete for the same species - equilibrium models are not capable of predicting either situation.

However, in the specific applications above, the precipitation reactions were dominated by the single mineral struvite (up to 97% of the precipitant), so that assessment of the kinetic model for multiple mineral precipitation was limited. In this Chapter, multiple mineral precipitation is explored further, through application of the kinetic model to aeration treatment of SWW and ADL.

6.3.2 Model Application

The kinetic model was applied to describe the time dependent three phase reactions that occur when SWW and ADL are aerated, using experimental data in the literature. All simulations were with the computer program AQUASIM (Reichert, 1994).

6.3.2.1 Aeration of swine wastewater (SWW) (Suzuki *et al.*, 2002)
Suzuki *et al.* (2002) experimentally investigated aeration treatment of SWW. Screened (1.5mm mesh) batches (3 ℓ) of SWW were aerated (3h) to stimulate CO_2 stripping and hence pH increase. pH, total inorganic carbon (C_T), and total soluble (3000rpm) Mg, Ca and P were monitored with time, as well as initial and final crystallized Mg, Ca and P. The increase in pH caused mineral precipitation, apparently principally struvite and calcium phosphate (accepted by the authors as hydroxyapatite, HAP, but more likely amorphous calcium phosphate, ACP, see below). Both minerals or their equivalents are included in the integrated chemical physical processes model, which facilitated model application.

6.3.2.2 Aeration of anaerobic digester liquor (ADL) (van Rensburg *et al.*, 2003)
Similarly to Suzuki *et al.*(2002), van Rensburg *et al.* (2003) experimentally investigated the aeration treatment of ADL from the (CFWWTP, Cape Town, South Africa) to resolve struvite precipitation problems being experienced at this treatment plant, and to aid possible struvite recovery. Batches (10 ℓ) of settled ADL were aerated (at 20°C) and conductivity, pH, total soluble (Whatman's No 1 filtrate acidified, then 0.45μm filtered) Mg, Ca, P, Fe, K and Na, total soluble (not acidified 0.45 μm filtrate) $H_2CO_3^*$ alkalinity and short-chain fatty acids (together with pH, used to determine C_T), and FSA (Whatman's No1 acidified filtrate) monitored with time. They applied the kinetic model to the experimental data and obtained a good correlation between predicted and measured data. Further, the model was also applied to theoretically examine the effect of changing initial concentrations of Mg and P, and the aeration rate. They found that in the CFWWTP ADL the struvite precipitation was limited by the availability of Mg, and significant ACP precipitation did not occur. This caused residual Ca and P to be present. However, in their simulations values for the ACP precipitation rate constants could not be accurately determined, so this is investigated further in this chapter. The ADL aeration batch test of van Rensberg *et al.* (2003) in which later samples drawn from the test had NaOH added to increase the pH, is also simulated.

6.3.3 Model Calibration

In the model, values are required for: (i) Weak acid/base equilibrium constants (pK_a), (ii) weak acid/base kinetic rate constants (K_{ra}), (iii) ion pair stability constants (pK_{ST}), (iv) mineral solubility products (pK_{SP}), (v) ion pair kinetic rate constants (K_{rIP}), (vi) mineral precipitation rate constants (K_{ppt}) and (vii) gas stripping rate constants ($K_{rG} = K_{LaG}$). In the calibration, weak acid/base constants (i) and (ii) were regarded as model constants and not changed. Large values for the reverse dissociation rate constants were applied to ensure rapid equilibrium, and the relative values for the forward and reverse dissociation rate constants were related via the appropriate equilibrium constant (i) obtained from the literature (Musvoto *et al.*, 1997, 2000abc). The ion pair stability constants (iii) were also obtained from the literature and regarded as model constants and not changed (Musvoto *et al.*, 2000c). The mineral solubility product constants (iv) were calibrated within the range of values quoted in the literature and have been used

successfully in all subsequent simulations, and hence were retained unmodified from Musvoto *et al.* (2000a,c). Values for the ion pair kinetic rate constants (v) accepted by Musvoto *et al.* (1997, 2000bc) were incorrectly calibrated such that formation of the ion pairs were not instantaneous as should be, and is an oversight in their calibration (Wentzel *et al.*, 2001). Accordingly the values of van Rensburg *et al.* (2003) of 10^7/d were accepted to ensure the ion pair reactions were effectively instantaneous as required. Values for the mineral precipitation rate constants (vi) of van Rensburg *et al.* (2003) were initially accepted, which are the same as Musvoto *et al.* (1997, 2000bc) except that the struvite precipitation rate constant was increased from 300/d to 1000/d. The gas stripping rate constants (vii) were calibrated for each specific test; This is expected, as the gas stripping rates are linked to the aeration rate. In calibrating the gas stripping rates for CO_2, the K_{La} for O_2 was calibrated, and the value for CO_2 determined via the proportionality of the diffusivities of O_2 and CO_2 (Munz and Roberts, 1989). The CO_2 gas dissolution rate was calculated from Henry's Law constant for CO_2. For the pH values attained in the experiments to be simulated (pH < 9) and the short periods at the higher pH values, NH_3 stripping is not a significant process, and hence the exact value for the NH_3 stripping rates is not of importance.

Except for the gas stripping rates, it was endeavoured to use the same set of 'default' constants for all applications and exceptions are mentioned below. Changes to constants were made by visual trial and error fitting of predicted to measured data. Previous applications (Musvoto *et al.*, 2000c; van Rensburg *et al.*, 2003; Wentzel *et al.*, 2001) indicated that visually there was little discernable difference between results from this calibration method and the results obtained with the parameter estimation facility in AQUASIM (Reichert, 1994).

6.3.4 Results and Discussion

6.3.4.1Aeration of swine wastewater (Suzuki *et al.*, 2002)

Measured and predicted results for the aeration of the SWW batch test of Suzuki *et al.* (2002) are shown in Fig 6.1. In the simulations, the 'default' values for the model constants above were accepted, except for the CO_2 gas stripping rate constant ($K_{La,CO2}$) and the ACP precipitation rate constant ($K_{ppt,ACP}$), which were adjusted by trial and error fitting predictions to the measured data. For $K_{La,CO2}$, this was calibrated via the $K_{La,O2}$ for oxygen (see above) = 800/d. This constant is batch test specific (aeration rate, mixing, solids, etc.). For $K_{ppt,ACP}$, in simulating this test, an inconsistency between predictions and measurements for Ca became apparent - the model could not correctly predict the observed changes in Ca concentration with time. The value for $K_{ppt,ACP}$ accepted (700/d) gave the best match between the measured and predicted initial and final Ca values. With this value the predicted Ca data were consistently less than that measured between the initial and final values (Fig 6.1d). In examining possible causes for this inconsistency, precipitation of hydroxyapatite (HAP) was included in the model instead of ACP (HAP was the calcium phosphate precipitant accepted by Suzuki *et al.*, 2002). Although this improved the pH predictions marginally, it did not resolve the Ca concentration inconsistency. Further, it has been noted that ACP acts as a precursor to HAP, with ACP slowly transforming to HAP over time (months to years), and that the conditions present in ADL (similar to SWW) stabilise ACP and slow its transformation to HAP (Musvoto *et al.*, 2000c). It is unlikely that HAP forms within the time-scale of the test, and accordingly ACP precipitation was accepted as the dominant CaP precipitant. Accepting that the change in Mg species across any time interval is due to struvite precipitation, then the P in this struvite can be calculated from this mineral's stoichiometric

formulation (molar ratio Mg:N:P = 1:1:1). Subtracting the struvite precipitated P from the measured change in P, then the non-struvite P precipitated can be determined. Comparing this with the measured decrease in Ca, gives a Ca:P ratio of about 11:1 for the first 0.25h of the test, where-after the ratio decreases to 1.25 then 1:1. No CaP precipitant with such a large Ca:P ratio could be identified from the literature, nor any Ca mineral (with or without P) not included in the model that would precipitate under the conditions present in the test. Hence this inconsistency could not be resolved - either there is an error in the Ca data or an unknown Ca mineral precipitates that is not accounted for in the model. This illustrates the immense value in applying mass balances based models to experimental data, to gain a deeper understanding of the underlying processes and identify possible errors in data.

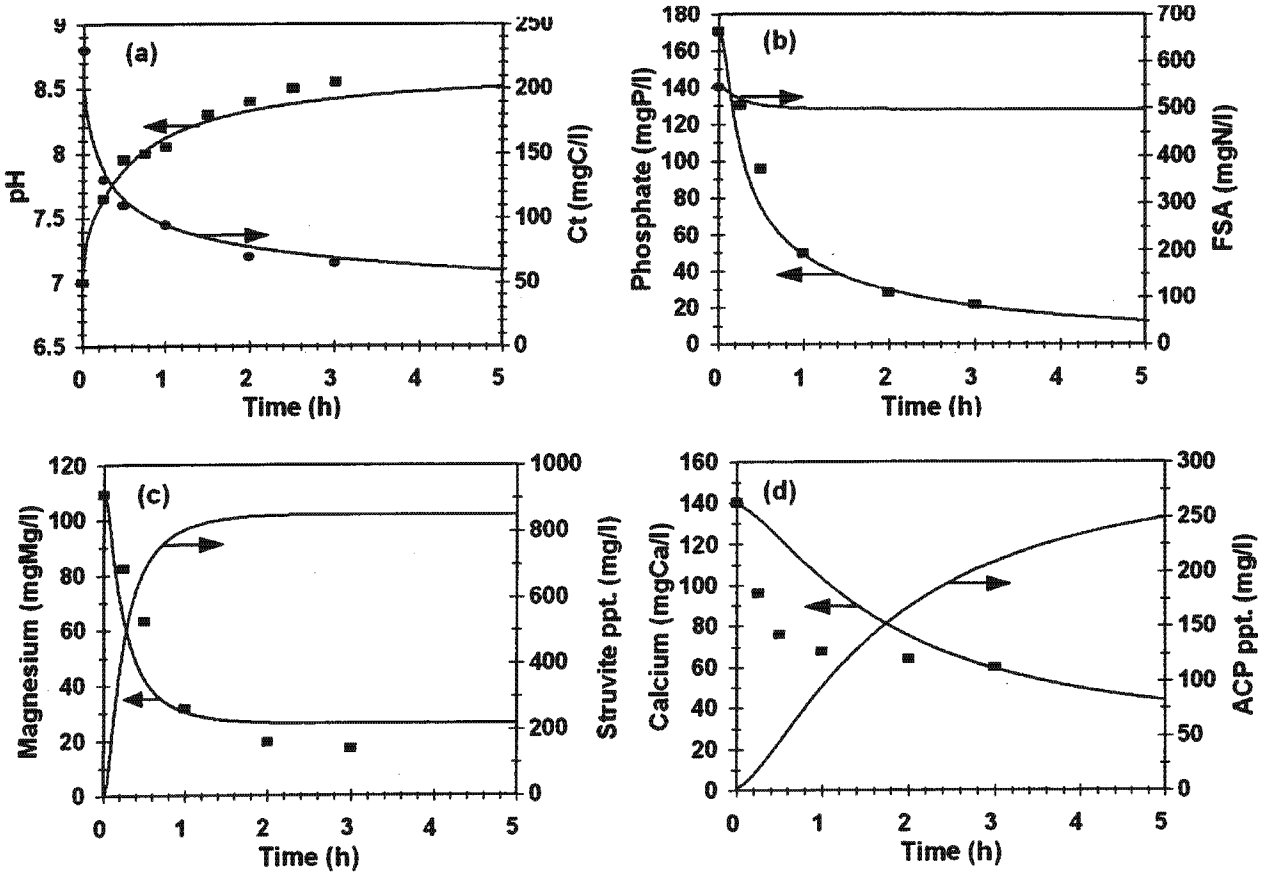

Fig. 6.1: Predicted (—) and measured (■,●) concentrations for pH and total inorganic carbon (C_T, Fig 6.1a, top left), soluble phosphate and free and saline ammonia (FSA, Fig 6.1b, top right), soluble magnesium and precipitated struvite (Fig 6.1c, bottom left) and soluble calcium and precipitated amorphous calcium phosphate (ACP, Fig 6.1d, bottom right) for aerobic batch test on SWW.

Accepting the inconsistency in the Ca values, with the 'default' values for the model constants with the exception of the two constants calibrated as above, close correlation was obtained between experimental and measured data (Fig 6.1). Also, the 3 hour simulated mass precipitations are in close agreement with the measured mass precipitation values: Measured Mg, Ca and P precipitated = 86, 84 and 155 mg/ℓ respectively and predicted = 83, 81 and 150 mg/ℓ respectively. From the simulations, as expected aeration strips CO_2 from the wastewater (observed as the decrease in C_T, Fig 6.1a) causing the pH to increase (Fig 6.1a). This increase in pH causes struvite to become supersaturated and precipitate (Fig 6.1c); The initial solution is very close to struvite saturation. Also, with time ACP precipitates (Fig 6.1d); The initial solution is slightly supersaturated with respect to ACP, but the precipitation rate is relatively slow. Over the 3 hour test period about 850 mg/ℓ struvite (as $MgNH_4PO_4 \cdot 6H_2O$ = 475 mg/ℓ as $MgNH_4PO_4$) and 81 mg/ℓ ACP (as $Ca_3(PO_4)_2$, the hydration water is unknown) precipitate and negligible newberyite, calcite and magnesite precipitate, in agreement with literature observations. In the precipitation of the minerals, the struvite and ACP essentially compete for P - if ACP precipitation is inhibited by, for example, removing Ca, or if additional P is added (in excess), additional struvite precipitates (about 200 mg/ℓ), and *vice versa*. Hence, it can be concluded that the struvite precipitation with time in the test is controlled by the change in pH, but that the final quantity that precipitates is influenced by the availability of P. The competition between struvite and ACP for P effectively reduces the P available for struvite precipitation. However, due to the rapid rate of struvite precipitation compared with ACP, the majority of P is precipitated in struvite. From the simulations it became evident that for the SWW the molar ratios of Mg, Ca and P are particularly favourable for induced struvite and ACP precipitation, but with P slightly deficient for optimal precipitation.

The close correlation between predicted and measured values (except Ca) enabled theoretical investigation with the model of the precipitation reactions. (1) *Extending aeration:* Aeration was theoretically extended for 1 hour beyond the experiment (Fig 6.1). Only minor additional ACP precipitation occurred, with minimal additional P and Ca removal. (2) *Aeration rate:* Increasing the aeration rate 2.3 (Suzuki *et al.*, 2002) times ($K_{La,O2}$ = 1600/d) causes the pH to increase more rapidly, which causes the precipitation rates to increase (rate constants remain unchanged), and *vice versa*. However, the final condition of the solution and the mass of precipitants remains largely unchanged provided sufficient time is allowed for precipitation at the lower aeration rates, in agreement with experimental observations (Suzuki *et al.*, 2002). Varying the aeration rate, therefore, impacts mainly on reactor retention time and, provided this is appropriately selected, not the removals via precipitation. (3) *Hydroxide dosing:* If instead of aeration, the pH is increased through hydroxide dosing at the start of the test, struvite precipitation is induced to approximately the same extent as with aeration, but the precipitation is much more rapid, virtually immediate. ACP precipitation does not occur immediately, but is a time dependent reaction. Further, depending on the pH attained, calcite and magnesite precipitation may occur reducing the Mg and Ca species available for struvite and ACP respectively. The effect of reduced Mg in struvite precipitation is compensated for by the increased availability of P due to non competition for P by ACP precipitation. However, due to lower P availability, reduced ACP precipitation with time occurs.

If hydroxide is dosed at the end of the aeration (3h), no significant additional minerals precipitate (except for some calcite and magnesite depending on the final pH). Thus, hydroxide dosing, whether instead of or after aeration, offers no significant advantages over aeration, except more

rapid struvite precipitation with dosing instead of aeration, reducing reactor retention times.

6.3.4.2 Aeration of anaerobic digester liquor (ADL) (van Rensburg *et al.*, 2003)
Accepting the ACP precipitation rate constant determined from the SWW simulations above, of $K_{ppt,ACP}$ = 700/d, and the $K_{La,O2}$= 130/d of van Rensburg *et al.*(2003), the batch ADL aeration tests of van Rensburg *et al.*(2003) were re-simulated (Fig 6.2). Close correlation between predicted and measured data was obtained. The increased $K_{ppt,ACP}$ value caused an increase in predicted ACP precipitation from 16 (van Rensburg *et al.*, 2003) to 75 mg/ℓ, but did not influence the struvite precipitation. Although the ACP and struvite compete for P species, in this test the P is available in excess and Mg is limiting in the struvite precipitation - increasing the initial Mg concentration increased predicted struvite precipitation significantly from 545 (van Rensburg *et al.*,2003) to 1000 mg/ℓ for increase in initial Mg from 65 to 130 mg/ℓ. Comparing the predicted and measured Ca concentrations, unfortunately the quality of the measurements is inadequate to make a judgement as to whether ACP precipitation (and hence Ca removal) is predicted more

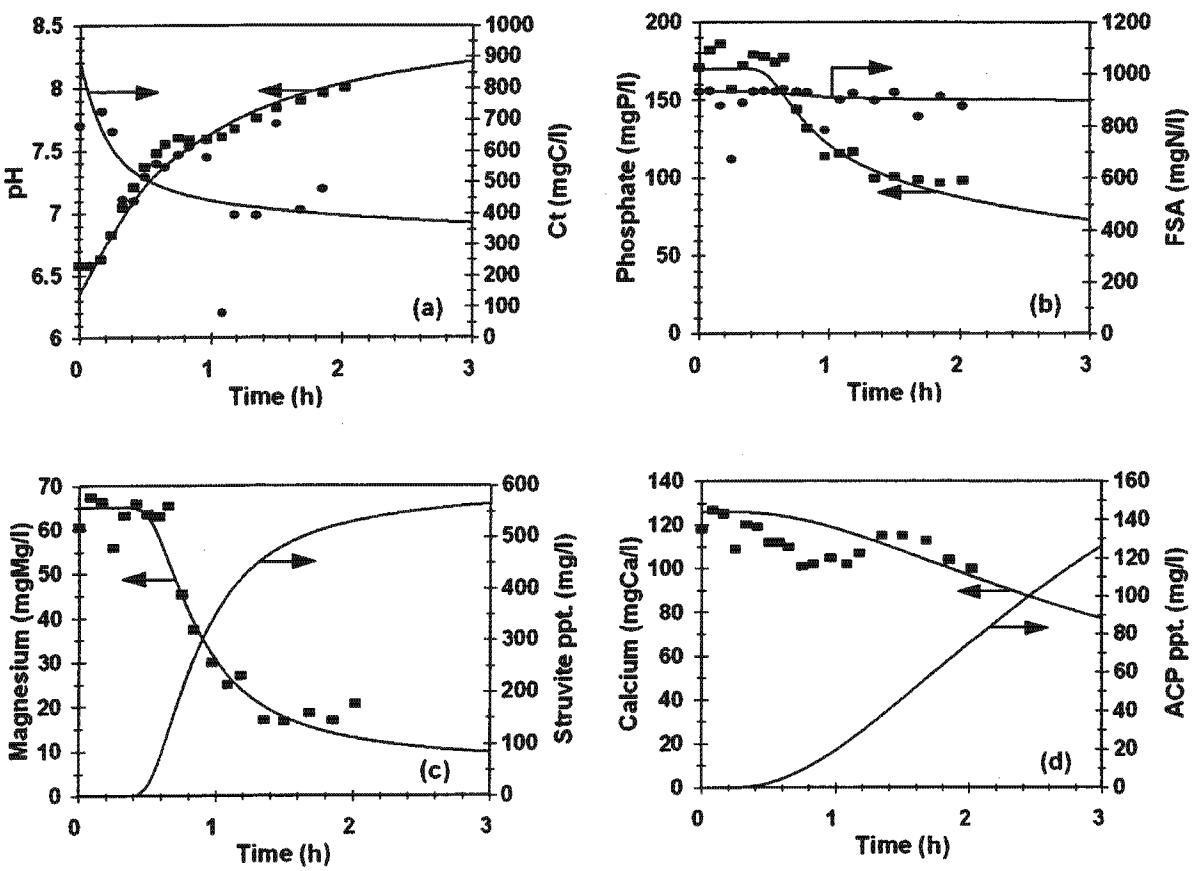

Fig 6.2: Predicted (—) and measured (■,●) concentrations for pH and total inorganic carbon (C_T, Fig 6.2a, top left), soluble phosphate and free and saline ammonia (FSA, Fig 6.2b, top right), soluble magnesium and precipitated struvite (Fig 6.2c, bottom left) and soluble calcium and precipitated amorphous calcium phosphate (ACP, Fig 6.2d, bottom right) for aerobic batch test on anaerobic digester liquor from CFWWTP digester treating primary and waste activated sludge.

correctly than in van Rensburg *et al.* (2003). In contrast to the SWW above, in the ADL initially the solution is significantly under saturated with respect to struvite, so that with pH increase saturation is only attained after about 30 minutes aeration, and struvite starts to precipitate. Theoretically, dosing hydroxide instead of aerating has the same effect as for the SWW above; Dosing hydroxide at the end of the test to increase the pH to 9 gives minimal additional precipitation (545 to 610 mg/ℓ struvite). Effect of aeration rates on precipitation reported by van Rensburg *et al.* (2003) remains unchanged. From the simulations, for this wastewater, the molar ratios of Mg, Ca and P are not as well suited for struvite precipitation as for the SWW - the P is in excess so that after aeration and precipitation significant P remains (about 100 mg/ℓ). Extended aeration (Fig 6.2) induces only minor additional ACP precipitation and P removal. If the objective is minimising struvite precipitation in subsequent unit operations then the aeration treatment will achieve this. However, if P recovery is the objective, additional P precipitation needs to be induced - this can be best achieved through Mg addition.

The additional test on aeration on ADL from the CFWWTP by van Rensberg *et al.* (2001) was also simulated. In this test, additionally to the aeration, NaOH was added to sample numbers 5 to 10 to increase pH further. To accommodate this, in the simulations OH was dosed to the test from sample number 5 ($\geq$1.4h), at quantities to match the measured pHs and the volume of OH dose was kept small so that dilution would not have a significant influence on concentrations. The values for all constants were as above, except for $K_{La,O2}$ which was set at 50/d, to match the observed initial pH increase ($\leq$1.4h); As noted above, the value for this constant is situation specific. Predicted and measured data are compared in Fig 6.3, and as can be seen from Fig. 6.3, close correlation was obtained. In this test it is evident that despite the increased ACP precipitation rate constant, significant ACP precipitation does not occur (Fig 6.3d). In this test the initial Ca concentrations were very much reduced (25 mg/ℓ) compared with the test above (125 mg/ℓ), so that ACP is initially under saturated, and only marginally supersaturated as the pH increases. As with the ADL aeration test above, at the end of the aeration significant P remains (90 mgP/ℓ). Dosing Ca to the initial solution does give increased P removal, but Mg dosing is far more efficient due to the relatively rapid struvite precipitation rate compared with ACP.

6.3.5 Closure

The considerable value of the integrated chemical physical processes three phase (aqueous/gas/solid) mixed weak acid/base kinetic model as a tool for evaluating experimental data and design options has been demonstrated. In particular, the integrated kinetic model is able to predict the time dependent weak acid/base reactions and the final equilibrium state for situations where multiple minerals competing for the same species (or not) precipitate either simultaneously, sequentially or both (as demonstrated here). This characteristic of the kinetic model represents a deficiency in equilibrium chemistry based algebraic models such as those incorporated in IWA Anaerbic Digestion Model No. 1 (Batstone *et al.*, 2002).

The three phase kinetic based weak acid/base chemistry model, and the approach on which it is based, has proved to be a very useful framework for research into and design of wastewater treatment systems in which several weak acid/bases influence the behaviour. For research, the model helps to focus attention on issues not obvious from direct experiment and allows determination of mineral precipitation rates for a particular wastewater from a single batch test.

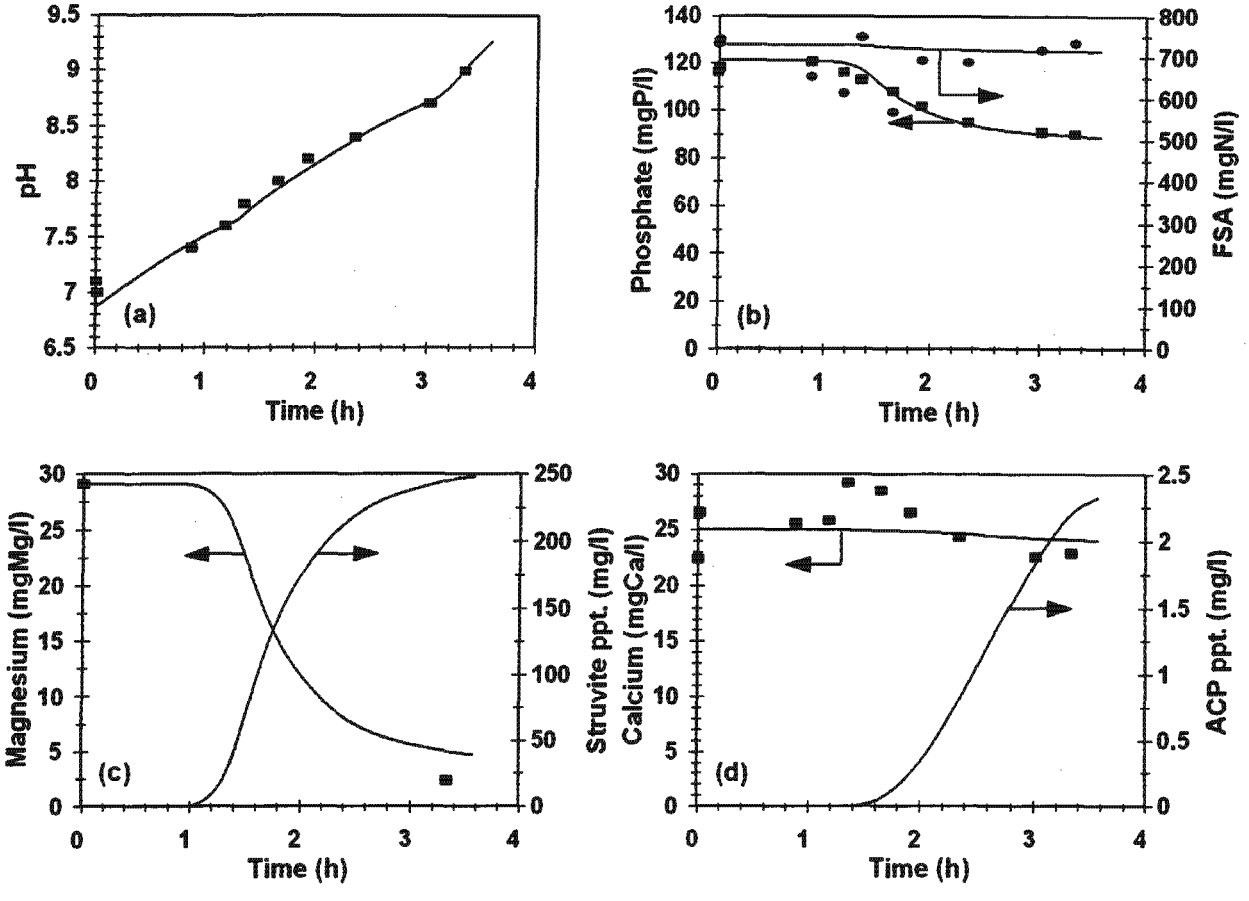

Fig 6.3: Predicted (—) and measured (■,●) concentrations for pH (Fig 6.3a, top left), soluble phosphate and free and saline ammonia (FSA, Fig 6.3b, top right), soluble magnesium and struvite precipitated (Fig 6.3c, bottom left) and soluble calcium and precipitated amorphous calcium phosphate (ACP, Fig 6.3d, bottom right) for aerobic batch test on anaerobic digester liquor from CFWWTP digester treating primary and waste activated sludge; NaOH added from sample 5 (>1.4h) to raise pH.

Once calibrated with the precipitation (and gas stripping if included) rates, this kind of model can be used to predict the performance of different treatment systems to identify for investigation those that appear technically and economically viable. In Chapter 3, this modelling approach (for two phases, aqueous and gas) was extended to include biological processes such as those for biological nutrient removal activated sludge and anaerobic digestion (Chapter 4). This allowed modelling of biological treatment systems together with the mixed weak acid/base chemical systems within which the biological processes operate or combined biological/chemical systems such as simultaneous chemical/biological P removal (de Haas *et al.*, 2001) in a seamless way. In Chapters 3 and 4, treatment processes modelling was taken a quantum step further by developing integrated kinetic chemical, physical and biological processes models that can deal with the interaction between the biological processes and the two phase mixed weak acid/base

chemistry 'background' in which these operate.

This Chapter illustrates that the integrated kinetic approach to modelling the three phase (aqueous, gas and solids) mixed weak acid/base chemistry is general and can be applied to any combination of mixed weak acid/base systems, mineral precipitations (simultaneous or sequential), ion pairs and physical gas exchange reactions. Further, the solids precipitation (or solids phase) can readily be included with the kinetics for the combined two phase chemical/physical and biological processes models developed in Chapter 3 (C and N removal activated sludge) and Chapter 4 (anaerobic digestion). Extending the models developed in Chapters 3 and 4 with the third (solids) phase is beyond the scope of this thesis project report, but this Chapter illustrates the capabilities of the three phase (aqueous-gas - solid) mixed weak acid/base kinetic model and also shows that the third (solids) phase can readily be integrated in the biological, 2 phase chemical and physical processes kinetic models developed in Chapters 3 and 4. The approach has opened the door to modelling in an integrated way systems governed by chemical, physical and biological processes, such as anaerobic digestion, activated sludge treatment of low alkalinity municipal wastewater, simultaneous precipitation in biological nutrient removal activated sludge and biological sulphate removal and sulphur recovery from acid mine drainage.

CHAPTER 7

CONCLUSIONS AND RECOMMENDATIONS

As part of a larger objective to develop steady state and dynamic simulation COD (electron), carbon (C), nitrogen (N), phosphorus (P), alkalinity (proton), calcium (Ca) and magnesium (Mg) and inorganic suspended solids (ISS) concentrations mass balances models for whole municipal wastewater treatment plants (WWTPs) comprising primary sedimentation, secondary treatment with activated sludge and aerobic and anaerobic sludge stabilization of primary (PS) and secondary (waste activated, WAS) sludges, this thesis project makes a number of significant contributions, viz.

(1) Set up a simple mass balances (COD, N and P) WWTP steady state and kinetic simulation models (UCTOLD) with primary sedimentation, anoxic aerobic activated sludge and aerobic digestion of primary and waste activated sludge and compared and verified these models.

(2) Extend the activated sludge simulation model (ASM1) to a two phase (aqueous/gas) chemical, physical and biological processes one incorporating pH as a predictive parameter and validate it against literature data. This extension is restricted to aerobic and anoxic/aerobic C and N removal activated sludge systems.

(3) Integrate the biological processes of anaerobic digestion into a two phase (aqueous/gas) version of the chemical/physical processes model developed by Musvoto *et al.* (1997, 2000) to construct a mass balances (COD, C, N, O, H) based integrated chemical physical biological processes model capable of predicting digester pH (UCTADM1) and verify it with laboratory and literature data.

(4) Simplify UCTADM1 into a steady state model for initial design of AD systems and integration into the steady state WWTP (1) model.

(5) Review three phase (aqueous/gas/solid) mixed weak acid/base chemical physical processes for inclusion of multiple mineral precipitation of calcium and magnesium phosphate and carbonate based minerals in the two phase kinetic models (2 and 3) developed above.

In the development of these models, requirements were that (i) they should be as far as possible combinations of the existing biological and the mixed weak acid/base chemistry models, so that the chemical physical processes within which the biological processes take place are modelled as well as the biological processes themselves, (ii) the integration between the biological and chemical physical processes is seamless with the hydrogen ion (i.e. pH) being modeled as a process compound like all the others, and (iii) the models of the different unit operations such as N removal activated sludge, anaerobic digestion, primary sedimentation etc. can be readily combined to form a mass balances based kinetic model for the whole WWTP.

7.1 THE STEADY STATE MASS BALANCES MODEL AND SINGLE (AQUEOUS) PHASE BIOLOGICAL KINETIC MODEL

A steady state mass balances (COD, N and P) spreadsheet program was developed. This steady state mass balances spreadsheet is capable of the following:

(1) Characterizes the raw and settled WWs COD, TKN, FSA, TP and OP, each into their unbiodegradable and biodegradable soluble and particulate components, from the given (measured) concentrations and fractions and PS COD, VSS, ISS, TSS, OrgN, OrgP, also each into their unbiodegradable and biodegradable soluble and particulate components from mass balances around the PST.

(2) Calculates the design parameters for the fully aerobic, ND or ND BEPR systems treating the raw and settled WW at long (>20d) and short (4-20d) sludge ages respectively.

(3) Calculates the design parameters for a single reactor aerobic digester by taking the PS and WAS flows and concentrations (including the liquid stream), blending and concentrating them to the selected thickened concentrations, aerobically digesting the blended and thickened sludge to a selected residual biodegradable organic content. Checks material mass balances (COD, N and P) over the aerobic digester.

(4) Explores aerobic digestion of fully aerobic and ND WAS sludge in single, double and triple compartment digesters with and without PS and with separate PS and WAS thickening before blending.

(5) Checks the COD, N and P mass balances around the WWTP comprising (i) raw WW treatment in a long sludge age AS system, where the sludge age is selected long enough for sludge stabilization in the reactor and direct discharge of WAS to drying beds (i.e. extended aeration), and (ii) PSTs, short sludge aged activated sludge system, PS and WAS thickening and aerobic digestion of PS and WAS to the same residual biodegradable organics as (i) above.

This steady state mass balances spreadsheet brings a step closer the modelling of a WWTP as a whole, in an integrated fashion with common compounds at the interconnections. The steady state mass balances spreadsheet includes a link (i) between the primary settler and the aerobic digester and (ii) between the AS system and the aerobic digester which assess and quantify the interdependencies of the PS, AS and aerobic digester unit operations.

It was shown further, that there is a very close match between the formal complex dynamic simulation WWTP model in which UCTOLD (Dold *et al.*, 1991) is used to model the AS and aerobic digester systems and the much simpler steady state model. Only one parameter had to be changed in the UCTOLD (Dold *et al.*, 1991) model, i.e. the K value of the switching function for the nitrogen requirement for aerobic growth from 0.10 to 0.0001 mgN/ℓ. This switching function controls the uptake of FSA for growth, and if insufficient, allows nitrate to be taken up instead.

Together with developing an integrated *steady state* mass balances model for the whole WWTP system to select and size its sequence of unit operations and interconnecting flows, there is also a need to develop a similar integrated *dynamic* model for the whole WWTP system that is built up around the same mass balances principles of the steady state mass balances model. This requires consideration of the links between the most common unit operations of a WWTP, viz (i) the PST - anaerobic digester link, (ii) the AS system - aerobic digester link, (iii) the AS system

- anaerobic digester link and (iv) the PST - aerobic digester link. Because the anaerobic digestion system is the most different to activated sludge and requires the major weak acid/base systems in three phases to predict its pH, it is the most difficult one for which to find common compounds at their links. Attention was therefore focussed in this thesis on integrating weak acid/base chemistry into the activated sludge model to facilitate connection with the anaerobic digester.

7.2 INTEGRATED BIOLOGICAL, CHEMICAL AND PHYSICAL PROCESSES KINETIC MODELLING: ANOXIC/AEROBIC C AND N REMOVAL IN THE ACTIVATED SLUDGE SYSTEM

The biological processes of the nitrification/denitrification (ND) activated sludge model No 1 (ASM1, Henze *et al.*, 1987) were integrated into a two phase (aqueous/gas) subset of the three phase mixed weak acid/base chemical/physical kinetic model of Musvoto *et al.* (2000). In this integration, a number of additions were made to ASM1, such as (i) production and/or utilization of CO_2, H^+, NH_3, and H_3PO_4 in heterotrophic (OHO) and autotrophic (ANO) growth and death (endogenous respiration) processes and (ii) the effect of pH (i.e. H^+) on the biological processes, in particular on the autotrophic nitrifiers (ANOs).

The integrated chemical, physical and biological (CPB) processes activated sludge model simulations were compared with those of ASM1 (Dold *et al.*, 1991) and experimental data in the literature. Identical simulation results were obtained with both models and the correlation of both models with experimental data was good. While the CPB model gave some interesting insights into the behaviour of the inorganic carbon and N systems, strictly, these comparisons serve only as model verification because, although included, the weak acid/bases and pH have no significant effect on the biological processes in the cases considered. However, because the CPB model was developed by integrating previously individually validated models, rigorous independent experimental validation of the integrated model was not deemed necessary, except where the chemical/physical processes interact strongly with the biological processes. The principal interaction is the effect of pH on nitrification and this interaction was based on literature information and so is calibrated as best as possible. It is concluded from this integration that:

(1) The total organic carbon (TOC) to chemical oxygen demand (COD) ratio of the wastewater does not significantly influence the reactor pH because most of the CO_2 generated is stripped by aeration.
(2) The free and saline ammonia (FSA) to total Kjeldahl nitrogen (TKN) ratio and concentrations does affect the pH due to alkalinity generation.
(3) Nitrate uptake for OHO growth once ammonia is depleted (assimilative denitrification) also affects the pH.
(4) The extent of denitrification and
(5) the extent of CO_2 stripping from the aerobic reactor by aeration also have an effect on the reactor pH.
(6) The pH in the anoxic reactor is higher than that in the aerobic reactor due to the lack of CO_2 stripping from the anoxic reactor.

Experimental determination of the inorganic carbon concentration (C_T) in outflows from full scale N removal activated sludge aerobic reactors indicated that these were about 20% supersaturated with CO_2 gas, so that CO_2 gas exchange by aeration in the aerobic reactor does

not yield CO_2 equilibrium with the atmosphere.

From simulation of long sludge age nitrification/denitrification (ND) activated sludge systems with incrementally decreasing influent $H_2CO_3^*$ alkalinity, when the effluent $H_2CO_3^*$ alkalinity falls below about 50 mg/ℓ as $CaCO_3$, the aerobic reactor pH drops below 6.3, which severely retards nitrification and causes the minimum sludge age for nitrification (R_{sm}) to increase up to the operating sludge age of the system. Therefore, when treating low $H_2CO_3^*$ alkalinity wastewaters, such as those from the Western and Southern coastal areas of South Africa, the minimum sludge age for nitrification (R_{sm}) varies with temperature and reactor pH and for low effluent $H_2CO_3^*$ alkalinity (< 50 mg/ℓ as $CaCO_3$), nitrification becomes unstable and very sensitive to dynamic loading conditions resulting in increases in effluent ammonia concentration and reduced N removal. For effluent $H_2CO_3^*$ alkalinity < 50 mg/ℓ, lime should be dosed raise the aerobic reactor pH and stabilize nitrification.

7.3 INTEGRATED CHEMICAL/PHYSICAL AND BIOLOGICAL PROCESSES MODELLING: ANAEROBIC DIGESTION OF SEWAGE SLUDGES

For connecting to the primary settling tank and the activated sludge system, an integrated two phase (aqueous/gas) mixed weak acid/base chemistry and biological processes anaerobic digester kinetic model for sewage sludge was developed. The salient features of this model are:

(1) As an alternative to characterizing the sewage sludge feed into carbohydrates, proteins and lipids, as is done in IWA ADM1 (Batstone *et al.*, 2002), it is characterized in terms of total COD, its particulate unbiodegradable COD fraction (f_{PSup}), the short chain fatty acid (SCFA) COD and the CHON content of the particulate organics, i.e. X, Y, Z and A in $C_XH_YO_ZN_A$. This approach characterizes the sludge in terms of measurable parameters and allows COD, C and N mass balances to be set up over the anaerobic digestion system. With this approach, the interactions between the biological processes and weak acid/base chemistry could be correctly predicted for stable steady state operation of anaerobic digesters. While not validated for dynamic flow and load conditions, the model has the capability of being applied to dynamic flow and load conditions.

(2) The COD, C and N mass balances and continuity basis of the model fixes quantitatively, via the interrelated chemical, physical and biological processes, the relationship between all the compounds of the system so that for a given biodegradation the digester outputs (i.e. effluent COD, TKN, FSA, SCFA, $H_2CO_3^*$ Alk, pH, gaseous CO_2 and CH_4 production and partial pressures) are governed completely by the input sludge (and aqueous) characteristics. All the kinetic and stoichiometric constants in the model, except those for hydrolysis, were obtained from the literature so that model calibration reduced to determining (i) the unbiodegradable particulate COD fraction of the sewage sludge (f_{PSup}), (ii) the hydrolysis kinetics formulation and associated constants and (iii) the sewage sludge CHON composition, i.e. the X, Y, Z and A values in $C_XH_YO_ZN_A$.

(3) Interactively with determining the hydrolysis kinetics ((4) below), the unbiodegradable particulate fraction of the sewage sludge was estimated at 0.32 - 0.36 for the sewage sludge fed to the mesophilic anaerobic digesters of Izzett *et al.* (1992) ranging over 7 - 20 days retention time, depending on the type of hydrolysis kinetics selected. These values are very close to the value of 0.36 determined by O'Rourke (1968) and the values estimated from a COD mass balance around the primary settling tank from typical raw

and settled wastewater characteristics (0.32 - 0.36 for COD removals of 40 - 35%).

(4) Four formulations for the hydrolysis rate of sewage sludge particulate biodegradable organics were evaluated, see 7.4 below. Surface mediated reaction (Contois) kinetics similar to that used by Dold *et al.* (1980) and IWA Activated Sludge Model 1 (Henze *et al.*, 1987) for slowly biodegradable organics in activated sludge systems, were selected. Once calibrated against the Izzett *et al.* (1992) data, this formulation showed the required sensitivity of gas production and unfiltered effluent COD concentration to variation in retention time, without changing the constants in the hydrolysis rate equation.

(5) From the influent COD, organic N and VSS measurements of Izzett *et al.*, the stoichiometric formulation of the influent sewage sludge was estimated to be $C_{3.4}H_7O_2N_{0.192}$. With the sludge biodegradability and hydrolysis process rate defined, to match the anaerobic digester performance data of Izzett *et al.* (1992) ranging over 7 - 20 days retention time, (i.e. effluent COD, TKN, FSA, SCFA, $H_2CO_3^*$, Alk, pH, gaseous CO_2 and CH_4 production and partial pressures), the sewage sludge composition was refined to $C_{3.5}H_7O_2N_{0.196}$ to conform to the COD, C and N mass balances of the model. This formulation was confirmed with undigested primary sludge CHON composition tests, the average of which was $C_{3.65}H_7O_{1.97}N_{0.19}$. The model predicted CHON content and molar mass of the PS was therefore 95.9%, 100%, 98.5%, 94.5% and 98.7% of the measured values. This provides persuasive validation of the UCTADM1 model. It would appear that because the CHON composition of the biodegradable primary sludge organics obtained from the mass balances model and that measured on undigested primary sludge, which comprises biodegradable and unbiodegradable organics, that the latter is of similar composition as the former.

(6) Validation of the AD model under steady state conditions validates only its stoichiometry and the system rate limiting process, which is hydrolysis. However, the model, which includes the influence of high hydrogen partial pressure on the acidogenesis and acetogenesis processes, showed the expected sensitivity to a digester upset initiated by temporary inhibition of the acetoclastic methanogens, which is the usual cause of digester failure in practise. The model demonstrated that even a brief inhibition of this organism group causes an irreversible failure of the digester (pH < 6.6).

The proposed surface mediated reaction (or Contois kinetic) hydrolysis rate equation reproduced the observed change in biodegradable particulate COD acidified versus retention time with the same kinetic constants. Based on the Izzett *et al.* (1992) anaerobic digester data, a Monod type hydrolysis rate equation also showed consistency of constants over 7 to 20 d retention time, but simple first order and first order specific hydrolysis rate equations yielded different rate constants at different retention times. However, by changing the unbiodegradable particulate COD fraction of the sewage sludge (f_{PSup}) the fit of both the first order and first order specific hydrolysis rate equations to the experimental data of Izzett *et al.* (1992) could be significantly improved (with concomitant deterioration in the fit with Contois and Monod kinetics). Experimental work to *inter alia* refine the modelling of the hydrolysis process was conducted on mesophilic methanogenic and sulphidogenic anaerobic digester systems (Ristow *et al.*, 2004a,b,c). Modelling the Ristow *et al.* (2004a) experimental data with their unbiodegradable particulate COD fraction (0.33) and hydrolysis rate constants and a surface mediated reaction (or Contois kinetic) hydrolysis rate equation resulted in a reasonable correlation between the experimental and simulated data. However, because of considerable scatter in the Ristow *et al.* (2004a) experimental data, it proved difficult to derive hydrolysis rate constants that would result in a

better fit of the experimental and simulated data. Hence, the Izzet *et al.* anaerobic digester data set is too limited and the Ristow *et al.* (2004a) data too variable to make a definitive conclusion as to which is the best equation to model the hydrolysis process, and what the best value for f_{PSup} is. Intuitively and based on its widespread application in activated sludge systems acting on the same biodegradable particulates, the surface mediated reaction (Contois) kinetics has been selected for hydrolysis.

- The characterisation of sewage sludge in terms of its CHON(P) content appears a sound approach. While testing primary sludges for the UCTADM1 model validation, a range of other sewage sludges were also tested, such as waste activated, anaerobic digested and mixtures of primary and waste activated. From the tests done to date, it seems that the CHON contents of sludges are consistent and grouped approximately in conformity with type. It appears likely, therefore, that typical CHON(P) contents of the different sludges may be selected, and that the standard characterisation tests such as COD, TKN and VSS, are sufficiently discerning and accurate for modelling AD of sewage sludges. Measurement of sewage sludge composition is continuing and its effect on digester pH and gas composition will be evaluated when more information has been collected.

7.4 A STEADY STATE MODEL FOR ANAEROBIC DIGESTION OF SEWAGE SLUDGES

The complex simulation AD model was simplified to a steady state one for incorporation into the steady state mass balances WWTP model (7.1 above). It comprises three sequential parts, (i) a kinetic part with which the influent COD hydrolyzed/ utilized, gas and biomass production and effluent COD concentration are calculated for a given retention time, (ii) a stoichiometry part with which the gas composition (or partial pressure of CO_2), ammonia released and alkalinity generated are calculated from the COD utilized and the CHON composition of the hydrolyzed COD and (iii) a carbonate system weak acid/base chemistry part with which the digester pH is calculated from the partial pressure of CO_2 and alkalinity generated. This model shows that for a given %COD removal, the partial pressure of CO_2 and alkalinity generated, and hence the digester pH, are governed entirely by the influent sludge composition, i.e. X, Y, Z and A in $C_XH_YO_ZN_A$ and the undissociated volatile fatty acids (VFA) species concentration of the influent.

The hydrolysis kinetic part of the model was calibrated against AD data for two types of sewage sludge, (i) a primary and humus sludge mixture extending over a retention time range of 7 to 20 days (Izzett *et al.*, 1992) and (ii) a 'pure' primary sludge extending over a retention time range of 7.5 to 60 days (O'Rourke, 1968). Also, four hydrolysis kinetic rate (r_h) equations were calibrated against both sludge types, viz. (i) first order ($r_h = K_h S_{bp}$), (ii) first order specific ($r_h = K_H S_{bp} Z_{AD}$), (iii) Monod [$r_h = K_m S_{bp}/(K_s + S_{bp}) Z_{AD}$] and (iv) saturation [$r_h = K_M (S_{bp}/Z_{AD})/(K_S + S_{bp}/Z_{AD}) Z_{AD}$]. Once calibrated against the particular sludge type and taking due account of experimental error, the %COD removals predicted by the four hydrolysis kinetic equations were closely similar, which made it difficult to select the best kinetic equation. Also, by varying the unbiodegradable COD fraction ($f_{PS'up}$) of the sewages sludges within a narrow range (~2%) changed the coefficient of variation (C_{var}) for the first order and first order specific kinetic equations, and the correlation coefficient (R^2) for the Monod and saturation kinetic equations. Within the 2% range in unbiodegradable COD fraction, the different hydrolysis kinetic equations yielded best statistical fits between theoretically predicted and experimentally measured COD

removals (or gas production) at different $f_{PS'up}$ values. It is concluded that for both types of sewage sludge, taking due account of experimental error (i.e. COD mass balance errors) each calibrated kinetic equation is equally good for calculating the %COD removal and gas production versus retention time. For each sewage sludge type, different hydrolysis kinetic rates and unbiodegradable COD fractions were obtained which showed that the pure primary sludge hydrolysed significantly faster and had a lower unbiodegradable particulate COD fraction ($f_{PS'up}$ = 0.33) than the primary and humus sludge mixture ($f_{PS'up}$ = 0.36). Anaerobic digesters treating pure primary sludge therefore will achieve higher COD or VSS removals at shorter retention times than digesters treating a primary and humus sludge mixture.

Once the COD removal is known from the hydrolysis kinetics part of the model, the CHON composition of the COD removed and the dissociated acetate species concentration in the influent (all utilized in the digester) fixes the gas composition (or partial pressure of CO_2), the ammonia released and the bicarbonate generated (equal to alkalinity generated) through the C, H, O and N mass balances based stoichiometry part of the model. From the influent COD, C and N masses of the primary and humus sludge digesters, a sludge composition of $C_{3.5}H_7O_2N_{0.196}$ was determined. With this sludge composition and measured influent VFA concentration and pH, from which the dissociated acetate species concentration was calculated, the stoichiometry part of the model predicted the experimentally observed gas composition (or CO_2 partial pressure), ammonia released and alkalinity generated well, taking due account of experimental error. With the CO_2 partial pressure and alkalinity generated, the digester pH was calculated from the carbonate system weak acid/base chemistry part of the model. The model predicted pH was significantly lower (by ~0.30 pH units) than that experimentally measured. From the observed CO_2 partial pressure and alkalinity, which can be measured reliably, there is an error in the measured digester pH, probably due to CO_2 gas loss in sampling and measurement. The 'corrected' measured pH should be between 6.84 and 6.88 for the 7, 10, 12, 15 and 20 day retention time systems and the predicted pH is 0.08 to 0.12 pH units higher than these corrected values. A significantly closer correlation between theoretically calculated and experimentally measured digester effluent FSA, alkalinity and pH can be obtained if the N content of the feed sludge is decreased from 0.196 to 0.186 based on the measured N mass exiting the digesters rather than on that entering the digesters. Taking into consideration experimental error (C and N mass balances errors) it is concluded that the steady state model predicts very well the observed 7 to 20 day retention time primary and humus sludge digester performance. The stoichiometry and carbonate system weak acid/base chemistry part of the model could not be checked against the 'pure' primary sludge digester data set of O'Rourke (1968) because the N concentrations in the effluent were not measured for this data set. The steady state AD model also correlated very closely with the predictions of the two phase (aqueous/gas) integrated chemical, physical and biological processes dynamic simulation anaerobic digester model (UCTADM1). Provided the hydrolysis rate of the particulate biodegradable organics is known for a particular sewage sludge, the steady state model is useful to (i) estimate retention time, reactor volume, gas production and composition for a required system performance like COD (or VSS) removal, (ii) investigate the sensitivity of the system performance to the design and operation parameters, (iii) provide a basis for cross-checking simulation model results, and (iv) estimate product stream concentrations for design of down- (or up-) stream unit operations of the wastewater treatment plant.

Because the predicted results from the steady state and dynamic simulation model were so close,

the steady state model was not applied to the Ristow *et al.* (2004a) data set - the results also would have been almost identical because the same process governs the model outputs, i.e. sludge hydrolysis.

7.5 MODELLING PHYSICAL/CHEMICAL PROCESSES IN 3 PHASES - TOWARDS INCORPORATING THE SOLID PHASE IN THE KINETIC MODEL FOR ANAEROBIC DIGESTION

The considerable value of the integrated chemical physical processes three phase (aqueous/gas/solid) mixed weak acid/base (inorganic carbon, phosphorus, ammonia, short chain fatty acids and water) kinetic model as a tool for evaluating experimental data and design options has been demonstrated. In particular, the integrated kinetic model is able to predict the time dependent weak acid/base reactions and the final equilibrium state for situations where multiple minerals competing for the same species (or not) precipitate either simultaneously, sequentially or both (as demonstrated), a deficiency in equilibrium chemistry based algebraic models such as those incorporated in IWA Anaerobic Digestion Model No. 1 (Batstone *et al.*, 2002).

The three phase mixed weak acid/base, multiple gas and mineral precipitation model developed is accurate, stable and reliable. Therefore, the solids precipitation (or phase) can be included with the kinetics for the two phase chemical/physical and biological processes models for C and N removal activated sludge and anaerobic digestion of sewage sludges. Extending these two kinetic models with the third (solid) phase is beyond the scope of this thesis project, but the capabilities of the three phase (aqueous/gas/solid) mixed weak acid/base kinetic model were demonstrated and it appears, that the third (solids) phase can be integrated in the biological, two phase chemical and physical processes kinetic models developed in this thesis.

The three phase kinetic based weak acid/base chemistry model, and the approach on which it is based, has proved to be a very useful framework for research into and design of wastewater treatment systems in which several weak acid/bases influence the behaviour. For research, the model helps to focus attention on issues not obvious from direct experiment and allows determination of mineral precipitation rates for a particular wastewater from a single batch test. Once calibrated with the precipitation (and gas stripping if included) rates, this kind of model can be used to predict the performance of different treatment systems to identify for investigation those that appear technically and economically viable.

The integrated kinetic approach to modelling the three phase (aqueous, gas and solids) mixed weak acid/base chemistry is completely general and can be applied to any combination of mixed weak acid/base systems, mineral precipitations (simultaneous or sequential), ion pairs and physical gas exchange reactions. The approach has opened the door to modelling in an integrated and seamless way systems governed by chemical, physical and biological processes, such as anaerobic digestion, activated sludge treatment of low alkalinity municipal wastewater, simultaneous precipitation in biological nutrient removal activated sludge and biological sulphate removal and sulphur recovery from acid mine drainage.

7.6 FURTHER RESEARCH

This thesis project made some significant advances towards developing mass balances based integrated WWTP models for steady state and diurnal flow and load conditions which link primary sedimentation, activated sludge and aerobic or anaerobic digestion of primary and waste activated sludges. The most significant of these are development of the two phase mixed weak acid/base chemical, physical and biological processes simulation model (i) the N removal activated sludge system, (ii) for anaerobic digestion (AD) of primary sludge (PS) and (iii) the steady state simplification of the two phase AD model.

In further research, the four main links between common unit operations of WWTPs need to be considered further, using the mass balances based steady state models for the activated sludge system and aerobic and anaerobic digestion. Attention should also be given to biological N and P removal AS systems including the inorganic suspended solids (ISS) and where required, steady state models developed or extended for unit operations in which the biological processes dominate (e.g. N and P removal activated sludge, aerobic digestion and anaerobic digestion), to allow integrated design of the different unit operations making up the WWTP. Unit operations in which physical processes dominate, such as primary sedimentation, sludge thickening before and dewatering after sludge digestion can be regarded as solid/liquid separators and solids concentrators only. Several complex issues which require further experimental research remain around aerobic and anaerobic digestion of activated sludge including the polyphosphate accumulating organisms (PAOs), in biological excess phosphorus removal (BEPR) activated sludge systems.

More specifically, to develop steady state and kinetic simulation models for the whole WWTP, the following tasks require attention:

Steady state WWTP model:

(1) The steady state anaerobic digestion model needs to be incorporated into the steady state WWTP mass balances tracking model developed so far. This would require that the inputs for the AD model (i.e. the feed sludge characteristics) be included in the upstream unit operations. In addition to the parameters already in the mass balances model, this would include C, alkalinity, and possible SCFA production in the PST. Also, and very importantly, it needs to be established whether or not the unbiodegradable particulate organic material from the influent wastewater, and those generated in the activated sludge reactor (endogenous residue) as defined by the activated sludge (aerobic) system, are unbiodegradable also under anaerobic digester conditions.

(2) Recycling of various liquors (e.g. sludge thickening liquors) from downstream unit operations to upstream ones, and the characteristics of these recycle stream would have to be included.

(3) The steady state mass balances WWTP model needs to be extended to include biological P removal. This is not a simple task. In the activated sludge system, the ordinary heterotrophic (OHO) and polyphosphate accumulating (PAO) organisms have different endogenous respiration/die off rates, the former high (b_{H20} = 0.24 /d at 20 °C) and the latter low (b_{G20} = 0.04 /d at 20°C). These b rates influence the rates at which the nutrients N and P bound in the cell mass are released in aerobic (and anaerobic) digestion. The

release rates of N and P from the cell bound phase to the dissolved phase under aerobic and anaerobic digestion conditions also needs to be investigated.

Kinetic simulation WWTP model:

(1) The integrated biological, chemical and physical processes kinetic model for C and N removal in the activated sludge system should be extended to include biological P removal. This would require research into the interaction of the biological aspects of the polyphosphate accumulating organisms with the aquatic chemistry of the bulk liquid - as was done for the heterotrophic and autotrophic organisms in the kinetic C and N removal model.

(2) The integrated biological, chemical and physical process kinetic model for anaerobic digestion should be extended to include P, for anaerobic digestion of biological N and P removal waste activated sludge.

(3) Once P has been included in the kinetic anaerobic model, the solid phase should be integrated to enable the kinetic anaerobic model to predict multiple mineral precipitation, which would be helpful in the design and operation of anaerobic digesters.

(4) Even though multiple mineral precipitation is not expected to occur in activated sludge systems, the compounds for multiple mineral precipitation should be included in the kinetic activated sludge model, because in a wastewater treatment plant, its output (e.g. WAS) is the input to the anaerobic digester, and hence the kinetic anaerobic digestion model.

CHAPTER 8

REFERENCES

American Public Health Association (1971). Standard methods for the examination of water and wastewater. 13th edition.

Antoniou P, Hamilton J, Koopman B, Jain R, Holloway B, Lyberatos G and Svoronos S A (1990). Effect of temperature and pH on the effective maximum specific growth rate of nitrifying bacteria. *Water Res*earch **24** (1) 97-101.

Barker PS and Dold PL (1997) General model for biological nutrient removal activated sludge systems - Model presentation. *Water Environ. Research* **69**(5) 969-984.

Barnard (1984) Activated primary tanks for phosphate removal. *Water SA*, **10**(3), 121-126.

Batstone DJ, Keller J, Angelidaki I, Kalyuzhnyi SV, Pavlostathis SG, Rozzi A, Sanders WTN, Siegrist H and Vavilin VA (2002). *Anaerobic digestion model No 1*, Scientific and Technical Report (STR) No 13, International Water Association, London. ISBN 19 00222 787.

Borgerding J (1972). Phosphate deposits in digestion systems. *J. Water Pollution Control Fed.*, **44**(5) 813-819.

Bryers JD (1985) Structural modelling of anaerobic digestion of biomass particulates. *Biotech & Bioeng.* **27** 638-649.

Capri M and Marais GvR (1975) pH adjustment in anaerobic digstion. *Water Research* **9**(3) 307-314.

Casey TG, Wentzel MC and Ekama GA (1999). Filamentous organism bulking in nutrient removal activated sludge systems. Paper 10: Metabolic behaviour of heterotrophic facultative aerobic organisms under aerated/unaerated conditions. *Water SA* **25**(4) 425-442.

Cout D, Gennon G, Ranzini M and Romano P (1994). Anaerobic co-digestion of municipal sludges and industrial organic wastes. In: Proceedings of the 7th International Symposium on Anaerobic Digestion. Johannesburg, South Africa.

Dold PL, Ekama GA and Marais GvR (1980) A general model for the activated sludge process. *Prog. Wat. Tech.* **12**(6): Tor 47 - 77.

Dold PL and Marais GvR (1985). Evaluation of the general activated sludge model proposed by the IAWPRC task group. *Water Sci. Technol.* **18** 63-89.

Dold PL, Wentzel MC, Billing AE, Ekama GA and Marais GvR (1991). Activated sludge system simulation programs. Published by the Water Research Commission, Private Bag X03, Gezina, 0031, South Africa, ISBN 0-947447-19-9.

Downing AL, Painter HA and Knowles G (1964). Nitrification in the activated sludge process. *J. Proc. Inst. Sewage Purif.*, 130-153.

Drozd JW (1976). Energy coupling and respiration in *Nitrosomonas europaea*. *Arch. Microbiol.*, **110**, 257-262.

Eastman JA and Ferguson JF (1981) Solubilization of particulate organic compounds during the acid phase of anaerobic digestion. *Journal WPCF* **53**(3) 352-366.

Eckenfelder WW Jr (1980) *Principles of water quality management.* CBI Publishing Company Inc., Boston, Massachusetts, USA.

Ekama GA and Wentzel MC (2004). Modelling inorganic material in activated sludge systems. *Water SA* **30**(2) 153-174.

Eliosov B and Argaman Y (1995) Hydrolysis of particulate organics in activated sludge systems *Water Research* **29**(1) 155 - 163.

Ferguson JF and McCarty PL (1971). Effects of carbonate and magnesium on calcium phosphate precipitation. *Environ. Sci. Tech.*, **5**(6) 534-540.

Friend JFC and Loewenthal RE (1992). STASOFT III - Chemical conditioning of low and medium salinity waters. Water Research Commission, P/Bag X03, Gezina 0031, South Africa, ISBN 1874858306.

Gujer W and Zehnder AJB (1983). Conversion processes in anaerobic digestion. *Wat. Sci. Tech.* **15**(8/9): 127 - 167.

Gujer W (1993). ASIM - Activated sludge simulation program version 2.2. EAWAG, Dubendorf, CH-8600, Switzerland.

Henze M and Harremoës P (1983) Anaerobic treatment of wastewater in fixed film reactors - A literature review. *Water. Sci. Technol.* **15** 1-101.

Henze M, Grady CPL, Gujer W, Marais GvR and Matsuo T (1987). Activated sludge model No. 1. IAWPRC Scientific and Technical Reports No 1, International Association on Water Pollution Research and Control, IAWPRC, London, ISSN 1010-707X. 33pp.

Henze M, Gujer W, Mino T, Matsuo T, Wenzel MC and Marais GvR (1995). Activated sludge model No. 2. IWA Scientific and Technical Report No. 3, Iwa London. ISBN 1-900222-00-0, 32pp.

Henze M, Gujer W, Mino T, Matsuo T, Wentzel MC, Marais GvR and van Loosdrecht MCM (1999). Activated sludge model No 2d (ASM2d) *Water Sci. Technol.* **39**(1) 165-182.

Hill DT and Barth CL (1977). A dynamic model for simulation of animal waste digestion. Technical Contribution No. 1318. *Journal WPCF* Oct 2129 - 2143.

Izzett HB, Wentzel MC and Ekama GA (1992). The effect of thermophilic heat treatment on the anaerobic digestibility of primary sludge. Research Report W76, Univ. of Cape Town, Dept. of Civil Eng. Rondebosch 7701, Cape, South Africa.

Janus HM and van der Roest HF (1997). Don't reject eh idea of treating rejected water. *Wat. Sci. Tech.* **35**(10) 27-34.

Katehis D, Diyamandoglu V and Fillos J (1998) Stripping and recovery of ammonia from centrate of anaerobically digested biosolids at elevated temperatures *Water Environ. Research* **70**(2) 231 - 240.

Kayhanian M and Tchobanoglous G (1992). Pilot investigation of an innovative two-stage anaerobic digestion and aerobic composting process for the recovery of energy from the organic fraction of MSW. In: Proceedings of the 5th International Symposium on Anaerobic Digestion. Venice, Italy.

Kiely G, Tayfur G, Dolan C and Tanji K (1997). Physical and mathematical modelling of anaerobic digestion of organic wastes. *Water Research* **31**(3) 534 - 540.

Koutsoukos P, Amjad Z, Tomson MB and Nancollas GH (1980) Crystallization of calcium phosphates: A constant composition study. *J. Am. Chem. Soc.* **27** 1553-1557.

Lahav O and Loewenthal RE (2000). Measurement of VFA in anaerobic digestion: The five-point titration method revisited. *Water SA*, **26**(3), 389-392.

Lehninger AL (1977) *Biochemistry*. 2nd Ed, Worth Publishers, New York, ISBN 0-87901-047-9.

Levenspiel O (1972) *Chemical reaction engineering*. 2nd Ed. John Wiley, New York, 465 - 469.

Lilley I D, Wentzel M C, Loewenthal R E, Ekama G A and Marais GvR (1990). Acid fermentation of primary sludge at 20°C. *Research Report W64*, Dept. Civil Eng., Univ. of Cape Town, Rondebosch 7701, South Africa.

Loewenthal RE, Wiechers HNS and Marais GvR (1986). *Softening and stabilization of municipal waters*. Water Research Commission, P/Bag X03, Gezina 0031, South Africa, ISBN 0 908356 54 4.

Loewenthal RE, Ekama GA, Marais GvR (1988). STASOFT - An interactive computer program for softening and stabilization of municipal waters. Published by the Water Research Commission, P/Bag X03, Gezina 0031, South Africa, ISBN0908356943.

Loewenthal RE, Ekama GA and Marais GvR (1989). Mixed weak acid/base systems: Part 1 - Mixture characterization. *Water SA* **15**(1) 3-24.

Loewenthal RE, Wentzel MC, Ekama GA and Marais GvR (1991). Mixed weak acid/base systems Part 2 - Dosing estimation, aqueous phase. *Water SA* **17**(2) 107-122.

Loewenthal RE, Kornmuller URC and Van Harden EP (1994). Struvite precipitation in anaerobic treatment systems. *Wat. Sci. Tech.*, **30**(12) 107-116.

Loewenthal RE and Morrison (1997). Manual for STASOFT 3, Water Research Commission, Private Bag X03, Gezina, 0031, RSA.

Loveless JE and Painter HA (1968). The influence of metal ion concentration and pH value in the growth of *Nitrosomonas* strain isolated from activated sludge. *J. Gen. Micro.* **52** 1 -14.

Malan WN and Gouws EP (1966). Geaktiveerde slyk vir rioolwatersuiwering op Bellville. Research report, Council for Scientific and Industrial Research, Nov. 1966.

Mamais D, Pitt PA, Cheng YW, Loiacono J and Jenkins D (1994). Determination of ferric chloride dose to control struvite precipitation in anaerobic sludge digesters. *Water Environ. Res.*, **66** (7).

Marais GvR, Ekama GA (1976). The activated sludge process part 1 - steady state behaviour. *Water SA*. **2** (4) 164-200.

McCarty PL (1964). Thermodynamics of biological synthesis and growth. 2nd Int. Conf. Water Pollut. Research, Pergammon Press, New York, 169 - 199.

McCarty PL (1972). Stoichiometry of biological reactions. Proceedings of the international conference towards a unified concept of biological waste treatment design, Atlanta, Ga.

McCarty PL (1974) Anaerobic processes. Presented at International Association of Water Pollution Research (IAWPR, now IWA) short course on Design Aspects of Biological Treatment, Birmingham, UK, 18 Sept. 1974.

Mohajit KK, Bhattarai E, Taiganides EP and Yapp BC (1989). Struvite deposits in pipes and aerators. *Biol. Wastes*, **30** 133-147.

Moosbrugger RE, Wentzel MC, Ekama GA and Marais GvR (1992). Simple titration procedures to determine H_2CO_3* alkalinity and short chain fatty acids in aqueous solutions containing known concentrations of ammonium, phosphate and sulphide weak acid bases. Water Research Commission, Private Bag X03, Gezina, 0031, South Africa. ISBN 1 874858 54 3.

Moosbrugger RE, Wentzel MC, Ekama GA and Marais GvR (1993). Grape wine distillery waste in UASB systems - Feasibility, alkalinity and pH control. *Water SA* **19**(1) 53-68.

Morel FMM and Hering JG (1993). Principles and applications of aquatic chemistry, 2nd edition. Wiley-Interscience, New York.

Muller A, Wentzel MC, Ekama GA and Loewenthal RE(2003). Heterotroph anoxic yield in anoxic aerobic activated sludge systems treating municipal wastewater. *Water Research* **37**(10) 2435-2441.

Munz C and Roberts PV (1989). Gas and liquid phase mass transfer resistances of organic compounds during mechanical surface aeration. *Water Research* **23**(5) 589-601.

Musvoto EV, Wentzel MC, Loewenthal RE and Ekama GA (1997). Kinetic based model for mixed weak acid/base systems. *Water SA* **23**(4) 311-322.

Musvoto EV, Wentzel MC, Ekama GA (1998). Mathematical modelling of integrated chemical, physical and biological treatment of wastewaters. Research Report W97, University of Cape Town, Dept. of Civil Engineering, Private Bag, Rondebosch, 7701, South Africa.

Musvoto EV, Ekama GA, Wentzel MC and Loewenthal RE (2000a). Extension and application of the three phase mixed weak acid/base kinetic model to the aeration treatment of anaerobic digester liquors. *Water SA* **26**(4) 417-438.

Musvoto EV, Wentzel MC, Loewenthal RE and Ekama GA (2000b). Integrated chemical - physical processes modelling. I - Development of a kinetic based model for mixed weak acid/base systems. *Water Research* **34**(6) 1857-1867.

Musvoto EV, Wentzel MC and Ekama GA (2000c). Integrated chemical-physical processes modelling. II - Modelling aeration treatment of anaerobic digester supernatants. *Water Research* **34**(6) 1868-1880.

O'Rourke JT (1968). Kinetics of anaerobic treatment at reduced temperatures. PhD dissertation, Department of Civil Engineering, Stanford University.

Orhon D, Sözen S and Artan N (1996). The effect of heterotrophic yield on the assessment of the correction factor for the anoxic growth. *Water Sci. Technol.* **34** (5/6) 67-74.

Pavlostathis SG and Giraldo-Gomez E (1991) Kinetics of anaerobic treatment. *Wat. Sci. Tech.* **24**(8) 35-59.

Payne W J (1981). *Denitrification.* Wiley Interscience, New York.

Pitman AR, Deacon SL, Alexander Wv, Nicholls HA, Boyd RSA and Minson D (1989). New methods for conditioning and dewatering sewage sludges in Johannesburg. Proceedings, WISA 1st Biennial Conference, Cape Town, South Africa.

Pitman AR, Deacon SL and Alexander WV (1991). The thickening and treatment of sewage sludge to minimize phosphorus release. *Water Research* **25**(10) 1285-1294.

Pitman AR (1995). Practical experiences with biological nutrient removal on full scale plants in South Africa. Presented at the Internationale Konferenz zur Vermehrten Biologischen Phosphorelimination, Hanover, Germany.

Reichert P (1998). Aquasim 2.0 - Computer program for the identification and simulation of aquatic systems. EAWAG, Dubendorf CH-8600 Switzerland, ISBN 3-906484-17-3.

Reichert P (1998) *Concepts underlying a computer programme for the identification and simulation of aquatic systems (Aquasim 2.0).* Swiss Federal Institute of Environmental Science and Technology (EAWAG), CH-8600, Switzerland.

Ristow NE, Sötemann SW, Loewenthal RE, Wentzel MC and Ekama GA (2004a) Hydrolysis of primary sewage sludge under methanogenic, acidogenic and sulphate reducing conditions. *WRC Report 1216/1/04*, Water Research Commission, P/Bag X03, Gezina 0031, South Africa.

Ristow NE, Sötemann SW, Wentzel MC, Loewenthal RE and Ekama GA (2004b) The effects of hydraulic retention time and feed COD concentration on the rate of hydrolysis of primary sewage sludge. *10th World Congress on Anaerobic Digestion, AD2004*, Montreal, Canada, 29 August - 2 September.

Ristow NE, Sötemann SW, Wentzel MC, Ekama GA and Loewenthal RE (2004c). Considerations for the use of primary sludge and sulfate-reducing bacteria for the treatment of sulfate-rich wastes. *Procs. WISA Biennial*, Cape Town, South Africa, 2-6 May, CD-ROM ISBN 1-920-01728-3, 1533 - 1541.

Sam-Soon PALNS, Wentzel MC, Dold PL, Loewenthal RE and Marais, GvR (1991). Mathematical modelling of upflow anaerobic sludge bed (UASB) systems treating carbohydrate waste waters. *Water SA* **17**(2): 91 - 106.

Sötemann SW, van Rensburg P, Ristow NE, Wentzel MC, Loewenthal RE and Ekama GA (2005a) Integrated chemical, physical and biological processes modelling Part 2 - Anaerobic digestion of sewage sludges. *Water SA* (submitted).

Sötemann SW, Musvoto EV, Wentzel MC and Ekama GA (2005b) Integrated chemical, physical and biological processes modelling Part 1 - Anoxic-aerobic C and N removal in the activated sludge system. *Water SA* (submitted).

Sperandio M, Urbain V, Audic J-M, and Paul E (1999). Use of carbon dioxide evolution rate for dentrifying heterotrophic yield characterizing denitrifying biomass. *Water Sci. Technol.* **39**(1) 139-146

Stern LB and Marais GvR (1974). Sewage as the electron donor in biological denitrification. Research report W7, Dept. of Civil Engineering, University of Cape Town, Private Bag, Rondebosch, 7701, South Africa

Still DA, Ekama GA, Wentzel MC, Casey TG and Marais GvR (1996). Filamentous organism bulking in nutrient removal activated sludge systems. Paper 2: Stimulation of the selector effect under aerobic conditions. *Water SA* **22**(2) 97-118.

Suzuki I (1974). Mechanisms of inorganic oxidation and energy coupling. *Ann. Micro.*, **28** 85-101.

Suzuki K, Tanaka Y, Osada T and Waki M (2002) Removal of phosphate, magnesium and calcium from swine wastewater through crystallization enhanced by aeration. *Water Research* **36** 2991-2998.

van Haandel AC, Ekama GA, Marais GvR (1981). The activated sludge process: Part 3 - Single sludge denitrification. *Wat. Res.* **15** 1135-1152.

van Haandel AC, Catunda PFC and Araujo L (1998). Biological sludge stabilization Part 1 - Kinetics of aerobic sludge digestion. *Water SA* **24**(3) 223-230.

van Rensburg P, Musvoto EV, Wentzel MC and Ekama GA (2000) Mineral precipitation from anaerobic digester supernatant at the Cape Flats treatment plant. *Research Report W105*, Dept. of Civil Eng., Univ. of Cape Town, Rondebosch 7701, Cape, South Africa.

van Rensburg P, Musvoto EV, Wentzel MC and Ekama GA (2003) Modelling multiple mineral precipitation in anaerobic digester liquor. *Water Research* **37** 3087-3097.

Vavilin VA, Lokshina Lya (1996). Modelling of volatile fatty acids degradation kinetics and evaluation of microorganism activity. *Biores. Tech.* **57**(1): 69 - 80.

Warner APC, Ekama GAE, Marais GvR (1986). The activated sludge process part 4: Application of the general kinetic model to anoxic / aerobic digestion of waste activated sludge. *Water Research*, **20** (8) 943-958.

Wentzel MC, Dold PL, Ekama GA and Marais GvR (1985) Kinetics of biological phosphorus release. *Water Sci Technol.* **17** 57-71.

Wentzel MC, Ekama GA, Dold PL and Marais GvR (1990). Biological excess phosphorus removal - Steady state process design. *Water SA* **16**(1) 29-48.

Wentzel MC, Ekama GA and Marais GvR (1992). Processes and modelling of nitrification denitrification biological excess phosphorus removal systems - a review. *Wat. Sci. Tech.* **25** (6) 59-82.

Wentzel MC, Musvoto EV and Ekama GA (2001) Application of integrated chemical physical processes modelling to aeration treatment of anaerobic digester liquors. *Environmental Technology* **22** 1287-1293.

Wiechers HNS (1978). Engineering aspects of calcium carbonate and magnesium hydroxide precipitation in waste water reclamation. PhD thesis, University of Cape Town, Department of Civil Engineering, Private Bag, Rondebosch, 7701, South Africa.

Wild HE, Sawyer CN and McMahon TC (1971). Factors affecting nitrification kinetics. *J. Water Pollut. Control Fed.*, September.

Wild D and Siegrist H (1999). The simulation of nutrient fluxes in wastewater treatment plants with EBPR. *Water Research* **33**(7) 1652-1662.

WRC (1984) *Theory, design and operation of nutrient removal activated sludge processes.* Ed. Wiechers HNS, Water Research Commission, Private Bag X03, Gezina, 0031, RSA. ISBN 0 908356 13 7.

Zehnder AJB and Wuhrmann K (1977) Physiology of a methanobacterium strain AZ. *Arch Mikrobiol.* **III** 199-205.

Zehnder AJB, Huser BA, Brock TD and Wuhrmann K (1980) Characterizing an acetate decarboxylating non-hydrogen oxidizing methane bacteria. *Arch. Microbiol.* **124** 1-11.

APPENDIX A

PRIMARY AND WASTE ACTIVATED SLUDGE CHARACTERISATION RESULTS

A.1 INTRODUCTION

During the development of the model for anaerobic digestion of sewage sludges, initially the primary sewage sludge composition was assumed to be the same as the generally accepted stoichiometric formulation for activated sludge: $C_5H_7O_2N$ (WRC, 1984). However, since the output (pH, gas volume and composition) from the digester is a direct consequence of the input and its composition, $C_5H_7O_2N$ could not reflect the output of the system that was used to calibrate the anaerobic model (the anaerobic model was calibrated using data from Izzet *et al.*, 1992), and had to be changed accordingly. Through a series of calculations the general formulation for the primary sewage sludge used by Izzet *et al.* (1992) experiments was found to be $C_{3.5}H_7O_2N_{0.196}$. This stoichiometric formulation for primary sewage sludge was accepted for all subsequent simulations of the Izzet *et al.* (1992) experiments.

It is not certain whether this composition applies to primary sewage sludges in general or not, and this prompted further investigations into characterising primary and waste activated sludges (WAS). Different sewage sludges (primary sludge, waste activated sludge and anaerobic digester sludge) were sampled and analysed for C, H and N (by an external laboratory) and COD, N, P and settleable solids (in the water research laboratory at the University of Cape Town). With this measured data the CHON composition can be calculated for each of the sludges and the primary sewage sludge compared with that estimated from the anaerobic digester model, and the WAS with the 'standard' value of $C_5H_7O_2N$.

A.2 CALCULATION METHOD

One litre of the sludge of interest was drawn, and the following analysis was done on the sludge in the water research laboratory at the University of Cape Town:

(i) Mixed liquor volatile (VSS) and total (TSS) suspended solids.
(ii) Chemical oxygen demand (COD).
(iii) Total Kjeldahl nitrogen (TKN) and free and saline ammonia (FSA).
(iv) Total phosphorus and orthophosphates.

The laboratory analysis above was done according to the respective methods contained in 'Standard Methods for the Examination of Water and Wastewater', American Public Health Association, 13th Edition, 1971.

The remainder of the sludge was dried in a drying oven at 100°C. After drying, the solids were pulverised using a mortar and pestle and sent to the ESCOM (TSI division) laboratories for CHN testing. ESCOM uses the Leco CHN 1000 Instrument for CHN testing. The dry samples are homogenised by micronising the nominal top size down to at least 212 micron and ideally 150 micron, after which the samples are analysed for CHN by the Leco CHN 1000 instrument. The results are returned as %C, %H and %N.

With the above analysis results available, the general CHON(P) composition can be calculated as follows:

From the carbon (C), hydrogen (H), nitrogen (N) and phosphorus (P) (% or mg) analyses, the respective compound masses are calculated from the TSS (or VSS). Since the masses of C, H, N, P and oxygen (O) must add up to the total TSS mass, once the masses of C, H, N and P are known, it is assumed that the remaining TSS mass is O. This assumption is not true in reality, because there may be minerals and other compounds present in the sample, however the O value is revised later on in the calculations to take account of this. As an example, consider the WAS from a laboratory scale MLE system (10 day sludge age, N removal only), (i) in Table A2 below:

For this WAS, the ESCOM analysis gave 37.34% C, 5.48% H and 5.45% N. The laboratory analysis results for this WAS are summarized in Table A1.

Table A1: Laboratory analysis results for sludge (i) in Table A2.

Test	Unit	
TSS	mgTSS/ℓ	2602.0
VSS	mgVSS/ℓ	2354.0
Total COD	mgCOD/ℓ	3319.0
TKN	mgN/ℓ	219.1
TP	mgP/ℓ	40.1
Soluble COD	mgCOD/ℓ	53.0
FSA	mgN/ℓ	14.1
OP	mgP/ℓ	11.0

From the above, the respective compound masses are 0.972g C, 0.143g H, 1.245g O, 0.205g N and 0.029g P. The values are converted into proportions of 1 gram of TSS. For the example WAS, 1 gram of TSS contains 0.3746 C, 0.055g H, 0.482g O, 0.079g N and 0.011g P. This is then converted to the molar scale (0.0311 mol C, 0.0546 mol H, 0.0301 mol O, 0.0056 mol N and 0.0003 mol P for the example WAS) and the moles of each of the compounds is divided by the molar mass of the compound with the smallest molar mass, which is usually P. This yields a general formulation in terms of C, H, O, N and P ($C_{86.4}H_{151.7}O_{83.6}N_{15.58}P_1$ for the example WAS). This general formulation has to be simplified further to resemble the generally accepted formulations, e.g. $C_5H_7O_2N$. It was decided to simplify the general formulation by bringing it to a H_7 basis, and in case of the example WAS, this simplification yields $C_{3.99}H_7O_{3.86}N_{0.72}P_{0.05}$.

This simplified general formulation is then used to calculate the theoretical COD, which is compared to the actual measured COD. If the theoretical and measured COD differ substantially, the COD is recalculated with the O as a variable and substituting the measured TSS and COD values, yielding a revised O. For the example WAS (not including P, assuming it has a negligible effect):

$$C_{3.99}H_7O_{3.86}N_{0.72} + 4.12H_2O \rightarrow 3.99CO_2 + 0.72NH_3 + 13.08H^+ + 13.08e^- \quad \text{(Reduction half reaction)} \qquad \text{(A1)}$$

$$13.08H^+ + 13.08e^- + 3.27O_2 \rightarrow 6.54H_2O \quad \text{(Oxidation half reaction)} \qquad \text{(A2)}$$

Noting that the molecular weight of $3.27O_2 = 104.63$g and that of $C_{3.99}H_7O_{3.86}N_{0.72} = 126.82$g, 0.825g $O/gC_{3.99}H_7O_{3.86}N_{0.72}$ is required. Therefore, the theoretical COD of 2602.0mgTSS/ℓ is 2146.7 mgCOD/ℓ. However, the measured COD of the solids is 3266.0 mgCOD/ℓ (total COD less soluble COD in Table A1), which is a substantial difference. Therefore, the COD is recalculated with the O as a variable in Equations A1 and A2 and substituting the measured TSS and COD values:

$$C_{3.99}H_7O_zN_{0.72} + (7.98 - z)H_2O \rightarrow 3.99CO_2 + 0.72NH_3 + (20.8 - 2z)H^+ + (20.8 - 2z)e^- \qquad \text{(A3)}$$

$$(20.8 - 2z)H^+ + (20.8 - 2z)e^- + \left(\frac{10.4 - z}{2}\right)O_2 \rightarrow (10.4 - z)H_2O \qquad \text{(A4)}$$

Therefore, from Equations A3 and A4, the particulate COD = (O required/molecular weight)xTSS:

$$COD = \frac{(10.4 - z)16}{53.17 + 16z} \cdot (2602) = 3266 \qquad (A5)$$

From Eq. A5, z = 2.762 and therefore in the case of the example WAS (i) in Table A2 the corrected O worked out to $O_{2.762}$. The corrected general formulation for the example WAS (i) is $C_4H_7O_{2.762}N_{0.72}(P_{0.05})$, as can be seen from Table A2.

The calculations were done on a TSS basis as well as a VSS basis, but it was found that the differences in the resulting general formulations were negligible.

A.3 RESULTS

In the first series of tests, the following sewage sludges were analysed:

(i) WAS from a laboratory scale MLE system (10 day sludge age, N removal only).
(ii) WAS from a laboratory scale UCT system (15 day sludge age, N and P removal).
(iii) WAS from a second laboratory scale MLE system (10 day sludge age, N removal only).
(iv) WAS form a laboratory scale UCT system (12 day sludge age, N and P removal).
(v) Primary sewage sludge from the Mitchell's Plain treatment plant in Cape Town.
(vi) Anaerobic digester sludge from a laboratory scale anaerobic digester (10 day retention time).
(vii) Primary sewage sludge from the Athlone treatment plant in Cape Town.
(viii) Anaerobic digester sludge from a laboratory scale anaerobic digester (10 day retention time)

Table A2 below summarises the results for all the sludges analysed during the first series of tests.

Table A2: COD/VSS, TKN/COD and calculated stoichiometric formulation for the sludges tested.

Sample	COD/VSS Ratio	TKN/VSS Ratio	Measured formulation	Literature formulation
(i) 10d MLE WAS	1.387	0.087	$C_4H_7O_{2.76}N_{0.72}$	$C_5H_7O_2N$
(ii) 15d UCT WAS	1.222	0.073	$C_{3.91}H_7O_{2.82}N_{0.54}$	$C_5H_7O_2N$
(iii) 10d MLE 2 WAS	1.147	0.086	$C_{4.32}H_7O_{3.44}N_{0.65}$	$C_5H_7O_2N$
(iv) 12d UCT WAS	1.181	0.081	$C_{4.31}H_7O_{3.39}N_{0.61}$	$C_5H_7O_2N$
(v) Mitchell's Plain PS	2.029	0.054	$C_{3.91}H_7O_{2.04}N_{0.16}$	$^*C_{3.5}H_7O_2N_{0.196}$
(vi) Anaerobic Digested Sludge	1.720	0.054	$C_{3.92}H_7O_{2.64}N_{0.35}$	$C_5H_7O_2N$
(vii) Athlone Primary Sludge	2.124	0.037	$C_{3.38}H_7O_{1.9}N_{0.21}$	$^*C_{3.5}H_7O_2N_{0.196}$
(viii) Anaerobic Digested Sludge	1.687	0.038	$C_{4.08}H_7O_{3.63}N_{0.22}$	$C_5H_7O_2N$

* Determined by the anaerobic digestion mass balances model.

In the second series of tests, the following sludges from the experimental investigation of Ristow *et al.* (2004a) were analysed:

(i) Feed batch (FB) 12 (Primary sludge from the Athlone treatment plant in Cape Town)
(ii) Feed batch 14 (Primary sludge from the Athlone treatment plant in Cape Town)
(iii) Feed batch 15 (Primary sludge from the Athlone treatment plant in Cape Town)
(iv) 8d retention time methanogenic laboratory scale anaerobic digester fed from FB12
(v) 15d retention time methanogenic laboratory scale anaerobic digester fed from FB12
(vi) 5d retention time methanogenic laboratory scale anaerobic digester fed from FB13
(vii) 15d retention time methanogenic laboratory scale anaerobic digester fed from FB13
(viii) 15d retention time methanogenic laboratory scale anaerobic digester fed from FB13
(ix) 10d retention time methanogenic laboratory scale anaerobic digester fed from FB13
(x) 8d retention time methanogenic laboratory scale anaerobic digester fed from FB13
(xi) 60d retention time methanogenic laboratory scale anaerobic digester fed from FB12
(xii) 8d retention time methanogenic laboratory scale anaerobic digester fed from FB14
(xiii) 6.67d retention time methanogenic laboratory scale anaerobic digester fed from FB14
(xiv) 3.33d retention time acidogenic laboratory scale anaerobic digester fed from FB15
(xv) 5d retention time acidogenic laboratory scale anaerobic digester fed from FB15
(xvi) 5.71d retention time methanogenic laboratory scale anaerobic digester fed from FB15
(xvii) 3.33d retention time acidogenic laboratory scale anaerobic digester fed from FB15
(xviii) 5d retention time acidogenic laboratory scale anaerobic digester fed from FB15

Table A3 below summarises the results for all the sludges analysed during the second series of tests.

Table A3: COD/VSS, TKN/COD and calculated stoichiometric formulation for the sludges from the experimental investigation of Ristow *et al.* (2004a).

Sample	COD/VSS Ratio	TKN/VSS Ratio	Measured formulation	Literature formulation
(i) FB12	2.074	0.038	$C_{4.15}H_7O_{2.42}N_{0.22}$	$^*C_{3.5}H_7O_2N_{0.196}$
(ii) FB14	1.837	0.041	$C_{4.31}H_7O_{3.03}N_{0.24}$	$^*C_{3.5}H_7O_2N_{0.196}$
(iii) FB15	1.907	0.036	$C_{4.06}H_7O_{2.43}N_{0.19}$	$^*C_{3.5}H_7O_2N_{0.196}$
(iv) Steady state 2	1.799	0.068	$C_{4.36}H_7O_{3.14}N_{0.26}$	$C_5H_7O_2N$
(v) Steady state 5	1.025	0.052	$C_{4.53}H_7O_{5.85}N_{0.22}$	$C_5H_7O_2N$
(vi) Steady state 9	1.880	0.068	$C_{4.35}H_7O_{3.02}N_{0.24}$	$C_5H_7O_2N$
(vii) Steady state 10	1.767	0.089	$C_{4.47}H_7O_{3.41}N_{0.23}$	$C_5H_7O_2N$
(viii) Steady state 11	1.434	0.070	$C_{5.11}H_7O_{4.58}N_{0.25}$	$C_5H_7O_2N$
(ix) Steady state 13	1.716	0.083	$C_{4.63}H_7O_{3.43}N_{0.24}$	$C_5H_7O_2N$
(x) Steady state 14	1.498	0.034	$C_{4.44}H_7O_{3.86}N_{0.21}$	$C_5H_7O_2N$
(xi) Steady state 17	1.501	0.079	$C_{4.62}H_7O_{4.40}N_{0.24}$	$C_5H_7O_2N$
(xii) Steady state 21	1.779	0.077	$C_{4.43}H_7O_{3.35}N_{0.26}$	$C_5H_7O_2N$

(xiii) Steady state 24	1.583	0.066	$C_{4.57}H_7O_{3.58}N_{0.26}$	$C_5H_7O_2N$
(xiv) Steady state 29	2.089	0.028	$C_{4.40}H_7O_{2.81}N_{0.23}$	$C_5H_7O_2N$
(xv) Steady state 30	2.254	0.053	$C_{4.13}H_7O_{2.44}N_{0.24}$	$C_5H_7O_2N$
(xvi) Steady state 31	1.828	0.006	$C_{4.50}H_7O_{2.85}N_{0.27}$	$C_5H_7O_2N$
(xvii) Steady state 32	2.296	0.041	$C_{4.12}H_7O_{2.23}N_{0.21}$	$C_5H_7O_2N$
(xviii) Steady state 33	2.193	0.051	$C_{3.92}H_7O_{2.37}N_{0.21}$	$C_5H_7O_2N$

* Determined by the anaerobic digestion mass balances model.

A.3 CONCLUSIONS

From Table A2 it can be seen that the general formulations calculated for the WAS (i, ii, iii and iv) deviate considerably from the generally accepted $C_5H_7O_2N$ formulation. The WAS tested here have a lower carbon content (~4 as opposed to 5), higher oxygen content (~3 as opposed to 2) and lower nitrogen content (~0.5-0.7 as opposed to 1) than the generally accepted formulation. The lower oxygen and nitrogen values can also be seen from the measured COD/VSS and TKN/VSS ratios: The theoretical values are 1.48 and 0.1 respectively and it can be seen that all the values for the WAS samples are considerably lower than the theoretical ratios. This does not have an effect on the anaerobic sludge digestion model of primary sludge only, however it will have an effect when the model is used to simulate the digestion of WAS only, or a blend of WAS and primary sludge. If the WAS has a lower carbon content than the generally accepted formulation suggests, this will impact on the methane production and the carbonate weak acid/base system (which will in turn impact on the CO_2 produced and the pH of the system). Similarly, if the WAS has a lower nitrogen content than the generally accepted formulation suggests, this will have an impact on the effluent free and saline ammonia concentrations.

The general formulations for the Mitchell's Plain (Table A2, v) and Athlone (Table A2, vii; Table A3 i, ii and iii) primary sludges are reasonably close to the formulation that was found from the anaerobic model with the Izzett *et al.* (1992) data ($C_{3.5}H_7O_2N_{0.196}$). This indicates that the formulation used to calibrate the anaerobic model is in fact the correct one to use, and that the formulation for primary sewage sludge may be general and is not the same as that generally accepted for activated sludge ($C_5H_7O_2N$).

The anaerobic digester sludges (Table A2, vi and viii, Table A3 iv to xviii) seem to lie between the calculated formulations for waste activated sludge and primary sewage sludge, which is not unexpected. Anaerobic digester sludge is a blend of residual primary sludge and the active organism population that grow in the digester and effect anaerobic digestion, hence the general formulation for anaerobic digester sludge would be a combination of the general formulations for primary sewage sludge and that of the organisms (which may be similar to that of WAS).

The results from this investigation are encouraging and warrant a more in depth investigation into the general formulations of primary sewage sludges, waste activated sludges and anaerobic digester

sludges. More sampling on a wider range of samples would be required to ascertain whether:

1. Primary sewage sludges from other sources (treatment plants) than those tested in this investigation will have a similar calculated formulation.
2. The formulation of a blend of primary sewage sludge and WAS is in fact the sum of the general formulations of the separate primary sewage and WAS sludges.
3. The general formulation of anaerobic digester sludge is the sum of the general formulation for the organisms and the residual primary sewage sludge.

A more in depth investigation into the general formulation of primary sewage, waste activated and anaerobic digester sludges will help with the understanding of the sludges and have a valuable input to the anaerobic digestion model and the integrated mixed weak acid/base chemical, physical and biological processes activated sludge model.